UNIVERSITÀ DEGLI STUDI DI MILANO

Department of Agricultural and Environmental Sciences
Production, Landscape, Agroenergy (DiSAA)

PhD School in Plant Biology and Crop Production

Disciplinary sector: Agricultural Genetics (AGR/07)

Characterization and dissection of natural genetic diversity for culm traits in Barley (*Hordeum Vulgare*).

PhD program coordinator: Prof. Daniele Bassi

Supervisor: Dr. Laura Rossini

Co-supervisors: Dr. Salar Shaaf and Dr. Alessandro Tondelli

PhD candidate: Gianluca Bretani

XXXI cycle

Al bene negli occhi di Liliana,
alla forza nelle spalle di Marino
e al loro grande amore.

Sommario

ABSTRACT

Barley (*Hordeum vulgare* L.) is one of the most important crops, with a worldwide grain production of more than 137,98 mln tons per year, 41% of which are produced in Europe. Barley production is threatened by climate change and the associated growing frequency of extreme weather events which results for example in increased lodging. Morphological culm features have been linked to lodging resistance and biomass production in rice and wheat, but the genetic architecture underlying culm traits has not been investigated in barley. Within the ClimBar project, the objective of my PhD research was to dissect natural genetic variation related to culm morphological traits in barley through association mapping on a collection of 198 diverse spring barley cultivars. As a critical region for lodging, we targeted the structure of 2nd basal internode from main stem: internode samples were collected in 2016 and 2017 from field-grown plants at dough stage (in Italy) and pre-harvest stage in four European locations (Spain, Italy, Finland and United Kingdom). Phenotypic data for culm diameter and culm wall thickness were obtained using a newly developed image analysis protocol based on ImageJ software. The number of vascular bundles from dough stage samples was also counted. Data for plant height, days to heading, lodging, and grain yield were also considered for further comparisons. Statistical analyses indicated the existence of significant genetic variation for the studied traits as supported by high heritability values. Combined analysis of variance indicated the existence of interaction between genotype and environment and this was mainly due to location by genotype, while the interaction due to year was less important, indicating the stability of the genotypes across years within the same location. Internode diameter and other culm related traits showed interesting correlations with other agronomical features, describing a complex system of interactions among the different plant organs and how they respond to the surrounding environment. Genome-wide marker data from a 50k iSelect Infinium SNP panel were used to run Genome-Wide Association Studies (GWAS) for plant height as validation trait, recovering markers in close proximity to well-known genes. GWAS revealed significant marker-trait associations for culm traits located within genomic regions harboring potential candidate genes mainly involved in the modification of cell wall composition and interacting with hormonal pathways. However, some associations were location-specific, due to the existence of GxE interactions for the traits under study. Together, our results provide the first insights into the genetic basis of culm morphology in barley and support the value of natural genetic diversity for the improvement of barley yield under climate change.

RIASSUNTO

L'orzo (*Hordeum vulgare* L.) è una delle più importanti piante coltivate, con una produzione mondiale che supera i 137,98 milioni di tonnellate all'anno, di cui il 41% è prodotto in Europa. La produzione di orzo è minacciata dal cambiamento climatico e dal rispettivo aumento dell'incidenza di eventi climatici estremi con conseguenti problemi di allettamento.
L'importanza di diverse caratteristiche morfologiche del culmo nella resistenza all'allettamento è stata dimostrata in riso e frumento, ma informazioni sulle basi genetiche che regolano queste caratteristiche del culmo sono assenti in orzo.
All'interno del progetto europeo Climbar, questo progetto di Dottorato si è posto l'obiettivo di studiare e caratterizzare la naturale variabilità genetica dei diversi tratti morfologici relativi al culmo d'orzo, tramite mappatura di associazione in una collezione di 198 varietà primaverili di orzo.
Studi in letteratura identificano nei cereali il secondo internodo del culmo principale come punto determinante per la resistenza all'allettamento: campioni del secondo internodo sono stati collezionati da esperimenti di campo negli anni 2016 e 2017 da piante in stadio di maturazione cerosa (Italia) e pre-raccolta (Spagna, Italia, Finlandia e Inghilterra). Dati fenotipici riguardanti il diametro del culmo e il suo spessore sono stati ottenuti grazie all'utilizzo di un innovativo protocollo di analisi di immagine basato sull'utilizzo del software ImageJ. Il numero di fasci vascolari è stato inoltre valutato nei campioni allo stadio di maturazione cerosa. Sono stati inoltre considerati dati addizionali riguardanti l'altezza della pianta, la data di fioritura, l'indice di allettamento e la resa in granaglie. Analisi statistiche, eseguite tramite il software R, indicano un alto valore di ereditabilità per i tratti studiati. Analisi della varianza indicano l'esistenza di interazioni tra genotipo e ambiente, mentre interazioni tra genotipo e anno di semina risultano essere meno importanti, indicando un certo livello di stabilità tra i vari ambienti europei attraverso gli anni per quanto riguarda i tratti studiati. Il diametro dell'internodo e gli altri caratteri relativi al culmo d'orzo mostrano interessanti correlazioni con altri tratti agronomici, descrivendo un complesso sistema di interazione tra diversi organi e fra questi e l'ambiente. Successivamente, i dati fenotipici sono stati integrati con dati genotipici ottenuti mediante il 50k iSelect Infinium SNP array al fine di condurre *genome-wide association studies* (GWAS) per i caratteri studiati. Analisi iniziali sull'altezza della pianta hanno permesso di identificare marcatori molto vicini a geni notoriamente coinvolti nella regolazione dell'altezza in orzo, confermando così la validità del modello GWAS utilizzato. Ulteriori analisi hanno identificato significativi segnali di associazione tra marcatori e tratti permettendo l'individuazione di regioni genomiche contenenti geni coinvolti in *pathways* ormonali e nella composizione e modifica dei componenti della parete cellulare.
L'identificazione di segnali di associazione specifici di un sottoinsieme di prove di campo sottolinea l'esistenza di una importante interazione tra genotipo e ambiente. In conclusione i nostri risultati offrono un primo punto di partenza per lo studio di caratteri relativi alla struttura del culmo in orzo, enfatizzando inoltre il valore della diversità genetica naturale di questa pianta per futuri progetti di miglioramento.

1. INTRODUCTION

1.1 ECONOMIC IMPORTANCE OF BARLEY

Barley (*Hordeum vulgare* L., Family: Poaceae, Tribe: Triticeae) ranks in fifth position among the cultivated crops worldwide after corn (*Zeamays* L.), rice (*Oryza sativa*L.), wheat (*Triticum* spp. L.) and soy (*Glycinemax*L.). The global average production of barley seeds between 2010 and 2016 was of 137,98 mln tons, with an average harvested surface of 48,71 mln ha and an average yield production of 2,83 ton/ha (http://www.fao.org/faostat/en/#home). In 2016 the global harvested surface was of 46,92 mln ha, with a seed production of 141,28 mln tons and an average yield of 3,01 ton/ha. In the same year, the major barley producing countries were Russian Federation (17,99 mln of tons), Germany (10,73 mln of tons), France (10,31 mln of tons), Ukraine (9,44 mln of tons), Australia (8,99 mln of tons), Canada (8,70 mln of tons), Spain (7,89 mln of tons) and Turkey (6,70 mln of tons).Italy ranked 27thwith a production of 0,98 mln tons across 246,370 ha (Fig. 1.1 – 1.2).

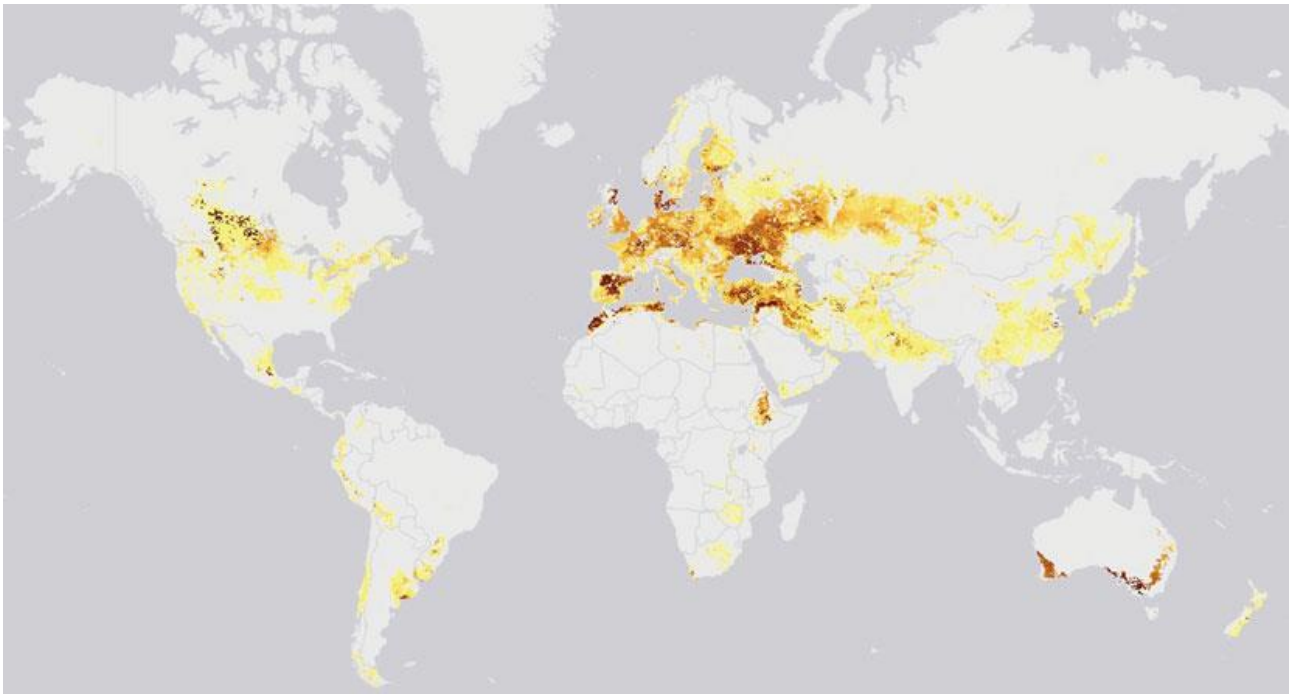

Fig. 1.1 Distribution of barley global production, darker areas represent regions with high percentage of land used for barley production (Langridge 2018).

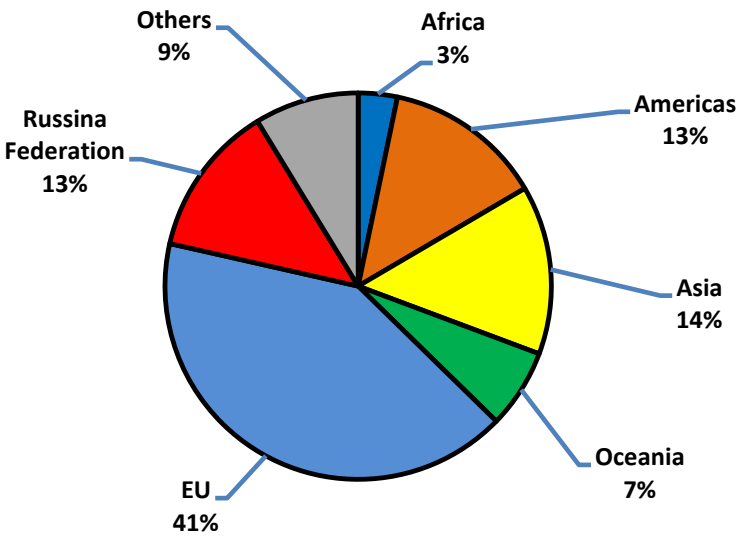

Fig. 1.2 Major barley producers worldwide.

From the latest FAO data, the European Union leads worldwide barley production covering 41% of the global barley production with 58,23 mln tons over a surface of 12,5 mln ha. Barley importance is not just limited to a grain yield evaluation, since 20% of the finest quality barley grains underpins the European brewing industries (whisky and beer), which are the largest in the world. The majority of the largest breweries worldwide are located in Europe, generating a total government income of ~ 57.5 billion euros/year approximately. Just in Europe 164,000 employees work for 3,800 breweries. For each of these, an additional job is generated in retail, two in the supply sectors and more than 12 in the hospitality sector (total >2.5M). Climatic changes and other threats concerning the supply of high quality barley in Europe in the incoming years would therefore have dramatic economic effects.

Due to its intrinsic plasticity, barley is more adaptable than corn and wheat, and can be cultivated in areas where these cereals could not, especially where the climatic conditions are cooler and/or dry, as in North America, North Europe, Middle East, North Africa and Andean areas of South America.

Of the total barley production, 55-60% is used in the feed industry (Ullrich 2011). Barley is the first and the third most used grain for animal feed in Europe and America, respectively, for its high quality/quantity of protein, vitamins and minerals compared to other cereals and may count up to 50% of total feed. Recently, partly because of the cost of feed, the value of sprouted barley as fodder has re-emerged in a number of locations. The controlled germination and early seedling growth in malt production improves the protein, starch and sugar contents of spent grain, which are better utilised in the rumen than dry grain and also reduce acidosis. Mineral and vitamin levels

increase (reported up to 20X) on sprouting; the reduced level of enzyme inhibitors improves absorption in the animal gut. As there is very little dry matter in sprouted barley grains, dry hay must also be provided in animal diets for roughage – with barley straw recognised as higher quality than that from wheat. Comparisons with other grains have concluded that barley sprouts best, grows fastest and is most cost effective. Farmers using sprouted barley fodder report increased milk/beef yields and reduced feed cost albeit with up-front infrastructure investment and additional energy/labour costs.

Indeed, barley is also an important food source in some areas like North Korea, China and Himalayan upland (Baik and Ullrich 2008). Barley is attracting increasing attention as a functional food for the nutraceutical potential associated with the high level of sterols, stenols, arabinoxylans, and soluble non-cellulosic polysaccharides in the form of (1,3;1,4)-ß-glucan (Ullrich 2011). Within the different varieties of barley, differences in ß-glucan concentration and composition are due to both genomic and environmental causes. Levels of (1,3;1,4)-ß-glucan have to be high in food barley for their positive health effects but on the other hand reduced quantity of (1,3;1,4)-ß-glucan in malting grains is an important feature since they can clog filters and stop production. Barley seed cell walls are composed of non-cellulosic polysaccharides which are not digested in human intestine, increasing the daily fibre intake with health benefits as reduction of colorectal cancer, cardiovascular disease and type II diabetes. Furthermore, The US Food and Drugs Administration (FDA) claimed that barley daily consumption lower the risk of heart disease (http://www.fda.gov/NewsEvents/Newsroom/PressAnnouncements/2005/ucm108543.htm).

While barley is not largely consumed by western society, it has recognised qualities that could be a worthy addition to the human diet. For example, (1,3;1,4)- ß -glucan is an excellent natural thickening agent that could find extensive application in the food industry. The effectiveness of non-cellulosic cell wall polysaccharides, including the (1,3;1,4)-ß-glucans, in improving health outcomes is related to their levels in grain, to their fine structures, and to their associated physicochemical properties.

Nonetheless, commercial and biological reasons motivate the use of barley as a break crop in intensive agriculture. While high quality malting barley can itself provide a good financial return, its different response (compared to other crops) to different biotic stresses are beneficial for the next sown crop. Planting a barley crop has additional benefits: its rapid and vigorous development provides extensive ground cover which acts to suppress weeds and its relatively early maturity allows ample time in autumn to harvest prior to planting winter wheat. Barley is more tolerant to

environmental stresses including drought and performs well in low moisture environments. Barley grows in regions where other cereal grains such as wheat or maize cannot, and has an important role in animal welfare, its straw being preferred over other sources of cereal straw. The recent reform of the European Common Agricultural Policy (CAP) has a 'Greening' element, one measure of which is the growing of three different crops on arable enterprises exceeding 30ha, which means that crops like barley will become more important in the overall rotational policy of individual farms.

Net primary biomass production from arable agriculture is estimated at around 8 billion tonnes of carbon per year. While barley represents only a small percentage of this, in regions where production is substantial (e.g. the UK) the unused portion of this biomass such as excess straw, could help offset an emerging energy gap, contribute to global energy security and reduce greenhouse gas (GHG) emissions through the sustainable production of both second generation bio-fuels and associated co-products. Using this biomass is attractive because it could be implemented without any major changes to agricultural production practices or procedures. The majority of the annually sequestered carbon is found in plant biomass as cell wall polysaccharides, making of cereal straw an economically convenient source of cellulose and hemicellulose for improving agricultural feedstocks for biofuel production. In the past ten years barley has become regarded as a renewable resource for the production of 2nd generation bioethanol. About 94,24 Tg of dry barley lignocellulosic material (straw) is obtained as a by product from the food/feed industry and could be theoretically converted into 29.21 billion litres of bioethanol (Han, Kang et al. 2013).

1.2 BARLEY ORIGIN AND DOMESTICATION

The origins of cultivated barley, and cereals in general, and their domestication have been a major focus of plant science research for centuries (von Humboldt and Bonpland 1807, Darwin 1859, Darwin and Gray 1868, de la Candolle 1882). At the beginning of the last century, the Russian scientist Nikolay Ivanovich Vavilov noted that most of the plant and cereal diversity is concentrated around mountainous areas (Vavilov 1926). In his research, Vavilov integrated de la Candolle's and Darwin's works to define the "centre of origin" concept, i.e. a geographically limited area where a crop was first domesticated (Hummer and Hancock 2015). Vavilov's hypothesis was that the level of genetic diversity for a given crop in a region is proportional to the duration of presence of that plant in a the specific location. Following this rationale, regions where a crop species exhibits its maximum genetic diversity are most likely the areas where that crop

existed for the longest time and where it was possibly domesticated, thus leading to their identification as “centre of origin” (Harlan 1951, Harlan 1971).

Vavilov identified and described 8 origin centres all around the world, and among them the Mediterranean centre is where wheat, barley and other crops probably originated (Vavilov 1992). Archaeological studies support Vavilov’s theory, identifying the Near East area, especially the region of the Fertile Crescent comprised between Turkey and Syria, as the starting point for agricultural practices due to favourable environmental and social conditions (Salamini, Özkan et al. 2002, Zohary, Hopf et al. 2012).

Cultivated varieties (cultivars) differ from their wild relatives for a series of features, known as the “domestication syndrome”(Salamini, Özkan et al. 2002, Kilian, Özkan et al. 2009, Olsen and Wendel 2013). Modification of these traits during crop domestication occurred as a result of unconscoius human selection of target genes involved in different aspects of plant development and metabolism (Doebley, Gaut et al. 2006). Key domestication traits improved the harvesting techniques and so the grain yields of early farmers, and in cereals they are the non-brittle rachis, free threshing and reduced seed dormancy.

- The non-brittle rachis is important because it avoids the shattering of the rachis with the spreading of the seeds before the harvest.
- The free threshing trait allows farmers to easily detach the glumes that wrap the cereal seeds for grains ready to be consumed.
- A reduce seed dormancy promotes uniform germination, resulting in plants reaching maturity together.

In barley for example, brittle rachis is used to discriminate between wild and domesticated plants (Pankin and von Korff 2017). Other traits often selected during domestication and breeding include increased seed size, seed hardness, spike row-type (in barley the six row varieties originated from the ancestral two-row form), plant height and tillering, photoperiod response, lack of vernalization requirements and heading date synchronicity (Salamini, Özkan et al. 2002, Kilian, Özkan et al. 2009, Olsen and Wendel 2013).

Cereal domestication lasted hundreds of years with humans cultivating wild species before selecting proper domesticated forms (Tanno and Willcox 2006, Weiss, Kislev et al. 2006, Willcox, Fornite et al. 2008).

Barley was domesticated from its wild progenitor *Hordeum vulgare ssp. spontaneum* (Pourkheirandish and Komatsuda 2007, Zohary, Hopf et al. 2012). To date, the oldest traces of

barley usage are seeds found in an excavation site by the Galilee sea, dating back to more than 21.000 years ago (Kislev, Nadel et al. 1992). Archaeological findings of ancient domesticated barley forms were revealed in the area of Ain Ghazal (today Israel-Jordan area), dating to 9.000/8.500 years ago for both two-row and six-row barley (Willcox 1998). *Hordeum vulgare ssp. spontaneum* is widespread covering a large area around the Fertile Crescent, colonizing eastern Mediterranean regions, western Asia up to Turkmenia and Afghanistan and reaching also north African regions as Abyssinia and Morocco (Harlan and Zohary 1966).

Beside archeobotanical approaches, molecular genetics and genomic approaches have revolutionized domestication studies sometimes providing different perspectives. Indeed, barley origin is still highly debated. Badr et al. (2000) claimed a monophyletic origin for the domestication of barley based on analysis of 400 polymorphic amplified fragment length polymorphism (AFLP) loci, on a population composed of 317 wild relatives and 57 cultivated varieties (Badr, M et al. 2000). The accessions from Israel–Jordan area were those most similar to the domesticated barley, supporting the hypothesis of the Israel–Jordan area as the centre of origin of barley(Badr, M et al. 2000). In a successive work, Morrell et al. (2007) proposed a polyphyletic model for barley origin: with a population structure study based on 684 SNPs on 18 genes, they discriminated 25 barley genotypes into two different subpopulations, one from the east and another from the west separated by the Zagros mountains (Fig. 1.3)(Morrell and Clegg 2007).

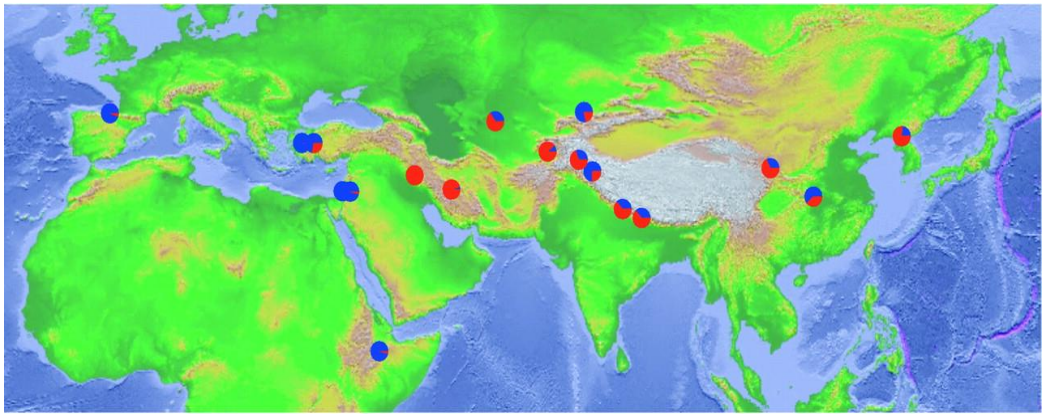

Fig. 1.3 Geographic distribution of barley landraces. The circles represent the estimated probability of western (blue) versus eastern (red) origin for each variety sample (Morrell and Clegg 2007).

The occurrence of two domestication events is consistent with the existence of two distinct tough rachis alleles in modern landraces (Komatsuda, Maxim et al. 2004). This interpretation is supported by the recent identification and characterization of two genes, *Brt1* and *Brt2*, controlling rachis shattering (Pourkheirandish, Hensel et al. 2015). Recessive alleles of these genes

confer the tough rachis trait and two combinations of these genes are present,*brt1 brt1/Brt2 Brt2* and *Brt1 Brt1/brt2 brt2*, characteristic of the western and eastern domestication centres respectively (Fig.1.4) (Komatsuda, Maxim et al. 2004, Pankin and von Korff 2017).

Fig. 1.4 Schematic representation of the two barley gene pools for the mutations in the two tough rachis locus (Pourkheirandish, Hensel et al. 2015).

In the genome sequencing era, recent techniques, based on collating large genomic data from representative collections of domesticated varieties versus wild relatives, are helping to clarify the genetic history of different domesticated species (Huang, Kurata et al. 2012, Hufford, Xu et al. 2012). These data are important to trace back the history of a genome or a specific genomic region to a precise area; combined with archaeological findings these results could greatly help to characterize the temporal and geographical origins of a species and how it was domesticated (Pankin and von Korff 2017).

In the case of barley, Poets et al. (2015) used genome-wide analyses with 6,152 SNPs genotyped in 803 landraces and 277 wild relatives from Europe, Asia, and North Africa(Poets, Fang et al. 2015).Their results show a different level of contribution of wild barley populations through the seven barley chromosomes of the studied landraces (Poets, Fang et al. 2015). A pattern of shared ancestry shaped by geography and human migrations is in contrast with one defined centre of origin (Fig. 1.5) (Poets, Fang et al. 2015, Pankin, Altmüller et al. 2018).

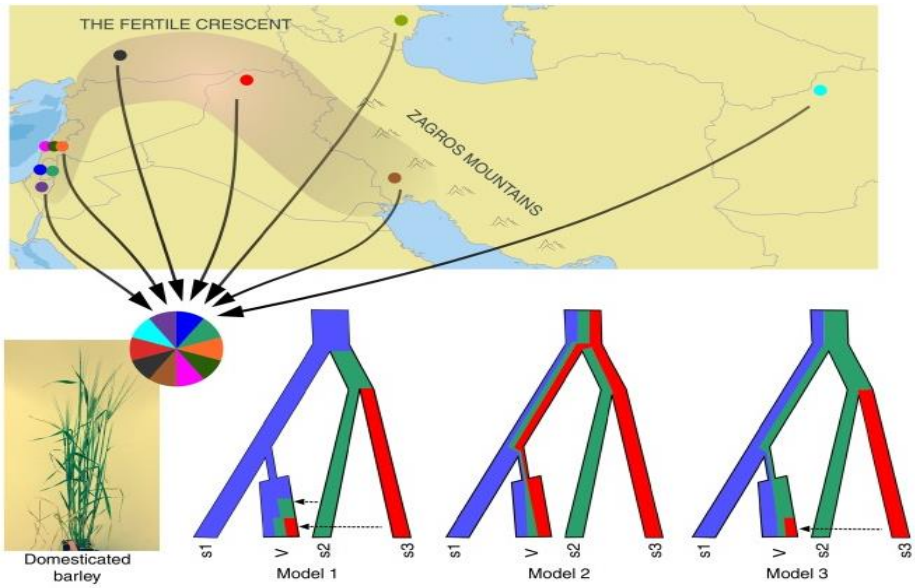

Fig. 1.5 Location of ancestral barley populations and different demographic models to explain barley domestication. Coloured dots on the map enlighten the positions of the wild populations. The pie chart is a schematic representation of the different genetic material of modern barely cultivar. The tree charts are simplified versions of the demographic models considering a single variety giving rise at domesticated *H. vulgare* genomes (V). In Model 1 the modern barley genomic pattern could have originated from introgression of wild genetic material (s2 and s3). In Model 2 it could have been inherited directly from the founder line. Finally Model 3 is a combination of the other two models (Pankin and von Korff 2017).

The separated origins of the tough rachis trait in barley and the mosaic pattern of the domesticated barley genome from different wild varieties, suggest that barley domestication occurred slowly across different regions.

In a recent work of Pankin et al (2018) further evidence for a polyphyletic origin model was reported; 344 wild barley accessions from the Fertile Crescent and 89 domesticated accessions were genotyped with a genome wide enrichment assay comprehensive of 544 000 SNPs (Pankin, Altmüller et al. 2018). Multiple domestication sweep regions were characterized on the whole genome. Domestication candidate genes in these regions were identified, influencing different aspect of plant physiology and development (i.e. shade avoidance, circadian clock and carbohydrate metabolism. Authors propose multiple domestication events may have occurred between the Levantine and Zagros areas with a continuous gene flow between domesticated and wild forms, which hindered genome-wide signature of independent domestication (Mascher, Schuenemann et al. 2016, Pankin, Altmüller et al. 2018). The identification of a third non brittle rachis mutation seems to confirm this hypothesis (Civáň and Brown 2017).

Ongoing research is expected to provide a better understanding of the complex ancestry of barley and unlock the genetic potential of wild relatives through the identification of adaptation and domestication genes and alleles to be used in breeding (Schmid, Kilian et al. 2018).

1.3 BARLEY PLANT ARCHITECTURE

Mature barley seeds contain an organized embryo divided in different regions with specific characteristics and functions (MacLeod and Palmer 1966). The scutellum mediates the release of hydrolytic enzymes and the nutrient transfer from the endosperm to the growing plant through the germination. Scutellum is a characteristic organ of cereal plants (Rudall, Stuppy et al. 2005). The radicle and root apical meristem (RAM) are enveloped into the coleorhiza. The epicotyl including the shoot apical meristem (SAM) and leaf primordia is protected by the coleoptile. The hypocotyl is the region between the epicotyl and the radicle area.

The structure of a barley plant can be considered as the result of the iterative repetition of a basic module known as the phytomer (Fig. 1.6).

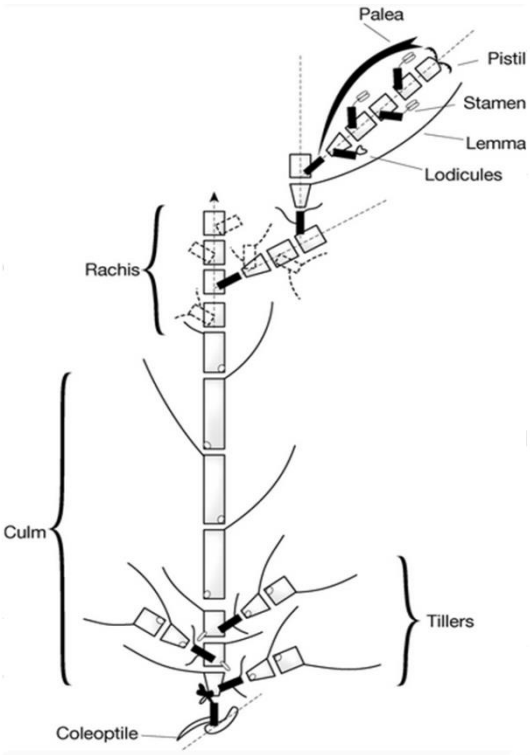

Fig. 1.6 Phytomer organization in barley (Forster, Franckowiak et al. 2007).

The classical vegetative phytomer is composed of distinct units: a node, an internode, a leaf and an axillary bud (Fig. 1.7) (Forster, Franckowiak et al. 2007).

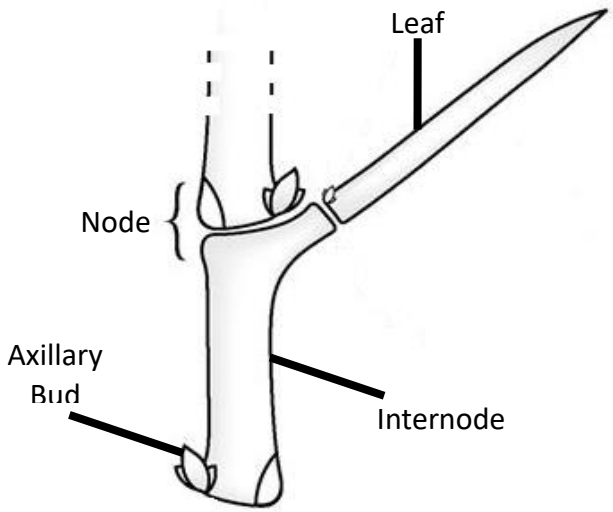

Fig. 1.7 Phytomer units (modified from Forster et al. 2007).

These modules are repetitively initiated by the SAM, progressively building the plant body. Barley seed germination involves the development of a coleoptile, from which the first leaf emerges, and seminal roots (Briggs 1978). If the seed is sown at an appropriate depth, the coleoptile grows until reaching the soil surface, while, if sown too deep, a "rhizomatous stem" develops just above the coleoptile which may produce several internodes with adventitious roots on the nodes (Briggs 1978). After emergence, leaves grow rolled up in the cylinder formed by the elder leaf sheaths - this structure is known as "pseudostem". Then the final part of the stem proximal to the soil surface starts growing producing the crown with adventitious roots (Fig. 1.8).

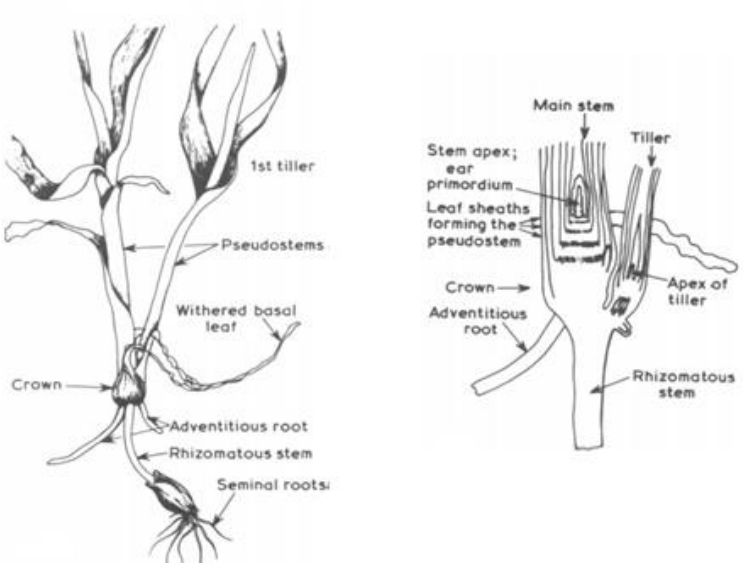

Fig 1.8 Seedling of barley, showing the position and shape of the organs during the first developmental stages (Briggs 1978)

Adventitious buds originate from the crown forming the main stem and the tillers.

During the jointing stage the stem (culm) starts to rapidly grow and differentiate a series of (between 5 and 8) cylindrical internodes hollow inside (medullar cavity). Each internode is separated from the others at the nodes by transverse septa (Briggs 1978).Nodes maintain a solid structure and represent the point of leaf insertion on the stem. Internodes become hollow while elongating due to the collapsing of the parenchymatic tissues producing the medullar cavity. On average the basal internodes are shorter and in many varieties each internode is longer than the one below. When the stems have almost reached their maximum extension, the root system can be considered fully developed. The canopy is usually composed of the main stem, a variable number of tillers depending on the genotype and the environment.

Internodes are delimited by silicified epidermis. On the stem surface, vertical stripes of photosynthetic tissue are alternated with sclerenchymatous fibres composed by lignified cells, located between the epidermis and the phloem. At the base of the internode the sclerenchymatous fibres are less developed.

During the growth of the leaf, the meristematic region from which it originatees divides: one side will produce the leaf sheath, while the other the leaf blade. Where the blade meets the sheath, two auricles grow as lateral colourless protrusions. Just above this area a short projection of epidermal tissue originates, the ligule.

The last apical leaf below the ear is called flag leaf and it has a critical effect on the development of grains.

The ear is organized around a central axis called rachis with a variable number of nodes, from 20 to 30. Each node carries three spikelets each containing a single floret. In two rowed barley varieties, only central spikelets are fertile while the laterals are sterile (von Bothmer and Komatsuda 2011). In contrast, in six rowed barley, all the spikelets are fertile (Fig. 1.9).

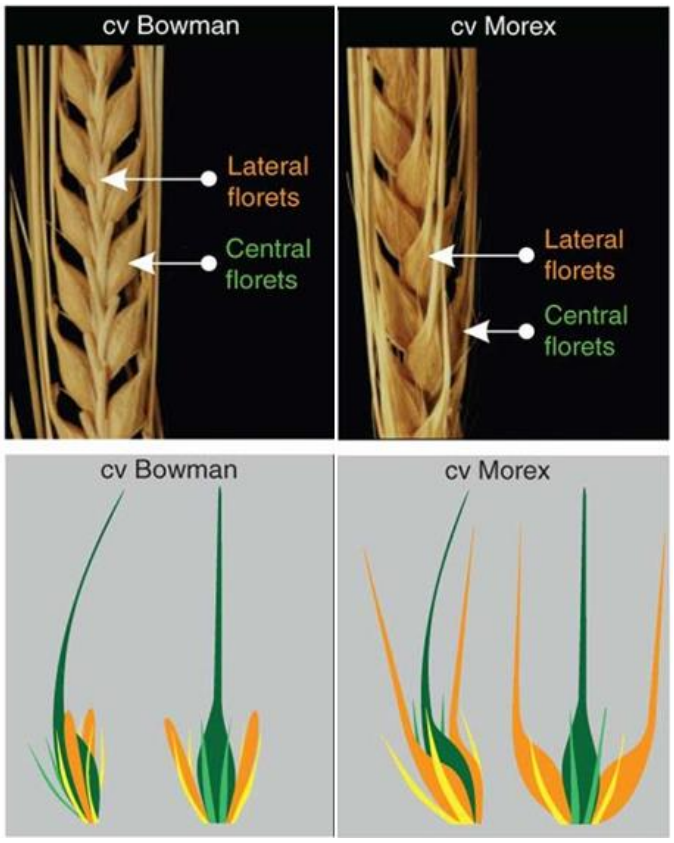

Fig. 1.9 Photographs of mature, dried barley inflorescences (lateral view) of the two-rowed cultivar Bowman and the six-rowed cultivar Morex at right, showing the lateral grain phenotypes that result from differential lateral floret development (Ramsay, Comadran et al. 2011).

Row-type is controlled by known genes with pleiotropic effects, for example two rowed varieties have a higher tillering capacity and heavier seeds compared with the six row types (Ramsay, Comadran et al. 2011, von Bothmer and Komatsuda 2011).

1.4 PHENOLOGY

Barley development can be divided into six growing phases, characterized by several stages. All these stages are described by the Zadoks scale and defined by a two digit number (Zadoks, Chang et al. 1974). The decimal code developed by Zadoks, Chang and Konzak is widely used all around the world by scientist and breeders. This two-digit code refers to a particular growing stage of the plant defined by specific morphological/developmental features. These features are not exclusive so a plant may be described in terms of the number of tillers elongating or in ear emergence by different Zadoks stages(Fig7) (Zadoks, Chang et al. 1974). The first digits refers to the principal growth stages (Fig 1.10).

1-digit code	Description
0	Germination
1	Seedling growth
2	Tillering
3	Stem elongation
4	Booting
5	Inflorescence emergence
6	Anthesis
7	Milk development
8	Dough development
9	Ripening

Fig 1.10 A decimal code for the principal growth stages of small cereals (Zadoks, Chang et al. 1974).

In order to classify in detail the plant development a second digit is introduced in the Zadoks scale, coded from 0 to 9, for each principal growth stage (Fig. 1.11) (Zadoks, Chang et al. 1974).

2-digit code	General description
	Germination
00	Dry seed
01	Start of imbibition
02	—
03	Imbibition complete
04	—
05	Radicle emerged from caryopsis
06	—
07	Coleoptile emerged from caryopsis
08	—
09	Leaf just at coleoptile tip
	Seedling growth
10	First leaf through coleoptile
11	First leaf unfolded*
12	2 leaves unfolded
13	3 leaves unfolded
14	4 leaves unfolded
15	5 leaves unfolded
16	6 leaves unfolded
17	7 leaves unfolded
18	8 leaves unfolded
19	9 or more leaves unfolded
	Tillering
20	Main shoot only
21	Main shoot and 1 tiller
22	Main shoot and 2 tillers
23	Main shoot and 3 tillers
24	Main shoot and 4 tillers
25	Main shoot and 5 tillers
26	Main shoot and 6 tillers
27	Main shoot and 7 tillers
28	Main shoot and 8 tillers
29	Main shoot and 9 or more tillers

Fig 1.11 An example of a two-digit Zacoks scale for growth stages. Is it possible to notice how Zadoks stage are not exclusive and that a certain biological moment in a plant's life can be described by more Zadoks stages depending on which organ development we want to focus on; for instance a given plant could be described by both Zadoks stages 13 (3 leaves unfolded) and 22 (main shoot emerged plus 2 tillers).

Zadoks scale is mainly focused on the above ground plant's organs, because it was thought to be used in field and green house conditions as a collating standard for cereal development.

Germination is the first phase and it starts with the emergence of the coleorhiza from the base of the grain, from which the main root will develop, and of the first plume, enveloped into the coleoptile (Zadoks stage 05-07). Next, the first seminal roots emerge and the coleoptile makes its way up to the soil surface. The tillering phase starts with the growth of the tillers (Zadoks stage 20), side branches that develop from lateral meristems located at leaf axils (axillary meristems, AXMs). For the varieties sown in autumn, tillering starts at the beginning of winter, it stops during the winter and starts again in spring. As for wheat, also in barley there are winter varieties, which have a certain cold requirement before flowering (vernalization period) and should be sown at the beginning of winter, and spring varieties that can be sown before the winter as in spring.
Tiller production is affected by genetic, environmental and agronomical factors. In cultivated barley, tillering ceases definitively during the shift between vegetative and reproductive period (which occurs for the winter varieties only if the vernalization requirement is satisfied). Upon transition of the shoot apical meristem from a vegetative to a reproductive identity (inflorescence meristem), the stem elongation phase begins in which the internodes rapidly grow (Zadoks stage 30). It starts when temperature starts rising and finishes at the booting stage, which is when the ear reaches the flag leaf and is completely enveloped by it. The next phase is the ear emergence, with the ear emerging from the flag leaf and the first spikelets of the ear just visible (Zadoks stage 49). Flowering phase starts approximately 5-6 days after ear emergence starting from the spikelets in the middle of the ear and proceeding acropetally and basipetally along the rachis. Seed ripening starts following pollination of the florets, kernels start to accumulate resources and the embryo develops (Zadoks stage 70). Ripening can be further divided into 4 phases:

1. Milk ripe stage: the kernels start to fill with a milky liquid.
2. Dough ripe stage: as grain filling continues, water is progressively lost so seeds start getting hardened and their colour starts turning from green to yellow.
3. Full ripe stage: nutrient storage stops but not the water loss. The colour of the seeds is yellow.
4. Death ripe: kernel moisture decrease down to 12-15%, optimal for harvest. Sometimes harvest can be done with higher moisture concentration in order to avoid grain loss.

1.5 BARLEY AS A MODEL PLANT FOR GENETIC STUDIES

For its diploid genome and autogamous reproduction, barley is a recognized model for genetic and genomic studies in the Triticeae tribe, which includes other important polyploid crops such as bread and durum wheats and rye . The haploid barley genome has an estimated size of 5300 mln

bp partitioned in 7 pairs of chromosomes, numbered from 1H to 7H (Blattner 2018), and was recently sequenced (Mascher, Gundlach et al. 2017). Barley has a great genetic variability originated from thousands of years of evolution in different environmental conditions. After the domestication occurred part of its genetic variability was lost due to the strong selection imposed by farmers and breeders trying to improve certain traits directly or indirectly related to yield, reducing the genetic pool from which most of the modern cultivars were bred (Martin, Blake et al. 1991).

1.6 GENOMIC TOOLS, MARKER PLAFORMS AND GENETIC MAPS

Barley researchers have developed an increasing range of genomic resources and tools supporting genetic analyses and breeding efforts.

Before the advent of whole genome sequencing approaches, large collections of expressed-sequence-tags (ESTs) were produced starting from the 1990s. ESTs are sequences 500-800 nucleotides of length, produced from a single sequencing run on cDNA clones. Beside representing a source of information about expressed transcripts, ESTs obtained from different varieties can be compared to identify gene-based Single Nucleotide Polymorphysms (SNPs) for mapping and diversity studies. Barley contigs assembled from overlapping ESTs sequences can be found in the HarvEST database (http://harvest.ucr.edu/). Close et al. identified approximately 22 thousand SNPs from barley ESTs and PCR amplicons (Close, Bhat et al. 2009). After filtering, 3.072 high confidence SNPs were select and integrated into two Illumina Golden Gate oligonucleotide pool assays (Fan, Gunderson et al. 2006) named BOPA1 and BOPA2, each consisting of 1536 SNPs. These two panels have been used to build a consensus map of 2.934 SNP loci on four barley mapping populations (Close, Bhat et al. 2009).

Further analysis of RNA sequencing-based polymorphisms of ten barley varieties allowed Comadran et al. to design an Illumina 9k SNP chip including also part of the SNPs developed by Close at al. (Close, Bhat et al. 2009, Comadran, Kilian et al. 2012). This panel included 7.864 SNPs and was used to genotype 360 barley recombinant inbred lines (RILs) produced crossing Barke x Morex to build a robust genetic framework map of 3.973 ordered markers, which was also used to assist the construction of a robust physical map based on ordering of BAC clones (Comadran, Kilian et al. 2012).

A further refined map was published by Mascher et al. in 2013, the POPSEQ barley genetic map (Mascher, Muehlbauer et al. 2013): SNP detection was performed by whole exome sequencing of 90 accessions from the RILs population characterized by Comadran et al. plus 82 double haploid

(DH) lines from the Oregon Wolfe Barley collection (OWB). Sequencing data were anchored to the barley physical map and used for building a genome annotation. POPSEQ map was built through segregation analysis in order to arrange sequence contigs on the target genome along with integration with already existing SNPs array map built on the same population (Comadran, Kilian et al. 2012). Gene annotation, genomic sequences, physical and genetic map are available at the MIPS barley genome database (http://mips.helmholtz-muenchen.de/plant/barley/).Comparative genomic analyses between barley and model cereals such as rice, Brachypodium and sorghum were of paramount importance to evaluate the level of synteny and transfer knowledge across species. Results from these efforts helped to estimate the number of barley genes, approximately 32.000, and ordering 86% of these pseudo-gene along the barley chromosomes (Mayer, Martis et al. 2011).

Another important resource is the Barley IPK genome database (http://webblast.ipk-gatersleben.de/barley/) which was developed by IPK to allow similarity searches against several barley databases, e.g. the POPSEQ map or the reference genome sequence (Mayer, Waugh et al. 2012, Mascher, Muehlbauer et al. 2013).

In the last years advances in DNA sequencing techniques and in bioinformatics made it possible for barley researchers to handle and work with large amount of data; Mascher at al. produced a platform able to capture through hybridization genomic coding sequences (Mascher, Richmond et al. 2013). This platform was designed from the coding portion of the genome (exomes), reducing the complexity of downstream analyses while allowing the detection of gene related sequence variants of potential functional importance.

In 2017, after publication of a new assembly of the barley genome with accurate gene annotation, a new marker panel 50k Illumina Infinium iSelect for barley was developed (see material and method chapter)(Mascher, Gundlach et al. 2017).

1.7 MAP-BASED APPROACHES FOR GENE IDENTIFICATION

The identification and functional characterization of genes is one of the core objectives of genetic studies in crops in order to not only increase our understanding in plant biology, but also to provide information for breeding new crop varieties that better suit human needs. Forward genetics –mutagenesis and comparison between mutant and wild type- has been the primary approach to investigate gene function. During the past decades, large mutant collection were accumulated offering powerful resources to identify and isolate genes though segregation analyses. Research on barley mutants begun in 1928 with Lewis Stadler. He showed that

treatment with ionizing radiations increase the occurrence of mutations that are also inherited by the offspring (Stadler 1928). Since then, barley scientists started to create, improve and characterize mutant collections composed of thousands of accessions (Druka, Franckowiak et al. 2011). The NordGen genebank in Sweden hosts one of the most important collections of barley mutants counting more than 10.000 different mutants for many traits (http://www.nordgen.org/).
Positional cloning relies on fine mapping using segregating populations and molecular markers to identify the genomic region harbouring the studied locus (Jander, Norris et al. 2002). Two flaking markers in tight linkage with the target locus should be identified and anchored to the genome sequence to discriminate the corresponding genomic interval. Gene annotation is important to identify candidate genes contained in this genome segment (Tanksley, Ganal et al. 1995). In barley, this approach was successfully applied to clone the causative genes for several morphological mutants, e.g. the meristem regulatory gene *Hooded/Bkn3* (Müller, Romano et al. 1995); *uzu* and *slender1* for plant height (Chandler, Marion-Poll et al. 2002, Chono, Honda et al. 2003); *six-rowed spike*1 and 4 for row type (Komatsuda, Pourkheirandish et al. 2007, Koppolu, Anwar et al. 2013); *Cly*1 for cleistogamy (Nair, Wang et al. 2010); NAKED CARYOPSIS for hull adhesion (Taketa, Amano et al. 2008); *Cul4* for tillering (Tavakol et al., 2015).
In this context, a milestone is represented by the work of Druka et al. (Druka, Franckowiak et al. 2011), where 979 introgression lines (ILs) of barley were obtained through backcrossing hundreds of mutant alleles with the Bowman variety. Genotyping of these lines with 3.072 SNPs allowed anchoring of the respective mutant loci to chromosomal positions on the barley genome (Close, Bhat et al. 2009, Druka, Franckowiak et al. 2011).
While forward genetic studies based on mutant analysis have greatly contributed to gene identification, different and complementary approaches are needed to investigate natural variation for traits defined as continuous variables and often regulated by many genes with additive effect, i.e. quantitative trait loci (QTL). Two strategies have mainly been used for this purpose: biparental QTL mapping and association studies (aka genome wide association studies, GWAS) (Mackay, Stone et al. 2009).
The first step in QTL mapping involves the development of a segregating population through crossing of two parental lines contrasting for the traits under study. The resulting progeny is then genotyped and phenotyped in different years/environments and statistical analyses allow to find markers strongly associated with the trait under investigation. In its basic form, QTL mapping relies on the simple interval mapping (SIM) method which tests a model for the presence of a QTL

at many positions between two marker loci, producing an estimate of the position of the QTL in the interval between the linked markers (Lander and Botstein 1989). Improvements in the methodology were made through the years to incorporate normal and non-normal distribution phenotypic data, considering also the effect of different cofactors that can influence the analysis. Genome wide association studies (GWAS) aim at identifying marker-trait associations with the natural populations of unrelated individuals(Huang and Han 2014). This approach differs from QTL mapping approach in two ways: 1) traditional mapping approaches study populations originated from a single cross between two individuals, and consequently deals with a restricted amount of genetic variation; 2) in QTL mapping the number of recombination events is limited to those occurring in 1 or few crossing generations affecting the resolution of the analysis. Relying on natural populations, where each individual/variety has a specific genetic history, GWAS explores a potentially high number of historical recombination events, thus increasing mapping resolution, as well as dealing with a wider pool of genetic variation.

The rationale behind GWAS is the use of linkage disequilibrium (LD) to identify associations between markers and causative loci for the trait of interest. In a population where mating occurrence and allele segregation are completely random, the frequency of a haplotype is equal to the product of each allele frequencies in every locus taken in account. This is the case of a hypothetical population in linkage equilibrium (Fig 1.12). However, several phenomena (migration, recombination, genetic drift, mating system, mutation, environmental causes, selection and linkage) act on allele segregation and mating, producing different levels of linkage disequilibrium (Fig. 1.13). Practically, the association between two markers/genes is not random (Lewontin 1964).

Fig. 1.122 Schematic representation of the state of linkage disequilibrium. Left: locus 1 and 2 are in linkage equilibrium; Right: locus 1 and 2 are in total linkage disequilibrium.

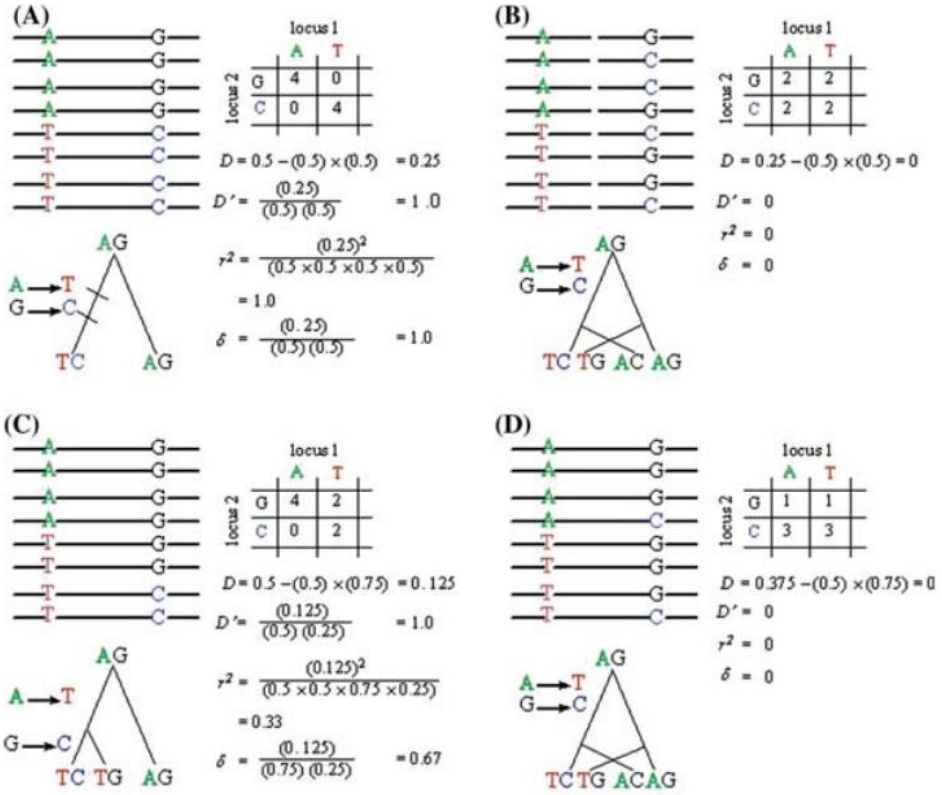

Fig 1.13 diagram representing linkage disequilibrium (LD) between two SNPs showing behaviour of D, D' and r^2statistics: (A) No recombination (mutations at two linked loci not separated in time); (B) Independent assortment (mutations at two loci separated in time); (C) No recombination (only mutations separated in time); (D) Low recombination (mutations at two loci separated in time)(Gupta, Rustgi et al. 2005).

LD can be evaluated with different methods but those mainly used are the D value, D' value and the r^2.

The D value follows the formula:

$$D = p(AB) - p(A) * p(B)$$

Where p(AB) is the frequency of gametes with allele A and allele B in the respective loci, while p(A) and p(B) are the frequencies of the alleles A and B. Assuming that allele A occurs with a frequency equal to p(A) at one given locus, while at a different locus allele B occurs with a frequency equal to p(B) and let p(AB) be the frequency of alleles A and B occur together in the same gamete, D represents the difference between the observed gametic frequencies of haplotypes (first term of the formula) and the Hardy-Weinberg gametic frequency of the same haplotype (second term of the formula).

The association between A and B should be regarded as random (independence) when the presence of one allele does not influence the presence of the other; in that case the probability of

A and B occurring together is given by p(A)*p(B). Thus, in this particular case p(AB)=p(A)*p(B), consequently D=0 and so it is said that alleles A and B are in linkage equilibrium. When D≠0 instead, the frequency of occurrence of the two alleles is not independent and they are in linkage disequilibrium. Since the D value is not always suited to describe the linkage disequilibrium because it is based on the frequencies of the two alleles, comparison between different allelic pairs is not always feasible. D' is the normalized value of D suggested as a correction by Lewontin and obtained by the following formula(Lewontin 1964):

$$D' = D/D_{max}$$

Where

$$D_{max} \begin{cases} max[pA * pB, pa * pb] \; when \; D < 0 \\ min[pA * pb, pB * pa] \; when \; D < 0 \end{cases}$$

Where *a* is equal to (1-pA) and expresses the frequency of occurrence of the alternative allele to A at the same locus and *b* is equal to (1-pB)and represents the frequency of occurrence of the allele alternative to B at the same locus, considering both loci as dimorphic.
An alternative to D' is the r^2 correlation coefficient between couples of loci, which follows the formula:

$$r^2 = \frac{D}{\sqrt{pA * pa * pB * pb}}$$

r^2 expresses mutation and recombination history in the population. r^2 can also be used to indicate how marker in a specific locus is correlated with a QTL of interest, and is thus often used in genetic studies (Abdallah, Goffinet et al. 2003). Values of 0.1/0.2 are regarded as the minimum significance association threshold for r^2 between pairs of loci (Fig.22) (Zhu, Gore et al. 2008).

It is important to note a significant difference between LD and linkage. Linkage represents the physical link between two loci on a chromosome as manifested from the tendency of correlated inheritance between the two; instead LD represents the correlation between alleles within a population (Flint-Garcia, Thornsberry et al. 2003). Thus, LD is not only related to the physical position on a chromosome: while two alleles at linked loci may have a high LD value, it is also possible to find alleles with elevated LD value for unlinked loci, in some cases even on different chromosomes (Flint-Garcia, Thornsberry et al. 2003).

LD extent is influenced by different factors; here we will examine the most important for genomic studies on barley.

- Mating highly affects LD (Myles, Peiffer et al. 2009). In self crossing species such as barley, rice and wheat, the occurrence of effective recombination is reduced because of high homozygosity (Nordborg 2000, Garris, Tai et al. 2005, Zhang, Bai et al. 2010) with an increase of LD extent if compared to out-crossing species as corn, rye and grapevine (Tenaillon, Sawkins et al. 2001, Myles, Peiffer et al. 2009, Li, Haseneyer et al. 2011).
- History of recombination events and genetic heterogeneity in the population under study are other factors influencing the extent of LD. Higher recombination rate and genetic variability reduce the LD extent. In corn, as in other out-crossing species, the population composition influences LD varying from 1kb in landraces, to almost 2kb in inbred collections reaching up several hundred kb in commercial cultivars(Jung, Ching et al. 2004) .
- Selection (human or naturally driven) increases the LD affecting not just the locus under selection but also adjacent regions (genetic hitchhiking). Complex situations with different genomic regions under LD can be noticed in cultivars around those areas harbouring genes affecting domestication traits or other important agronomical traits (Lewontin 1964, Slatkin 2008).
- Genetic drift may remove variability from the available genetic pool, thus increasing the LD extent (Flint-Garcia, Thornsberry et al. 2003).
- Presence of subdivisions and clustering (population structure) within the population due to relatedness has a dramatic effect on LD especially among loci that are not physically linked. Population structure is determined by characteristic allelic frequencies with different historical origins among linked or unlinked loci (Slatkin 2008).

Maize as an out crossing species has a short LD decay rate: analysis of a global collection of 632 inbred lines from different breeding programs based on 1,229 SNP markers across 582 loci showed that LD extent varied from 1 to 10 kb among chromosomes (Yan, Shah et al. 2009).
By contrast, rice and wheat, both selfing species, have a LD decay that extends for longer distances. Mather et al. (2007) studied different rice populations reporting that LD decay for temperate japonica, tropical japonica and indica is about 500 kb, 150 kb and 75 kb respectively (Mather, Caicedo et al. 2007).

Barley LD condition is similar: Zhou et al.(2012) studied the extent of the LD decay in a population of 3840 cultivars genotyped with 3072 SNPs. The software STRUCTURE identified nine subpopulations and LD decay was estimated ranging from 4.0 to 19.8 cM (Zhou, Muehlbauer et al. 2012). In a more recent work, Bengtsson and colleagues genotyped 180 Nordic barley breeding lines with 48 SSR and 7842 SNPs (9k iSelect) markers. The total LD decay was spanning between 0 and 4 cM across all the population (Bengtsson, Åhman et al. 2017).

1.7.1 ASSOCIATION MAPPING AND GWAS

One of the main applications of LD is association mapping where large natural populations are genotyped and phenotyped in order to identify significant associations between genetic variants and phenotypic traits (Fig. 1.14)(Rafalski 2010).

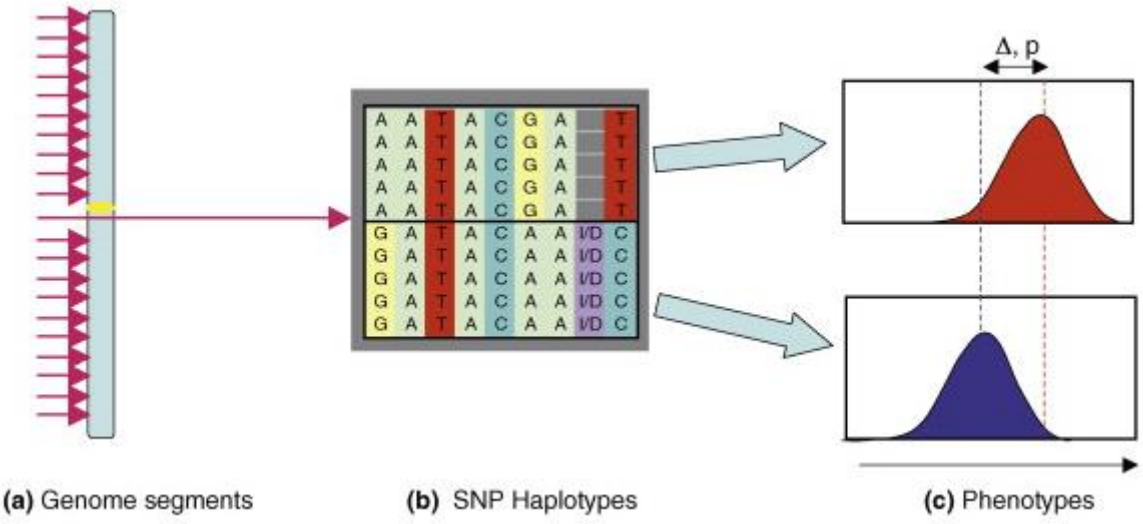

Fig. 1.14 Association mapping rationale: (a) A panel of individuals with different genotypes is analysed for genomic variants at different loci distributed across the genome; (b) the individuals are divided in clusters with common haplotype or individual marker variant in every locus studied; (c) Phenotypic scores distribution for each haplotypes/variants are tested in order to identify significant association between the marker and the trait (Rafalski 2010).

Association mapping was first used in case-control studies to identify alleles influencing human hereditary diseases, comparing the frequencies of different alleles between a group of unrelated people showing the disease (case) and another group of unrelated non-affected people of the same size (control)(Abdurakhmonov and Abdukarimov 2008).

Different tests could be used to identify significant association of one or more alleles and the occurrence of a disease, depending on several parameters as the number of observations, number of replicates and factors influencing the individuals; the most used are Fisher's exact test, The Pearson chi-square test and Yates continuity correction (Ohashi, Yamamoto et al. 2001, Schulze and McMahon 2002).

For traits that are not categorical but quantitative, as plant height or leaf length, different tests are used to assess the significant allele frequency variation associated with the distribution of phenotypic measurements (Fig.1.14). Analysis of variance (ANOVA) or linear regression (or general linear model, GLM) could assess if different haplotypes have an effect on phenotypic variation (Fig. 1.15)(Balding 2006).

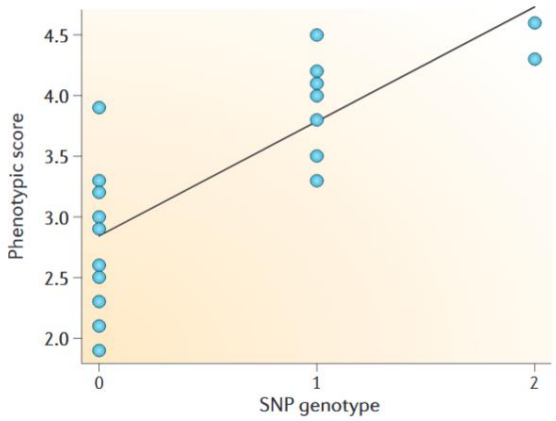

Fig. 1.153 Example of GLM for a single SNP with two alleles and three genotypes (aa/Aa/AA). Blue dots represent the individuals considered for this analysis. On the Y axes the range of phenotypic values, while on the X axes the different genotypes at the tested markers. Genotypes are considered like different levels of the same treatment. Distribution of the individual's phenotypic scores for each genotype should be normally distributed and with a non-significantly different variance, in order to not violate the model assumptions (Balding 2006).

The GLM model follows the linear equation

$$y = ax + b$$

where y, the dependent variable, is the phenotype value, x is the non-dependent variable which corresponds to the genetic marker with number of levels equal to the number of genotypes for each marker, a is the regression coefficient and b the intercept.

A genome wide association study (GWAS) can be seen as a series association study that can be a chi-square test (for categorical data as case-control study) or a regression model (e.g. GLM for continuous traits). Basically, a GWAS study is like performing a number of regression analyses (or chi-square tests) equal to the number of markers where the dependent variable Y is the phenotypic data and the independent variable X are the genotypic variants. Covariates can be added to correct for particular confounding factors (i.e. unequal related among the accessions). The basic approach of a GWAS study can be summarized as in Fig. 1.16.

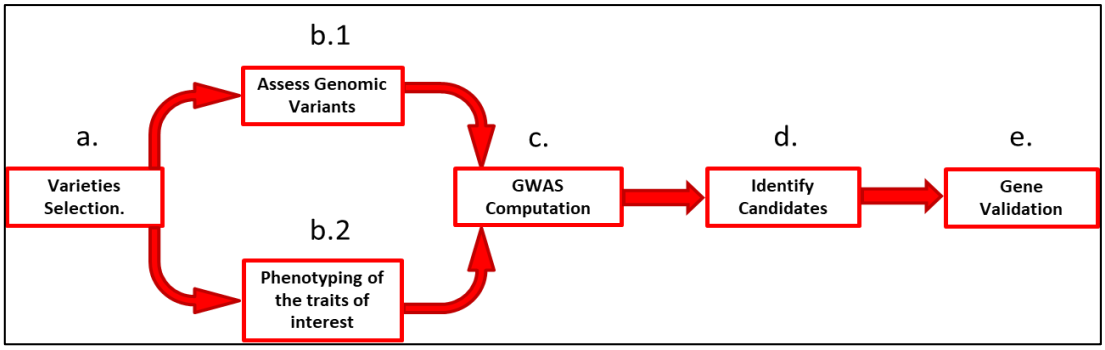

Fig. 1.16. General GWAS workflow. a. Identify a panel of varieties that fit the research objectives; b.1. Collect genotypic data on the population identifying a large set of molecular markers with an appropriate density and avoiding ascertainment bias; b.2. Collect phenotypic data on the population, preferably replicated over different environments/years; c. Identify significant marker-trait associations with proper models; d. Search the identified QTL regions for the most likely genes (candidate gene, CG); e. Validate the function of the candidate genes through a range of techniques, e.g. TILLING, genome editing, expression analyses etc.

The success of GWAS depends on several elements. First of all the composition of the population panel is a critical factor (Flint-Garcia, Thornsberry et al. 2003, Breseghello and Sorrells 2006, Yu, Pressoir et al. 2006); choosing varieties that are too closely related will reduce the genetic variation and consequently decrease the resolution of the analysis resulting in non informative results; on the other hand, choosing accessions that have a too divergent history can complicate the analysis for example because of sub-structuration of the population that needs to be adequately accounted for to minimize false positive associations. The selection of the accessions for the panel should be a fine balance between these two extreme situations. Usually plant populations used in GWAS are composed of breeding varieties, landraces or wild relatives, these collections experienced many recombination events increasing the genetic diversity if compared with a QTL mapping biparental population (Fig. 1.17).

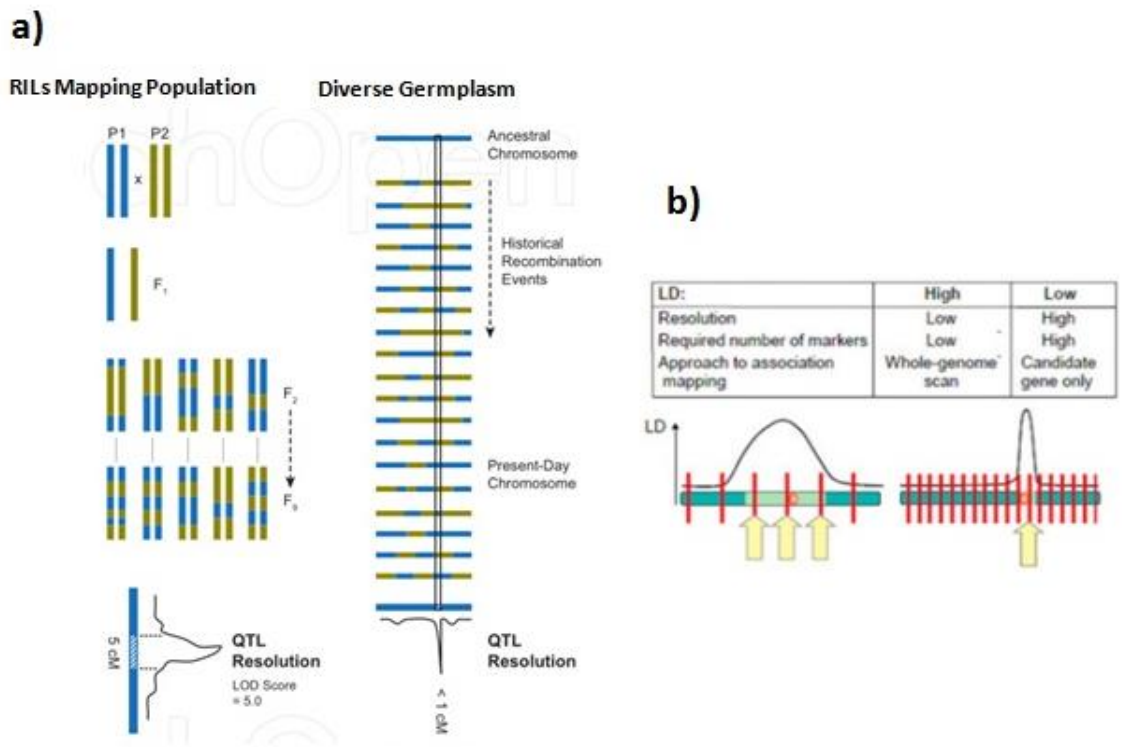

Fig. 1.17 a) Comparison of mapping resolution between biparental QTL mapping (left) and GWAS (right). RIL mapping population shows a low QTL resolution due to the few recombination events accumulated, while the GWAS panel affords a high QTL resolution due to the diverse genetic history of germplasm (Soto-Cerda and Cloutier 2012). b)Implications of high and low LD for mapping resolution.

The number of accessions plays an important role in the analysis in two ways: 1) the more genotypes we include the more chance we have to spot a causative variant even for complex traits, where several genes explain a modest amount of phenotypic variation; 2) the more replicates of these genotypes we include the more reliable phenotypic data we can collect reducing misleading and confounding effects, that by chance could affect the trait we want to study. Clearly, increasing the number of accessions and replicates involves higher investment in phenotyping efforts. Finally, the number of accessions will depend on the resources available, the expertise involved and the aims of the experiment (Abdurakhmonov and Abdukarimov 2008).

The quality of phenotypic data is another critical factor influencing GWAS (Falconer and Mackay 2004). Complex phenotypic traits (e.g. fitness, yield or stress resistance) should be seen as cumulative traits, since they incorporate the effects of other upstream traits (for example the production of a certain enzyme or a particularly thick epidermis); cumulative traits may involve from few to many interactions between genes and between genes and the environment (GxE). In the case of cumulative traits, the choice of upstream or component traits may be more effective, for example yield components such as grain weight and grain number may be more tractable than yield per se.

In parallel to phenotypic data, high quality genome-wide genotypic data are required for the whole germplasm panel. Marker density is a key factor to maximize chances of identifying significant marker-trait associations. While whole genome re-sequencing certainly provides maximum coverage and is widely used in species with small genomes, the costs of such kind of analysis are still too high for species with large and complex genomes such as barley (>5 Gbp) and wheat (17 Gbp) (Bolger, Weisshaar et al. 2014). This is due to two main factors: the amount of repetitive and transposable elements (in barley more than 84% of the genome is composed by mobile or repetitive elements) and the level of ploidy (as in the case of wheat)(Gill, Appels et al. 2004, Gregory, Nicol et al. 2007, Mayer, Waugh et al. 2012).

Viable alternatives to whole genome re-sequencing, are represented by SNP arrays, targeted resequencing for example of exome capture or reduced representation sequencing approaches such as genotyping-by-sequencing(Poland, Brown et al. 2012, Mascher, Richmond et al. 2013, Lowry, Hoban et al. 2017). Depending on the genotyping approach, a smaller or larger proportion of missing data may occur (i.e. lack of information for certain markers in certain samples) potentially causing problems in downstream analyses. To circumvent this problem, dedicated software was created to impute the missing data based on different imputation methods (Halperin and Stephan 2009, Marchini and Howie 2010, van Leeuwen, Kanterakis et al. 2015). More complex approaches such as fast-PHASE (Scheet and Stephens 2006) take advantage of inferred LD from the population. Others use pedigree information in order to impute the missing data, e.g. those implemented in *Beagle* (Browning and Browning 2016). Finally other software needs to be "trained" using a high quality linkage training set as IMPUTE2 (Howie, Fuchsberger et al. 2012). Regardless of all the techniques cited above, it is still possible for the causative variants to be missing in the selected marker panel. In this case, it is still possible to identify the "lost" variant if it is in strong linkage disequilibrium (LD) with other markers represented in the panel.

Each association analysis will produce a P-value, which is the probability of obtaining the specific association just by chance, and is used to identify those associations that significantly influence the trait of interest. Manhattan plots are frequently used for graphical representation of association results (Fig. 1.18).

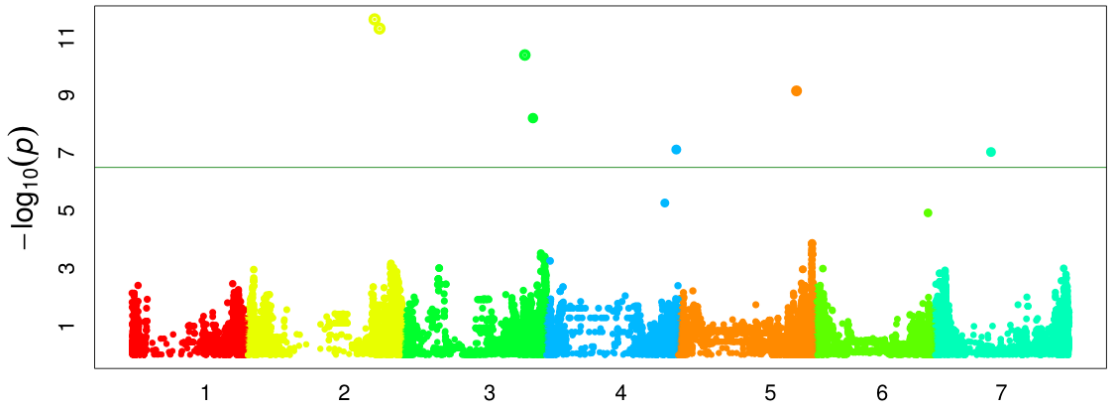

Fig. 1.184 Example of a Manhatthan plot for a certain barley trait. On the Y axis there is the - log_{10} of the P value for each marker included in the analysis; the higher it is the stronger the association between the trait analysed and the marker. While on X axis there is the position of each marker on the genome, the numbers and the different colours are needed to discriminate between the different chromosomes. The red line represent the significant threshold after Bonferroni correction.

In such plots, each dot represents a marker, the Y-axis represents the negative logarithm of marker-trait association p-values, while values along X-axis correspond to the genomic positions of the considered markers. Dots that stand out over the threshold level are significantly associated with the trait studied. Usually in biology the threshold to look at in order to divide significant from non-significant associations is 5% (0.05). However, in the case of genome-wide studies corrections for multiple-hypothesis testing should be introduced: one approach implemented by most GWAS softwares is the Bonferroni correction which adjusts the level of significance based on the number of the statistical tests conducted. This correction is the most conservative since, it ignores the linkage between markers (Johnson, Nelson et al. 2010). An alternative to avoid false positives is to use the false discovery rate (FDR) method. This method estimates the proportion of false positives for a given threshold (usually 0,05), considering that under the null hypothesis we should have a normal distribution of p-values. FDR corrects for the number of expected false positive, producing an estimate of the number of true significant results (Hochberg and Benjamini 1990, van den Oord 2008).

Another correction method, even if extremely computationally demanding, is permutation testing. It produces for a given collection of samples an empirical distribution of test statistics considering the null hypothesis H0 as true by assigning at random the phenotypic value of a variety to another. This technique removes any association between markers and phenotypic data under the null hypothesis. Permutation testing can be done in software such as PLINK (http://zzz.bwh.harvard.edu/plink/) (Purcell, Neale et al. 2007).

Several open source packages have been developed to run GWAS analyses: currently, two of the most widely used packages are TASSEL (http://www.maizegenetics.net/tassel) and FarmCPU (http://www.zzlab.net/FarmCPU/) (Bradbury, Zhang et al. 2007, Liu, Huang et al. 2016). Regardless of the software used, a critical point for the analysis is the reliability of the model to describe the data and produce accurate results. The quantile-quantile plot (QQ plot) can summarize how the model fits the analyzed data comparing the negative $\log_{10}$p-values from the GWAS model versus the expected negative $\log_{10}$p-values under the null hypothesis of no association (Fig. 1.19) (Chen, Wang et al. 2016).

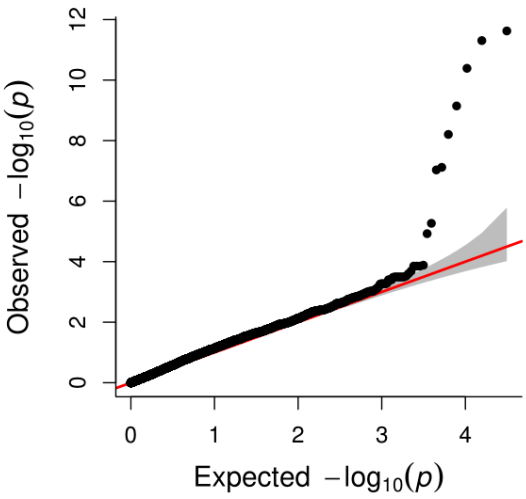

Fig. 1.195.QQ-plot of P-values. On the Y axis are the observed $\log_{10}$P-values and on the X axis are the expected $\log_{10}$P-values under the assumption of no association. The grey area represents the 95% confidence interval under the assumption of no association between the markers and the trait of interest.

If the observed P-values strongly deviate from the expected then the analysis may be flawed by one of several factors. The most common is the structure of the population, which represents the degree of relatedness among the individuals as the presence of specific allele frequencies among groups of kin (Vilhjálmsson and Nordborg 2012). It can originate from non-random mating between individuals due to different geographical origins or breeding selection (Soto-Cerda and Cloutier 2012). Population structure influences the results increasing the number of false positives because if the studied trait covaries with the structure of the population then many non-associated genetic variants will be associated with the phenotype just because of relatedness (Fig. 1.20)(Schulze and McMahon 2002).

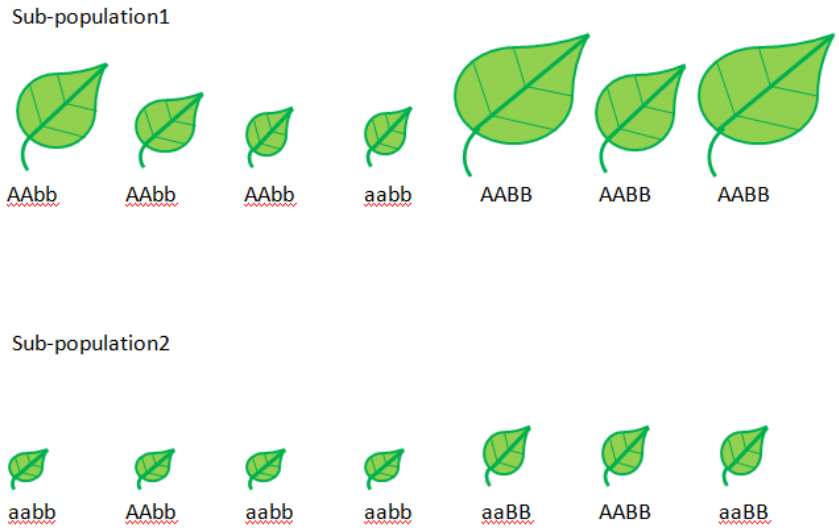

Fig. 1.206 Leaf dimension is larger in subpopulation 1, which has a higher frequency of allele A, so it could be possible to conclude that the locus A/a influence the leaf dimension, even if it is not true. On the other hand, allele frequencies for locus B/b are the same in the two subpopulations and actually in both the presence of B alleles has an effect on leaf size. Due to population structure locus B may be undetected by GWAS if proper correction is not applied.

Recent GWAS software uses mixed linear models (MLM) to correct for this confounding effect (Yu, Pressoir et al. 2006). Even if MLM are computationally demanding they can control for spurious association between markers and phenotype due to population structure incorporating Q and K matrices as cofactors in the general MLM formula (Yu, Pressoir et al. 2006):

$$y = M + Q + K + e$$

Where y is the phenotype, M the molecular marker, Q and K the two matrices and e the residuals. The Qmatrix accounts for the number of subpopulations and can be built with two statistical methods;

- STRUCTURE software (https://web.stanford.edu/group/pritchardlab/structure.html) infers the number of subpopulations and the level of membership of each individual with a Bayesian method based of genotype variants (Pritchard, Stephens et al. 2000). It produces a Q matrix composed of different fixed factors (columns, one for each inferred subpopulation) describing the different level of relatedness for each individual (Hubisz, Falush et al. 2009).
- Principal component analysis (PCA) evaluates the genotypic correlations among individuals in order to find “main axes” of variation within the accession panel (Price, Patterson et al. 2006). In this type of matrix columns represent the axes of variation with the position for each individual along the axes (Ringnér 2008).

Instead, K matrix corrects for non-random association between markers due to co-ancestry among the individuals. K matrix is calculated collating all genotype against each other to produce a k x k table, with k equal to the number of individuals. Each pair wise comparison assigns a kinship coefficient. GWAS software like TASSEL and FarmCPU have implemented algorithms to calculate the K matrix (Bradbury, Zhang et al. 2007, Liu, Huang et al. 2016).

Accounting for population structure is not an easy task, since it is hard to choose which and how many covariates to use in the analysis, especially if considering that adding unneeded covariates may hamper the detection of true associations or increase the false positive rate (Zhang, Wang et al. 2008, Atwell, Huang et al. 2010).

Marker-trait associations provide a starting point to identify genes and allelic variants controlling the trait of interest. To this end, the genomic region around the significant marker(s) is initially explored in order to find potential candidate genes. Accurate gene annotation is important in this step while LD can define the area to screen around the peaks (Abdurakhmonov and Abdukarimov 2008): on this basis, candidate genes can be proposed based on a priori knowledge of the biology underlying the trait studied (Houston, Burton et al. 2015). Expression data, if available, are a powerful tool to identify genes expressed in relevant tissues/stages that are closely located to the GWAS signal. An expression atlas can be crossed with GWAS results in order to identify those candidate genes that most likely have a biological effect on the trait (Jia and Zhao 2014, Schaefer, Michno et al. 2017).

The last step is the validation of the candidate genes, to confirm the effect of the gene on the trait of interest, and it can be performed both with statistical tests or with molecular biology approaches. To reconfirm a CG with statistical methods, a solution could be to rerun the experiment on a different population of the same species or very closely related, since it is very unlikely to find the same results in two different GWAS experiments (Chanock, Manolio et al. 2007, Pease, Haak et al. 2016). However, quantitative traits may greatly vary across different growth conditions and environments implying that results from two different trials may be different. Another way to validate CG s from GWAS is through use of mutant resources, biparental populations or other genetic stocks segregating for allelic variants in the gene of interest. In barley such approaches were successfully deployed to validate CGs from GWAS that control different traits of agronomical interest (Pasam, Sharma et al. 2012, Wang, Jiang et al. 2012).

Finally, the real benchmark to validate a candidate gene relies on the many reverse genetic approaches like RNA interference or CRISPR-Cas9gene editing (Small 2007, Lowder, Zhang et al. 2015)

1.8 PLANT IDEOTYPE

"Ideotype breeding" is a concept introduced by Donald in 1968 as complementary to traditional breeding methods based on yield selection (Donald 1968). Ideotype breeding relies on genetic and physiological knowledge of the plant in order to design a plant model with selected improved characteristics and controlled behaviour for a specific purpose and environment (Martre, Quilot-Turion et al. 2015). Successful application of ideotype breeding has been argued to rely on certain prerequisites including:

1. Knowledge of the interactions and trade-offs among plant features in different climatic conditions;
2. Access to plant collections hosting a consistent level of genetic diversity (mutants and wild varieties);
3. High-throughput phenotyping techniques and tools for precise trait scoring to explore available genetic diversity and accelerate selection (Donald 1968, Tao, Rötter et al. 2016);
4. Availability of genotype sequencing data, reliable and dense genetic marker panels and genome annotation to support the identification of relevant genes and the deployment of the most valuable alleles.

The ideotype model is defined as series of model features relating for example to plant morphology, physiology, agronomical and/or biochemical aspects and affecting in different ways fitness and yield (Kawano, Yamaguchi et al. 1966, Thorne 1966). Breeding by ideotype could be applied to different extent to design dual-purpose crops: plants can produce other useful resources than just grains from lignocellulosic biomass for biofuel production fermentation to forage for grazing (Li, Chaney et al. 2003, Giunta, Motzo et al. 2015, Townsend, Roy et al. 2017). While considering the choice of traits to improve, ideotype design needs to pay due attention to the complex dynamics that regulate plant development and physiology, e.g. organ symmetries and compensation/correlation mechanisms among plant features. This system of proportion and compensation is influenced by the environment but also by pleiotropic effects, epistatic effects and genetic linkage (Chandler and Harding 2013, Rebolledo, Luquet et al. 2013, Nadolska-Orczyk,

Rajchel et al. 2017). To establish good breeding programs diverse ideotypes for different crop/environmental combinations are then needed resulting in a great range of models to evaluate (Rasmusson 1991, Martre, Quilot-Turion et al. 2015).

A unique ideotype for a specific crop variety cannot perform efficiently if it is not designed for a particular environment; changes in climatic conditions affect greatly plant morphology and development. Therefore

ideotype development should also consider the fluctuation of the environment's features where the plants are sown (Rötter, Tao et al. 2015). Crop models do not need necessarily to be developed considering tested environments, they can be designed to fit in environments that were never tested before, studying the climatic context and crop development in other environments, or in an artificial environment (e.g greenhouses) with improved agronomical characteristics (Bucklin, Fowler et al. 2004, Kacira, Giacomelli et al. 2012).

A paradigmatic example of ideotype breeding is offered by the reduction of cereal stature attained by breeders of the Green Revolution: semi-dwarfing alleles were used to breed varieties with shorter culms, which in modern agricultural systems improve the yield gain thanks to enhanced tolerance to nitrogen fertilizer application and lodging resistance (Gooding, Addisu et al. 2012, Xu, Jia et al. 2017). Beside plant height, tillering and leaf morphology are largely investigated by scientists and breeders as they have a strong effect on the mobilization and storage of plant resources (Zhu, Long et al. 2010, Mathan, Bhattacharya et al. 2016, Wang, Smith et al. 2018). These and other morphological traits were the focus of the New Plant Type (NPT) ideotype breeding programme initiated by the International Rice Research Institute (IRRI) in the 1990s (Peng, Khush et al. 2008, Khush 2013). The NPT programme aimed to increase yield potential up to 20-25% compared to Green Revolution semi-dwarf rice cultivars, under a tropical environment during the dry season. The NPT model was designed based on the results of simulation modelling and the selected traits were mostly morphological since they are easier to evaluate than physiological traits in breeding programs (Yang, Peng et al. 2007). To reduce unproductive tillers the proposed rice plant had low tillering capacity (three to four tillers when direct seeded) and enhanced panicle size since primary and early secondary tillers have a significant influence on total grain yield (Peng, Khush et al. 2008). The first NPT lines showed poor yield because of limited biomass production, reduced panicle size and a low grain filling-percentage (the latter probably due to the lack of apical dominance within the panicle and limited number of vascular bundles) (Yang, Peng et al. 2007, Khush 2013). In the second generation of NPT lines, first

generation lines were crossed with elite *indica* varieties to increase tillers and grain production. In 2002/2003 the second generation NPT performed better than first generation NPT in four flooded field experiments (Peng, Laza et al. 2004). Yield increased because of the introgression of *indica* genes that augmented tiller number and grain quality (Khush 2013). The result achieved by the second generation NTP stimulated the Chinese government to launch the "super rice" breeding program, which combined inter-subspecific heterosis and ideotype breeding approaches to further improve rice yield (Wenfu, Zhengjin et al. 2007, Khush 2013, Qian, Guo et al. 2016) . This strategy is largely based on the introduction of male sterile lines which are used to develop hybrid varieties following different methodologies (Qian, Guo et al. 2016).

Compared to the NPT, one of the points of strength of the "super" rice program was the specific quantification of the angles of the 3 uppermost rice leaves: 5° for the flag leaf, 10° for the 2nd and 20° for the 3rd(Peng, Laza et al. 2004, Yuan 2017). In 1998-2005 rice lines from the "super" program were commercialized, producing a yield gain of 6.7 millions of tons compared to local Chinese cultivars (Peng, Khush et al. 2008).

The development of plant ideotypes integrates interdisciplinary skills and competences from agronomy, modelling, ecological statistic, developmental biology, crop physiology, high throughput phenotyping, genomics, genetics and breeding to design and select new cultivars combining the most suitable traits for defined environments (Rasmusson 1991, Tao, Rötter et al. 2016). Experience in rice shows that progress in these different disciplines is key to identify the most promising crop characteristics/genes/alleles to tailor breeding programs to changing climate and agricultural practices (Bergez, Colbach et al. 2010, Dumont, Basso et al. 2015). In the last years, crop modelling in particular showed a great potential in ideotype breeding (Li, Zhu et al. 2012, Rötter, Tao et al. 2015, Gouache, Bogard et al. 2017). In this context "ensemble modelling techniques" can infer through several simulations' models the performance of different crop ideotypes across different environments (Tao, Rötter et al. 2016, Wallach, Mearns et al. 2016). In parallel, high throughput technologies for better and more reliable phenotyping are allowing a more complete examination of cumulative and complex traits (Fiorani and Schurr 2013). Other critical points are the characterization and conservation of wild varieties and landraces as reservoirs of adaptive genetic variation (Tavakol, Bretani et al. 2017, Szareski, Carvalho et al. 2018) and the renewed focus on mutant identification studies to identify genes affecting critical traits.

1.9 LODGING

Lodging is a permanent displacement of the plant from the erect position, and is one of the major constraints affecting cereal production by reducing the crop yield potential and impeding harvest (Berry and Spink 2012, Berry 2013). In a recent query on the choice of cereal varieties for the future climate changes, 410 German farmers and 114 advisors ranked lodging resistance as one of the first 3 traits to consider when choosing cultivars (Macholdt and Honermeier 2016).

Lodging can affect the plant after stem elongation, but the occurrence of lodging after anthesis greatly reduces yield (Piñera-Chavez, Berry et al. 2016). In wheat, Weibel and Pendleton reported the different average levels of yield reduction just after anthesis; 31% reduction at ear emergence, 25% reduction at milk stage, 20% and 12% at soft dough stage and hard dough stage, respectively (Weibel and Pendleton 1964).

There are three type of lodging (Fig.1. 21) (Hirano, Ordonio et al. 2017).

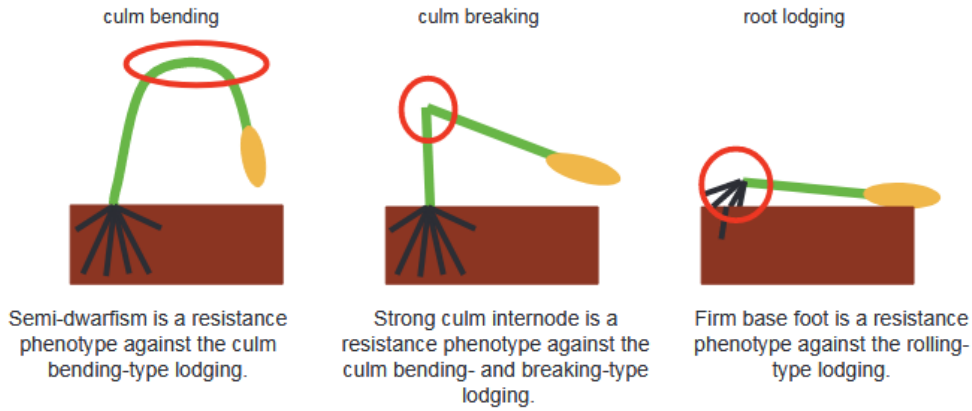

Fig. 1.21 Different types of plant lodging (Hirano, Ordonio et al. 2017).

The first type is the “culm bending”, that happens when plant is not able to withstand the strength exerted by wind, rain and ear weight; usually this occurs in the apical internodes of the hollow stem. Semi-dwarf varieties introduced during the Green Revolution have lower centre of gravity with reduced lodging moment and therefore are less prone to this type of lodging (Fig. 1.22) (Kashiwagi, Hirotsu et al. 2007).

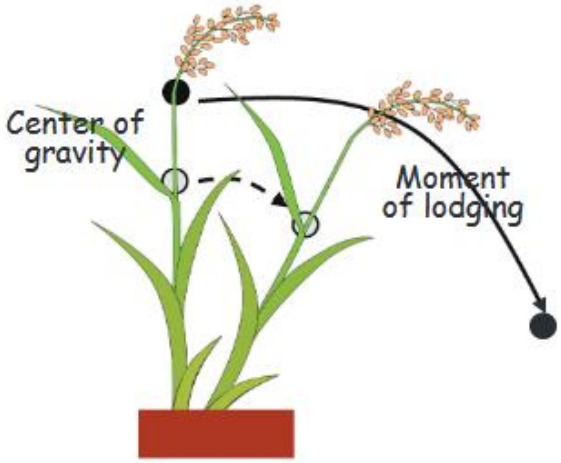

Fig. 1.22 Dynamics of lodging; plants with a lower centre of gravity have a low moment of lodging (Hirano, Ordonio et al. 2017).

The second lodging type is the “culm breaking”, which occurs at the basal internodes; taller plants tolerate less bending on the upper internodes, which exert a greater leverage on the basal internodes producing the failure of the plant (Islam, Peng et al. 2007). The third type is “root lodging” and it happens when roots fail to maintain the plant anchored; it is mainly due to poor soil conditions and agronomical practices, but also the lateral root plate spreading plays a significant role in this process (Berry, Sterling et al. 2004). However it does not affect in a critical way crops like barley, wheat and rice (Watanabe 1997).

In early vegetative stages, lodging has less deleterious effects on plant performance thanks to the plasticity of the stem that can rapidly recover from the flattened position through a process known as kneeing (Berry, Griffin et al. 2000, Berry, Sterling et al. 2004).

In barley it was estimated that lodging can reduce yield from 4 up to 65% (Jedel and Helm 1991, Sameri, Nakamura et al. 2009). When crops lodge, several aspects concur to yield loss: reduced mineral uptake, reduced carbon assimilation which increases tissues respiration and chlorosis, reduction of chlorophyll because of mutual shading between lodged plants; also all these factors promote the spread of pests and diseases (Foulkes, Slafer et al. 2011). Among pest and diseases, fungal infections are particularly deleterious decreasing size, weight and quality of grains (Foulkes, Slafer et al. 2011). In this situation, milling and malting quality are often compromised for wheat and barley respectively (Nakajima, Yoshida et al. 2008, González-Curbelo, Herrera-Herrera et al. 2012).

Plant inclination is one of the first visible lodging effects and a measure of lodging severity; wider inclination angles are correlated with higher yield losses in wheat, oat and barley and inclination of 45° causes a yield reduction of 25-50% compared with an angle of 80° (Berry, Griffin et al. 2000).

Lodging resistance is a complex trait to study since it is affected by several factors as climatic conditions (wind and rain), agronomical practices, topography, diseases and soil type (Berry 2013). Several studies also identified plant morphological features, anatomical characteristics and biochemical composition that are involved in lodging control (Table 1.1).

Trait (s)	Correlation with lodging	Reference(s)
A. Morphological Traits		
Plant height	+	(Verma, Worland et al. 2005)(wheat); (Zeid, Belay et al. 2011)(tef); (Kashiwagi, Sasaki et al. 2005)(rice); (Yao, Ma et al. 2011)(wheat)
Internode length	+	(Huang, Cloutier et al. 2006)(wheat); (Kelbert, Spaner et al. 2004)(wheat); (Sameri, Nakamura et al. 2009)(barley)
Internode diameter	-	(Kashiwagi, Togawa et al. 2008)(rice);(Wang, Zhu et al. 2006)(wheat); (Kaack, Schwarz et al. 2003)(*Miscanthus*);(Ookawa, Hobo et al. 2010)(rice)
Internode wall thickness	-	(Tripathi, Sayre et al. 2003)(wheat); (Wang, Zhu et al. 2006)(wheat); (Peng, Chen et al. 2014)(wheat); (Hai, Guo et al. 2005)(wheat); (Chuanren, Bochu et al. 2004)(rice); (Yao, Ma et al. 2011)(wheat);(Ookawa, Hobo et al. 2010)(rice)
Ear weight	+	(Zuber, Winzeler et al. 1999)(wheat); (Baker, Berry et al. 1998)(wheat); (Tripathi, Sayre et al. 2003)(wheat); (Ma and Yamaji 2006)
Stem weight per unit length	- (increase pushing resistance)	(Kashiwagi, Togawa et al. 2008)(rice); (Yao, Ma et al. 2011)(wheat);(Kong, Liu et al. 2013)(wheat)
B. Anatomical Traits		
Number of vascular bundles	-	(Ishimaru, Togawa et al. 2008)(rice); (Chuanren, Bochu et al. 2004)(rice)
Mechanical tissues (Schlerenchyma layer)	-	(Ishimaru, Togawa et al. 2008)(rice); (Dunn and Briggs 1989)(barley); (Kong, Liu et al. 2013)(wheat)
C. Biochemical Traits		
Lignin concentration	-	(Okuno, Hirano et al. 2014)(rice); (Tanaka, Murata et al. 2003)(rice); (Kong, Liu et al.

		2013)(wheat); (Ma and Yamaji 2006); (Jones, Ennos et al. 2001)(*Arabidopsis*);(Wang, Zhu et al. 2012)(wheat)
Cellulose and hemicellulose concentration	-	(Jones, Ennos et al. 2001)(*Arabidopsis*); (Tanaka, Murata et al. 2003)(rice);(Kong, Liu et al. 2013)(wheat); (Ookawa and Ishihara 1992)(rice);(Wang, Zhu et al. 2012)(wheat)
Carbohydrates concentration	-	(Kashiwagi and Ishimaru 2004)(rice)
Starch concentration	- (increases culm bending strength and stiffness)	(Kashiwagi and Ishimaru 2004)(rice); (Kashiwagi, Madoka et al. 2006)(rice);(Ishimaru, Togawa et al. 2008) (rice)
Silicate concentration	- (increase physical stem strength)	(Zhang, Jin et al. 2010)(rice);(Fallah 2012)(rice);(Ma and Yamaji 2006).

Table 1.1 Plant traits correlated with lodging susceptibility in cereal crops (adapted from Noor Shah et al. 2016) .

Plant height, in cereal crops as rice, wheat and barley, is by definition the distance between the tip of the ear and the soil, and is one of the key traits engineered during the Green Revolution for preventing lodging susceptibility (Tamm 2003, Berry, Sterling et al. 2004, Kong, Liu et al. 2013, Okuno, Hirano et al. 2014).

1.9.1 Green Revolution

With Green Revolution we mean a period in the recent past started in the '60s that brought a significant increase in the yield of cereal crops. This scientific advance helped to avoid threats to the food security system due to the increase of the human population worldwide (Khush 2001). Genetic selection operated by the breeders during the Green Revolution improved production, adaptability, reduction of the plant biological cycle, resistance to biotic and abiotic stress (Khush 2001). But the greatest leap of the Green Revolution was in the control of several plant architecture related traits, such as reduction of in the height of the plant (improving the lodging resistance and making the plant able to tolerate higher nitrogen treatment) and the increase of tiller number with a consequent increase in the number of ears (Khush 2001). The world population is in constant increase and is expected to reach 9,772 billion for 2050 (United Nations 2017) with a rise of their alimentary needs, that should be satisfied with a reduced environmental impact, with particular attention at the harvestable surface, water use and chemicals use. It is

therefore necessary to breed varieties with an high yield potential, but also high yield stability to face the climatic changes (Khush 2001).

Up to now to reduce the occurrence of lodging events many approaches were tested, but the one which produced best results is the control over the plant height. In order to do that during the Green Revolution semidwarf varieties were introduced; these varieties present a reduced plant height, increased harvest index (which is the weight of the seeds over the total weight of the plant aboveground biomass) and increased number of tillers thanks to a deficit in gibberellin production or gibberellin response pathways (Sasaki, Ashikari et al. 2002).

During the Green Revolution, semi-dwarfing genes helped to reduce lodging occurrence (Khush 2001, Chandler and Harding 2013). Genes responsible for plant height reduction in wheat and rice were identified and characterized, showing their involvement in the pathway of the gibberellin (GA) growth hormones (Peng, Richards et al. 1999, Sasaki, Ashikari et al. 2002). In rice, the *Semi_Dwarf-1* (*SD-1*) locus was causally linked to loss-of-function mutations of the GA biosynthesis gene *GA_20_oxidase2* (*GA20ox2*) (Sasaki, Ashikari et al. 2002). In wheat, *Reduced_height-1* (*Rht-1*) genes are responsible for the production of DELLA proteins that act as suppressor of GA-signalling (Peng, Richards et al. 1999). In barley there are several kinds of dwarf and semi-dwarf mutants such as *semi-dwarf 1* (*sdw1*) and *semi-brachytic 1* (*uzu1*), both largely used in barley breeding programs (Kuczyńska, Surma et al. 2013). Like rice *SD-1*, barley *Sdw1* encodes a gibberellin 20-oxidase protein, while the *uzu* phenotype is caused by a missense mutation of a single nucleotide in the*HvBRi1* gene encoding the receptor of another important class of phytohormones, brassinosteroids (Chono, Honda et al. 2003, Kuczynska and Wyka 2011). These genes are widely used to develop barley dwarf varieties (Fig. 1.23) (Xu, Jia et al. 2017).

Fig. 1.23 Different juvenile barley growth habits: erect plants with the dominant *Sdw1* allele (left) and prostrate plants with the mutant *sdw1* allele (right) (Kuczyńska, Surma et al. 2013).

The introduction of these genes did not solve the lodging problem. Nonetheless these mutants present several unfavourable characteristics like temperature sensitivity, late flowering and reduced grain quality (Rajkumara 2008, Okuno, Hirano et al. 2014).

As major players in hormonal pathways, Green Revolution semi-dwarfing genes pleiotropically affect a range of traits, occasionally with some undesirable effects. For example, GA plays a key role in seed germination and use of strong alleles of the barley *sdw1* gene has been limited to feed barley, likely due to a negative impact of GA deficiency on malting quality (Thomas, Powell et al. 1991, Chen, Phillips et al. 2013). Also, size reduction due to dwarfing genes negatively affects plant photosynthesis rate and production of biomass with a reduction in stem mechanical resistance (Islam, Peng et al. 2007, Okuno, Hirano et al. 2014). This trade-off between plant height and stem resistance was investigated by Okuno et al. (2014) in rice, through the study of several GA related mutants with dwarf, semi-dwarf and tall phenotypes (Okuno, Hirano et al. 2014). Results confirmed the increase of bending type lodging resistance in dwarf and semi-dwarf varieties as a result of plant height reduction; however, this favourable trait was accompanied by a reduction in stem diameter and cell wall components quality and quantity (cellulose, hemicellulose, lignin), increasing the occurrence of breaking type lodging. For the tall GA mutants the results were opposite compared to the dwarf GA mutants (Ookawa and Ishihara 1992, Okuno, Hirano et al. 2014). These results were partially confirmed by Ookawa et al. (2016) working on a near isogenic line (NIL) population carrying contrasting alleles for the Sd-1 gene (Ookawa, Aoba et al. 2016). Lines carrying the functional *SD-1*allele were taller with larger diameter and improved

morphological culm features compared to recessive *sd-1* lines (Ookawa, Aoba et al. 2016). These examples point to a paradox regarding the manipulation of culm architecture to achieve lodging resistance through alteration of the GA pathway (Hirano, Ordonio et al. 2017). Plant stature cannot be reduced under a certain threshold and new solutions to lodging are needed especially in light of ongoing climate change(Dawson, Russell et al. 2015, Hirano, Ordonio et al. 2017, Rockström, Williams et al. 2017)

1.9.2 ALTERNATIVES TO PREVENT LODGING

Nowadays alternative ways are investigated to control lodging occurrence. An alternative to plant height control is exemplified by wheat variety Baviacora 92, exhibiting a stature on average higher than 1 m and improved lodging resistance (Rajkumara 2008), as a result of the greater diameter at the basal internodes compared with other cultivars with similar height (Sayre, Rajaram et al. 1997). Indeed, engineering of culm traits related to stem diameter is an attractive alternative method to improve lodging resistance (Ookawa, Hobo et al. 2010, Kuczyńska, Surma et al. 2013, Zhang, Wu et al. 2016). Stem diameter and thickness are highly correlated with plant height, number of grains per ear/panicle and leaf sheath length and width, whereas they have negative correlations with tiller number and number of ears per square meter (Fig. 1.24)(Berry, Sterling et al. 2004).

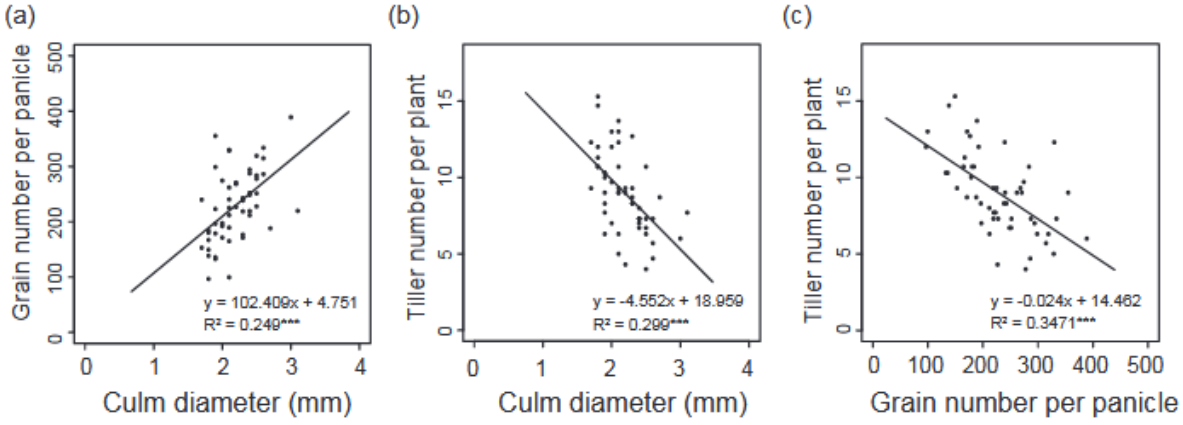

Fig. 1.24 Correlations between culm diameter, grain number per panicle and tiller number per plant in 53 rice accessions.

In wheat, Zuber et al. (1999) observed a positive correlation of culm diameter and thickness with lodging resistance (Zuber, Winzeler et al. 1999). In barley, wheat and rice, culm diameter is on average wider at the basal internodes becoming smaller in the upper internodes (Li, Zhang et al. 2011). Several studies reported that wider culm diameter and thickness improve lodging resistance (Islam, Peng et al. 2007). In rice, Hirano et al. (2014) identified a mutant line called

smos1 (*small organ size*) showing increased culm diameter, thickness, cell wall composition and therefore less subject to lodging (Hirano, Okuno et al. 2014). *Smos1* encodes an auxin-responsive APETALA2 (AP2) transcription factor (Aya, Hobo et al. 2014) acting in the cell expansion process: defective alleles of the gene result in wide and stiff culm (Hirano, Okuno et al. 2014). Ookawa et al. (2010) used a chromosomal segment substitution population, between the two rice lines Habataki and Sasanishiki (Ookawa, Hobo et al. 2010), to dissect the *Strong Culm2* (*SCM2*) QTL, identified as a mild mutation of the *ABERRANT PANICLE ORGANIZATION* (*APO1*) gene, which increases the plant diameter with positive effect on lodging resistance (Ookawa, Hobo et al. 2010).
All these evidences indicate culm diameter and culm wall thickness of basal internodes as important traits to improve lodging resistance in future breeding programs. Beside diameter and thickness, number of vascular bundles and sclerenchyma thickness also influence lodging resistance in rice and wheat (Chuanren, Bochu et al. 2004, Berry 2013, Fu, Feng et al. 2013, Kong, Liu et al. 2013).

Biochemical features as concentration of cellulose, hemicelluloses, lignin, sugar and silicate play an important role in lodging resistance (Kashiwagi, Madoka et al. 2006, Ma and Yamaji 2006, Arai-Sanoh, Ida et al. 2011). Among cell wall components, cellulose, hemicelluloses and lignin are the most important in determining culm strength and rigidity (Kong, Liu et al. 2013). Plants with lower cellulose and lignin content show a reduction in flexibility and rigidity and increased culm fragility (Jones, Ennos et al. 2001, Tanaka, Murata et al. 2003). Lignin in particular plays a role in stem strength and rigidity: a study in wheat showed significant correlation among lignin content and internode mechanical resistance (Peng, Chen et al. 2014). Nonetheless, cellulose and hemicellulose play a role in the structural properties of the plant stem (Reddy and Yang 2005, Ookawa, Yasuda et al. 2010). Li et al. (2009) studied the *brittle culm1* rice mutant finding that cell wall thickness and culm mechanical resistance are a consequence of the accumulation of cellulose, hemicelluloses and lignin (Li, Deng et al. 2009). Physical properties of cellulose fibers (e.g. crystallinity) were investigated showing a correlation with culm strength (Reddy and Yang 2005). Ma et al. (2002) in wheat investigated the expression of the COMT gene which is involved in improved lignin biosynthesis and accumulation in the culm (Ma, Xu et al. 2002).

Linkage and association mapping analyses can be useful in dissecting the genetic basis of the traits involved in lodging resistance, as shown in corn , wheat (Zuber, Winzeler et al. 1999, Peiffer, Flint-

Garcia et al. 2013) and rice (Kashiwagi and Ishimaru 2004, Ookawa, Hobo et al. 2010). Identification of mild alleles could allow a better manipulation of the features under study, avoiding aberrant and deleterious phenotypes(Ookawa, Hobo et al. 2010). Pyramiding, as the combination of different favourable QTLs, from different donors/parent lines, revealed to be a powerful tool to ideotype design controlling non synonymous mechanism for a given trait, in one variety. It could be an effective strategy to control complex traits while avoiding drastic phenotypes (Fig. 1.25) (Ashikari, Sakakibara et al. 2005, Takeda and Matsuoka 2008, Hirano, Ordonio et al. 2017).

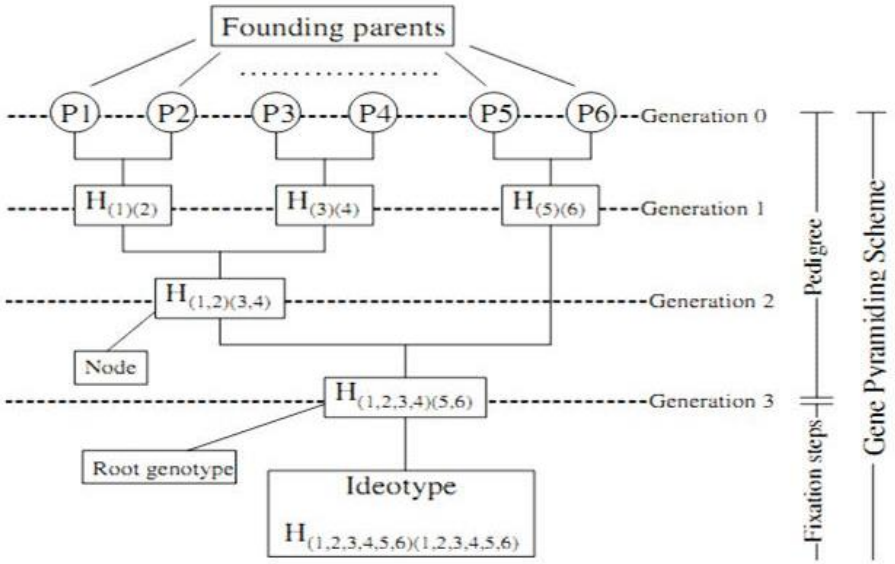

Fig. 1.25 Pyramiding breeding scheme for six target genes/QTLs. Each founding parent carries a gene/QTL of interest. These favourable genetic regions are coupled in Generation 1 and 2. Generation 3 produced an individual with all the six genes/QTLs present in a single individual (Kumar Malav, Indu et al. 2016).

Yano et al (2015) using a Koshihikari rice as background introgressed two QTLs for culm resistance, SCM2 and SCM3 (Yano, Ookawa et al. 2015). An additive effect of the two QTLs, resulting from the alteration of two different hormonal pathways, resulted in an improved diameter size and lodging resistance and, in terms of grain yield, in an increase in the number of grains per panicles (Yano, Ookawa et al. 2015).

Despite the difficulties of studying such complex traits, the first results in characterizing lodging susceptibility in wheat and rice clearly support the importance of culm architecture traits in lodging resistance. However, despite its economic importance and uses, nothing is known about the genetics of these traits in barley.

1.10 PHENOTYPING AND IMAGE ANALYSIS

With the term phenotyping we mean the collection of morphological, physiological and biochemical data for specific traits on several individuals, chose for the sampling and associated with allelic variants (Ghanem, Marrou et al. 2015, Tardieu, Cabrera-Bosquet et al. 2017). With the advance of genetic and genomic resources, phenotyping procedures have become a bottleneck in plant sciences, as in the case of quantitative/population genetic studies on large collections of individuals (Coppens, Wuyts et al. 2017, Ubbens and Stavness 2017). This deficit in phenotyping techniques is caused by absence of proper tools to measure a specific trait, lack of common protocols shared among the scientific community and sometimes also inadequate knowledge on how to score the traits of interest that can bring to misleading results (Stützel, Brüggemann et al. 2016). Beside these problems, many of the available phenotypic protocols involve the destruction of samples, which are thus excluded from further investigation.

The development of accurate and inexpensive phenotyping protocols has paramount implications in advancing plant biology and breeding programs. Measurement of phenotypic traits is still largely performed with manual devices (i.e. ruler for plant height, calliper for culm diameter) or visually scored (i.e. lodging ratio or different colours of leaves) (Thomas and Howarth 2000, Cobb, DeClerck et al. 2013). All these measurements are subjected to human error and therefore not reliable and repeatable with a waste of economic and labour resources (Masuka, Atlin et al. 2017). For instance, measurement of plant height for 3000 rice plots takes one hour with an ultrasonic height sensor, while with a manual scoring system it takes on average one hour for 45 plots (Tanger, Klassen et al. 2017). In this context, different solutions emerged in recent years relying on high-throughput phenotyping methods based on the use of new image analysis tools with advanced software and special platforms (Agnew, Bray et al. 2017).

Modern phenotyping techniques are based on remote sensing tools and include many different sensors (able to catch multispectral, fluorescence and thermal radiation) and cameras (image acquiring techniques)(Deery, Jimenez-Berni et al. 2014, Pauli, Chapman et al. 2016).

In particular digital RGB (red-green-blue) cameras and scanners represent low-cost solutions for high-throughput phenotyping through collection and analysis of digital images (Fig. 1.26).

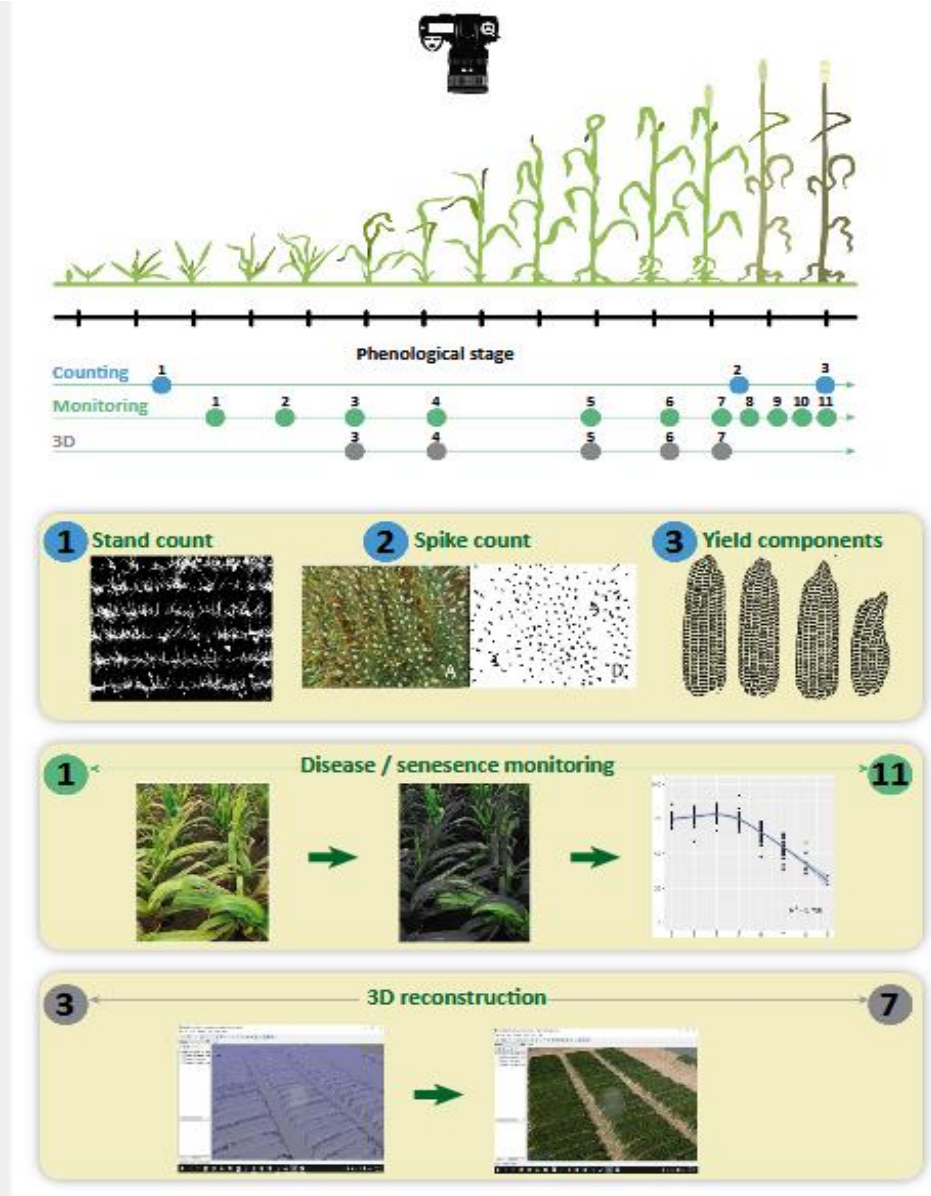

Fig. 1.26 Possible uses of RGB digital camera in plant phenotyping. Several classes are represented in the picture as crop characterization and monitoring plant growth.

Image analysis is already employed in routine scoring of several traits for different crops and private breeding companies also moved toward this kind of phenotyping methods [i.e. https://www.google.com/patents/US20090046890 ; https://www.google.com/patents/US9335313; https://www.google.com/patents/WO2017021285A1](Araus, Kefauver et al. 2018). Gauge and colleagues developed a Tassel Image-based Phenotyping System to quickly extract from corn tassel images morphological features of 3530 individuals tassels from a diverse maize inbred population; the system showed a high repeatability (0.85) and high correlation with conventional manual measurements (0.89)(Gage, Miller et al. 2017).Another example is given by Miller et al (2017) for an imaging system that can measure maize ear, cob and kernel

characteristics from office scanner pictures, showing a very high correlation among manual methods and software analysis (>0.9)(Miller, Haase et al. 2017). Tanabata et al. (2012) used a dedicated software to scan images from rice grains for several shape descriptor traits of kernels, these data were used to run QTL mapping and identifying 2 and 4 QTLs on chromosomes 8 and 11 (Tanabata, Shibaya et al. 2012). In another QTL mapping study, Moore et al. (2013) used 3200 dpi Arabidopsis seed images obtained with a flat office scanner to extract phenotype data: several significant QTLs were identified for traits related to seed area and diameter (Moore, Gronwall et al. 2013). More recently, Zhang et al. (2017) screened 106 development-related traits through 16 growth stages in a corn Recombinant Inbred Line (RIL) population of 167 individuals identifying 988 QTLs with an automated phenotyping system. They collected precise RGB pictures of plants every three days from sowing to tasseling, accumulating 476 GB of images that can be reanalyzed in future studies as well (Zhang, Huang et al. 2017). High-throughput image phenotyping is used not just in cereal crop studies: 252 QTLs associated with fruit shape and size were identified in American Cranberry (*Vaccinium macrocarpon* L.) by analysis of a biparental population of 351 individuals (Diaz-Garcia, Covarrubias-Pazaran et al. 2018).

Beside their extensive use in counting plants/plant's organs and measuring plant features, RGB imaging techniques are already being used in a wide application range: crop development, disease detection and 3D reconstruction (Shakoor, Lee et al. 2017, Gibbs, Pound et al. 2018, Lee, Chang et al. 2018).

This is paralleled by extensive implementation of image analysis software (many of them gathered in the web archive https://www.plant-image-analysis.org/) available to researchers for characterization of various plant traits (Table 1.2)(Lobet, Draye et al. 2013, Lobet 2017).

Tissue	Software	Purpose and design	Reference
Roots	WinRhizo Tron	Morphological descriptions of root area, volume, length, etc	https://www.regentinstruments.com/assets/winrhizotron_about2.html
	KineRoot	2D analysis of root growth and curvature	(Basu, Pal et al. 2007)
	PlaRoM	Platform for measuring root	(Yazdanbakhsh and Fisahn 2009)

		extension and growth traits	
	EZ-Rhizo	2D analysis of root system architecture	(Armengaud, Zambaux et al. 2009)
	RootTrace	Counting and measuring root morphology	(Naeem, French et al. 2011)
	DART	2D analysis of root system architecture	(Le Bot, Serra et al. 2010)
	SmartRoot	ImageJ plugin for the quantification of growth and architecture	(Lobet, Pagès et al. 2011)
	RootReader3D	3D analysis of root system architecture	(Clark, MacCurdy et al. 2011)
	RootReader2D	2D analysis of root system architecture	(Clark, Famoso et al. 2013)
	Gia-Roots	2D analysis of root system architecture	(Galkovskyi, Mileyko et al. 2012)
Shoots/Leaves	WinFolia	Morphological measurements of broad leaves	http://regent.qc.ca/assets/winfolia_about.html
	TraitMill	Platform for measuring various agronomic characteristics	(Reuzeau, Frankard et al. 2007)
	PHENOPSIS	Automated measurement of water deficit-related traits	(Granier, Aguirrezabal et al. 2006)
	LeafAnalyser	Rapid analysis of leaf shape variation	(Weight, Parnham et al. 2008)
	LAMINA	Quantification of leaf size and shape	(Pasam, Sharma et al. 2012)
	HYPOTrace	Analysis if hypocotyl growth and shape	(Wang, Uilecan et al. 2009)
	LEAFPROCESSOR	Analysis of leaf shape	(Backhaus, Kuwabara et al. 2010)
	Lamina2Shape	Analysis of lamina shape	(Dornbusch and Andrieu 2010)
	HTPheno	ImageJ plugin for morphological shoot measurements	(Hartmann, Czauderna et al. 2011)
	LEAF-GUI	Analysis of leaf vein structure	(Price, Symonova et al. 2011)

	LemnaTec 3D Scanalyzer	Comprehensive platform for analysis of color, shape, size, and architecture	(Golzarian, Frick et al. 2011)
	GROWSCREEN-Rhizo	Simultaneous analysis of growth rate, leaf area, and root growth	(Nagel, Putz et al. 2012)
Seeds /Grain	WinSEEDLE	Volume and surface area measurements of seeds and needles	https://www.regentinstruments.com/assets/winseedle_about.html
	SHAPE	Quantitative evaluation of shape parameters	(Iwata and Ukai 2002)
	ImageJ	General image analysis software for area, size, and shape; applied to grain	(Herridge, Day et al. 2011)
	SmartGrain	High-throughput measurement of seed shape	(Tanabata, Shibaya et al. 2012)

Table 1.2 List of software available for phenotype analysis (adapted from Cobb et al. 2013).

A particular mention is needed for ImageJ software (https://imagej.net/Welcome) and all its different open-source distributions (https://fiji.sc/ ; https://bio7.org/). These computer programs offer a flexible set of image editing and analysis toolkits that can be used by researchers for different purpose without a deep knowledge of programming thanks to an intuitive graphic user interface. As open-access informatics tools, they allow researchers/programmers to share among other users their custom developed code pipelines to expand the functionalities of each plugin for a wider range of cases and experiments (Austenfeld and Beyschlag 2012, Schindelin, Arganda-Carreras et al. 2012, Rueden, Schindelin et al. 2017).

Most image analysis techniques are laboratory oriented or with particular requirements (environmental or sample pre-treatment) and therefore have limited applicability in the field or to analyze large population (Zhang, Huang et al. 2017, Diaz-Garcia, Covarrubias-Pazaran et al. 2018, Lee, Chang et al. 2018). The need for additional technical improvements expendable in the fields, brought remote sensing tools such as RGB cameras and thermal sensors to be incorporated into phenotyping platforms. Phenotyping platforms are experimental facilities that can work indoor in

completely controlled environmental conditions or designed to collect images and data from plots outdoor (Fig. 1.27-1.28)(Virlet, Sabermanesh et al. 2017, Lee, Chang et al. 2018, Atkinson, Pound et al. 2019).

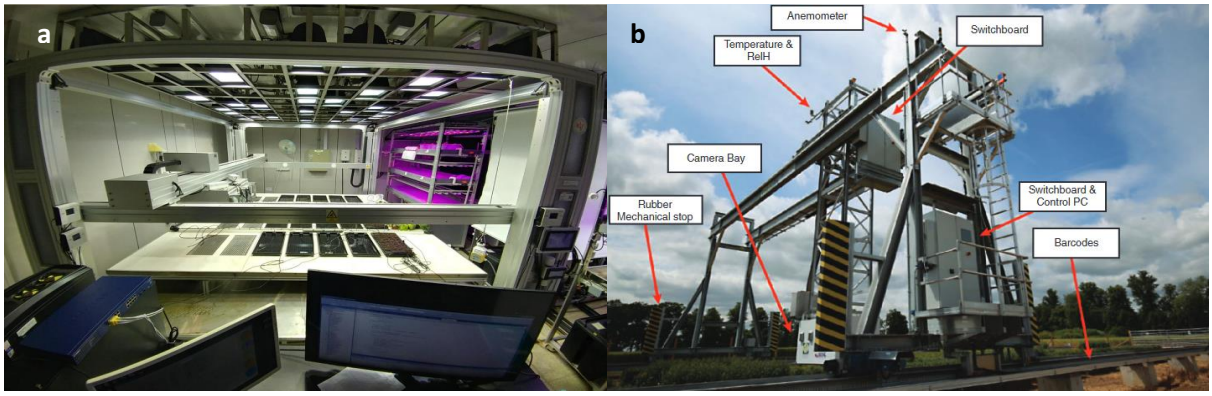

Fig. 1.27 Examples of phenotyping platforms: a) indoor phenotyping platform with robotic arms and cameras (Lee, Chang et al. 2018); b) outdoor platform (Field Scanalyzer phenotyping platform installed at RothamstedResearch UK) (Virlet, Sabermanesh et al. 2017).

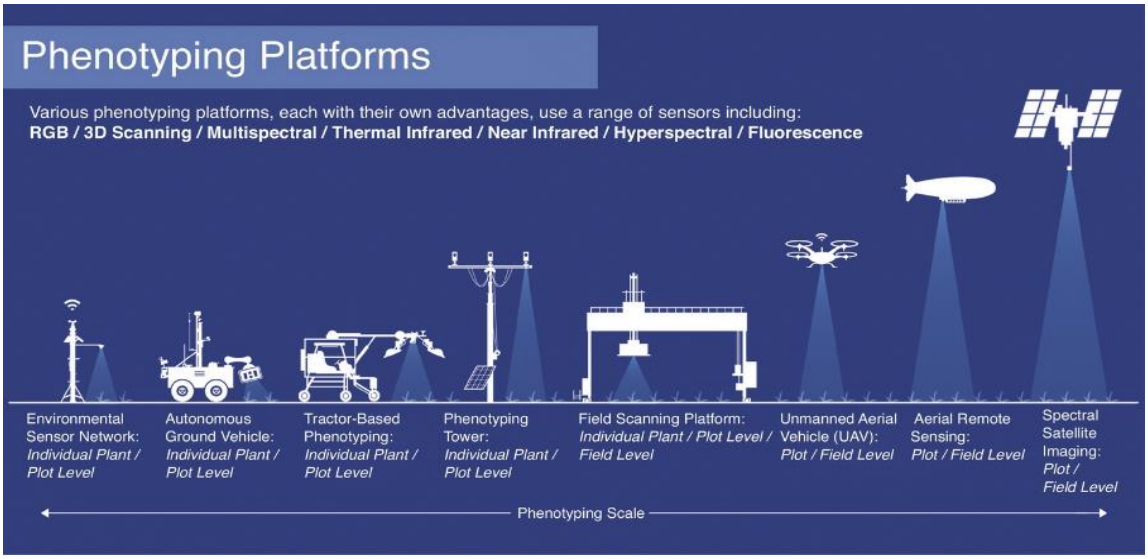

Fig. 1.28 Different types of outdoor phenotyping platforms (Shakoor, Lee et al. 2017).

Of particular interest, smartphone apps have recently been developed as mobile toolkit for plant phenotyping to collect georeferenced and precise data using the ordinary RGB camera or other built-in sensors (Kim, Lee et al. 2013, Francone, Pagani et al. 2014). The image analysis field is further expanding to the use of drones, phenotyping platforms and microsatellite to collect high resolution images of wider areas (Jain, Srivastava et al. 2016).
Finally, the analysis of such complex data and their exploitation in genetics and breeding programmes requires multidisciplinary expertise integrating quantitative genetics, crop modelling, statistics and biological knowledge (Cobb, DeClerck et al. 2013, Tardieu, Cabrera-Bosquet et al. 2017).

2.OBJECTIVES

Culm development and architecture are now regarded as key traits for improving plant performance, and knowledge of the genetic factors controlling culm morphology is of paramount importance to breed new varieties able to face the threats of climate change. In barley, the second internode of the main stem is a critical point in lodging resistance, but very little is known about the genes influencing its diameter, thickness, and the number of vascular bundles. The relationship between these culm-related traits and lodging is still not understood; also, information is lacking about the proportionality and compensatory effects acting between culm traits and yield related features such as plant height, harvest index and grain yield.

In order to fill these gaps, efficient, reliable and robust phenotyping protocols are essential.

This project had two objectives:

1. To characterize culm related traits in the second barley main culm internode, studying how they correlate with important traits, such as grain yield or lodging occurrence, in a collection of 198 barley spring accessions (162 two rowed and 36 six rowed) sown in 4 European locations (UK, Italy, Spain and Finland) for two consecutive years (2016 and 2017) and in two distinct developmental stages (dough stage and harvest stage).
   To this end, two different phenotyping protocols were created, taking advantage of image editing and image phenotyping techniques, in order to extract precise and accurate phenotyping data from the specimens. Images of the barley samples were taken using a flat office scanner (for the samples at harvest stage) and a stereo microscope (for the samples at dough stage), then images were filtered and processed using two dedicated custom-made macro commands for the open access software ImageJ. As a validation step for the image-based phenotyping protocols, data for culm diameter were compared with data obtained for the same samples by manual measurement with a caliper. Furthermore, measurements from the second barley internode were compared with those of other internodes, to evaluate it as a representative model of the overall plant stem. Finally, we investigated heritability values, correlations and similarities of the different barley traits.

2. To identify genomic regions and candidate genes involved in the control of these traits in barley, with a special focus on QTLs shared across locations/growth stages. To this end, we conducted genome-wide association studies, integrating the obtained phenotypic data with 31,360 SNP markers from the 50k iSelect marker panel (kindly provided by Dr. Robbie

Waugh, James Hutton Institute, Scotland, UK). Across trials, the ten most significant markers were taken into consideration to find shared marker-trait associations. Candidate genes were then identified based on genomic annotations for barley and other species (rice and *Arabidopsis*) and published literature on development-related genes in plants.

3. MATERIALS AND METHODS

3.1 PLANT MATERIAL AND EXPERIMENTAL DESIGN

This PhD thesis is based on a barley germplasm panel representing a subset of the wider Climbar collection: it is composed of 198 spring barley cultivars (Appendix A), and was sown for two consecutive years, 2016/2017 in four European field stations: Fiorenzuola d'Arda, Piacenza, Italy (44°55'N and 9°53'E); Balruddery, Perthshire, United Kingdom (56°28'N and 3°6'W); Zuera, Zaragoza, Spain (41°51'N and 00°39'W); Museopelto, Helsinki, Finland (60°13'N and 25°01'E). The experimental fields were organized in completely randomized blocks following an alpha lattice design with 2 replicates; each plot covered on average 1,5m² with a sowing rate of 350-360 seeds per m². Sowing date, harvest date and treatments for each location are reported in Table 3.1. All the trials were rainfed.

The only exception is the Spanish trial of 2016, which was sowed in two replicas with 12 rows each and not in plot. In every rows six barley varieties were sown.

Location	Year	Sowing	Harvesting	Treatment
Fiorenzuola (ITA)	2016	05/11/15	21/06/16	Prophylactic fungicide, weedingand 200kg/ha N
Fiorenzuola (ITA)	2017	08/11/16	10/07/17	Prophylactic fungicide, weeding and 200kg/ha N
Zaragoza (SPA)	2016	11/11/15	30/06/16	Prophylactic fungicide and weeding No fertilization added
Zaragoza (SPA)	2017	15/11/16	13/06/17	Prophylactic fungicide and weeding No fertilization added
Helsinki (FIN)	2016	11/05/16	27/08/17	Prophylactic fungicide, weeding and 92kg/ha N
Helsinki (FIN)	2017	19/05/17	29/08/17	Prophylactic fungicide, weeding and 92kg/ha N
Dundee (UK)	2016	16/03/16	29/08/16	Prophylactic fungicide, weeding and 60kg/ha N
Dundee (UK)	2017	29/03/17	24/08/17	Prophylactic fungicide, weeding and 80kg/ha N

Table 3.2 Trails arrangement in the four locations across 2016/2017.

3.2 AGRONOMICAL DATA

Trained personnel of each research center in charge of running the trial, scored traits of known agronomic importance for each plot (Table 3.2). Zadoks scale was used through all the trials in

order to define the specific developmental stage for the measurements and organize the field works consistently (Zadoks, Chang et al. 1974).

Variable Name	Protocol
On a plot basis	
Maturity Date (MD)	Scored when 50% of the plot is at Zadoks91 (fully mature) and peduncles turned to yellow. Plot averages are used for downstream analyses.
Plant Height (PH)	With a ruler, measure the distance in cm from the soil to the tip of the ear. Taken after dough stage (Zadoks87) on the main culm, average value of 3 measures per plot. Plot average are used for downstream analyses.
Grain Yield (GY)	Grain weight (g) of the plot after combine threshing and drying (if appropriate). Expressed in t/ha.
Lodging (LoD)	Percentage of plot lodging immediately prior to harvest. 0% is when all the plants in the plot keep an erect position while 100% is scored if all plants have an inclination inferior to 45 degrees from horizontal axis. Plot averages are used for downstream analyses.
On a plot subsample (25x25 cm)	
Harvest Index (HI)	The full plant subsample taken from the centre of the plot is weighted at maturity. After threshing, weight of the grain is obtained as well. Harvest Index is estimated by the following formula: $\frac{\text{Grain Weight}}{\text{above ground Plant Weight}}$ Plot averages are used for downstream analyses.

Table 3.3 Agronomical traits measured in each field trial by the technicians of each research centre.

Regarding culm traits, two distinct growth stages were considered (Zadoks83-85 and 90), focusing on culm features reported in the literature to be critical for lodging resistance in cereals (paragraph 1.5)(Table 3.3). Zadoks stage 83-85 was investigated because it is when the vegetative growth definitely stops and the grain filling starts: at this stage most serious lodging damage and yield losses occur (Weibel and Pendleton 1964). On the other hand, working on samples at Zadoks stage 83-85 is very time consuming; samples at Zadoks stage 90 are easier to handle and do not require expensive equipment to be analyzed, while being still representative of the culm architecture. Furthermore samples at Zadoks stage 90 have a different and more uniform cellular composition (Luo, Tian et al. 2007, Gui, Wang et al. 2018).

VariableName	Protocol
Scored at Zadoks stages 83-85 and 90	
Diameter (Diam)	Scored using a custom macro-command on the software ImageJ (see below). Considering the culm section as an elliptical shape, this parameter is obtained through the average *major axis* and the *minor axis* of the total scan of a singular section. Plot averages are used for downstream analyses.
Thickness (TK)	Obtained through the following formula: $$\frac{(Major\ outer\ axis + minor\ outer\ axis)}{2} - \frac{(Major\ inner\ axis + minor\ inner\ axis)}{2}$$ Where the first term refers to the *major* and *minor axes* of the total section shape while the second refers to the *major* and *minor axes* of the medullar cavity, all extracted using the ImageJ macro-command. Plot averages are used for the analyses.
Stem Index (SI)	Stem index is calculated with the following formula (Sowadan, Li et al. 2018): $$\frac{Stem\ Diameter}{Plant\ Height} * 100$$ This is an adimensional index proven to be related to lodging resistance and to other yield related traits as well (Sowadan, Li et al. 2018). Plot averages are used for the analyses.
Stiffness (ST)	Stiffness index is calculated with the following formula: $$\frac{Stem\ Diameter}{Stem\ Thickness}$$

	This is an adimensional index we obtained analyzing our data correlated to lodging resistance and to other yield related traits. Plot averages are used for the analyses.
Scored for samples at Zadoks stage 83-85	
n. of Vascular Bundels (n.VB)	The number of vascular bundles was obtained from counting manually from images collected from culm sections (see below). Plot averages are used for the analyses.

Table 3.4 Culm related traits; all these traits were obtained using the custom made ImageJ macro techniques. Only exception are the vascular bundles that were counted by hand.

3.3 CULM PHENOTYING – ZADOCKS STAGE 90

An *ad hoc* image analysis-based protocol was developed in order to obtain quantitative data for measuring the different traits related to the architecture of the second internode of the barley main stem. From previous studies on lodging resistance in cereals (wheat and rice) we identified the 1st and 2nd basal internodes as critical points for the lodging occurrence (Berry, Sterling et al. 2004, Berry, Sylvester-Bradley et al. 2007). Because of the great plasticity of first internode we decided to focus just on the second internode (Fig. 3.1) as a critical point for lodging resistance and a good descriptor of the other internodes characteristics.

Second internode is identified as the internode following the first internode longer than 1 cm above the root crown (Berry, Sterling et al. 2004, Berry, Sylvester-Bradley et al. 2007, Berry 2013). This analysis was performed for all samples from all four locations in both 2016 and 2017, only exception was FIN 2016 trial, where the diameter data were taken using the caliper, and no data about the thickness and stiffness are available.

At Zadock stage 90 (fully mature), three randomly selected plants for each plot were uprooted, avoiding those on the plot's borders. For each plant, the main stem was identified based on two criteria: i) the main stem is usually the tallest; ii) in the hypocotyl area just below the main stem the caryopsis is visible. Once the main stems were identified, the second basal internode was excised cutting just below and above the subtending nodes.

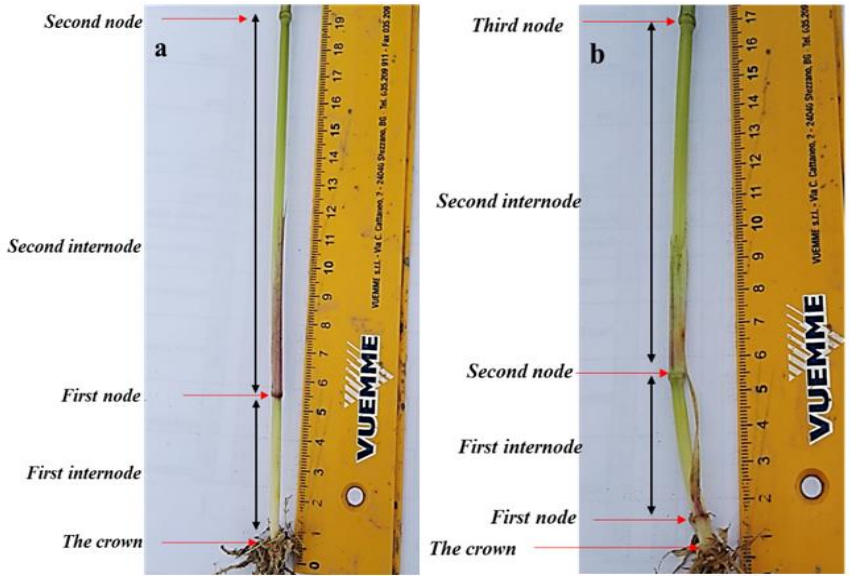

Fig. 3.1 Identification of the second internode.

Using a custom made circular saw (Fig. 3.2a), internodes were cut in the central position to produce 5 mm tall sections: in this step it is important to perform blunt cuts (Fig. 3.2b).

Fig. 3.2 sections cutting. a)Custom circular saw example; b) sections with blunt edges .

The resulting internode sections were attached with cyanoacrylic glue (Super Attak) to a black A4 cardboard. The card board is divided into 3cm x 5cm cells, labeled with the plot's field coordinates (column and row). Three samples (each from a distinct plant from the same plot) were glued in the same cells shown in Fig. 3.3. On the side of each cardboard a paper ruler was attached in order to allow the software calibration during image analysis.

Fig. 3.3 Example of the cardboard with sections attached

Each section was then colored with a white marker (Uni-ball Posca, 0,7 mm) to increase the contrast with the black background.

All cardboards were scanned with a flat office scanner in order to obtain 600 dpi images saved in .tiff format. A total of 10800 sections were collected and analyzed over the two years of study (plus 1440 sections were measured with a caliper in the Finland 2016 trial).

The images are then analyzed with a custom made macro command in Java language on the software ImageJ (Schindelin, Arganda-Carreras et al. 2012). In order to extract quantitative measurements in mm, the first step involves setting of the right scaling ratio, using the "Analysis -> Set Scale" menu. Since the images have a resolution of 600 dpi, 234 pixels correspond to 1 cm.

The last operation before running the macro consists in setting the desired measurement in the menu "Analysis->Set Measurements". Here we checked "Area", "Shape Descriptors", "Perimeter", "Fit Ellipse", and "Display Label". For further information the reader is referred to the ImageJ User manual (https://imagej.nih.gov/ij/docs/guide/user-guide.pdf). The complete script of the macro can be found in the Appendix B.

The macro command performs two series of operations on each image: i) apply filters and ii) analysis, in the following order:

i) Apply filters

1. Enhance contrast: in this step, the image contrast is enhanced by using either histogram stretching or histogram equalization techniques. In our case, the default option histogram

stretching was used. Histogram stretching, contrast stretching or simply normalization is an image-enhancement technique that attempts to improve the image contrast by "stretching" the range of intensity values it contains to span a desired range of values for each channel (red, green, blue). The saturated pixel level, which determines the number of pixels in the image that are allowed to become saturated in order to increase the contrast, is set to 3.0% after several trials (Fig. 3.4).

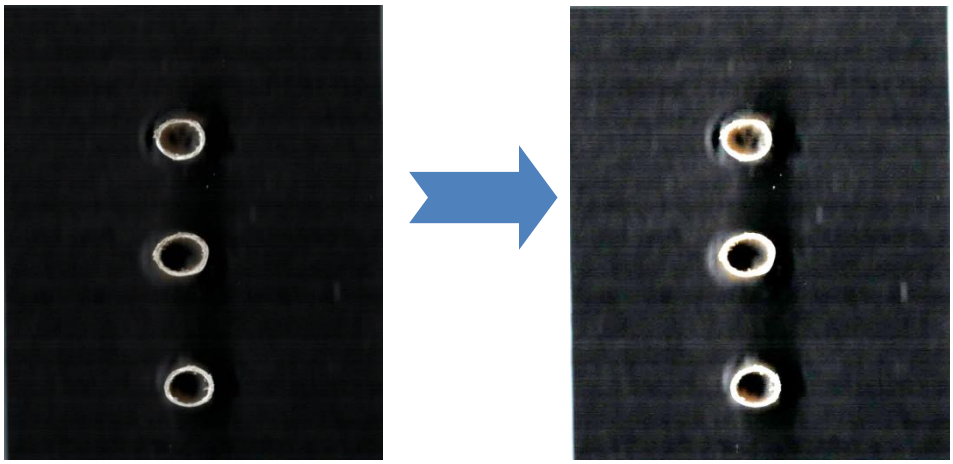

Fig. 3.4 Example of the cardboard with sections attached. On the left the original image, on the right the image after the enhance contrast command.

2. Bandpass filter: this command removes high spatial frequencies (adding blur to the image)and low spatial frequencies (subtracting blur from the image) (Fig. 3.5) . It can also remove horizontal or vertical stripes that were created by scanning an image line by line. In this way the algorithm reduces edge artifacts. The filter can target selectively objects in the image that fall between a determined span of pixels ("Filter Large Structures Down to" and "Filter Small Structure Up to") so as to remove interferences due either to the background or to small objects. An important option is "Autoscale after filtering" which can be used - after the filtering step to set the lowest intensity in the image equal to 0 and the highest equal to the maximum allowed for the type of image for each channel, preserving all the intensities. In this step all options are left as default: "Filter Larger Structure Down to"=40, "Filter Small Structure Up to"=3, "Suppress Stripes"=None, "Tolerance direction"=5, "Autoscale After Filtering"= checked.

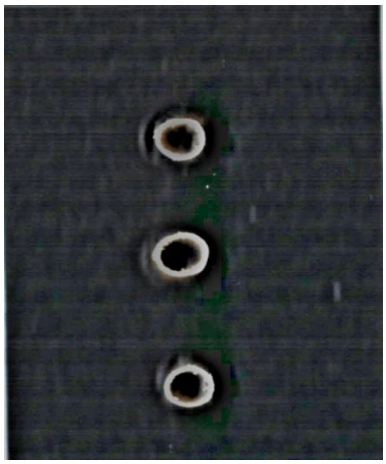

Fig. 3.5 Bandpass filter command

3. 8-bit transformation: this command coverts the Image into an 8-bit grayscale image. This step further simplifies our image, making it easier to analyze (Fig. 3.6).

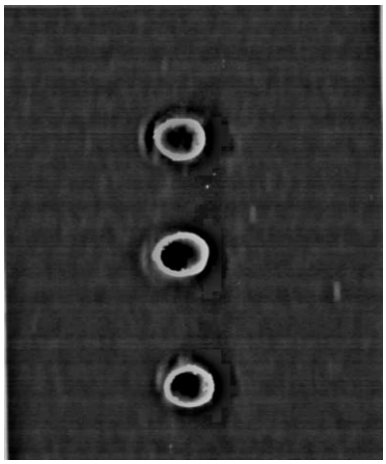

Fig. 3.6 8-bit transformation command

4. Set AutoThreshold: with this command it is possible to set lower and upper threshold values, segmenting grayscale images. All values below or above the threshold will be converted to the maximum and minimum value set by the user. In our case the maximum intensity was 255 (which corresponds to black) and minimum was 70 (making all the pixel with intensities below 70 equal to 70). The “Black Background” option should be set as “TRUE”. This command reduces the image to a black&white image with the culm section completely black and the background white (Fig. 3.7). Other options were left as default.

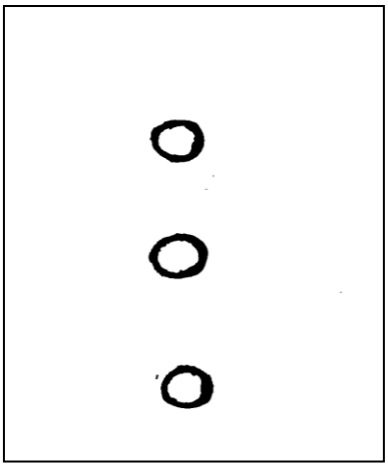

Fig. 3.7 Auto threshold command for whole section measurements.

5. Remove outliers: this command replaces a pixel by the median of the pixels around it if its value deviates from the median by more than the threshold value. The option "Radius" determines the area (pixels) around each pixel for the median estimate and was set to 5. The "Threshold" option instead was set to 0, in order to correct the noise created by the texture of the paper or by any other cofounding agent. This command can correct both white outliers and black outliers; for this reason, it was run twice in order to remove the two kinds of outliers (Fig. 3.8).

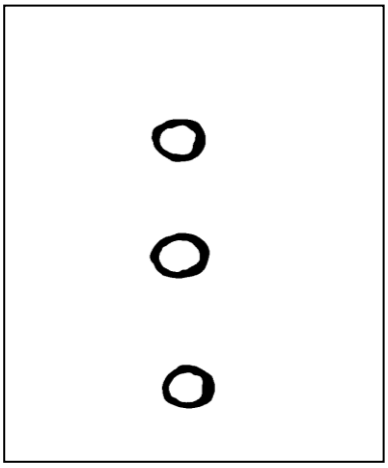

Fig. 3.8 Remove outliers command.

ii) Analysis

1. Set regions of interest (ROI):this command is present in the toolbar area and allows the selection of rectangular areas in the image defined by starting position, width and height. With this command, we selected the first cell including the 3 sections. The coordinates

depend on how each cardboard was prepared.

2. Analyze particles: this useful command counts and measures objects in binary or thresholded images. Analysis is performed on the previously selected region of interest. It works by scanning the ROI (every line of pixels will be scanned; from left to right, from top to bottom) until it finds the edge of an object. It then outlines the object (the same as using the "Wand Tool" command in the toolbar), measures it, fills it to make it invisible and then resumes scanning until it reaches another object or the end of the ROI. Several options were checked prior to analysis:

2.1. Size: objects with area outside the range specified are ignored. Value may range between 0 and "infinity". For scaled images values are expressed with the defined parameter. This parameter should be set depending on the general size of the samples, in our case it was set to a span of 0.03 – 0.5 cm^2;

2.2. Circularity: the circularity parameter can span between 0 (line) and 1 (circle). Objects with a size circularity outside the desired range are just ignored. This parameter should be set depending on the general circularity of the samples, in our case the range set was from 0.6 to 1. Circularity is a shape descriptor calculated with the following equation:

$$Circularity = \frac{Object\ Area}{(Object\ Perimeter)^2}$$

2.3. Display: this option was checked to produce a results table with measurements for all the analyzed objects in the ROI;

2.4. Include Hole: this option was checked in order to fill the medullar cavity prior to analysis and include interior holes in the object measure;

2.5. Summarize: this option was checked to show descriptive parameters as objects count, total object area, average object size, area fraction and other descriptive parameters in a separate summary table;

2.6. Add to the Manager: this option was checked to add measured objects in the ROI's manager;

3. Repeat steps for Analysis 1. and 2.The abovementioned steps are repeated on each cell of the cardboard. This protocol allows to evaluate the total shape of each section. In order to

investigate the medullar cavity of each section, few steps must be changed as follows, to take into account the different dimension of the culm hollow area:

i)Apply filters

1. Set AutoThreshold: in this step, the option “Black Background” should be left as “FALSE”. In this case the background and the medullar cavity will be left black while the section will be white. If necessary, adjust the intensities coherently (Fig. 3.9).

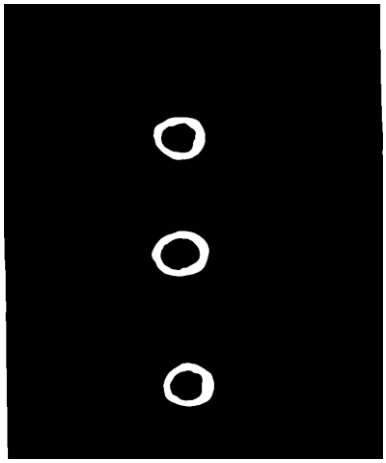

Fig.3.9 Auto threshold command for measurements of the medullar cavities

ii) Analysis

2. Analyze particles: at the point 2.1 the span size of the objects was set between 0.01 and 0.2 cm^2 while at point 2.2 the circularity range was set between 0.4 and 1.

Once the Analyze particles command finishes to analyze the objects in the different ROIs a results window, summarizing the measurements, and a summary window, with the number of section analyzed in each ROIs, appear. Measurements in the result window are labeled with the name of the picture they come from and a progressive number. Each line correspond to a distinct section, and the number of lines depends on the number of sections on each cardboard.
The summary window tells us how many sections are present for a certain plot, in that way it is possible to divide by plot all the measurements present in the results window. Results window and summary window can be saved as a .txt or .xls file; alternatively they can be copied on the clipboard and pasted in any excel spreadsheet.

3.4 CULM PHENOTYPING: ZADOCK STAGE 83-85

A distinct image analysis protocol was also developed to measure traits related to the architecture of the second internode of the barley main stem at Zadocks stage 83-85 (dough stage). This analysis was performed for all samples from trials carried out at CREA research center of Fiorenzuola d'Arda, Piacenza, Italy, in the years 2016 and 2017.

Two randomly selected plants for each plot were selected and uprooted, avoiding those on the plot's borders. For each plant, the main stem was identified and second internodes were indentified and excised as described in paragraph 3.3. Internodes were cut in half and stored in 15 ml Falcon tubes filled with Farmer's solution[3:1 ethylic alcohol (95%) to glacial acetic acid] for 3 days at 4°C. Next, samples were placed under vacuum with a Chemistry Vacuum System (https://www.vacuubrand.com/en/page736.html) at pressure of 7 mbar/room temperature to expel the air still present in the samples and allow a complete penetration of the solution into the tissues (Fig. 3.10-3.11). Sections were then moved to ethanol (70%) and stored at 4°C until sectioning.

Fig.3.10 Falcon tubes, containing samples, are sealed with pierced parafilm and placed in the vacuum pump.

Fig.3.11 Vacuum pump.

With a sharp razorblade, samples were manually dissected to obtain 3 sections(thickness 0.3/0.4

mm)from the central part of each internode, yielding 6 sections for each plot (3 sections x 2 plants). Sections were stained for few seconds with 0,1% Safranin aqueous solution (Euromex) coloring lignified tissues in red. Stained section were placed on a glass microscope slide and covered with 0,2% agarose solution to keep them hydrated avoiding the formation of air bubbles. Images of the specimens were taken with a stereo microscope Leica MZ6 with integrated m Megapixel Leica DFC295 connected with a computer: a dedicated software (Leica Software) is used to visualize the samples, edit and save sample images (Fig. 3.12). The magnification level changed between samples but a proportionality bar of 2mm was kept constant throughout the experiment.

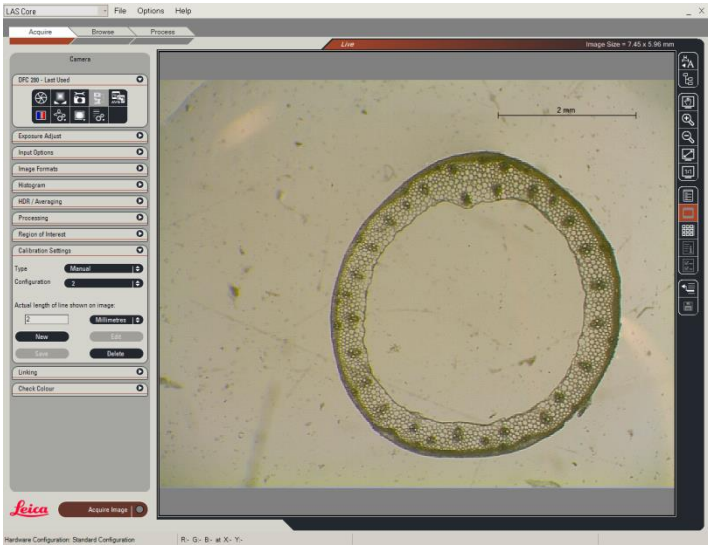

3.12 Images of a specimen under the Stereomicroscope visualized on the computer .

No particular settings or filters were used. All images were saved in .tiff format, a total of 6480 images from both years were collected.

Images were analyzed with a custom made macro command similar to the one mentioned in section 2.3.2 using Java language on the software ImageJ. To properly set the right scale ratio we used the proportionality bar on each image adjusting the correct pixel ratio in the “Analysis -> Set Scale” menu. The last operation before running the macro was to check “Area”, ”Shape Descriptors”, ”Perimeter”, ”Fit Ellipse”, and “Display Label” parameters in the “Analysis->Set Measurements” menu, as in paragraph 3.3. The complete script of the macro can be found in the Appendix C.

The macro command performs two operations on each image: i) apply filters and ii) analysis, in the following order:

i) Apply filters

1. Bandpass Filter: See paragraph 3.3, (Fig. 3.13).

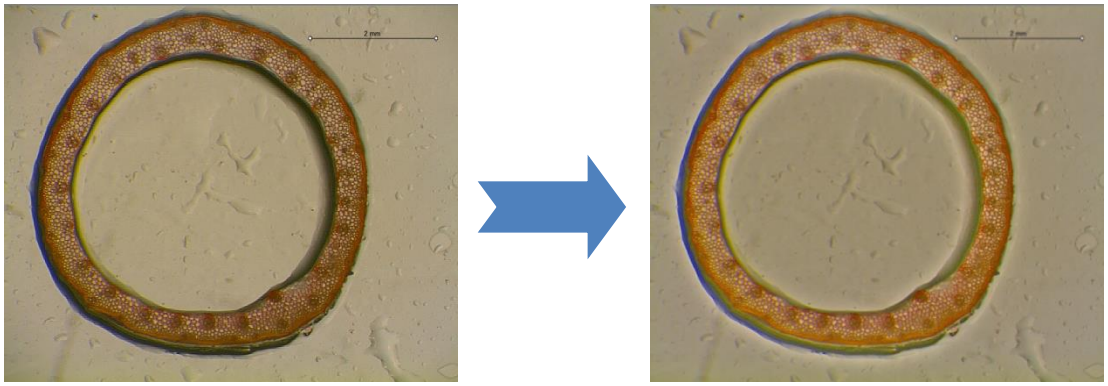

Fig. 3.13 Example of a safranin stained section. On the left the original image, on the right the image after the bandpass filter command.

2. Subtract Background: this step removes smooth continuous backgrounds from images (Fig. 3.15). It is based on the "rolling ball" algorithm described by Sternberg Stanley in 1983 (Sternberg 1983)(Fig. 3.14). Options in this command are left as default with few exceptions:

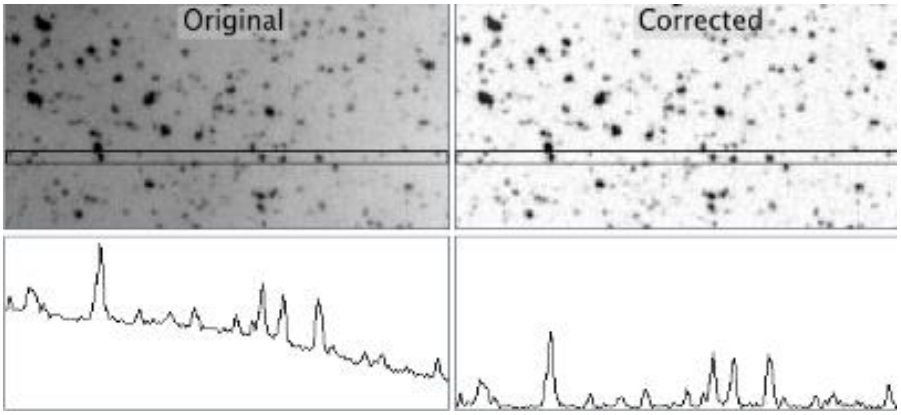

Fig. 3.14 Example of the subtract background command.

2.1 "Rolling Ball Radius" was set to 50, which defines the radius of the paraboloid curvature. Authors suggest to set it at least as large as the radius of the largest object in the image (no background).

2.2 "Light Background" sets the requirements to edit an image with bright background.

2.3 "Separate Colors" allows the Subtract Background command to operate on the brightness as well on the hue and saturation..

2.4 "Sliding Paraboloid": this command replaces the "rolling ball" algorithm with "sliding paraboloid" algorithm (the sliding paraboloid algorithm was written by Michael Schmid (https://imagej.nij.gov/ij/docs/guide/146.html)) . It allows to use radius smaller than 1 (which is the maximum for the "rolling ball" algorithm) down to 0,0001. "sliding paraboloid" code

improvement produces more reliable and precise correction, if compared with the “rolling ball” algorithm which can create some minor edge artefacts.

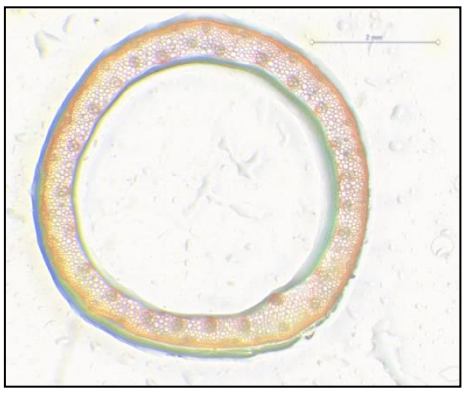

Fig. 3.15 Subtract background command.

3. Enhance contrast: See paragraph 3.3, (Fig. 3.16).

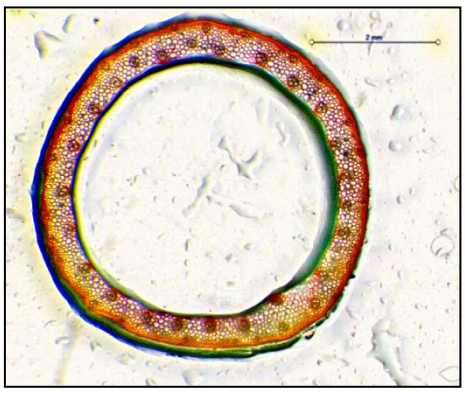

Fig. 3.16 Enhance contrast command.

4. Find Edges: listed in the “Process” menu, this command uses a Sobel edge detector to highlight sharp changes in intensity in the active image or selection. This command permits to find edges and borders of structures in the picture (Fig. 3.17).

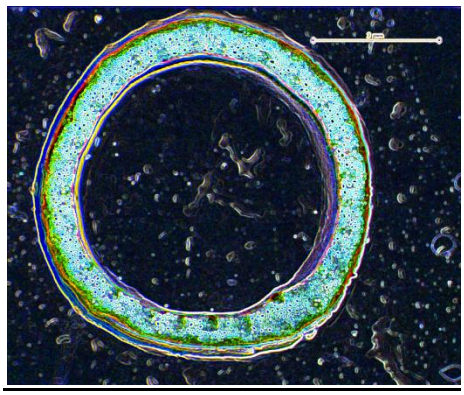

Fig. 3.17 Find edges command.

5. 8-bit transformation: See paragraph 3.3, (Fig. 3.18).

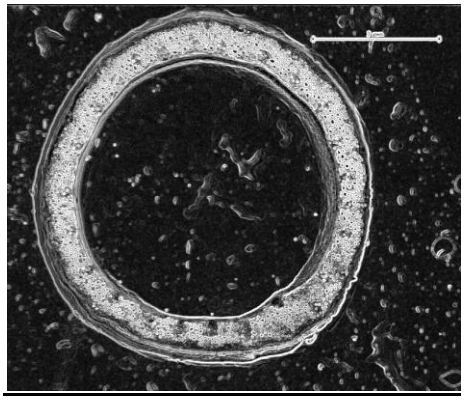

Fig. 3.18 8-bit transformation command.

6. Set AutoThreshold: See paragraph 3.3

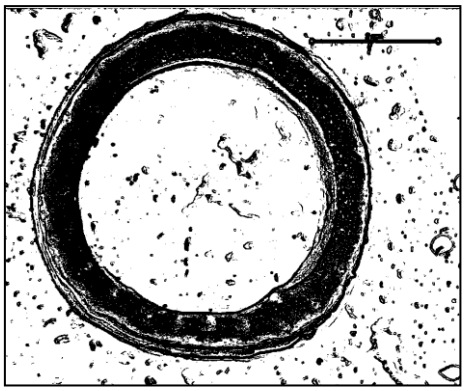

Fig. 3.19 Auto threshold command for whole section measurements.

7. Remove outliers: See paragraph 3.3.

8. Fill Holes: This command fills holes (4–connected background elements) in objects by filling the background (the algorithm was contributed by Gabriel Landini (https://imagej.nij.gov/ij/docs/guide/146.html)).

9. Remove outliers: as in step 7 (See paragraph 3.3) but in this case the radius for the median estimate of the correction is increased to 15 (Fig. 3.20).

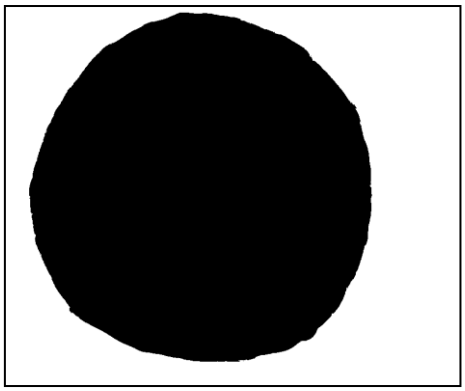

Fig. 3.20 Remove outliers command

ii) Analysis

1. Analyze particles: this command is used in the same way as in the paragraph 3.3, with the following differences:

   1.1. Size: in our case was set a span of 0.01 – infinity cm^2;

   1.2. Circularity: in our case the range set was from 0.6 to 1.

The above protocol aims at evaluating the total shape of the section. For analysis of the medullar cavity of each section few steps must be changed in the Apply Filters section, to take into account the different pattern of the culm hollow area:

i)Apply filters

2. Set AutoThreshold: In this passage the option "BlackBackground" should be left as "FALSE". In this case the background and the medullar cavity will be left black while the section will be white. Intensity was set to 0 for the minimum and 100 for the maximum (Fig. 3.21).

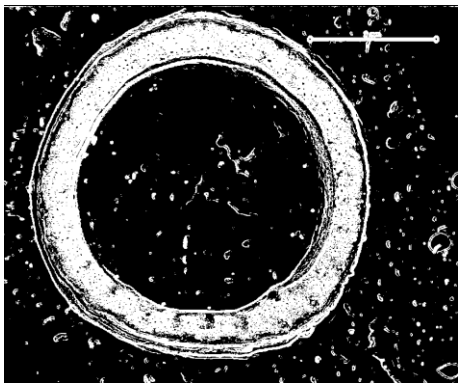

Fig. 3.21 Auto threshold command for medullar cavity measurements.

3. Remove outliers: In this passage it is necessary to remove first the dark outliers setting the radius to 2.

4. Remove outliers: Instead of using the “filling hole” command it is necessary run another time “remove outlier” , to remove bright outliers with a radius of 6 (Fig. 3.22).

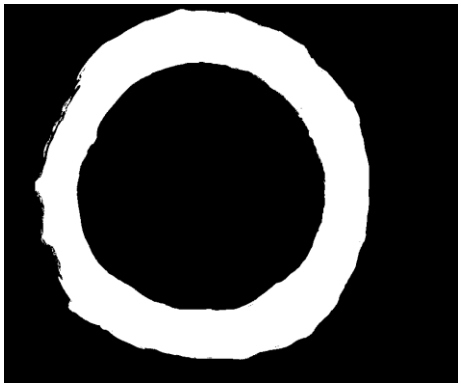

Fig. 3.22 Remove outliers command.

3.5 GENOME-WIDE SNPs GENOTYPING

The molecular marker panel used in this project is the 50K Illumina Infinium iSelect (Bayer, Rapazote-Flores et al. 2017) designed combining 6,251 SNPs from the 9k iSelect marker panel (maintaining sequence orientation and allele calling for a backward compatibility with the 9k SNP chip) with 37,789 SNPs obtained from exome capture technology producing a total of 44,040 SNPs. Genotyping data were kindly provided by Prof. Robbie Waugh (James Hutton Institute) in the context of the ClimBar collaborative project. Data were provided in a “raw” form for all the SNPs. SNPs failed were removed from the panel.

The software Tassel (V.5.0) was used to impute the missing values through the kNNi algorithm (Bradbury, Zhang et al. 2007). This imputation method can be used with data of different kind (continuous, discrete, ordinal and categorical) and consists of matching a point with its closest k neighbors: the rationale behind the method is that any missing marker value (allelic state) for a particular genotype can be approximated by the values of the markers that are closest to it, based on other variable; in our case other genotypes.

3.6 POPULATION STRUCTURE ANALYSIS

Markers were filtered excluding SNPs with a MAF <5% (Bellucci, Tondelli et al. 2017). Principal component analysis (PCA) was run in Tassel (V5.0) and R studio, scatter plots were inspected to study subpopulations.

STRUCTURE V. 2.3.3 software was used to analyze population structure of the collection, as well as to confirm PCA results (Bellucci, Tondelli et al. 2017). The software builds a model to cluster each

individual into subgroups (k=number of subgroups) based on genotypic data, and the fit of the model is then tested. The software tested the number of subgroups k increasing the value for each analysis from 1 to 10 with the reduced set of SNPs (50 SNPs from across all the genome) .Burn-in iterations and Markov Chain Monte Carlo (MCMC) were both set at 10,000 for each run. Each value of *k* was tested in 10 replicates. The software output was then screened using Structure Harvester (http://taylor0.biology.ucla.edu/structureHarvester/) (Earl and vonHoldt 2012).

3.7 LINKAGE DISEQUILIBRIUM ANALYSIS

Linkage disequilibrium (LD) pattern for each chromosome was investigated using the R package LDcorSV (Desrousseaux, Sandron et al. 2017), which can correct r^2 for population structure and relatedness among the genotyped individuals, as described by Mangin et al (Mangin, Siberchicot et al. 2012). Prior to Intra-chromosomal LD decay evaluation, the marker panel was pruned using the R package SNPrelate. High levels of pairwise LD in SNP data may lead to biased conclusion in the LD decay analysis; to avoid this situation we kept one SNPs every five markers. This approach will produce a subset of approximatively independent markers and consequently removing spurious substructure patterns.

After this filtering step, the total number of markers used to evaluate the LD decay was 5293, distributed across the genome as shown in Table 3.4.

	n.markers
chrm1	518
chrm2	931
chrm3	790
chrm4	627
chrm5	1056
chrm6	632
chrm7	739
TOT	5293
MEAN	756

Table 3.4 Number of markers used to evaluate the linkage disequilibrium decay.

The corrected r2values were then plotted and a second-degree smooth LOESS curve was fitted on the plotted data. The 95th percentile of r2 values for unlinked loci was calculated to establish a threshold for markers not in LD. The projection onto the x axis of the interception point between the fitted curve and the critical r2 is the estimate of the average chromosome LD decay distance.

3.8 STATISTICAL ANALYSES OF PHENOTYPIC DATA

All statistical analyses were performed using the R software version 3.4.4. In order to evaluate the heritability in each trial, variance components were computed for Diameter, Thickness, Stem index, Stiffness, Plant Height, number of Vascular Bundles considering the number of replicates and the year as fixed factors and genotypes, row, column as random factors. This was done taking advantage of the R package "lme4" version 1.1.18 using the function "lmer"(Bates, Maechler et al. 2015).

Broad-sense heritability for the trait studied was evaluated for single trial according to (Knapp, Stroup et al. 1985):

$$h\,2\ = \sigma\,2\,g/(\sigma\,2\,g\ +\ (\sigma\,2\,e/n))$$

Where σ 2 g is the genetic variance, σ 2 e is the error variance, n is the number of replicates.

Best Linear Unbiased Estimators (BLUEs) of the traits under study were calculated as the phenotypic values estimated for each genotype in a mixed linear model implemented by "lmer" function, where genotype and replicate were set as fixed factors and column and row as random factors.

Genome wide association analyses (GWAS) were calculated based on BLUEs, while for the Pearson's correlations the raw experimental data were evaluated.

3.9 GENOTYPE BY ENVIRONMENT ANALYSES

Additive main effect and multiplicative interaction (AMMI) model in GenStat v.12 was used to determine the stability of the genotypes across environments. The AMMI model combines the features of analysis of variance (ANOVA)along with the Multiplicative Interaction effects of principal components analysis (PCA). The ANOVA estimates the additive main effects of the two-way additive components for the main effects of genotypes (g_i), environments (e_j– in our case 8 environments; 4 locations * 2 years) and multiplicative components for the interaction effect $(ge)_{ij}$. Therefore, the model equation implemented by the software for the *i*-th genotype in the *j*-th environment in *r* blocks (replicate) is (Gauch 1992):

$$Y_{ijr} = \mu + g_i + e_j + b_r(e_j) + \sum_{k=1}^{n} \lambda_k \alpha_{ik} \gamma_{jk} + \rho_{ij} + \varepsilon_{ij}$$

where Y_{ijr} is the phenotypic trait (e.g. culm diameter) of genotype *i* in environment *j* for replicate *r*, μ is the grand mean, g_i are the genotype main effects as deviations from μ, e_j are the environment

main effects as deviations from μ, λ_k is the singular value for the Interaction Principal Component (IPC) axis k, α_{ik} and γ_{jk} are the genotype and environment IPC scores (i.e. the left and right singular vectors) for axis k. $b_r(e_j)$ is the effect of the block r within the environment j, r is the number of blocks, ρ_{ij} is the residual containing all multiplicative terms not included in the model; n is the number of axes or principal components (PC) retained by the model, and ε_{ijr} is the experimental error, assumed independent with identical distribution.

The AMMI model is a robust statistical method widely used to analyze multiple-environment trials. Its purpose is to unveil complex genotype*environment interactions. AMMI analysis can help to identify the most performing combinations of genotypes and environments concerning a specific variable.

3.10 GWAS ANALYSES

Genome wide associations scans (GWAS) were performed with FARM cpu package version 1.02 (Liu, Huang et al. 2016) implemented in the in R software. For the identification of significant marker-trait associations FARM cpu performs an analysis that incorporates both the multi-locus mixed-model approach (MLMM)(Segura, Vilhjálmsson et al. 2012) and the factored spectrally transformed linear mixed models (FaST-LMM-Select)(Lippert, Listgarten et al. 2011, Listgarten, Lippert et al. 2012). This technique improves the classical mixed linear model approach (MLM)(Yu, Pressoir et al. 2006) by removing the confounding effects due to both population structure (Q) and kinship (K), which result in better control of false positive while avoiding over-fitting (Liu, Huang et al. 2016).

The first 2 components of PCA (used to correct the population structure) and the kinship matrix [calculated in FARMcpu with the VanRaden method (VanRaden, 2008)], were used in the model. Results were analyzed to identify significant marker-trait associations and QTLs comparing results from all the 5 traits tested in the 8 different trials. The p-values were adjusted based on Bonferroni correction, separately for each trait/trial, and the threshold value for significant association was set at 0,05. Thus, it was decided not to systematically exclude marker-trait associations without a significant p-value after the Bonferroni adjustment but to evaluate every signal within its context, considering: *1)* how many markers were significant from the same or different analysis mapping at similar positions and *2)* presence of known genes regulating the trait considered in the region. The

genomic area surrounding these signals was then investigated using the online database Barley Floresta (http://Floresta.eead.csic.es/barleymap/).

4.RESULTS

4.1 PROTOCOL VALIDATION

In order to automate the extraction of accurate measurements from images of culm sections, we developed a dedicated macro to be used in combination with ImageJ (paragraph 3.3). To assess the reliability of our macro-driven protocol, we used mature samples from the Finnish field trial of 2017 to compare culm diameter measurements taken with a caliper with those extracted from the images by the software.

The two distributions show a minor but significant differences (Tab. 4.1): minimum, maximum and mean values are consistent between the two, but, as shown by the standard deviation, data extracted with the calliper are less compact.

Diameter data extracted with the software show a normal distribution (Skewness and Kurtosis comprised between -1 and +1 (Sowadan, Li et al. 2018))

	Min.	Mean	Max.	SD	Skewness	Kurtosis
Caliper (cm)	0.18	0.3256	0.5154	0.044	0.59	1.074
ImageJ (cm)	0.24	0.3443	0.485	0.041	0.76	0.622

Table 4.1 Descriptive statistics regarding the diameter data taken with the caliper and with the software.

Although the t-test and the Kolmorogov-Smirnov test show a significant difference between the two methods (both inferior to 0.001) because of the marked difference between the two phenotyping systems, the correlation between the two is high, positive and significant (Fig. 4.1). Results are very similar even if the data extracted with the software have a more compact distribution (Fig. 4.2-4.3), as shown by skewness and kurtosis, and a lower standard deviation (Tab. 4.1).

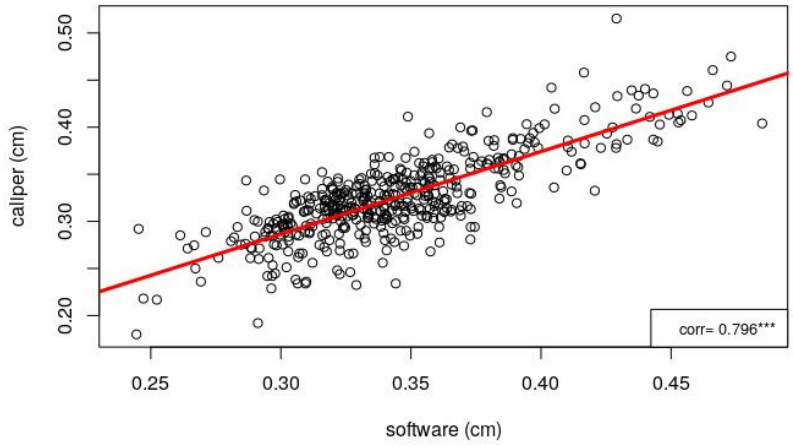

Fig. 4.1 Correlation between caliper and software measurements. The correlation among the two is 79.6% and significant.

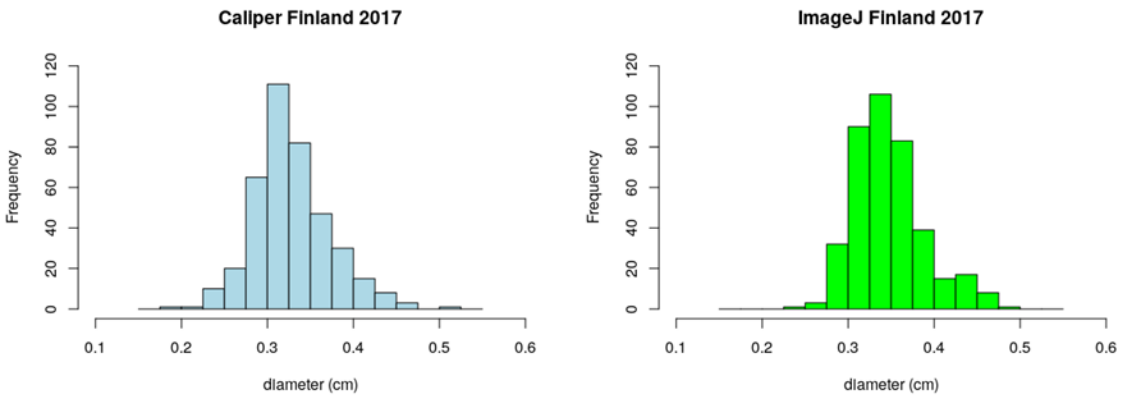

Fig. 4.2 Comparison of the distributions among the caliper (light blue –left) and software (green-right) diameter data sets. The two data sets show a normal distribution, and similar min, MAX and mean values.

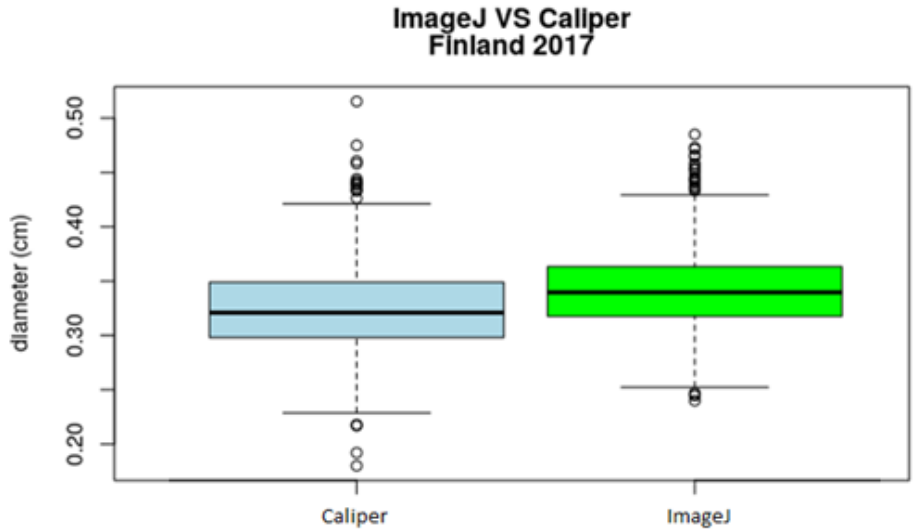

Fig. 4.3 Box plots comparing the distributions of caliper (light blue –left) and software (green-right) derived diameter data sets.

Compared to manual measurement with the caliper, the software is more time-efficient and less subject to human error. Importantly, the software can also extract other shape descriptor values allowing a precise evaluation of the shape of the medullar cavity, a region that is not easily measurable with the caliper.

Taken together, these results demonstrate that our image analysis-based protocol can be used for accurate phenotyping of culm diameter and other culm morphological traits.

4.2 PROPORTIONALITY WITHIN THE STEM

In this work, we analyzed morphological features of the second elongated internode at the base of the plant as a critical point for lodging in barley; however, lodging may occur also at internodes (Berry, Sterling et al. 2004, Berry, Sylvester-Bradley et al. 2007). For this reason, we decided to analyze morphological parameters of the second internode along with those of other internodes of the same culm to evaluate if the second internode can be used as a proxy for the whole culm,

e.g. if accession A has larger second internode diameter compared with accession B, is this true also for other internodes?

To this end, we conducted two experiments to analyze internode length, diameter and thickness of six barley internodes sections coming from the same stem.

In the first experiment, we considered three replicates of ten randomly selected barley varieties from the 2017 Italian field trial (Table 4.2).

Variety	Rows types	Habitus
Chariot	2	spring
Elo	2	spring
Odin	2	spring
Midas	2	spring
Abava	2	spring
Deba-Abed	2	spring
Maris-mink	2	spring
Corgi	2	spring
Riviera	2	spring
Calgary	2	spring

Table 4.2 List of barley varieties used for the proportionality test for the trial Italian trial of 2017.

In the second experiment, we analyzed three replicates from five two-row and five six-row varieties randomly selected from the 2017 Scottish field trial (Table 4.3).

Variety	Rows types	Habitus
Krystal	2	spring
Freja	2	spring
Dandy	2	spring
Roxana	2	spring
Stendes	2	spring
Morex	6	spring
Jarle	6	spring
Vairogs	6	spring
Jadar	6	spring
Loviisa	6	spring

Table 4.3 List of barley varieties used for the proportionality test for the trial English trial of 2017.

For each plant, we identified the main culm and collected up to the sixth internode from the first above the crown. Internode length was measured with a ruler and diameter and thickness from each section using the protocol described in paragraph 2.3.2.

In agreement with the literature, length of internodes progressively increased from basal to more apical internodes, so that each internode is longer than the one below (Briggs 1978). Results for the internode length, diameter and thickness confirmed observations from the first study, although a higher correlation between internode length and internode number was found in the Scottish trial compared to the Italian one (0.911 and 0.66 respectively).

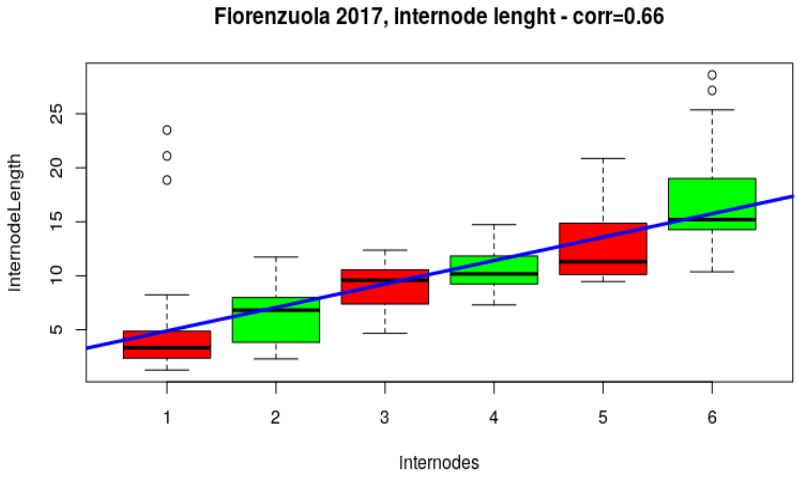

Fig. 4.4 Length of the barley internodes from the first to the sixth, from the Italian trial of 2017. Blue line represent the correlation. The graph shows a progressive increase of the internode length from the basal internodes up to the apical.

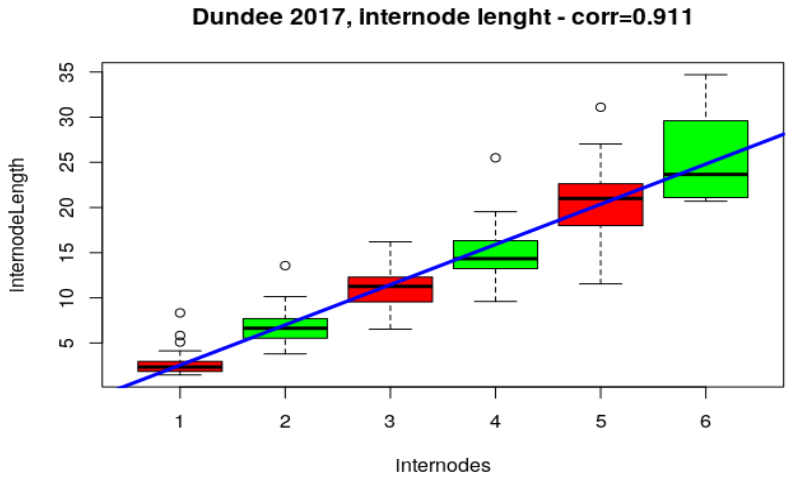

Fig. 4.5 Length of the barley internodes from the first to the sixth, from the UK trial of 2017. Blue line represent the correlation. The graph shows a progressive increase of the internode length from the basal internodes up to the apical.

Regarding culm diameter, the 2nd, 3rd and 4th internodes have a wider diameter compared to the other internodes of the same culm. These data depict the stem structure as a pipe with an ogival– rather than cylindrical- shape. The internodes at the extremities of the stem are those with smaller diameter.

Concerning the diameter no clear differences were found between experiments: the bell shaped pattern is confirmed with the third and the fourth internodes having the wider diameter. The correlations of the two experiments are similar (-0.01 and 0.069).

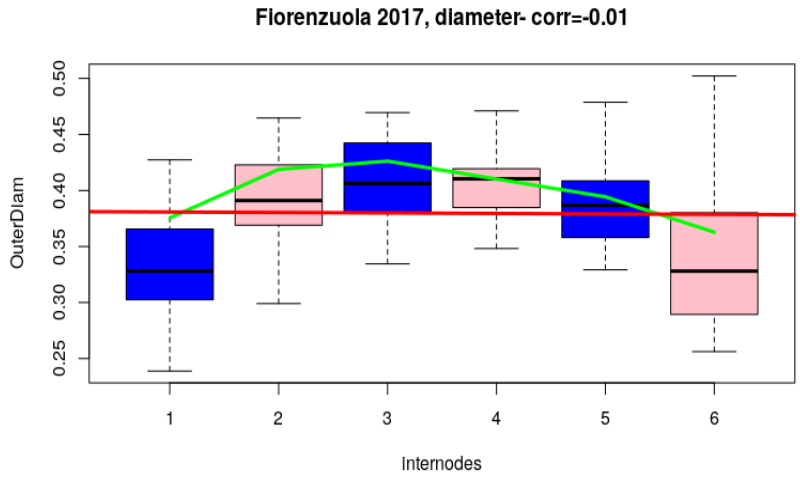

Fig. 4.6 Diameter of the barley internodes from the first to the sixth, from the Italian trial of 2017. The red line represent the correlation, while the green line the mean general trend. The graph shows that the third and fourth internodes have on average a wider diameter if compared to the basal or apical internodes.

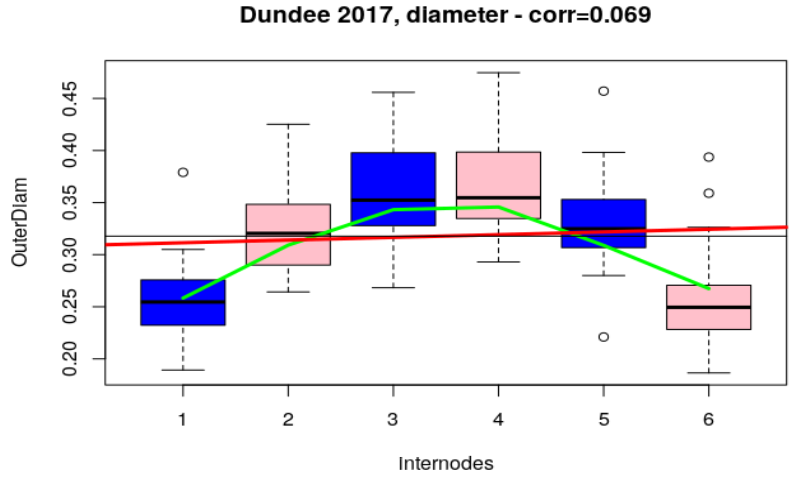

Fig. 4.7 Diameter of the barley internodes from the first to the sixth, from the UK trial of 2017. The red line represent the correlation, while the green line the mean general trend. The graph shows that the third and fourth internodes have on average a wider diameter if compared to the basal or apical internodes.

Furthermore, culm wall thickness progressively decreased from basal to more apical internodes in both experiments, showing a pattern that is opposite to the one of internode length.

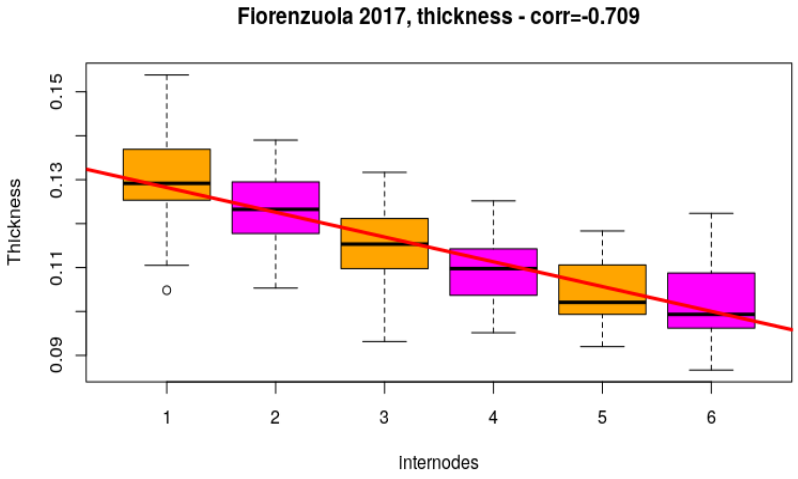

Fig. 4.8 Thickness of the barley internodes from the first to the sixth, from the Italian trial of 2017. The red line represent the correlation, while the green line the mean general trend. The graph shows a progressive decrease of the internode thickness from the basal internodes up to the apical.

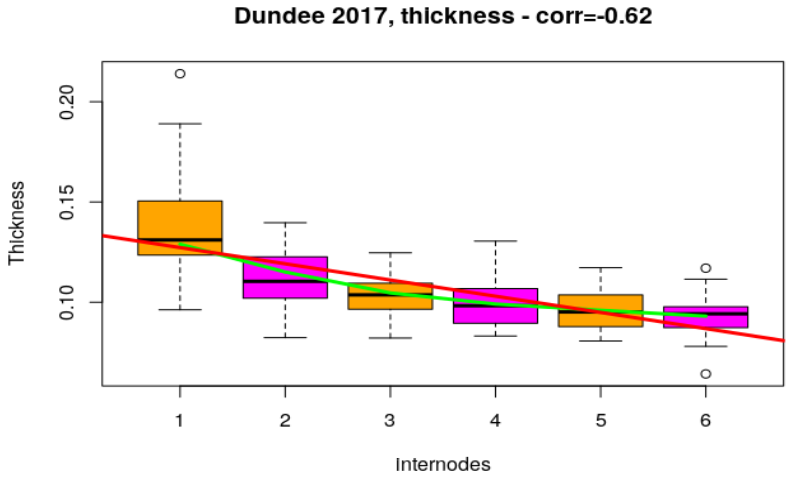

Fig. 4.9 Thickness of the barley internodes from the first to the sixth, from the UK trial of 2017. The red line represent the correlation, while the green line the mean general trend. The graph shows a progressive decrease of the internode thickness from the basal internodes up to the apical.

We also performed ANOVA on diameter and thickness data in order to dissect variance components for these two traits. In the Italian trial diameter is significantly influenced by the genotype (P<0,05) while no significant effect was detected for internode position. Instead thickness is influenced by both internode position and genotype (P<0,001). In the UK trial, ANOVA results confirm that the genotype factor exerts a significant influence on diameter (P<0.01). Also, row-type has a strong influence on the diameter as expected (P<0,001).

Genotype and internode number both have a strong effect on culm wall thickness (P<0,001), while row type was not significant for this trait (P>0.5).

Then, in the Italian trial, we compared the 5 varieties showing second internode diameter/thickness values higher than the total mean with the 5 varieties with an average value of diameter/thickness at the second internode lower than the mean (Figs. 4.7-4.8).The pattern for culm diameter was consistent for the first 4 internodes, with wide-culm varieties clearly separated from thin-culm varieties (Fig.4.7). In the case of thickness, the pattern is consistent along the whole culm, although with more pronounced differences in more basal internodes (Fig. 4.8).

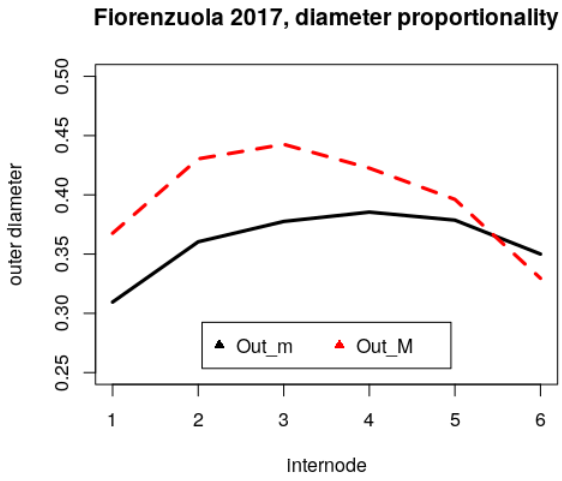

Fig. 4.10 Diameter proportionality across six barley internodes. The x axis refers the number of the internode (from 1 basal to 6 apical). The red dotted line represent the five varieties with diameter value higher than the total mean at the second internode, while the black line represents the other five with an average value of diameter/thickness at the second internode lower than the mean.

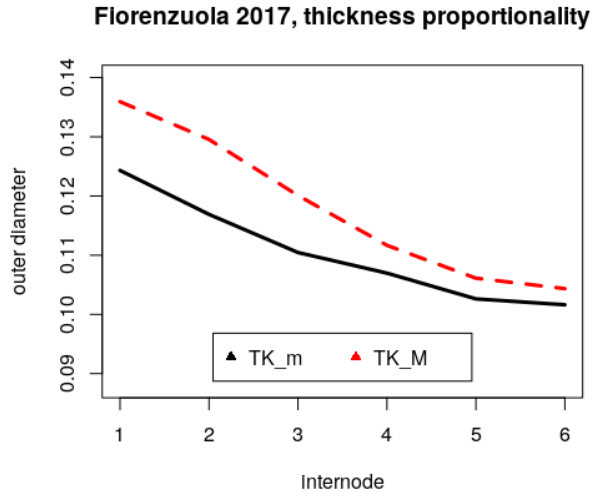

Fig. 4.11 Thickness proportionality across six barley internodes. The x axis refers the number of the internode (from 1 basal to 6 apical). The red dotted line represent the five varieties with thickness value higher than the total mean at the second internode, while the black line represents the other five with an average value of diameter/thickness at the second internode lower than the mean.

In the UK, irrespective of row-type, all plants exhibiting larger diameter/thickness at the second internode also showed higher values for these traits at the other internodes (Fig. 4.12). While six and two rowed barley with diameter/thickness lower than the average at the second internode

show similar trends, the six row barley with diameter above the average have consistently higher diameter/thickness value if compared with the two row all over the stem (Fig. 4.13) Again from the fifth internodes on the proportionality among the traits/groups became less sharp.

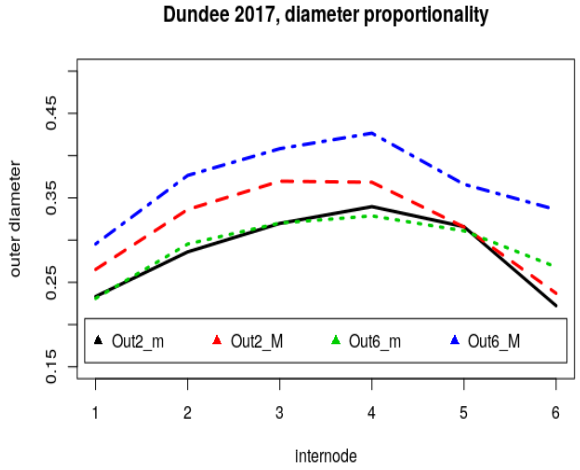

Fig. 4.12 Diameter proportionality across the stem of six- and two-rowed barley. Black line represents two-row varieties with a second internode diameter lower than the average, red line two-row varieties with second internode diameter higher than the average, green line six-row varieties with diameter lower than the average and blue line six-row varieties with diameter higher than the average.

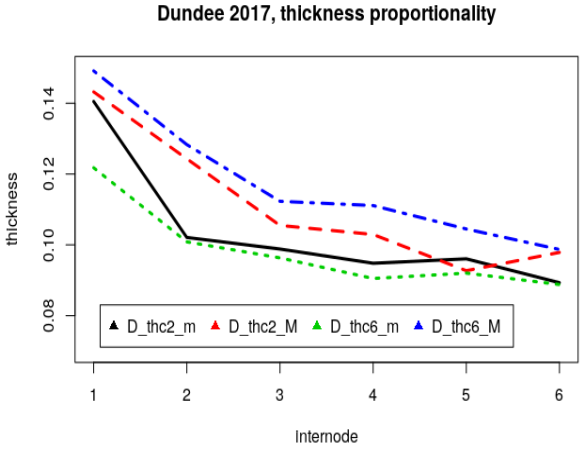

Fig. 4.13 Thickness proportionality across the stem of six- and two-rowed barley. Black line represents two-row varieties with a second internode thickness lower than the average, red line two-row varieties with second internode thickness higher than the average, green line six-row varieties with thickness lower than the average and blue line six-row varieties with thickness higher than the average.

Taken together, results of these experiments support the reliability of the second internode as a good descriptor of stem features. Graphics with the diameter and thickness trends for each variety can be found in Appendix D.

4.3 POPULATION STRUCTURE AND LINKAGE DISEQUILIBRIUM ANALYSES

After filtering (see paragraph 3.5), a total of 31,360 SNPs was used for subsequent analyses. Population structure analysis based on STRUCTURE and PCA identified two subpopulations according to row-type (two/six-row). Figure 4.17 shows the scatter plot for PCA where principal

component 1 (PC1) sharply discriminates between two- and six-row barley lines, explaining 25% of the variance. Principal component 2 (PC2) accounts just for a 3% of the population variance, and together they reach almost 30% of cumulative variance explained. The two principal components obtained from this analysis were used to correct for population structure in the GWAS.

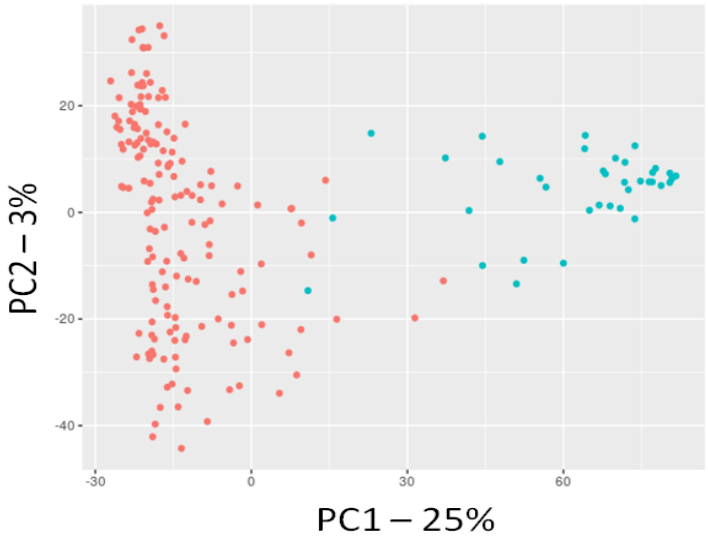

Fig. 4.17 Scatter plot of principal component 1 (PC1) plotted against principal component 2 (PC2). A clear division is visible between two row (red dots) and six row barley (blue dots).

The results obtained by STRUCTURE software were analyzed by Structure Harvester confirming PCA output (fig.4.18).

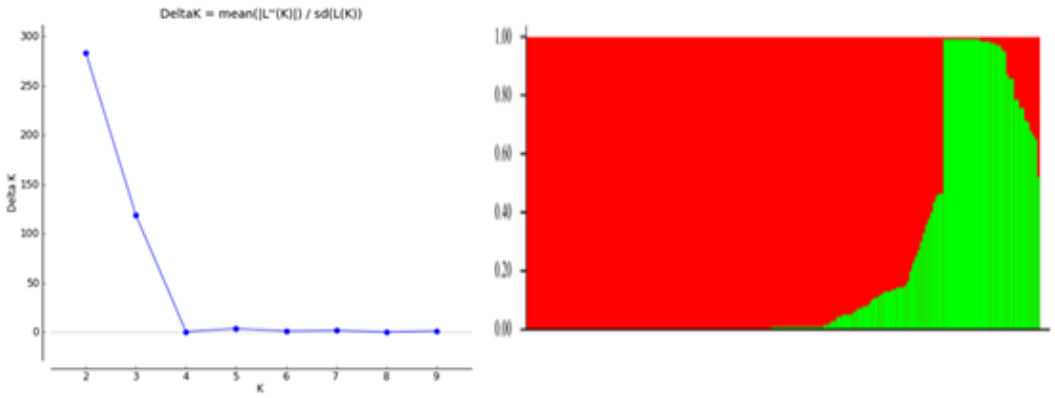

Fig. 4.18 Outputs from the STRUCTURE Harvester website concerning the structure of our population. The graph on the left is a scree plot and the position of the highest peak suggest the optimal number of subpopulation based on the Tracy -Widom method in our case two (Patterson, Price et al. 2006). The graph on the right instead shows how each variety could be clustered in these two subpopulation: the red area represents the % of belonging of a variety to the two row barley group, while the green area refers to the % of belonging of each variety at the six row group.

Linkage disequilibrium decay was evaluated based on a total of 2,103,851 significant pairwise comparisons between markers within the same chromosome. The genome-wide threshold value avarage was $r^2 = 0.18$ and the fitted smoothed LOESS curve crossed the threshold in different

positions for each chromosome. Using the R package LDcorSV we also corrected for population structure using the STRUCTURE file output (Mangin, Siberchicot et al. 2012).

The point on the x axis at the intercept of the LOESS curve and the r^2threshold is the estimated LD decay score for each chromosome. Average LD decay was 1.55, 1.02, 1.27, 0.87, 0.86, 1.22 and 1.17 Mbp for chromosomes, from 1H to 7H,respectively (Fig. 4.19). The average LD decay across the whole genome is 1.14 Mbp.

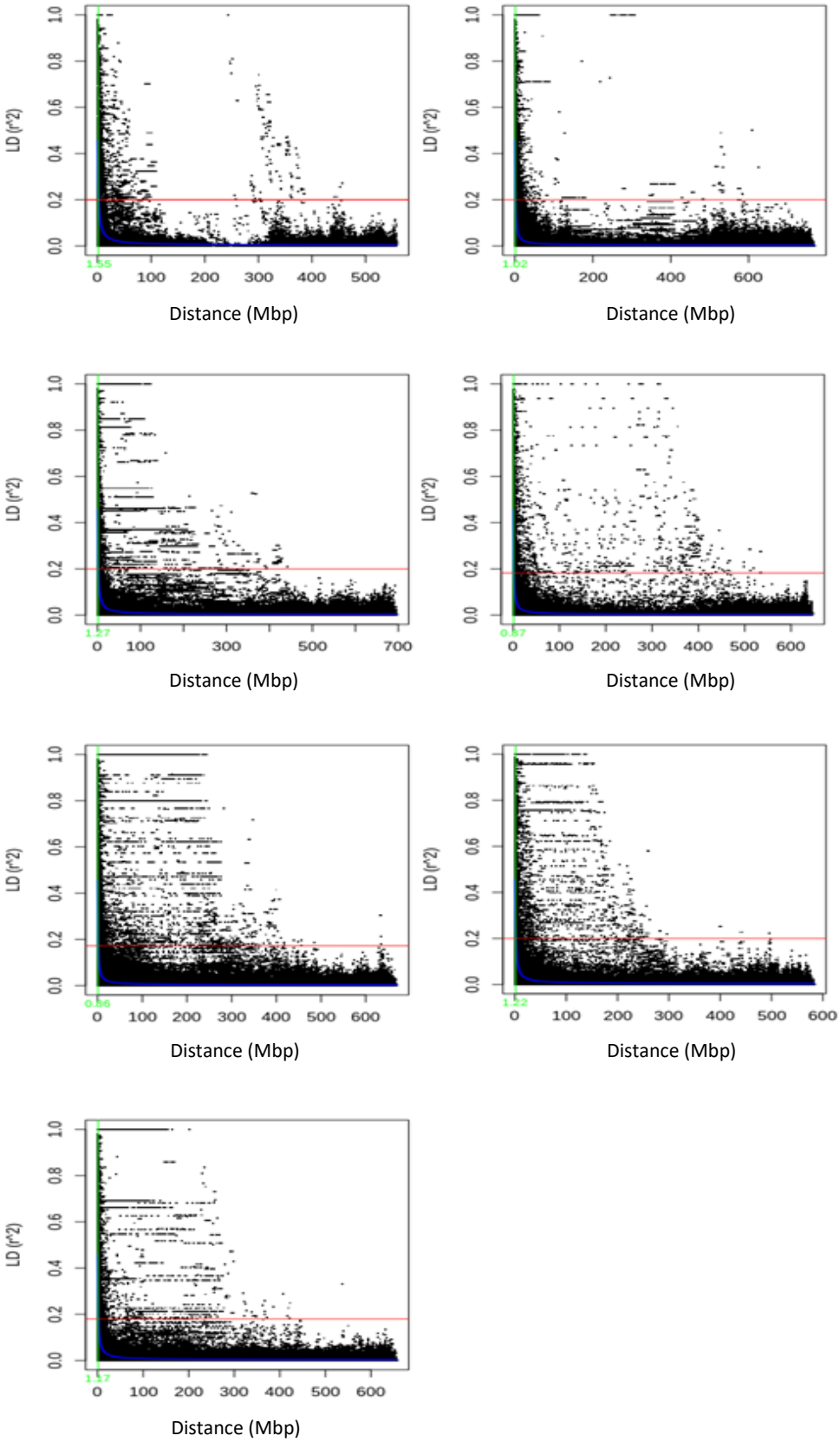

Fig. 4.19 LD decay plot for each of seven barley chromosomes.

4.4 PHENOTYPIC AND GENETIC ANALYSES OF CULM MORPHOLOGICAL TRAITS IN MULTI-ENVIRONMENT FIELD TRIALS (HARVEST STAGE – Zadoks 90)

4.4.1 Field trials

In order to explore phenotypic variation for culm traits, second internodes were collected from plants at Zadocks stage 90 (fully mature) in the years 2016 and 2017 from field trials conducted in four European locations in Italy (Fiorenzuola d'Arda), Spain (Zaragoza), Finland (Helsinki) and UK (Dundee). Our image analysis protocol (see section 3.3) was applied to extract quantitative data for culm diameter and culm wall thickness and their ratio (i.e. stiffness, ST); where available, data for plant height kindly provided by ClimBar partners were also considered and used to calculate stem index (SI), i.e. the ratio between culm diameter and plant height (plant height was not measured in the 2016 Spain field trial). Explorative statistics for these traits are presented for each location and year in Table 4.4.

	2016					2017				
Trial - trait	Min.	Mean	Max.	SD	HER %	Min.	Mean	Max.	SD	HER %
UK Diameter	0.243	0.3399	0.489	0.046	82.4	0.215	0.3308	0.472	0.039	70.5
UK Thickness	0.069	0.1075	0.169	0.017	69.2	0.065	0.1007	0.15	0.013	36
UK Stem Index	0.2655	0.4629	0.7353	0.082	85	0.2395	0.4019	0.6401	0.061	76.1
UK Stiffness	2.12	3.208	4.486	0.45	44.13	1.733	3.32	5.123	0.45	14.7
UK PlantHeight	49.5	74.99	133.25	12.74	94.34	51.25	83.36	132.25	10.95	93.9
ITA Diameter	0.303	0.4153	0.556	0.044	65.46	0.288	0.3886	0.507	0.039	53.6
ITA Thickness	0.079	0.1124	0.17	0.015	18.45	0.09	0.1205	0.159	0.011	55.33
ITA Stem Index	0.3157	0.4747	0.6649	0.064	66.64	0.2824	0.4675	0.6967	0.063	73.78
ITA Stiffness	2.343	3.742	5.433	0.493	28	2.147	3.241	4.307	0.337	12.8
ITA PlantHeight	60	88.3	125	9.39	84.37	58.33	83.81	113.67	8.39	85.51
FIN Diameter	0.18	0.2583	0.41	0.039	75.19	0.24	0.3479	0.485	0.04	74.5
FIN Thickness	NA	NA	NA	NA	NA	0.055	0.09817	0.14025	0.01	27.8
FIN Stem Index	0.3175	0.5115	0.7736	0.082	74.3	0.3077	0.4759	0.6807	0.064	80.1
FIN Stiffness	NA	NA	NA	NA	NA	2.499	3.561	4.638	0.35	30.4
FIN PlantHeight	35	51.19	84.4	8.37	93.1	52.4	74.13	113.6	11.94	96.4
SPA Diameter	0.361	0.5281	0.687	0.054	63.9	0.251	0.3422	0.482	0.041	76.5
SPA Thickness	0.095	0.1357	0.202	0.019	72.92	0.061	0.09173	0.146	0.014	81.13
SPA Stem Index	NA	NA	NA	NA	NA	0.3359	0.6228	0.9564	0.105	76.65
SPA Stiffness	2.741	3.933	5.179	0.42	54.9	2.11	3.787	5.557	0.53	60.1
SPA PlantHeight	NA	NA	NA	NA	NA	34	56.02	98.8	8.95	77.26

Table 4.4 Descriptive statistic regarding diameter, thickness, stem index, stiffness and plan height.

In the 2016 Finnish trial, it was not possible to measure culm thickness (and consequently stiffness) due to the use of a hand caliper to measure the samples. However, high correlation and uniform variance between results obtained from caliper and our image analysis-based protocol (paragraph 4.1) indicate that culm diameter data from this trial can be considered for downstream

analyses together with data from other trials. Also, plant height was not recorded in the 2016 Spanish trial so Stem index could not be calculated in this case.

Distribution of the traits is normal, with value of skewness and kurtosis comprised between -1 and +1 (see Appendix E for histogram and skewness/kurtosis (Sowadan, Li et al. 2018))

Heritability for culm diameter shows promising values with the minimum value in the ITA 2017 trial (53,6%). On the other hand, thickness has lower heritability values compared with diameter, with the exception of the Spanish trials were thickness showed high heritability values (63.9% in 2016 and 81.13% in 2017). Stem index reflects the combination of diameter and plant height with heritability values ranging between 66% (ITA 2016) and 85% (UK 2016). Stiffness instead shows low heritability values, probably as a result of thickness: the maximum value it reaches is 60%.

To compare phenotypic data from the same location in the different years, we conducted t-tests and Kolmorogov-Smirnov test. Results indicate significant differences between the two years, likely deriving from different environmental conditions (e.g. rainfall, temperature, etc.). Nevertheless, for all traits significant Pearson's correlations were obtained between the two years of study within the same location (Table 4.5).

	Diameter	Thickness	Stem Index	Stiffness	PlantHeight
ITA 2016/2017	0.521***	0.327***	0.638***	0.292***	0.548***
UK 2016/2017	0.642***	0.448***	0.729***	0.189*	0.865***
FIN 2016/2017	0.7***	NA	0.50***	NA	0.775***
SPA 2016/2017	0.574***	0.571***	NA	0.361***	NA

Table. 4.5 Pearson correlation tests among the two years for the traits under investigation. Asterisks indicate significant correlations (* for P<0,05, ** for P<0,01 and * for P<0,001).**

In order to explore interrelationships between different morphological and agronomic traits, pairwise Pearson's correlations were calculated for each location and year, considering Plant Height (PH), Grain Yield (GY), Lodging (LoD), Harvest Index (HI), as well as culm Diameter (D), Thickness (TK), Stem index (SI) and Stiffness (ST).

ITALY								
2016	PH	GY	LoD	HI	D	TK	SI	ST
PH	1	-0.24***	0.41***	-0.55***	0.18***	0.1*	-0.64***	0.03
GY		1	-0.32***	0.23*	-0.22***	-0.3***	0	0.14**
LoD			1	-0.42***	0.09	0.2***	-0.24***	-0.14**
HI				1	0	-0.12*	0.42***	0.14**
D					1	0.43***	0.63***	0.36***
TK						1	0.27***	-0.67***
SI							1	0.24***
ST								1
2017	PH	GY	LoD	HI	D	TK	SI	ST
PH	1	0.11*	0.37***	-0.34***	0.11*	-0.03	-0.67***	0.12

GY		1	0.01	0.26***	-0.07	-0.31***	-0.15**	0.22***
LoD			1	-0.29***	-0.2***	-0.12**	-0.41***	-0.09
HI				1	0	-0.01	0.24***	0.02
D					1	0.45***	0.65***	0.54***
TK						1	0.37***	-0.5***
SI							1	0.3***
ST								1

Table 4.6 Pearson correlation scores among the traits in the two Italian trials 2016/2017.

SPAIN								
2016	PH	GY	LoD	HI	D	TK	SI	ST
PH	1	NA	NA	NA	NA	NA	NA	NA
GY		1	NA	NA	NA	NA	NA	NA
LoD			1	NA	NA	NA	NA	NA
HI				1	NA	NA	NA	NA
D					1	0.65***	NA	0.1*
TK						1	NA	-0.68***
SI							1	NA
ST								1
2017	PH	GY	LoD	HI	D	TK	SI	ST
PH	1	0.02	0.41***	-0.24***	0.26***	0.17***	-0.71***	0.01
GY		1	-0.05	0.24***	-0.14**	-0.52***	-0.17**	0.44***
LoD			1	-0.12*	-0.11*	0.08	-0.4***	-0.17***
HI				1	0.02	0	0.2***	0.04
D					1	0.5***	0.46***	0.3***
TK						1	0.22***	-0.66***
SI							1	0.18***
ST								1

Table 4.7 Pearson correlation scores among the traits in the two Spanish trials 2016/2017.

UNITED KINGDOM								
2016	PH	GY	LoD	HI	D	TK	SI	ST
PH	1	-0.51***	0.3***	-0.52***	0.27***	0.34***	-0.69***	-0.14**
GY		1	-0.32***	0.29***	-0.33***	-0.32***	0.22***	0.07
LoD			1	-0.07	0.09*	0.14**	-0.18***	-0.08*
HI				1	0.08	-0.07	0.49***	0.15**
D					1	0.57***	0.49***	0.28***
TK						1	0.12*	-0.61***
SI							1	0.32***
ST								1
2017	PH	GY	LoD	HI	D	TK	SI	ST
PH	1	-0.39***	0.21***	-0.56***	0.25***	0.21***	-0.64***	0.01
GY		1	-0.31***	0.31***	-0.2***	-0.34***	0.16**	0.18***
LoD			1	-0.18**	-0.05	0.09*	-0.2***	-0.14*
HI				1	0.05	0	0.49***	0.04
D					1	0.41***	0.57***	0.46***
TK						1	0.14**	-0.61***
SI							1	0.35***
ST								1

Table 4.8 Pearson correlation scores among the traits in the two UK trials 2016/2017.

FINLAND								
2016	PH	GY	LoD	HI	D	TK	SI	ST
PH	1	-0.08	0.3***	-0.3***	0.42***	NA	-0.55***	NA

GY		1	-0.13**	0.61***	-0.25***	NA	-0.15*	NA
LoD			1	-0.08	0.3***	NA	-0.02	NA
HI				1	-0.34***	NA	-0.03	NA
D					1	NA	0.52***	NA
TK						1	NA	NA
SI							1	NA
ST								1
2017	PH	GY	LoD	HI	D	TK	SI	ST
PH	1	0.03	0.44***	-0.06	0.56***	0.38***	-0.69***	0.21***
GY		1	-0.04	0.38***	0.18***	-0.03	0.13*	0.23***
LoD			1	0.04	0.04	0.07	-0.47***	-0.03
HI				1	0.13**	-0.14*	0.19***	0.29***
D					1	0.6***	0.2***	0.47***
TK						1	0.09	-0.41***
SI							1	0.14**
ST								1

Table 4.9 Pearson correlation scores among the traits in the two Finnish trials 2016/2017.

In all cases, diameter and thickness show of a significant positive correlation, reflecting the strong association of these two trait regardless the environmental conditions. Generally, diameter and thickness also showed positive and significant correlations with plant height. As expected, plant height was positively correlated with lodging (Berry, Sylvester-Bradley et al. 2007, Berry 2013). At this developmental stage, culm diameter and thickness were also poorly correlated with grain yield, harvest index and lodging. The two indexes show similar correlations against the same trait across the trials. The stem index exhibited positive and significant correlation with harvest index and negative and significant correlation with the lodging scores, largely due to the well-known effect of plant height on lodging (Berry, Sylvester-Bradley et al. 2007, Berry 2013). Stiffness was positively correlated with harvest index and grain yield and negatively with lodging scores, although to lower extent compared with the stem index.

As confirmed by many studies row-type has a strong impact on barley plant architecture and morphology (Komatsuda, Maxim et al. 2004, Liller, Neuhaus et al. 2015). We evaluated the presence of significant differences between the two- and six-rowed barley for diameter, thickness, stem index, stiffness and plant height across the 8 trials. All data were tested with parametric (t-test) and non-parametric (Wilcoxon-Mann-Whitney test) approaches. The results are consistent between the two approaches. For both diameter and thickness, significant differences were uncovered between row-types, with the six-row varieties showing on average larger values than two-row (Fig. 4.14).

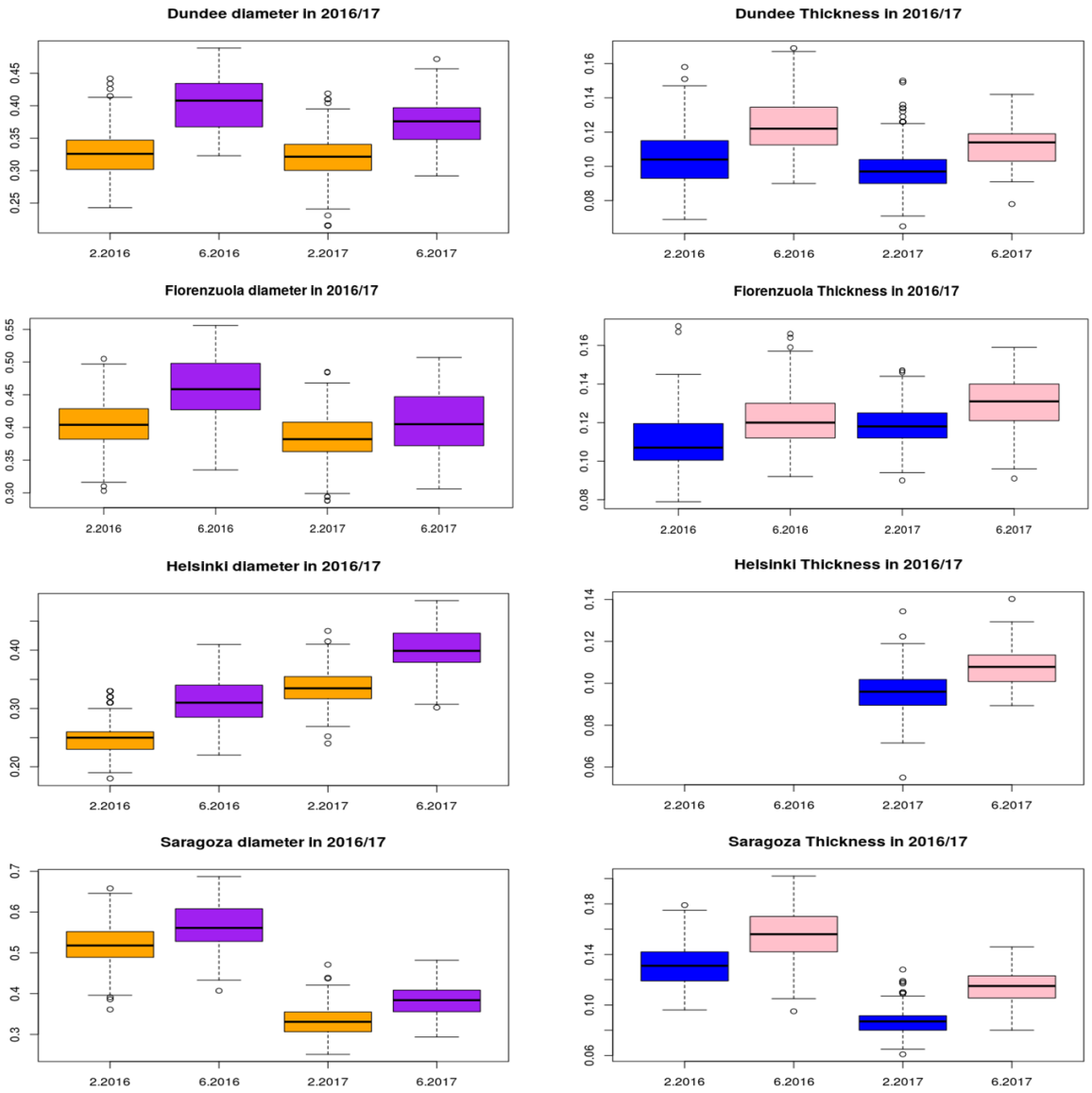

Fig. 4.14 Boxplots for the diameter (left) and thickness (right) in the 4 locations among the 2016/2017 trials. It is possible to see how six row varieties (purple for diameter, pink for thickness) have higher average values compared with the two row (orange for diameter, blue for thickness).

Accordingly, six-row barley cultivars had higher mean values of stem index (only in the 2017 Finnish trial two-row barley had higher values).

The situation for stiffness is more complex: in all Scottish and Italian trials, no clear difference was found between row-types, while in Spain, for both trials, two-row barleys had higher stiffness. In Finland 2017 stiffness is on average greater for the six-row varieties (Fig 4.15).

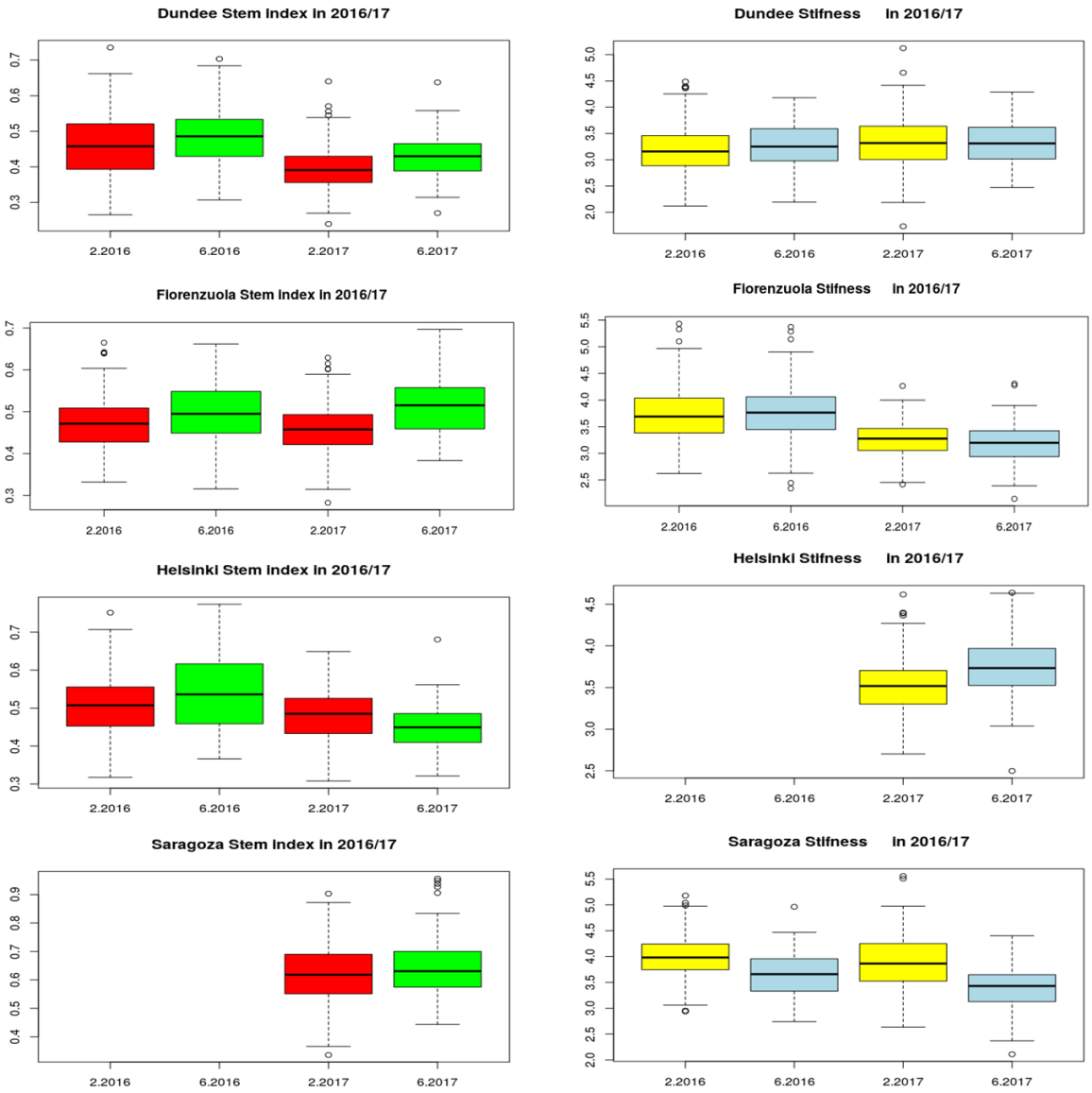

Fig. 4.15 Boxplots for the stem index (left) and stiffness (right) in the 4 locations among the 2016/2017 trials. For the stem index, six-row barely (green) have on average higher value compared with two-row (red); only exception is Finland 2016. For the stiffness there are no clear differences in the Italian and UK trials, but discrepancies appear in Finnish trial where six rowed barley (light blue) has an higher stiffness value if compared with the two rowed (yellow). Instead in both Spanish trials two row barley has a greater stiffness if compared with the six row.

In conclusion, good variability was found for the studied traits in all trials. Furthermore, high heritability values support the usefulness of the selected panel for genetic dissection to try to identify genomic regions and genes controlling our traits of interest. It is also important to notice that even if diameter and thickness show positive correlation with the plant height across the environments, it could be still possible to manipulate these traits separately from the plant height.

4.4.1 Genotype by environment interactions

The environmental conditions greatly differed among the eight field trials for climatic conditions, day-length and soil composition - all factors that directly affect plant development. To conduct

AMMI analysis 12 varieties were removed from each trial in order to guarantee a balanced condition necessary to run the ANOVA; those varieties are: Ceylon, Domen, Erkki, Herse, Isabella, Kenia, Kilta, Pirkka, Pohto, Rondo, Spartan and Stendes. As already mentioned, in the 2016 Spanish trial data for plant height were not collected, so this location was removed from the plant height and stem index AMMI analyses. Similarly, no data for culm thickness were available from the 2016 Finnish trial, causing the exclusion of this trial from the thickness and stiffness AMMI evaluation. A total of 185 varieties for each trial were tested in double replicate: environmental means and variances are presented in Table 4.10.

Env	N. obs	Diam (cm)	Diam σ^2	PH (cm)	PH σ^2	SI	SI σ^2	TK (cm)	TK σ^2	ST	ST σ^2
FIN16	370	0.2578	0.00154	51.11	69.1	0.5116	0.00694	NA	NA	NA	NA
FIN17	370	0.3455	0.00155	73.85	135.5	0.4745	0.00393	0.0978	0.000117	3.551	0.1233
ITA16	370	0.4135	0.00184	88.42	91.8	0.4721	0.00397	0.1118	0.000226	3.744	0.2314
ITA17	370	0.3883	0.00152	83.84	70.9	0.4675	0.00409	0.1204	0.000135	3.243	0.1157
SCO16	370	0.3406	0.00214	75.16	163.1	0.4626	0.00658	0.1079	0.000327	3.205	0.2077
SCO17	370	0.3291	0.00147	83.38	117.1	0.3997	0.00359	0.1001	0.000178	3.325	0.2087
SPA16	370	0.5270	0.00297	NA	NA	NA	NA	0.1350	0.000377	3.945	0.1770
SPA17	370	0.3410	0.00168	55.95	83.0	0.6220	0.0111	0.0912	0.000214	3.795	0.2933

Table 4.10 Environmental means and variance for each trial.

Culm diameter showed higher environmental means in the 2016 Spain trial, possibly as a result of specific management practices which could allow more vigorous plant growth (see paragraph 3.1). In southern locations, culm diameter was on average higher compared to northern sites, probably because of the longer growth period (Fig.4.16). For thickness the effect of the environment was more complex as shown in Figure 4.16, with no clear clustering of the different trials. Furthermore, stem index showed a peculiar pattern with most trials located in the top left of the plot except for SPA 2017, which showed a particularly high value of stem index. This result was partially confirmed by the data from SPA 2017 trial, which have low plant height considering the diameter (Tab. 4.10).

For plant height, no particular trend emerged (Fig. 4.16), with SPA 2017 and FIN 2016 clustering on the left side of the plot away from the rest of the trials.

AMMI analyses showed that on average higher stiffness values characterized southern locations compared to northern sites, with SPA 2017 showing the highest stiffness values.

The AMMI biplot showed that for the diameter SPA16 contributed the most part of the interaction, while genotypes from other environments indicated more stable values among each other. For the thickness genotype means from ITA16 and SPA16 were less stable than other

environments. For the stem index SPA17 contributed most part of the interaction. ITA17, FIN17, and SCO16 were among the environments contributing most part of the interaction for plant height.

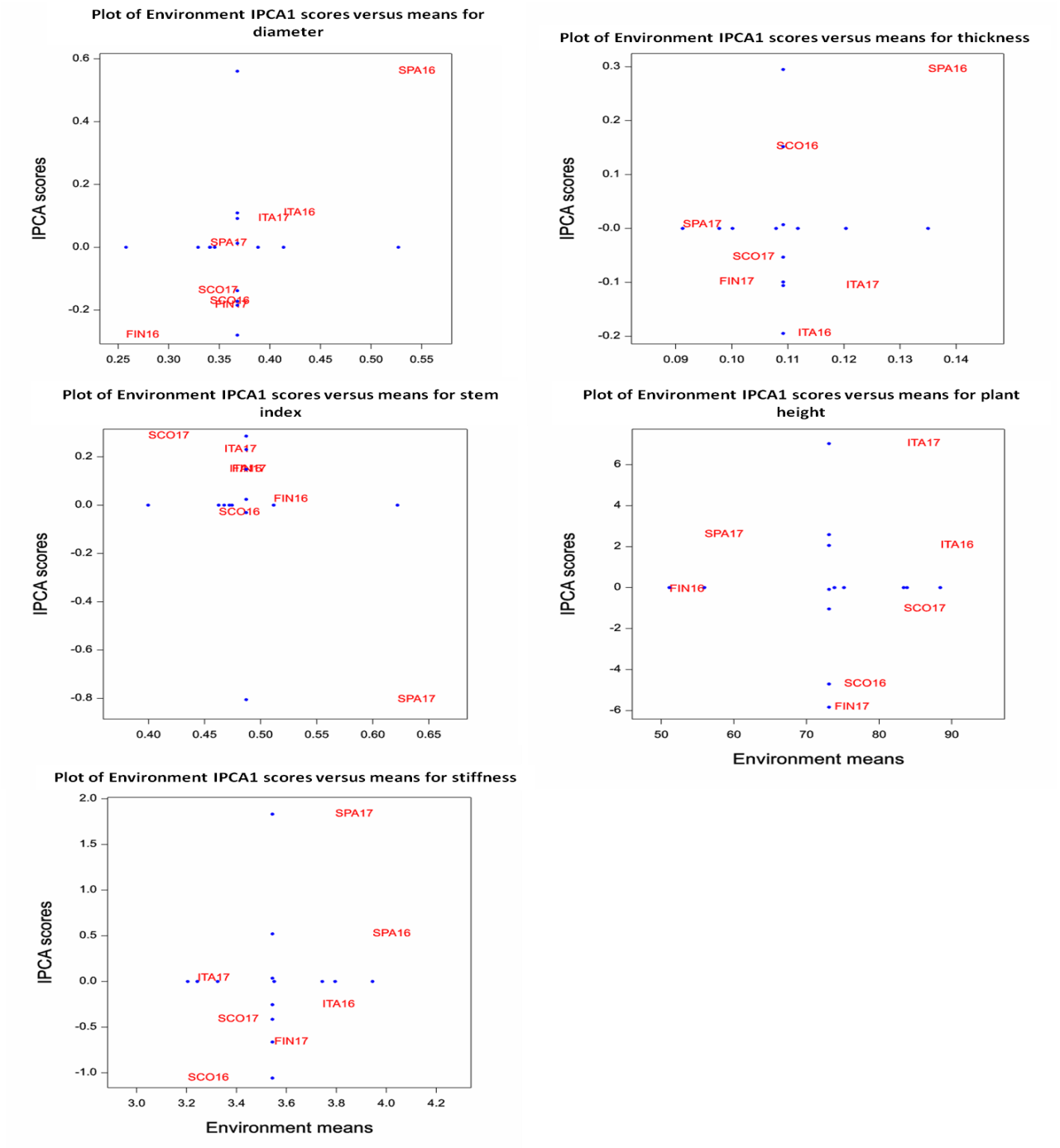

Fig. 4.16 Graphical representation of the AMMI analyses for the traits under investigation. Data for plant height and stem index from SPA 2016 trial are missing. Data for culm thickness and stiffness from FIN 2016 are missing.

Finally, SPA17 and SCO16 were among environments with the contribution to G*E effect for stiffness. The biplots also showed that amongst the studied traits, culm thickness was most affected by G*E interaction showing highly environment-dependent expression. AMMI analysis of

variance indicated highly significant (F < 0.001) effects of genotype, environment and interaction for all traits (Table 4.11). Genotypic factor accounted for largest proportion of the treatment (G+E+G*E) sum of squares for the traits under study.

.

meansquare	Diameter (cm)		Plant Height (cm) & Stem Index			Thickness (cm) &Stiffness		
Source	df	Diam (cm)	df	PH	SI	df	TK	ST
Treatments	1479	0.0136***	1294	540***	0.0171***	1294	0.00068***	0.377***
Genotypes (G)	184	0.0136***	184	928***	0.0426***	184	0.00101***	0.493***
Environments (E)	7	2.2945***	6	76367***	1.7140***	6	0.08223***	31.913***
Block	8	0.0061***	7	379***	0.0154***	7	0.00278***	2.487***
Interactions (G*E)	1288	0.0012***	1104	63***	0.0036***	1104	0.00018***	0.187***
IPCA1	190	0.0026***	189	146***	0.0073***	189	0.00031***	0.311***
IPCA2	188	0.0016***	187	91***	0.0046***	187	0.00026***	0.220***
Residuals	910	0.0009	728	34***	0.0025	728	0.00013	0.146
Error	1432	0.0009	1256	21	0.0023	1262	0.00014	0.148

sum of square	Diameter (cm)		Plant Height (cm) & Stem Index			Thickness (cm) &Stiffness		
Source	df	Diam	df	PH	SI	df	TK	ST
Treatments	1479	20.154	1294	698775	22.135	1294	0.883	488.4
Genotypes (G)	184	2.496	184	170770	7.839	184	0.1862	90.8
Environments(E)	7	16.062	6	458201	10.284	6	0.4934	191.5
Block	8	0.049	7	2653	0.108	7	0.0194	17.4
Interactions (G*E)	1288	1.596	1104	69803	4.013	1104	0.2034	206.1
IPCA1	190	0.492	189	27652	1.376	189	0.0591	58.8
IPCA2	188	0.296	187	17069	0.855	187	0.0482	41.2
Residuals	910	0.808	728	25082	1.783	728	0.0962	106.1
Error	1432	1.289	1256	26353	2.877	1262	0.1715	186.5
% treatments SS due to G	184	12.38	184	24.44	35.42	184	21.09	18.59
% treatments SS due to E	7	79.70	6	65.57	46.46	6	55.88	39.21
% treatments SS due to G*E	1288	7.92	1104	9.99	18.13	1104	23.04	42.20
% G*E SS due to IPCA1	190	30.83	189	39.61	34.29	189	29.06	28.53
% G*E SS due to IPCA2	188	18.55	187	24.45	21.31	187	23.7	19.99

Table 4.11 AMMI analysis results. The first (meansquare) table tell us if the factors (Source colum) have a significant influence on traits; the second table (sum of square) tell us the effect of the factors on each traits.

Genotypic effect accounted for 12,38% of the treatment sum of square (SS) for the Diameter (cm) whilst environment and G*E interaction accounted for 79,7% and 7,92% respectively. The first two interaction principal component axes (IPCA1 and IPCA2) accounted for 49,38% of the interaction sum of squares.For Plant height instead, 24,44% of the treatment sum of squares was due to genotype effect while environment and G*E interaction effect explained 65,57% and 9,9% of the variance, respectively. IPCA1 accounted for 39,61% with IPCA2 accounting for 24,45%.

Additive main effect and multiplicative interaction analysis ranked all the barley cultivars based on the traits under investigation for each environment. In Table 4.12 the 4 top ranking varieties for each trait are shown beside the environmental mean.

Env	DiamMean	1	2	3	4	PH Mean	1	2	3	4
FIN16	0.258	Niina	Teele	Pokko	Potra	51.110	Latvijas	Jadar	Stella	Isaria
FIN17	0.346	Niina	Teele	Pokko	Potra	73.850	Latvijas	Stella	Jadar	Teele
ITA16	0.414	Lise	Potra	Niina	Latvijas	88.420	Latvijas	Morex	Stella	Maskin
ITA17	0.388	Morex	Jadar	Quench	Latvijas	83.840	Latvijas	Isaria	Wisa	Morex
SCO16	0.341	Niina	Teele	Otra	Pokko	75.160	Latvijas	Jadar	Stella	Isaria
SCO17	0.329	Niina	Potra	Lise	Pokko	83.380	Latvijas	Jadar	Isaria	Vankkuri
SPA16	0.527	Artturi	Niina	Frisia	Lise	/	/	/	/	/
SPA17	0.341	Niina	Potra	Lise	Pokko	55.950	Morex	Latvijas	Stella	Maskin
Env	TK Mean	1	2	3	4	SI Mean	1	2	3	4
FIN16	/	/	/	/	/	0.512	Botnia	Pokko	Arra	Potra
FIN17	0.098	Teemu	Jadar	Morex	Arra	0.475	Quench	Cooper	Artturi	Perun
ITA16	0.112	Teemu	Stella	Asplund	Tammi	0.472	Quench	Cooper	Artturi	Eero
ITA17	0.120	Teemu	Artturi	Jadar	Arra	0.468	Quench	Arra	Potra	Artturi
SCO16	0.108	Pokko	Niina	Jadar	Potra	0.463	Quench	Botnia	Eero	Cooper
SCO17	0.100	Jadar	Morex	Niina	Arra	0.400	Quench	Artturi	Arra	Perun
SPA16	0.135	Artturi	Frisia	Eero	Agneta	/	/	/	/	/
SPA17	0.091	Jadar	Niina	Morex	Artturi	0.622	Botnia	Tammi	Eero	Pokko
Env	ST Mean	1	2	3	4					
FIN16	/	/	/	/	/					
FIN17	3.551	Quench	Forum	Teele	Annabell					
ITA16	3.744	Armelle	Agneta	Beatrix	Optic					
ITA17	3.243	Forum	Quench	Hanka	Pasadena					
SCO16	3.205	Agneta	Teele	Annabel l	Silja					
SCO17	3.325	Egmont	Asplund	Binder	Corgi					
SPA16	3.945	Hanka	Egmont	Binder	Quench					
SPA17	3.795	Smilla	Latvijas	Lux	Dandy					

Table 4.12 Top ranking varieties for the different traits in across all the trials.

Variety Niina has a good score for diameter in almost all locations, while it does not show the same trend for culm wall thickness , making of it a good candidate for future breeding programs. For plant height, cultivar Latvijas ranks first across all trials, followed by Jadar and Isaria. For culm wall thickness, the situation is not so uniform with different ranking of varieties in the different field trials, although Teemu and Jadar show high values for this trait in several environments. Quench and Botnia are the top ranking varieties for stem index, while in the case of stiffness, ranking of varieties is different for each field trial.

These results together depict a complex scenario for influence of the environments on the traits under investigation. Nonetheless, the genotype effects were considerable for these traits providing a starting point for further association mapping analyses.

4.4.2 Genome wide association mapping

To find markers associated with the traits under study the phenotypic data for culm diameter, plant height, culm wall thickness, stem Index and stiffness were integrated with the 50k iSelect markers panel (paragraph 3.5). After imputation and filtering for a minor allele frequency (MAF>5% the final number of SNPs markers used was 31360.

Analyses were run for each single environment correcting for population structure using PCA and kinship.

Plant height was initially used as a benchmark traits since several gene are known in barley to have direct effect on it (Kuczynska and Wyka 2011, Kuczyńska, Surma et al. 2013).

Considering all trials, 22, 32, 25, 15, 18 significant marker-trait associations for Diameter, Plant Height, Stem Index, Stiffness and Thickness, respectively, were detected using a Bonferroni correction to reduce the occurrence of false positive.

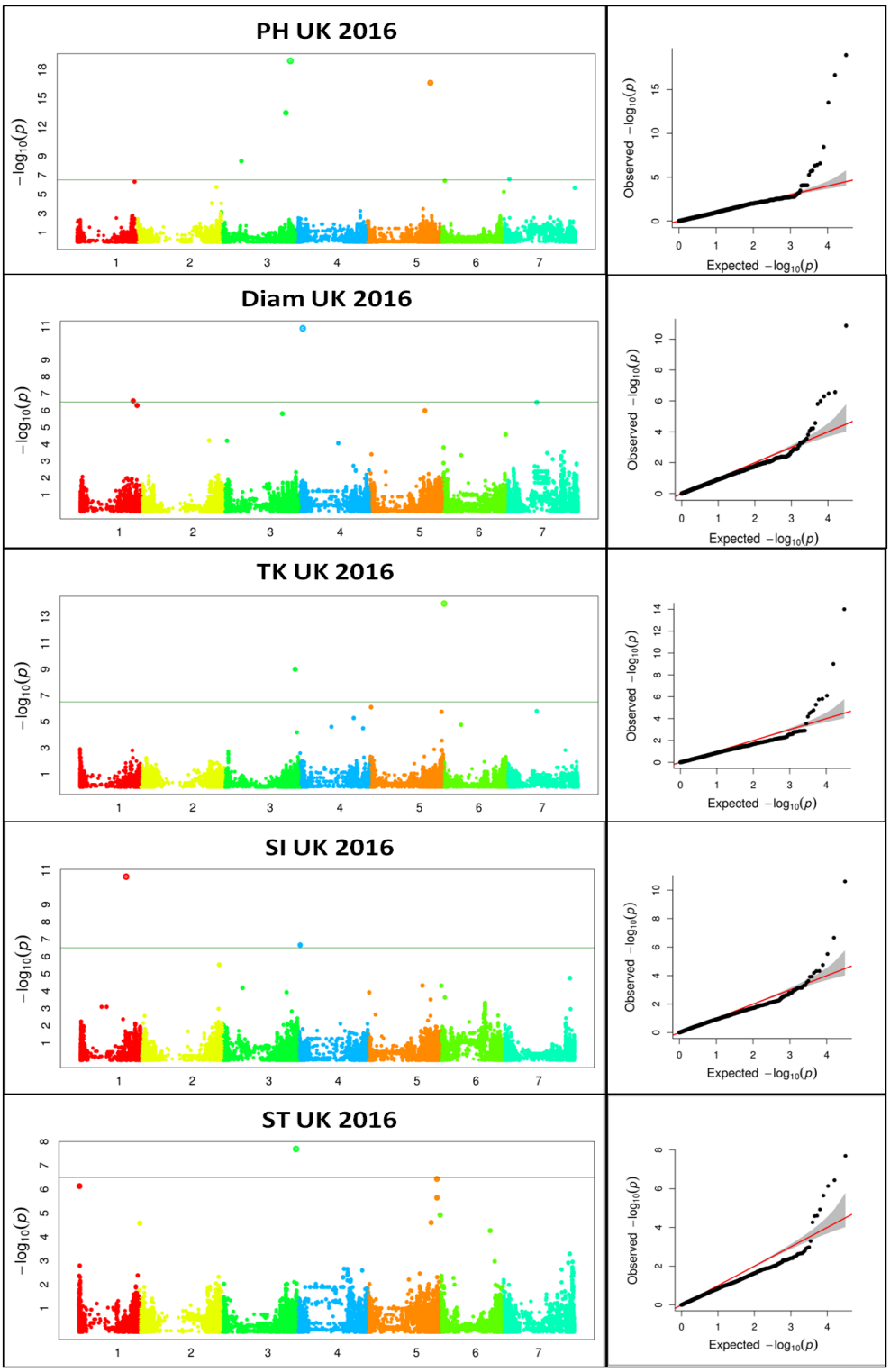

Fig. 4.17 Manhattan plot and QQ plot for the GWAS analyses carried out on the samples from UK 2016 trial. From the top to the bottom the traits analyzed are plant height (PH), diameter (diam), thickness (TK), stem index (SI) and stiffness (ST). In the Manhattan plot the green line represent the significance threshold calculated by the Bonferroni correction. The QQ plots show the expected distributions of association tests (X-axis) across the million SNPs compared to the observed association values of the SNPs (Y-axis). Any deviation from the X=Y line implies a consistent association of the SNP with the studied trait.

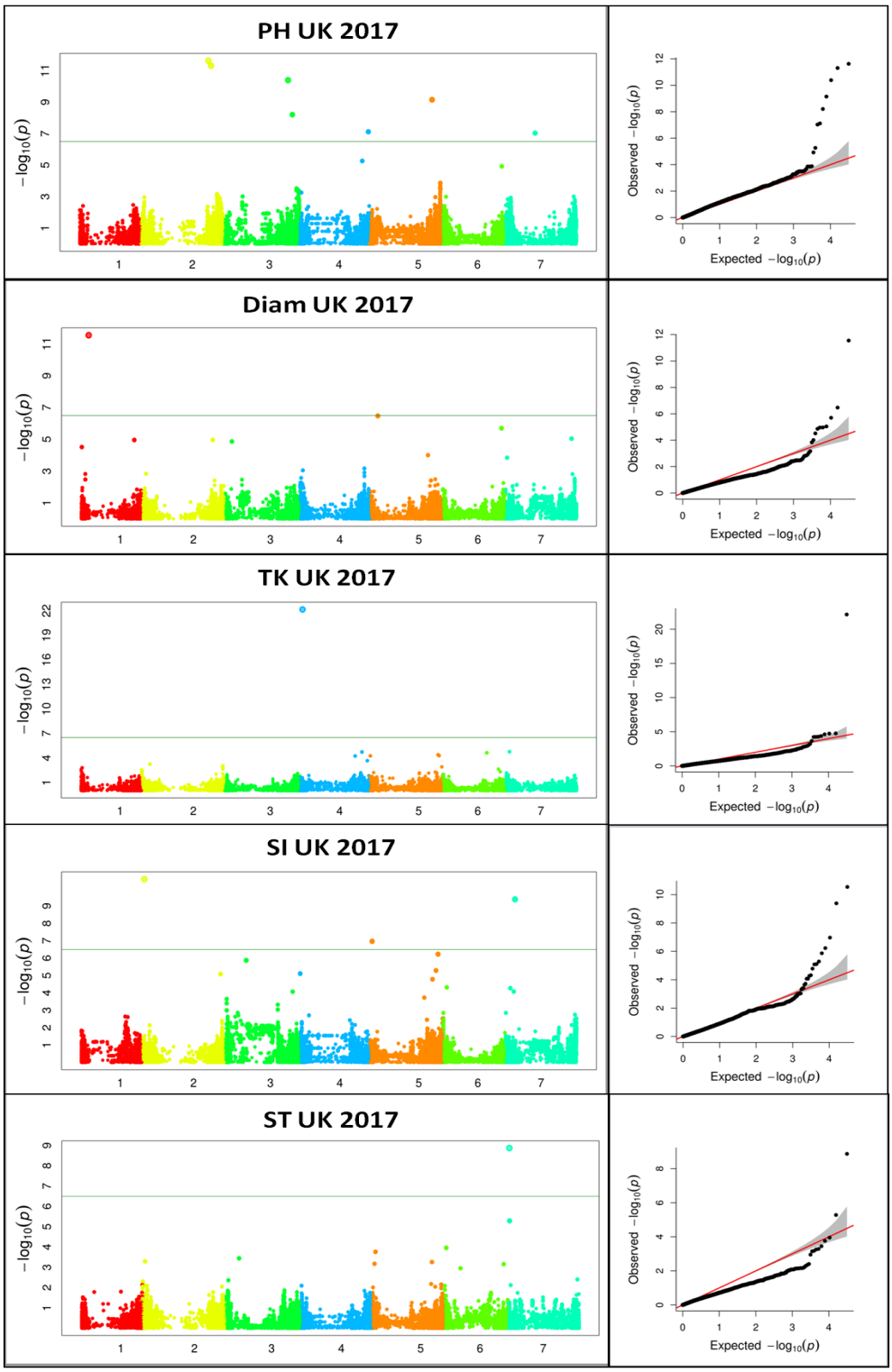

Fig. 4.18 Manhattan plot and QQ plot for the GWAS analyses carried out on the samples from UK 2017 trial. From the top to the bottom the traits analyzed are plant height (PH), diameter (diam), thickness (TK), stem index (SI) and stiffness (ST). In the Manhattan plot the green line represent the significance threshold calculated by the Bonferroni correction. The QQ plots show the expected distributions of association tests (X-axis) across the million SNPs compared to the observed association values of the SNPs (Y-axis). Any deviation from the X=Y line implies a consistent association of the SNP with the studied trait.

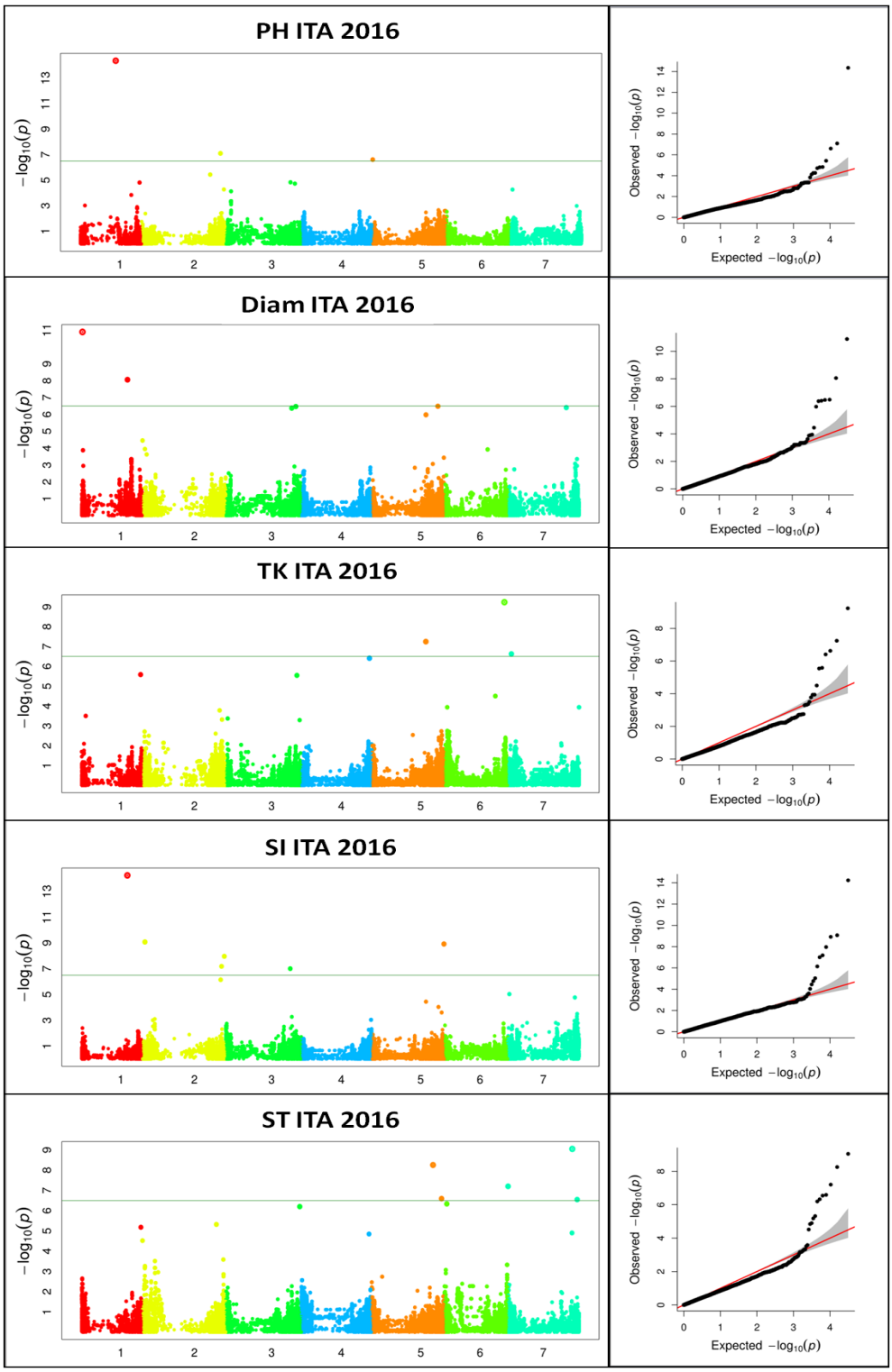

Fig. 4.19 Manhattan plot and QQ plot for the GWAS analyses carried out on the samples from ITA 2016 trial. From the top to the bottom the traits analyzed are plant height (PH), diameter (diam), thickness (TK), stem index (SI) and stiffness (ST). In the Manhattan plot the green line represent the significance threshold calculated by the Bonferroni correction. The QQ plots show the expected distributions of association tests (X-axis) across the million SNPs compared to the observed association values of the SNPs (Y-axis). Any deviation from the X=Y line implies a consistent association of the SNP with the studied trait.

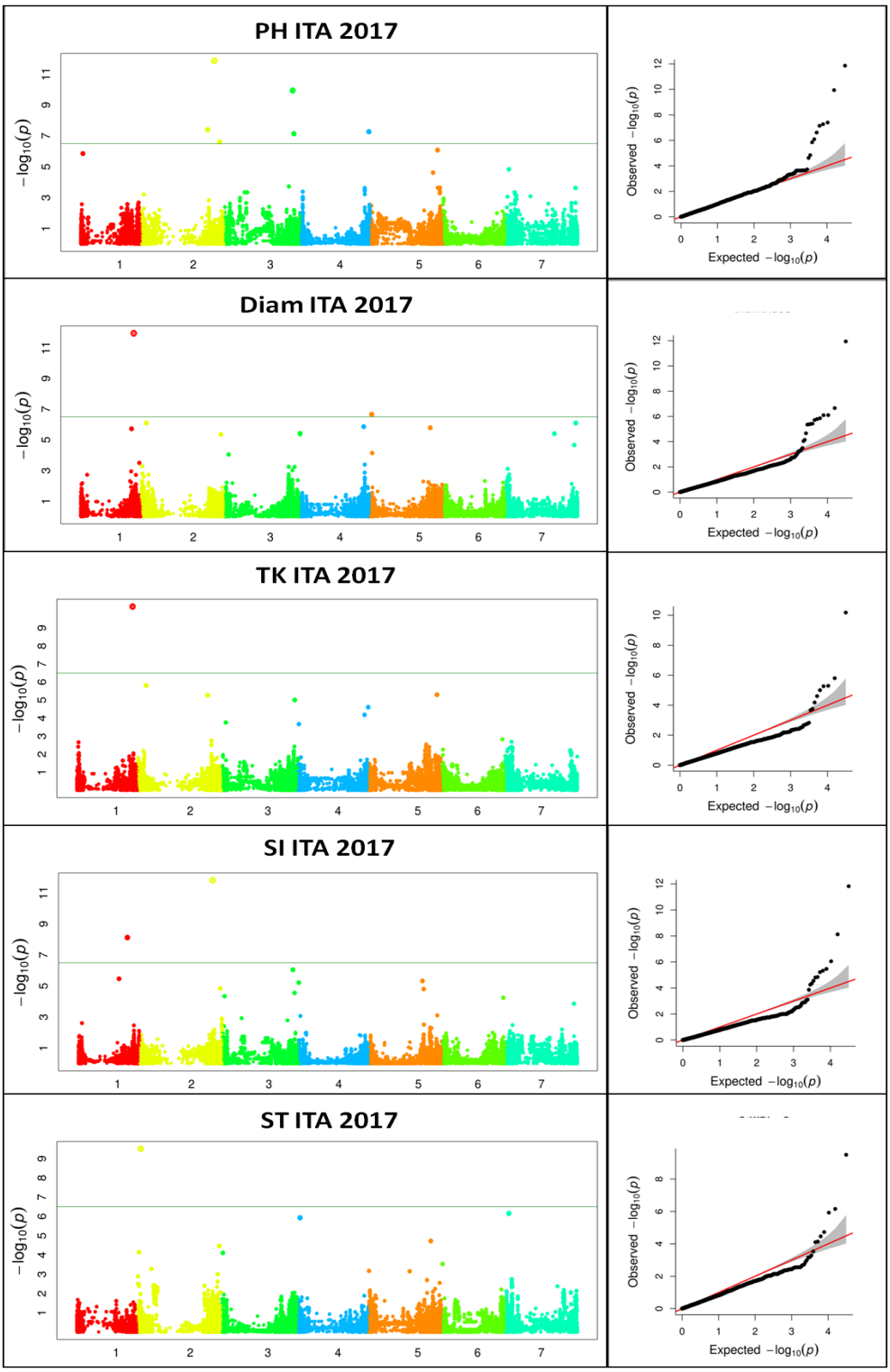

Fig. 4.20 Manhattan plot and QQ plot for the GWAS analyses carried out on the samples from ITA 2017 trial. From the top to the bottom the traits analyzed are plant height (PH), diameter (diam), thickness (TK), stem index (SI) and stiffness (ST). In the Manhattan plot the green line represent the significance threshold calculated by the Bonferroni correction. The QQ plots show the expected distributions of association tests (X-axis) across the million SNPs compared to the observed association values of the SNPs (Y-axis). Any deviation from the X=Y line implies a consistent association of the SNP with the studied trait.

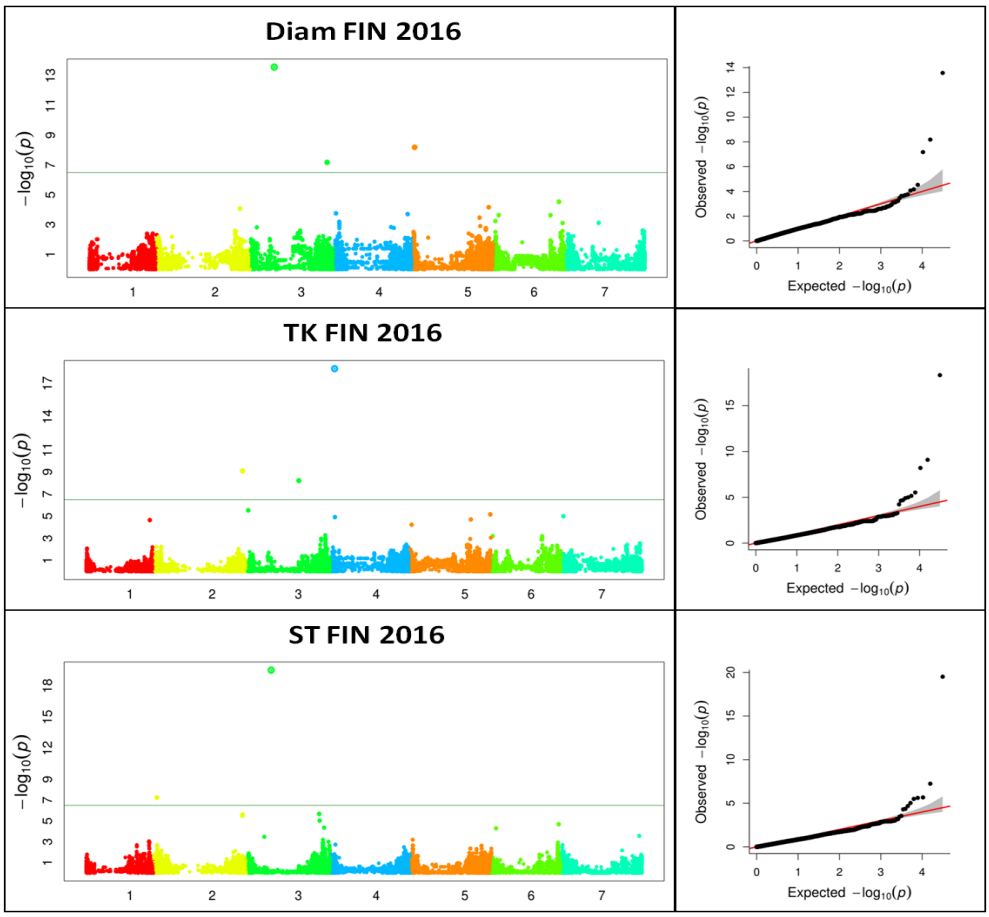

Fig. 4.21 Manhattan plot and QQ plot for the GWAS analyses carried out on the samples from FIN 2016 trial. From the top to the bottom the traits analyzed are plant height (PH), diameter (diam), thickness (TK), stem index (SI) and stiffness (ST). In the Manhattan plot the green line represent the significance threshold calculated by the Bonferroni correction. In this trial data about culm thickness and stiffness are missing. The QQ plots show the expected distributions of association tests (X-axis) across the million SNPs compared to the observed association values of the SNPs (Y-axis). Any deviation from the X=Y line implies a consistent association of the SNP with the studied trait.

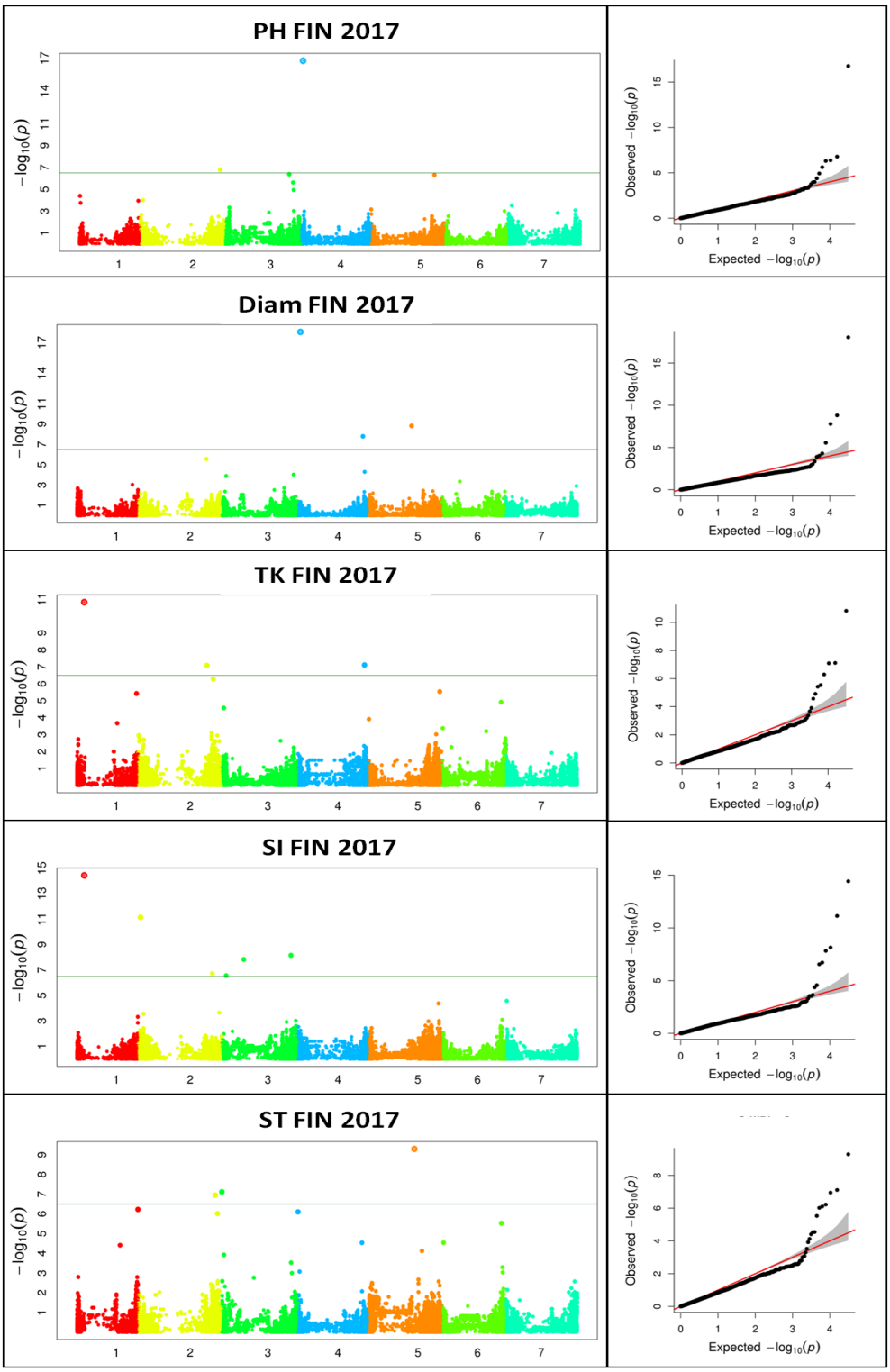

Fig. 4.22 Manhattan plot and QQ plot for the GWAS analyses carried out on the samples from FIN 2017 trial. From the top to the bottom the traits analyzed are plant height (PH), diameter (diam), thickness (TK), stem index (SI) and stiffness (ST). In the Manhattan plot the green line represent the significance threshold calculated by the Bonferroni correction. The QQ plots show the expected distributions of association tests (X-axis) across the million SNPs compared to the observed association values of the SNPs (Y-axis). Any deviation from the X=Y line implies a consistent association of the SNP with the studied trait.

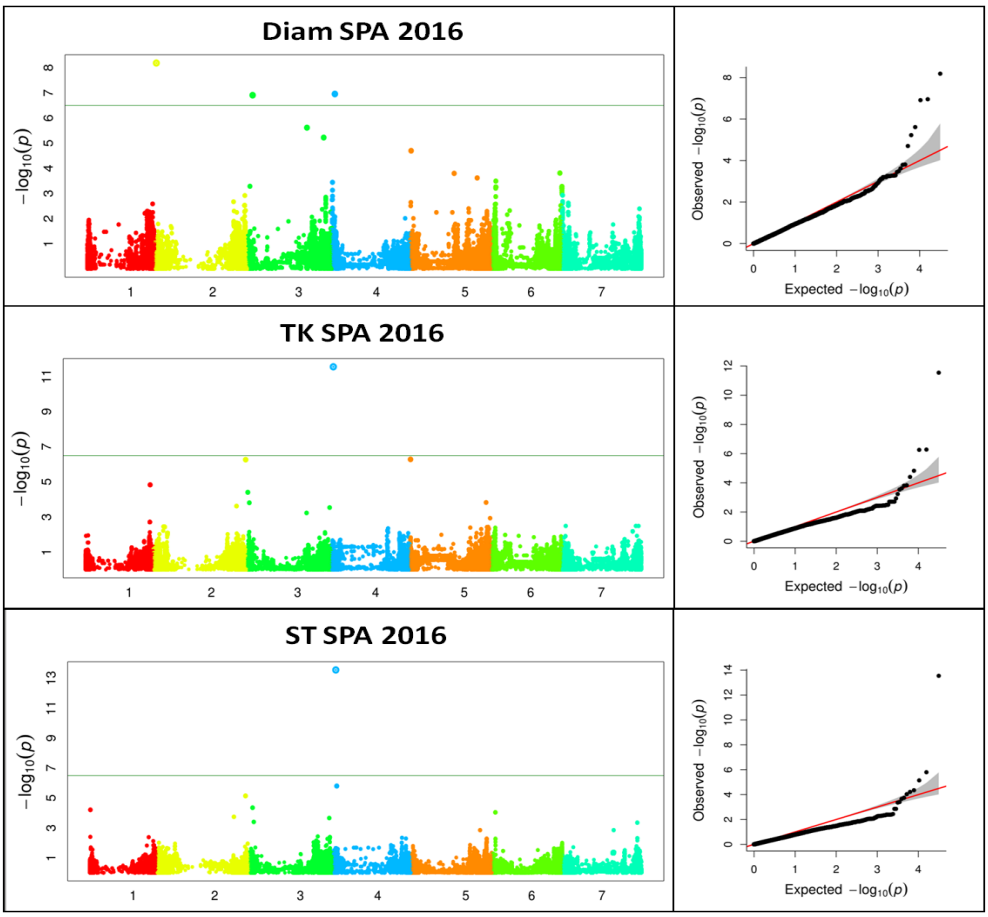

Fig. 4.23 Manhattan plot and QQ plot for the GWAS analyses carried out on the samples from SPA 2016 trial. From the top to the bottom the traits analyzed are plant height (PH), diameter (diam), thickness (TK), stem index (SI) and stiffness (ST). In the Manhattan plot the green line represent the significance threshold calculated by the Bonferroni correction. In this trial data about plant height and stem index are missing. The QQ plots show the expected distributions of association tests (X-axis) across the million SNPs compared to the observed association values of the SNPs (Y-axis). Any deviation from the X=Y line implies a consistent association of the SNP with the studied trait.

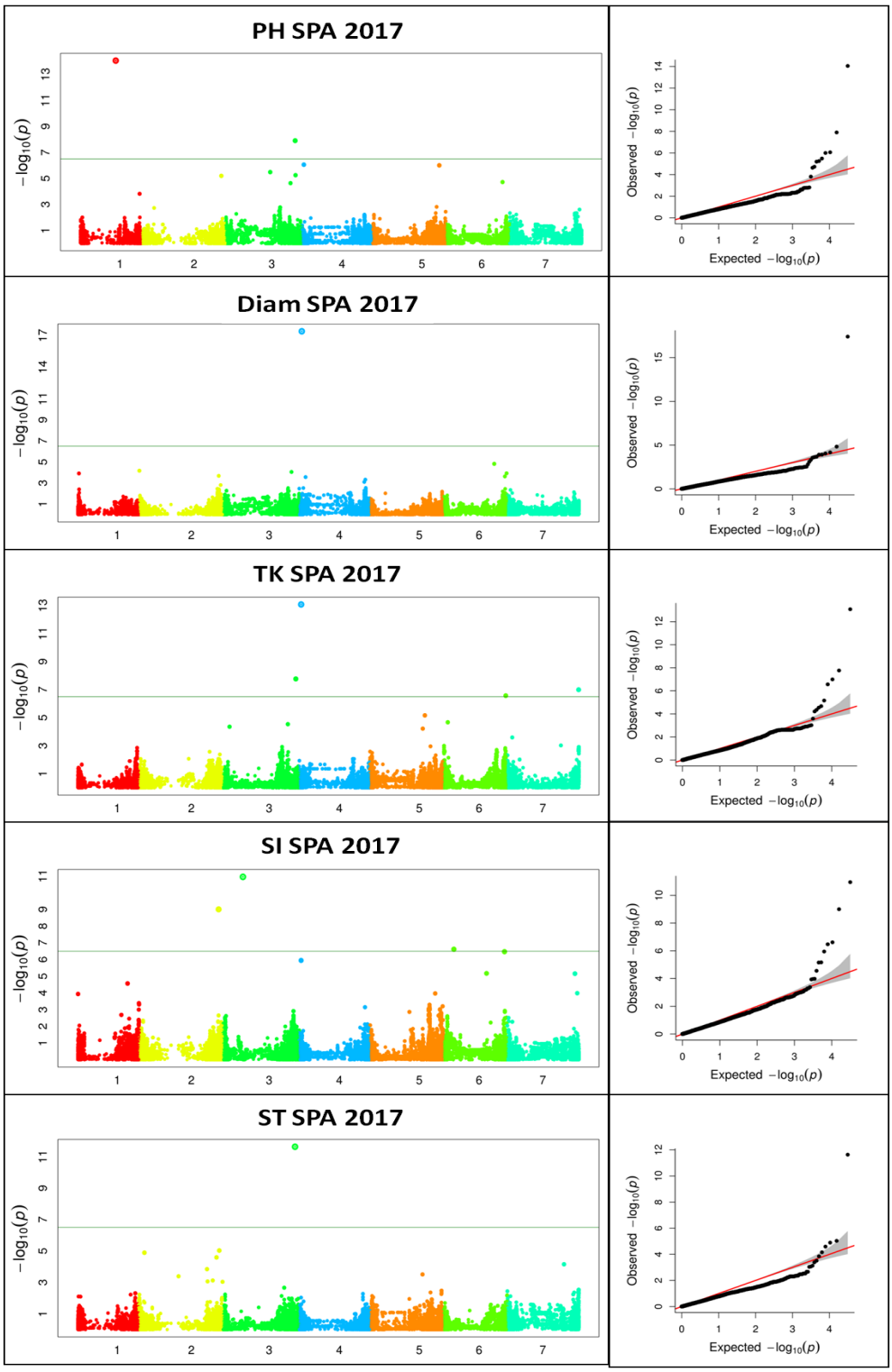

Fig. 4.24 Manhattan plot and QQ plot for the GWAS analyses carried out on the samples from SPA 2017 trial. From the top to the bottom the traits analyzed are plant height (PH), diameter (diam), thickness (TK), stem index (SI) and stiffness (ST). In the Manhattan plot the green line represent the significance threshold calculated by the Bonferroni correction. The QQ plots show the expected distributions of association tests (X-axis) across the million SNPs compared to the observed association values of the SNPs (Y-axis). Any deviation from the X=Y line implies a consistent association of the SNP with the studied trait.

Bonferroni correction is too conservative; thus, we decided to focus our attention on signals shared across trials/environments: the ten most significant markers divided by location are

summarized in Appendix F. Among them several shared signals were identified with relatively high P-values (Table 4.13).

trial	year	trait	SNP	Chromosome	Position	P.value	maf	effect
ITA	2016	ph	JHI-Hv50k-2016-197188	3	592.449.859	1.47E-05	0.454315	1.72609
SPA	2017	ph	JHI-Hv50k-2016-197229	3	592.562.958	2.32E-05	0.393401	-1.36161
FIN	2017	ph	JHI-Hv50k-2016-197260	3	592.639.168	4.21E-07	0.494924	-1.89336
SCO	2016	ph	JHI-Hv50k-2016-197260	3	592.639.168	3.04E-14	0.494924	-3.59849
SCO	2017	ph	JHI-Hv50k-2016-197260	3	592.639.168	4.08E-11	0.494924	-3.15694
ITA	2016	ph	JHI-Hv50k-2016-205000	3	632.318.274	1.90E-05	0.34264	1.794925
FIN	2017	ph	JHI-Hv50k-2016-205154	3	633.069.492	1.17E-05	0.30203	1.703317
SCO	2016	ph	JHI-Hv50k-2016-205269	3	633.303.897	1.12E-19	0.101523	8.76089
SCO	2017	ph	JHI-Hv50k-2016-205269	3	633.303.897	6.21E-09	0.101523	5.003685
FIN	2016	ph	JHI-Hv50k-2016-205398	3	634.190.153	6.65E-08	0.162437	2.624816
SPA	2017	ph	JHI-Hv50k-2016-205616	3	634.928.088	1.25E-08	0.177665	-3.23361
SCO	2016	ph	JHI-Hv50k-2016-325943	5	577.523.180	2.19E-17	0.21066	4.943762
ITA	2016	ph	JHI-Hv50k-2016-325943	5	577.523.180	0.000212	0.21066	1.427209
ITA	2017	ph	JHI-Hv50k-2016-325943	5	577.523.180	4.1E-07	0.21066	2.274116
FIN	2017	ph	JHI-Hv50k-2016-325973	5	577.531.748	4.86E-07	0.347716	2.099005
SCO	2017	ph	SCRI_RS_196437	5	577.776.518	7.11E-10	0.401015	-6.12079
SCO	2016	diam	JHI-Hv50k-2016-37634	1	486.872.133	2.71E-07	0.081218	-0.01269
ITA	2017	diam	JHI-Hv50k-2016-37651	1	488.799.253	1.12E-12	0.266497	-0.02599
SCO	2017	diam	JHI-Hv50k-2016-37651	1	488.799.253	1.10E-05	0.266497	-0.01401
SCO	2016	diam	JHI-Hv50k-2016-45614	1	522.492.014	5.11E-07	0.373096	-0.01865
FIN	2016	diam	JHI-Hv50k-2016-46233	1	523.388.034	2.30E-05	0.345178	0.011664
FIN	2017	diam	JHI-Hv50k-2016-231888	4	22.324.263	8.72E-19	0.162437	0.02392
SPA	2016	diam	JHI-Hv50k-2016-231905	4	22.331.283	1.10E-07	0.167513	-0.0227
SCO	2016	diam	JHI-Hv50k-2016-231992	4	22.933.768	1.34E-11	0.177665	0.02218
SPA	2017	diam	JHI-Hv50k-2016-231992	4	22.933.768	3.97E-18	0.177665	0.027531
FIN	2016	diam	JHI-Hv50k-2016-232164	4	23.603.729	4.58E-19	0.195431	0.026068
ITA	2016	diam	JHI-Hv50k-2016-309221	5	499.576.853	1.05E-06	0.423858	-0.02176
FIN	2016	diam	JHI-Hv50k-2016-309227	5	499.578.571	1.99E-05	0.464467	-0.01458
SCO	2016	diam	JHI-Hv50k-2016-309227	5	499.578.571	1.02E-06	0.464467	-0.01824
FIN	2017	diam	JHI-Hv50k-2016-515270	7	647.631.915	0.001219	0.398477	-0.00824
SPA	2017	tk	JHI-Hv50k-2016-231008	4	17.377.960	8.34E-14	0.182741	0.007098
SPA	2016	tk	JHI-Hv50k-2016-231078	4	18.335.761	2.85E-12	0.152284	-0.00896
SCO	2017	tk	JHI-Hv50k-2016-231962	4	22.861.735	6.92E-23	0.177665	-0.00846
SCO	2016	tk	JHI-Hv50k-2016-279209	5	6.367.937	7.97E-07	0.162437	-0.00441
SPA	2016	tk	JHI-Hv50k-2016-279888	5	7.561.397	5.27E-07	0.06599	-0.00789
ITA	2016	si	SCRI_RS_185319	2	22.770.072	8.41E-10	0.238579	0.01644
SCO	2017	si	JHI-Hv50k-2016-71249	2	22.853.879	2.88E-11	0.238579	0.015739

FIN	2016	si	SCRI_RS_198643	2	23.189.369	5.67E-08	0.281726	-0.01757
FIN	2017	si	JHI-Hv50k-2016-71784	2	23.484.021	7.32E-12	0.494924	-0.01832
FIN	2016	si	JHI-Hv50k-2016-130257	2	728.298.636	2.43E-06	0.274112	-0.01803
SPA	2017	si	JHI-Hv50k-2016-130260	2	728.298.989	9.97E-10	0.274112	0.035378
SCO	2016	si	JHI-Hv50k-2016-130387	2	728.830.270	3.03E-06	0.238579	0.016156
SCO	2017	si	JHI-Hv50k-2016-130387	2	728.830.270	8.28E-06	0.238579	0.012147
ITA	2016	si	JHI-Hv50k-2016-130413	2	728.831.999	6.49E-08	0.324873	-0.01428
ITA	2016	si	JHI-Hv50k-2016-197188	3	592.449.859	9.84E-08	0.454315	-0.0124
FIN	2016	si	JHI-Hv50k-2016-197342	3	593.275.528	2.14E-06	0.162437	0.023792
FIN	2017	si	JHI-Hv50k-2016-204951	3	632.243.848	7.23E-09	0.406091	-0.01498
FIN	2016	si	JHI-Hv50k-2016-205269	3	633.303.897	4.43E-05	0.101523	-0.02949
SPA	2016	st	JHI-Hv50k-2016-131986	2	733.393.195	7.22E-06	0.071066	0.13049
SPA	2017	st	JHI-Hv50k-2016-132250	2	733.685.021	9.32E-06	0.233503	0.098619

Table 4.13 List of the markers shared across the trials for the sample at harvest stage (Zadoks 90). The first column (trial) represents the location where the trial was run. The second column (year) is the year of the trial. Third column (trait) represent the trait taken into consideration. Fourth column (SNP) shows the SNP marker associated with the trait in a particular trial and year. The fifth and the sixth columns (Chromosome and Position, respectively) show on which chromosome and on which position (bp) the marker is located. The seventh column (P.value) represents the significance of the association between the marker and the trait. The eighth column (maf) instead represent the frequency of the minor allele for this particular marker in the population. Last column (effect) is the mean of trait value for allele I homozygotes versus allele II homozygotes.

To this end, we decided to group markers based on LD decay, i.e. if several markers for the same trait were identified in different location or at different growing stage and fell within an interval inferior to the LD decay specific for their chromosome, they were considered a group.

Plant height was used as a benchmark to test our GWAS model since different barley genes controlling this trait are known (Kuczynska and Wyka 2011, Kuczyńska, Surma et al. 2013). For plant height, three groups of markers were identified. On chromosome 3H, we detected two distinct groups of signals: one shared between UK 2016/2017, ITA 2016, FIN 2017 and SPA 2017 (position 592.449.859-592.639.168) and another in UK 2016/2017, ITA 2016, FIN 2016/2017, SPA 2017 (position 632.318.274-634.928.088). The third was on chromosome 5H and was detected in the north European trials UK 2016/2017 and FIN 2017 only (position 577.523.180-577.776.518).

For culm diameter, five groups of markers showed consistency between trials. The first was located at the end of chromosome 1H (position 486.872.133-488.799.253) and was shared between UK 2016/2017 and ITA 2017. The second was also found on chromosome 1H in UK 2016 and FIN 2016 (position 522.492.014-523.388.034). The third group of significant markers was located at the beginning of chromosome 4H (position 22.324.263-23.603.729) and shared between UK 2016, FIN 2016/2017 and SPA 2016/2017. Another group located at the end of chromosome 5H (position 499.576.853-499.578.571) was shared between ITA, FIN and UK 2016. The last was located on chromosome 7H (position 647.631.915) just for the FIN 2017 trial.

GWAS for culm thickness produced two groups of associated markers. The first group was detected in UK 2017 and SPA 20016/2017 at the beginning of chromosome 4H (position 17.377.960-22.861.735), partially overlapping with the second group of markers for culm diameter. Another group of markers associated with thickness was present at the beginning of chromosome 5H for the trials UK 2016/2017and SPA 2016 (position 3.438.902-7.561.397).
Four clusters of markers were identified for Stem Index. Two were located at the opposite ends of chromosome 2H: the first in UK 2017, ITA 2016 and FIN2016/2017 (position 22.770.072-23.484.021) while the second in UK 2016/2017, ITA 2016, FIN 2016 and SPA 2017 (position 728.298.636-728.831.999). Other two groups were located on chromosome 3H: one in the ITA 2016 and FIN 2016/2017 (position 592.449.859-596.522.095) whereas the other is present in both the FIN 2016/2017 trials (position 632.243.848-633.303.897). The last group of signals on chromosome 3H overlap with signals found for plant height, while no loci are shared between diameter and stem index signals. These observations indicate that genes involved in stem length play a major role in defining the ratio between diameter and plant height.
Finally, only one group of shared markers across FIN 2017 and SPA 2016/2017 trials was identified for stiffness on chromosome 2H (position 733.393.195-733.685.021). This is not totally surprising: stiffness is the trait with the lowest heritability on average across trials, so we can expect to hardly find shared peaks across the environments and growing stages.
All these clusters of markers were screened using the online database Barley Map (http://floresta.eead.csic.es/barleymap). As a preliminary approach to identify genomic regions for candidate gene searches, the LD decay calculated for each chromosome was used to investigate the regions surrounding the 15 loci we identified: subtracting/adding the LD decay distance at the positions of the most external markers of each group we defined the extremes of the region to investigate. We focused on gene models for which annotations of closely associated genes implied a possible functional link to our studied traits. Gene annotations were obtained from genome assemblies of barley, rice and Arabidopsis (Table 4. paragraph 4.6).

4.5 RESULTS: STUDY ON ZADOKS STAGE 83-85 PLANTS PHENOTYPIC AND GENETIC ANALYSES OF CULM MORPHOLOGICAL TRAITS IN ITALIAN FIELD TRIALS AT DOUGH STAGE (Zadoks 83-85)

4.5.1 Field trials

In order to evaluate the barley culm architecture and morphology at the dough stage (Zadoks 83-85), we collected and analyzed samples from the Climbar Italian trials 2016/2017. The analysis was

not extended to the other locations because of the great amount of time needed to prepare the samples. Samples were hand cut by a sharp razorblade, images of the sections were taken with a stereo microscope and analyzed with a dedicated macro command on ImageJ software (paragraph 3.4). In this series of experiments was possible also to consider the number of vascular bundles as a phenotypic trait, investigating the correlation it has with the other and its level of heritability. The raw phenotypic data were collected from plants at Zadoks stage 83-85 (dough stage) from the field trials grown at CREA research center of Fiorenzuola d'Arda, Piacenza, Italy, in the years 2016 and 2017. Explorative statistic of the traits scored is given in Table 4.14.

	2016					2017				
Traits	Min.	Mean	Max.	SD	HER%	Min.	Mean	Max.	SD	HER%
Diameter (cm)	0.104	0.3865	0.568	0.072	13.86%	0.297	0.4203	0.567	0.049	56.32%
Thickness (cm)	0.005	0.02946	0.078	0.012	45.58%	0.097	0.1485	0.24	0.027	60.86%
Stem Index	0.1175	0.4422	0.6791	0.089	45.08%	0.305	0.5066	0.8331	0.079	78.05%
Stiffness	4.542	15.398	71	7.66	42.64%	1.697	2.902	4.255	0.498	49.49%
n. VascularBundles	23	32.68	48.25	4.29	71.16%	20.33	30.05	43.67	4.144	68.24%

Table 4.14 Descriptive statistics regarding diameter, thickness, stem index, stiffness and number of vascular bundles.

Comparison between the two years was taken into consideration. After t-test and Kolmorogov-Smirnov test investigations, the two trials show consistent differences, likely reflecting different environmental conditions of the two years. In particular, a strong storm struck the field in the days prior to sampling activities in 2016. In agreement with a strong environmental year effect, Pearson's correlation between traits across the years revealed significant but very low correlations for most of the traits (Table 4.15). Stem index and number of vascular bundles are the exceptions. Stem index high correlation could be partially due to the effect of the plant (paragraph 4.4.1). Instead the high correlation of the vascular bundles count between the years, is a sign that the storm, which struck the field in the 2016 did not modify excessively the number of vessels.

	Diameter	Thickness	Stem Index	Stiffness	Vascular bundles
ITA 2016/2017	0.124***	0.149***	0.389***	0.165***	0.572***

Table 4.15 Pearson correlation test among the two Italian trials for the traits under investigation.

For all the two trials at Zadoks stage 83-85 pairwise Pearson's correlations were tested among the traits Plant Height (PH), Grain Yield (GY), Lodging (LoD), Harvest Index (HI), Diameter (D), Thickness (TK), Stem index (SI), Stiffness (ST) and number of Vascular Bundles (n.VB).

ZADOKS STAGE 83-85									
2016	PH	GY	LoD	HI	D	TK	SI	ST	n.VB
PH	1	-0.24***	0.41***	-0.55***	0.14***	0.01	-0.39***	0.04	0.22***
GY		1	-0.32***	0.23***	-0.14**	-0.18***	-0.02	0.10*	-0.17**
LoD			1	-0.42***	0.09*	-0.07	-0.12*	-0.11*	0.04
HI				1	0.06	0.18***	0.32***	-0.12*	-0.09
D					1	0.43***	0.85***	0.03***	0.20***
TK						1	0.42***	-0.71***	0.18***
SI							1	-0.02***	0.07
ST								1	-0.10*
n.VB									1
2017	PH	GY	LoD	HI	D	TK	SI	ST	n.VB
PH	1	0.11*	0.37***	-0.34***	-0.02	0.01	-0.66***	-0.04	0.15**
GY		1	0.01	0.26***	-0.11*	-0.35***	-0.18**	0.29***	-0.11*
LoD			1	-0.29***	-0.23***	-0.13*	-0.40***	-0.02	-0.21***
HI				1	0.09	-0.09	0.29***	0.17***	-0.05
D					1	0.39***	0.75***	0.27***	0.54***
TK						1	0.29***	-0.76***	0.29***
SI							1	0.21***	0.29***
ST								1	0.06
n.VB									1

Table 4.16 Pearson correlation scores among the traits in the two Italian trials 2016/2017.

Some correlations show different and even contrasting values between the two years of testing. A similar pattern was observed for Plant Height, which shows a shared trend with the exception of the correlations with grain yield and culm diameter, with marked differences between 2016 and 2017, especially for the latter trait. Correlations between diameter and lodging also differed between the two year: in 2016, no significant relationship was found in contrast with the following year where diameter is inversely correlated with lodging. Also in 2016, the correlation between diameter and Stiffness is surprisingly low. For thickness, correlations are consistent between the two years with the exception of the harvest index. The number of vascular bundles shows interesting significant correlations with Plant Height and Lodging resistance in 2017, while in the previous year only the high correlation with plant height was observed. Correlation of the vascular bundles with diameter and thickness is positive and significant in both years, even if it is larger in 2017. We suspect that many of the differences between the two years are due to the storm effects that influenced the ITA 2016 trial, bending many of the plants in the field before anthesis, and therefore, influencing the last developmental phases.

Furthermore, we compared correlation values in the two different developmental stages (Tables 4.6 – 4.16). For plant height correlation with the diameter is reduced in 2017 compared to 2016

for both stages, and no significant relationship was found with culm wall thickness regardless of the growth stage. Instead, for diameter/stiffness correlations there are significant difference among the Zadoks stage 83 and 90.

Interaction of our traits with row-type was also considered following a similar approach to what we did for Zadoks stage 90 (paragraph 4.4.1). Cultivars were divided in row-types and all data were tested with parametric (t-test) and non-parametric (Wilcoxon-Mann-Whitney test) approaches. Results are consistent between the two approaches.

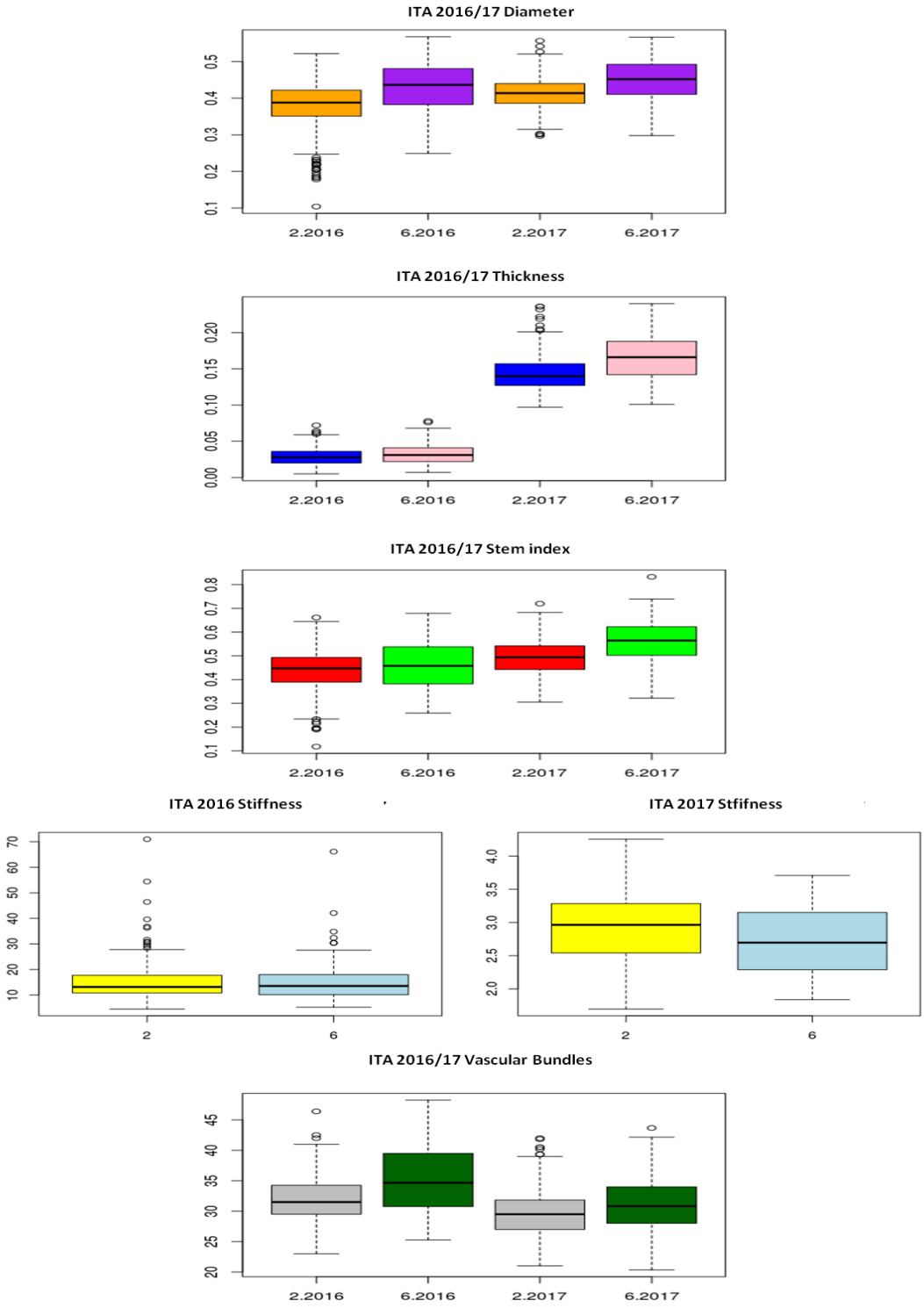

Fig. 4.25 Boxplots for the diameter (top), thickness, stem index, stiffness and vascular bundles (bottom). In each graph the distribution for two-row and six-row barley is presented at dough stage (Zadoks 83-85) for the two years (ITA 2016 and ITA 2017 trials).

Results for diameter at this growing stage are consistent with results at harvest stage (Zadoks 90) with six-row barley showing significantly wider diameter than two-row. For thickness and stem index, the difference is significant only in 2017, with higher values for six-row barley. Thickness

presents a great gap between the two years for, with really small values in the 2016, perhaps a consequence of the storm which stroke the field few days before the harvesting. For Stiffness, no significant difference was detected between two- and six-row at Zadoks stage 83-85 in 2016; on the other hand, in 2017 at the same growth stage, two-row barley showed higher stiffness compared with six-row. Furthermore, stiffness is greatly affected by thickness, therefore the strong differences between the two years are expected. As for the number of vascular bundles, six-row barley consistently had more vessels compared at two-row in both years.
Collating diameter results from Zadoks stage 83-85 and Zadoks 90 through 2016/2017 trials, an opposite trend is apparent between the two years. In 2016 plants increased their diameter towards maturity (probably because of the strong stress experienced) while the opposite occurred in 2017 (table 4.17).

	2016			2017		
Trial - trait	Mean	SD	HER %	Mean	SD	HER %
ZK 83-85 Diameter (cm)	0,3865	0,072	13,86	0,4203	0,049	56,32
ZK 83-85 Thickness (cm)	0,02946	0,012	45,58	0,1485	0,027	60,86
ZK 83-85 Stem Index	0,4422	0,089	45,08	0,5066	0,079	78,05
ZK 83-85 Stiffness	15,398	7,66	42,64	2,902	0,498	49,49
ZK90 Diameter (cm)	0,4153	0,044	65,46	0,3886	0,039	53,6
ZK90 Thickness (cm)	0,1124	0,015	18,45	0,1205	0,011	55,33
ZK90 Stem Index	0,4747	0,064	66,64	0,4675	0,063	73,78
ZK90 Stiffness	3,742	0,493	28	3,241	0,337	12,8

Table 4.17 Comparison of diameter, thickness, stem index and stiffness descriptive statistics between the two developmental stages and across the two years.

For thickness there is a great difference between the two years (average 0.029 in 2016 and average 0.148 in 2017) probably due to the storm's effect, in fact samples from 2016 present a smaller thickness with no difference between two and six-rowed barley, while samples of the following year have significant difference between six rowed and two rowed, with higher values. Samples at Zadoks stage 90 in the same trials did not show the same extent of difference between the two years (average 0.11 in 2016 and average 0.12 in 2017).
Clearly, these differences also impact Stiffness, which differs by one order of magnitude between the two years (average 15.39 in 2016 vs. 2.9 in 2017). Compared with stiffness results at Zadoks stage 90 (average 3.5 in 2016 and 3.7 in 2017), it is possible to notice a larger reduction in the 2016 while the increase in 2017 is due to reduction of the thickness.

Generally speaking in 2017 we can observe a reduction in size between Zadoks 83-85 toward Zadoks stage 90 that could be due to a translocation of carbon from the stem to the ear. On the other hand in 2016 after the storm the plants increase their stems from Zadoks stage 83-85 to 90, with a different etological strategy. More studies will be needed to characterize these size changes in different environmental situations.

4.5.2 Genome wide association mapping

In order to identified markers and genomic regions associated to culm morphological traits at dough stage, the collected phenotypic data were integrated with genome-wide genotyping data for a total 31360 SNPs after filtering for MAF<5%. The traits tested were culm diameter, culm wall thickness, stem Index, stiffness and number of vascular bundles. The same GWAS model used to analyze the morphological data from plant at Zadoks stage 90 was used, incorporating the first and the second principal components in order to correct for the population structure.
Considering both trials, 5, 3, 3, 6, 2 significant marker-trait associations for diameter, thickness, stem index, stiffness and number of vascular bundles respectively, were detected using a Bonferroni correction to reduce the occurrence of false positive (Fig. 4.26-4.27).

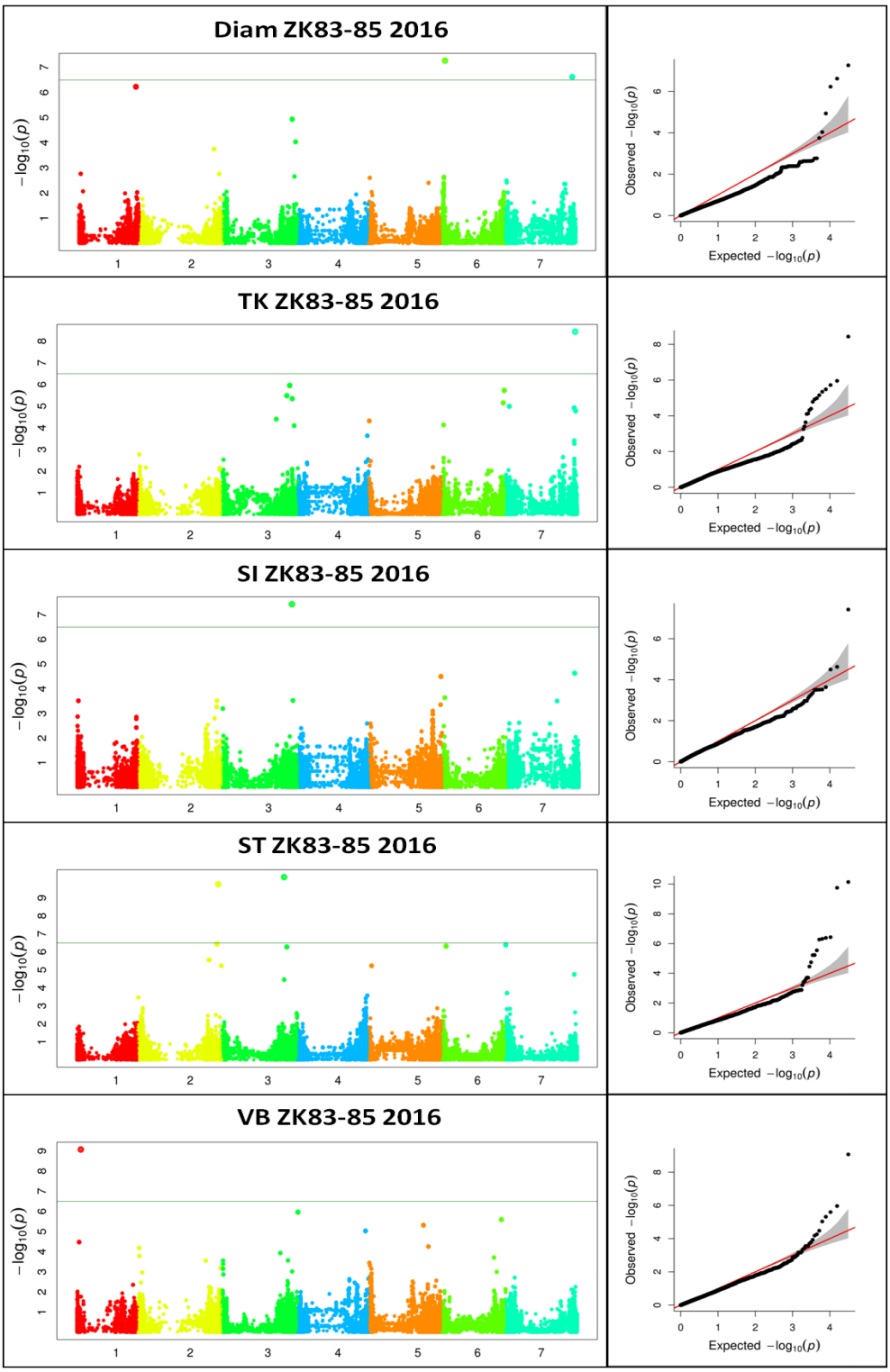

Fig. 4.26 Manhattan plot and QQ plot for the GWAS analyses carried out on the samples from ITA 2016 trial from plants at Zadoks stage 83-85. From top to bottom the traits analyzed are, diameter (diam), thickness (TK), stem index (SI), stiffness (ST) and number of vascular bundles (VB). In the Manhattan plot the green line represent the significance threshold calculated by the Bonferroni correction. The QQ plots show the expected distributions of association tests (X-axis) across the million SNPs compared to the observed association values of the SNPs (Y-axis). Any deviation from the X=Y line implies a consistent association of the SNP with the studied trait.

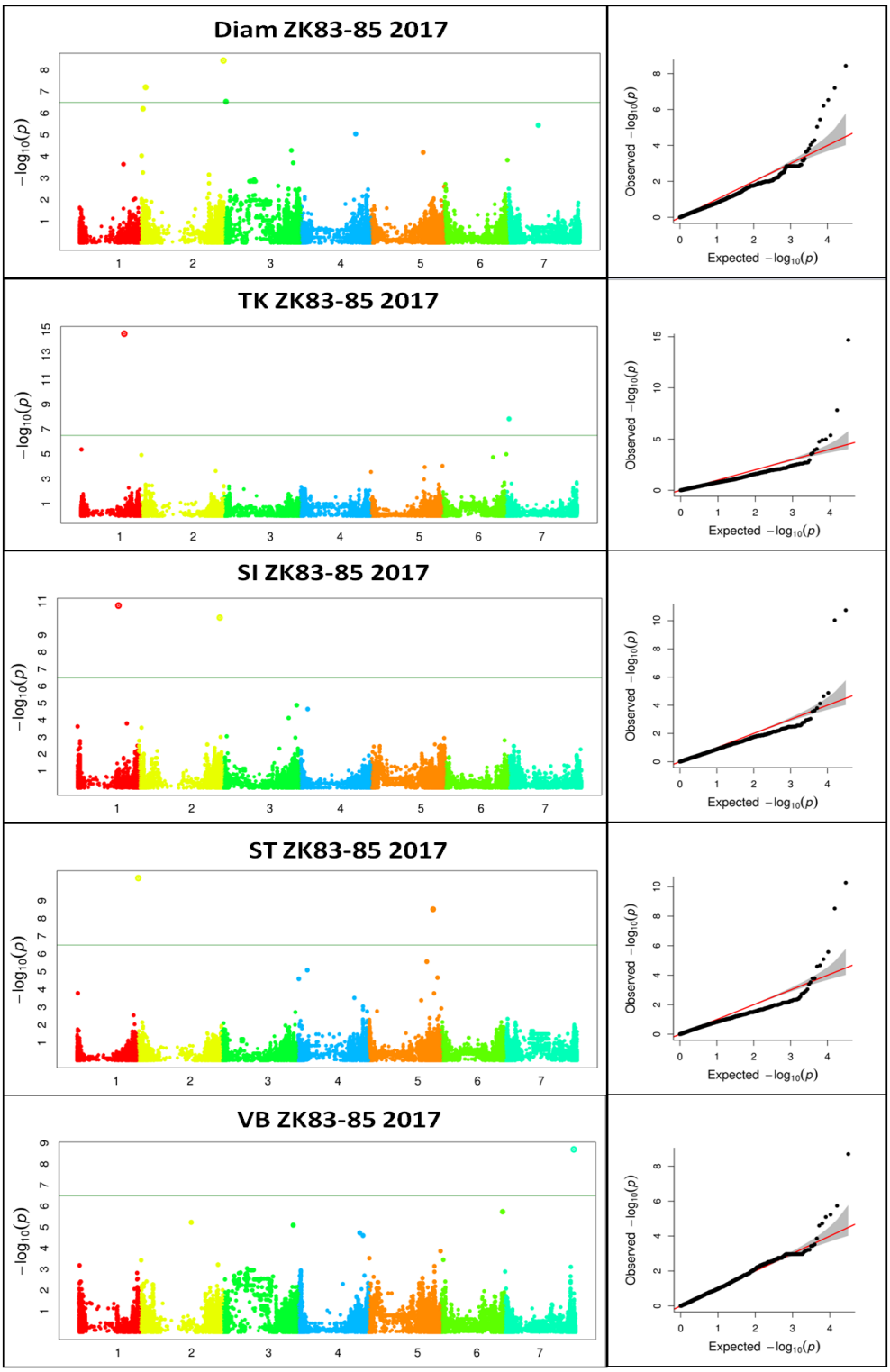

Fig. 4.27 Manhattan plot and QQ plot for the GWAS analyses carried out on the samples from ITA 2017 trial from plants at Zadoks stage 83-85. From top to bottom the traits analyzed are, diameter (diam), thickness (TK), stem index (SI), stiffness (ST) and number of vascular bundles (VB). In the Manhattan plot the green line represent the significance threshold calculated by the Bonferroni correction. The QQ plots show the expected distributions of association tests (X-axis) across the million SNPs compared to the observed association values of the SNPs (Y-axis). Any deviation from the X=Y line implies a consistent association of the SNP with the studied trait.

As we did for the GWAS results from samples at Zadoks stage 90 we investigated the ten most significant marker signals from these results in order to find those shared across growth stages

and trials (Appendix G). Among them several shared signals were identified with relatively high p-values (Table 4.13).

Six traits were analyzed for marker-trait association: Plant Height, Culm Diameter, culm wall thickness, Stem Index, Stiffness and number of Vascular Bundles. GWAS results with significant markers for each year are summarized in Table 4.18.

trial	trait	SNP	Chromosome	Position	P.value	maf	effect
2016	diam	JHI-Hv50k-2016-46776	1	524.629.926	5,94E-07	0,203046	-0,02596
2017	tk	JHI-Hv50k-2016-278792	5	5.590.301	0,000281	0,319797	-0,00389
2017	si	JHI-Hv50k-2016-71784	2	23.484.021	0,000282	0,494924	-0,01088
2017	si	JHI-Hv50k-2016-197188	3	592.449.859	7,49E-05	0,454315	-0,01147
2016	si	JHI-Hv50k-2016-205398	3	634.190.153	3,75E-08	0,162437	-0,03414
2016	st	SCRI_RS_161490	2	735.203.017	1,76E-10	0,106599	-3,41857
2016	vb	JHI-Hv50k-2016-65236	2	12.238.955	6,56E-05	0,286802	-1,31145
2016	vb	JHI-Hv50k-2016-65476	2	12.863.581	0,000164	0,154822	0,739947
2017	vb	JHI-Hv50k-2016-66847	2	14.345.320	0,000374	0,492386	-0,62198

Table 4.18 List of the markers shared across the trials for the sample at dough stage (Zadoks 83-85). The first column (trial) reports the year of the trial. The second column (trait) represent the trait taken into consideration. Third column (SNP) the SNP marker associated with the trait in a particular trial and year. The fourth and the fifth columns (Chromosome and Position, respectively) show on which chromosome and on which position (bp) the marker is located. The sixth column (P.value), represents the significance of the association between the marker and the trait. The seventh column (maf) instead represent the frequency of the minor allele for this particular marker in the population. Last column (effect) is the mean of trait value for allele I homozygotes versus allele II homozygotes.

These groups of markers are in close proximity with the groups of markers found with the GWAS run on the Zadoks stage 90 phenotypic data (paragraph 4.4.3).

For the diameter a single marker in 2016 trial on chromosome 1H (position 524.629.926) was found. For the stem index we found three distinct associations in common with the Zadoks 90 experiment: one on the chromosome 2H for the 2017 trials (position 23.484.021); the other two are located on chromosome 3H (positions 592.449.859 and 634.190.153). The marker in position 592.449.859 also overlaps with another marker for plant height. Stiffness shows high association with just one maker on chromosome 2H (position 735.203.017).

Thickness analysis produced one marker shared with the previous experiment on chromosome 5H (position 5.590.301).

GWAS on vascular bundles has no shared association between the two years except for a peak on chromosome 2H (position 12.238.955-14.345.320).

4.6 CANDIDATE GENES

From the GWAS studies on morphological data from different trials/growing stages (paragraphs 4.4.3 and 4.5.2) several groups of markers were identified (Tab. 4.19) associated with six barley culm related traits: plant height, stem diameter, thickness, stem index, stiffness and number of vascular bundles. Marker groups were investigated using Barley map database (http://floresta.eead.csic.es/barleymap). The database was created to study barley genetic markers and genes on the barley physical map and POPSEQ gene map (Mayer, Waugh et al. 2012, Mascher, Muehlbauer et al. 2013). The most recent version of the map takes advantage of the recently published Morex reference genome (Mascher, Gundlach et al. 2017). Information available on the barley map database are public and can be found at the MIPS (ftp://ftpmips.helmholtz-muenchen.de/plants/barley/public_data/), IPK (ftp://ftp.ipk-gatersleben.de/barley-popseq/) and Morex Genome data (https://webblast.ipk-gatersleben.de/barley_ibsc/downloads/) servers.

For each group of markers we subtracted/added the LD decay distance for the corresponding chromosome (paragraph 4.3) from the position of the most external markers in order to define a genomic area to screen for potential candidate genes, focusing on gene models for which annotations of closely associated genes implied a possible functional link to our studied traits. Candidate genes were selected based on their characterization (if present) in barley, alternatively references in rice (*Oryza sativa* L.) or *Arabidospis thaliana* were integrated to help defining the function of the candidate gene during the development and the effects on phenotype of mutants. For gene models in the investigated areas the HORVU were collected. The HORVU is an univocal identification code specific for a particular barley gene/locus. HORVU can be used to search the EnsemblPlants database for more specific information on the gene/locus (https://plants.ensambl.org/index.html), including intron-exon structure, gene expression profile from publicly available RNAseq data, annotated sequence variants from resequencing studies, publications, orthologs in other plant species, etc. We focused our attention on gene models with a direct effect on the plant developmental processes, affecting hormonal signaling , especially in modification of above ground biomass production, change in plant stem height/diameter and altered biochemical composition of the cell wall. In absence of clear evidences in literature about candidate genes characterization in barley, rice or *Arabidopsis* we indicated as candidate gene the gene embedding the markers, or the closest to it with a predicted function that can be involved in

the modification of the stem structure. Candidate genes characterized in literature are analyzed in the downstream paragraphs.

trial	year	trait	SNP	Chrm	Position	within the gene	Horvu	Gene position	Description	Ortholog in rice	Ortholog in Arabidopsis
ITA	2016	ph	JHI-Hv50k-2016-197188	3H	592.449.859	YES	HORVU3Hr1G081030	592.448.229 - 592.453.837	WRKY DNA-bindingprotein 46	WRKY21	N/A
SPA	2017	ph	JHI-Hv50k-2016-197229	3H	592.562.958						
FIN	2017	ph	JHI-Hv50k-2016-197260	3H	592.639.168						
SCO	2016	ph	JHI-Hv50k-2016-197260	3H	592.639.168						
SCO	2017	ph	JHI-Hv50k-2016-197260	3H	592.639.168						
ITA	2016	ph	JHI-Hv50k-2016-205000	3H	632.318.274						
FIN	2017	ph	JHI-Hv50k-2016-205154	3H	633.069.492						
SCO	2016	ph	JHI-Hv50k-2016-205269	3H	633.303.897						
SCO	2017	ph	JHI-Hv50k-2016-205269	3H	633.303.897						
FIN	2016	ph	JHI-Hv50k-2016-205398	3H	634.190.153	NO	HORVU3Hr1G090980	634.080.836 - 634.081.229	gibberellin 20-oxidase 3	SDW1	GA20Ox5
SPA	2017	ph	JHI-Hv50k-2016-205616	3H	634.928.088						
SCO	2016	ph	JHI-Hv50k-2016-325943	5H	577.523.180	NO	HORVU5Hr1G087000	577.607.441 - 577.607.734	Peroxidase	N/A	N/A
ITA	2016	ph	JHI-Hv50k-2016-325943	5H	577.523.180						
ITA	2017	ph	JHI-Hv50k-2016-325943	5H	577.523.180						
FIN	2017	ph	JHI-Hv50k-2016-325973	5H	577.531.748						

SCO	2017	ph	SCRI_RS_196437	5H	577.776.518						
SCO	2016	diam	JHI-Hv50k-2016-37634	1H	486.872.133	YES	HORVU1Hr1G070250	488.799.144 - 488.802.079	WRKY DNA-bindingprotein 33	WRKY70	WRKY33 WRKY26
ITA	2017	diam	JHI-Hv50k-2016-37651	1H	488.799.253						
SCO	2017	diam	JHI-Hv50k-2016-37651	1H	488.799.253						
SCO	2016	diam	JHI-Hv50k-2016-45614	1H	522.492.014	NO	HORVU1Hr1G079130	522.434.605 - 522.450.160	Pectine lyase	N/A	N/A
FIN	2016	diam	JHI-Hv50k-2016-46233	1H	523.388.034						
ZK83	2016	diam	JHI-Hv50k-2016-46776	1H	524.629.926						
FIN	2017	diam	JHI-Hv50k-2016-231888	4H	22.324.263	NO	HORVU4Hr1G008270	22.383.974 - 22.387.455	UDP-glucose 6-dehydrogenase family protein	UDG3 UDG5 UDG6	N/A
SPA	2016	diam	JHI-Hv50k-2016-231905	4H	22.331.283						
SCO	2016	diam	JHI-Hv50k-2016-231992	4H	22.933.768						
SPA	2017	diam	JHI-Hv50k-2016-231992	4H	22.933.768						
FIN	2016	diam	JHI-Hv50k-2016-232164	4H	23.603.729						
ITA	2016	diam	JHI-Hv50k-2016-309221	5H	499.576.853	NO	HORVU5Hr1G065330	499.628.232 - 499.633.970	cinnamoylcoareductase 1	cinnamoyl CoAreductase 19	CCR1 CCR2
FIN	2016	diam	JHI-Hv50k-2016-309227	5H	499.578.571						
SCO	2016	diam	JHI-Hv50k-2016-309227	5H	499.578.571						
ZK83	2017	diam	JHI-Hv50k-2016-515120	7H	647.471.990	NO	HORVU7Hr1G118390	647.543.664 - 647.544.217	Protein MOR1	N/A	N/A
FIN	2017	diam	JHI-Hv50k-2016-515270	7H	647.631.915						

SPA	2017	tk	JHI-Hv50k-2016-231008	4H	17.377.960	NO	HORVU4Hr1G008270	22.383.974 - 22.387.455	UDP-glucose 6-dehydrogenase family protein	UDG5 UDG6	UDG2
SPA	2016	tk	JHI-Hv50k-2016-231078	4H	18.335.761						
SCO	2017	tk	JHI-Hv50k-2016-231962	4H	22.861.735						
ZK83	2017	tk	JHI-Hv50k-2016-278792	5H	5.590.301	N/A	N/A	N/A	unknown	N/A	N/A
SCO	2016	tk	JHI-Hv50k-2016-279209	5H	6.367.937						
SPA	2016	tk	JHI-Hv50k-2016-279888	5H	7.561.397						
ITA	2016	si	SCRI_RS_185319	2H	22.770.072	NO	HORVU2Hr1G011460	22.876.332 - 22.876.703	Glycosyltransferase	N/A	N/A
SCO	2017	si	JHI-Hv50k-2016-71249	2H	22.853.879						
FIN	2016	si	SCRI_RS_198643	2H	23.189.369						
FIN	2017	si	JHI-Hv50k-2016-71784	2H	23.484.021						
ZK83	2017	si	JHI-Hv50k-2016-71784	2H	23.484.021						
FIN	2016	si	JHI-Hv50k-2016-130257	2H	728.298.636	NO	HORVU2Hr1G113360	728.433.055 - 728.469.599	GRAS family transcription factor family protein	N/A	N/A
SPA	2017	si	JHI-Hv50k-2016-130260	2H	728.298.989	NO	HORVU2Hr1G113480	728.896.619 - 728.897.566	GRAS family transcription factor family protein	N/A	N/A
SCO	2016	si	JHI-Hv50k-2016-130387	2H	728.830.270	NO	HORVU2Hr1G113490	728.906.883 - 728.907.830	GRAS family transcription factor family protein	N/A	N/A
SCO	2017	si	JHI-Hv50k-2016-130387	2H	728.830.270						
ITA	2016	si	JHI-Hv50k-2016-130413	2H	728.831.999						
ITA	2016	si	JHI-Hv50k-2016-197188	3H	592.449.859	YES	HORVU3Hr1G081030	592.448.229 - 592.453.837	WRKY DNA-bindingprotein 46	WRKY21	N/A

ZK83	2017	si	JHI-Hv50k-2016-197188	3H	592.449.859						
FIN	2016	si	JHI-Hv50k-2016-197342	3H	593.275.528						
FIN	2016	si	12_11322	3H	596.522.095						
FIN	2017	si	JHI-Hv50k-2016-204951	3H	632.243.848						
FIN	2016	si	JHI-Hv50k-2016-205269	3H	633.303.897						
ZK83	2016	si	JHI-Hv50k-2016-205398	3H	634.190.153	NO	HORVU3Hr1G090980	634.080.836 - 634.081.229	gibberellin 20-oxidase 3	SDW1	GA20Ox5
SPA	2016	st	JHI-Hv50k-2016-131986	2H	733.393.195	NO	HORVU2Hr1G114980	733.462.692 - 733.463.848	1-aminocyclopropane-1-carboxylate oxidase 1	N/A	N/A
SPA	2017	st	JHI-Hv50k-2016-132250	2H	733.685.021						
ZK83	2016	st	SCRI_RS_161490	2H	735.203.017						
ZK83	2016	vb	JHI-Hv50k-2016-65236	2H	12.238.955	YES	HORVU2Hr1G005650	12.232.966 - 12.244.042	Cullin-associated NEDD8-dissociated protein 1		CAND1
ZK83	2016	vb	JHI-Hv50k-2016-65476	2H	12.863.581						
ZK83	2017	vb	JHI-Hv50k-2016-66847	2H	14.345.320						

Table 4.19 Table of the groups of markers and candidate genes. The first two columns (trial and year) tell in which trial and in which year the marker was identified by GWAS analysis. The third column (trait) shows to which trait the marker was associated. Fourth column (SNP) reports the name of the associated marker. The fifth and the sixth columns (Chrm and Position) represent the location of the marker in the barley genome. The seventh column (within the gene) tells us if the marker is embedded into the candidate gene. The eight column (Horvu) reports the univocal identification code of the candidate gene. The ninth column (Gene Position) shows the position in base pairs of the candidate gene. The tenth column (Description) reports the annotation of the candidate gene. The last two columns (Ortholog in rice and Ortholog in *Arabidopsis*) report the annotation of rice and *Arabidopsis orthologs.*

.

4.6.1 Candidate genes for plant height.

In order to validate our GWAS model, we initially ran the analysis on plant height as a benchmark trait, that is well characterized in barley and in other members of the Triticeae tribe. Three clear clusters of signals were identified across European trials and developmental stages, two of which with gene models studied also in rice and *Arabidopsis Thaliana*:

The first group of 6 markers is located on chromosome 3H in an interval spanning between 592.449.859 and 592.693.168 bp. These 6 markers are located within or in close proximity to a WRKY transcription factor: HvWRKY46 (position 592.448.229-592.453.837, HORVU3Hr1G081030). Furthermore, also a group of markers associated with the stem index trait also cluster in the same area.

WRKYs are a class of plant transcription factors, that regulate many different plant processes (Bakshi and Oelmüller 2014), e.g. biotic and abiotic stress responses, but very little is known up to now about their roles in plant development and morphology. HvWRKY46 - also known as SUSIBA2 (sugar signalling in barley) - was previously identified and shown to activate sugar responsive elements (SURE) that regulate starch synthesis (Sun, Palmqvist et al. 2003). A rice ortholog of HvWRKY46, OsWRKY78, was characterized by Zhang and colleagues (Fig. 4.28 (Zhang, Xu et al. 2011).

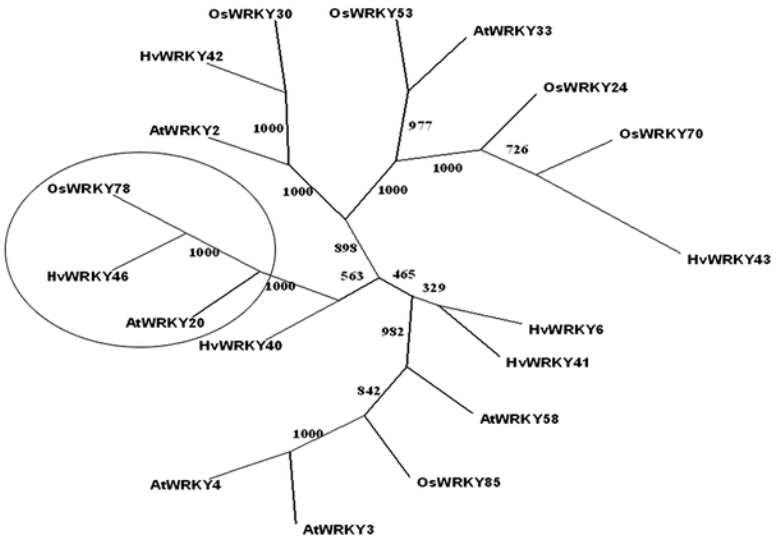

Fig. (4.28) Phylogenetic tree calculated on the basis of full length WRKY protein sequence. OsWRKY78, HvWRKY46 (SUSIBA2) and AtWRKY20 transcription factors are strictly related (circle). OsWRKY78 shares 80% of its amino acid sequence with barley HvWRKY46, and 43% with Arabidopsis AtWRKY20 (Zhang, Xu et al. 2011).

RNAi lines and loss of function mutants of OsWRKY78 produced rice plants with a dwarf phenotype and small kernels, probably because of a reduction in cell length. Analysis of the grain showed changes in endosperm starch structure. Zhang et al. suggested a possible role of

OsWRKY78 in the control of stem elongation and seed development (Zhang, Xu et al. 2011). More recently, HvWRKY46/SUSIBA2 has been overespressed in Nipponbare rice lines, altering the resource allocation toward the aboveground parts of the plant, resulting in increased dry weight of aboveground biomass and filled grains without an increase in plant height (Su, Hu et al. 2015).

The second group of markers counts 6 signals located on chromosome 3H in a range comprised between 632.318.274 and 634.928.088 bp. Associated markers were found in the same area also for Stem Index. This region hosts the well-known Sdw1 locus encoding gibberellin 20-oxidase 2 (GA20ox2, position 634.080.836-634.081.229, HORVU3Hr1G090980), a key enzyme in gibberellin biosynthesis: recessive mutations in this gene reduce plant height and improve lodging resistance (Kuczynska and Wyka 2011, Kuczyńska, Surma et al. 2013). Indeed *Sdw1*, along with *uzu* and ari-e.GP, is one of the major genes used for control plant height in barley. *Sdw1* is widely used in barley breeding programs, since it can reduce plant height up to 10-20 cm, conferring also a prostrate growth, while plants carrying dominant allele have an erect growth (Hellewell, Rasmusson et al. 2000, Górny 2001). Kuczyńska and Wyka (2011) showed that *sdw1* affects plant development by acting both on cellular growth and cell division frequencies, proving that *sdw1* interacts with a wide range of cells, tissues and organs with different dynamics (Kuczynska and Wyka 2011). Several other QTLs are located in the same area of *sdw1* locus, which may trigger pleiotropic interactions of these genes on plant height but also on different traits in LD with the *swd1* gene (Yin, Kropff et al. 1999, Hellewell, Rasmusson et al. 2000, Jia, Zhang et al. 2011). All these interactions are important for the design of plant ideotypes, and further research is needed to characterize them better through different developmental stages and environmental conditions.

4.6.2 Candidate genes for culm related traits.

GWAS analyses for culm related traits allowed us to identify several clusters of markers, shared also among different traits. In the present paragraph, we focus on gene models in close proximity to these marker groups, with orthologs characterized in either rice or *Arabidopsis.*

The first group of three markers falls in a region spanning from 486.872.133 to 488.799.253 on chromosome 1H and it associated with culm diameter. Of these three markers, two are located within a gene encoding WRKY DNA-binding protein 33 (position 488.799.144-488.802.079,

HORVU1Hr1G070250). Research in the EnseblPlants database and BLAST searches led to identify three close homologs of this gene: AtWRKY33, AtWRKY26 in Arabidopsis and OsWRKY70 in rice. As said in the previous paragraph WRKY transcription factors are mainly involved in the biotic and abiotic stress resistance in plants, but they are poorly characterized concerning their roles in plant development and growth.

In a recent research Li et al. (2015) characterized WRKY70 activity prioritizing defensive overgrowth. By increasing levels of jasmonic acid while reducing the levels of gibberellins, this mechanism may improve plant resistance to pest attacks (Li, Zhang et al. 2015). OsWRKY70 over-expression resulted in dwarfed plants displaying dark green leaves and delayed flowering, similar to known GA-deficient mutants (Sakamoto, Miura et al. 2004, Li, Zhang et al. 2015). Li and colleagues investigated the cause of this phenotypes finding consistent down-regulation of gibberellins 20 oxidase gene (GA20ox7) in OsWRKY70 over-expressing varieties, indicating an interaction between OsWRKY70 and gibberellins biosynthesis (Li, Zhang et al. 2015). While the effect of OsWRKY70 on culm diameter was not evaluated, previous work has shown interactions between plant height and diameter and gibberellin pathway affects stem diameter and thickness (Ookawa, Yasuda et al. 2010, Falcioni, Moriwaki et al. 2018).

Another group of markers located at the beginning of chromosome 4H was associated with culm diameter and thickness. Among gene models comprised in this chromosomal region, the most interesting is a UDP-glucose 6-dehydrogenase (UDG) family gene (position 22.383.974-22.387.455, HORVU4Hr1G008270). Based on sequence similarities, this gene is highly related to rice UDG 5/6 and *Arabidopsis* UDG2. Pectins and hemicelluloses are an important component of the plant cell wall, and they are mostly synthesized from UDP–glucuronic acid. The major enzymes involved in this process are the UDP-glucose dehydrogenase family (Fig. 4.29) (Klinghammer and Tenhaken 2007).

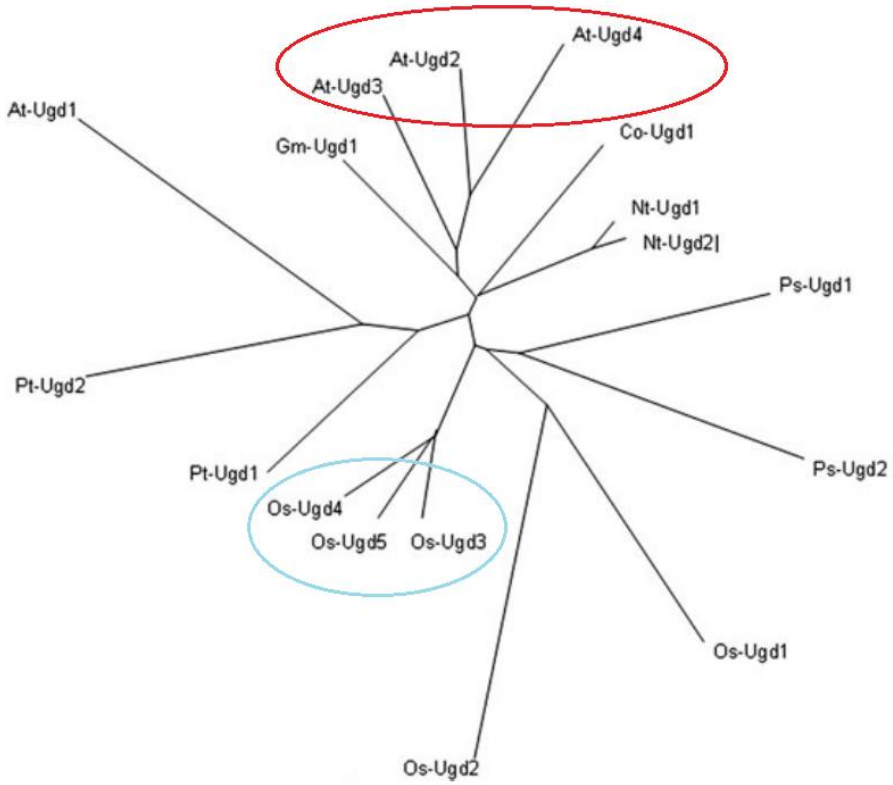

Fig. 4.29 Aligment of some plant UGD sequences. The UGDs from Arabidopsis cluster together in the upper part of the figure, while three rice UGDs are located in the lower part (Klinghammer and Tenhaken 2007).

From the study of Klinghammer and Tenhaken (2007) in Arabidopsis, UGD2 is the most abundant ezyme of the family expressed; real-time PCR analyses on UGD genes in *Arabidopsis* suggest that UGD2 is expressed at high levels in seedlings and in roots of seedlings. Furthermore, in cotyledons and hypocotyl, UGD2 expression is very high if compared to the other UGD genes (Klinghammer and Tenhaken 2007).

Pectin and hemicelluloses, as cell wall components, play an important role in the complex dynamics of cell proliferation and expansion during plant vegetative growth (Serrano-Mislata and Sablowski 2018). The effect of cell wall composition related genes during stem elongation is known (Minic, Jamet et al. 2009, Hall and Ellis 2013, Hall, Cheung et al. 2013), and the interaction of proteins controlling plant development, as RPL and DELLA, with genes that influence the cell wall composition is shown by recent studies (Etchells, Moore et al. 2012, Bencivenga, Serrano-Mislata et al. 2016, Serrano-Mislata, Bencivenga et al. 2017). Furthermore, in Arabidopsis was proven that the association between pectin and cellulose/hemicelluloses have a predominant role in the control of internode development (Phyo, Wang et al. 2017). All these evidences, even if not related directly to internode diameter modification, underline the effect of the UGD gene family , and more in general of the biochemical composition of the cell wall, as a promising way to explore

in order to control better plant development and therefore improve lodging resistance (Phyo, Wang et al. 2017, Serrano-Mislata and Sablowski 2018).

Another marker group is placed on chromosome 5H comprised between 499.576.853 and 499.578.571 bp and, based on the Barley Map website, in close proximity with a gene codifying for a Cinnamoyl-CoA reductase 1 (position 499.628.232-499.633.970, HORVU5Hr1G065330). The gene has orthologs in rice (Cinnamoyl-CoA reductase 19) and in *Arabidopsis* (Cinnamoyl-CoA reductase 1 and Cinnamoyl-CoA reductase 2) and in wheat (Cinnamoyl-CoA reductase 1). Cinnamoyl-CoA reductase (abbreviated CCR) is the first enzyme operating in the monolignol pathway for the production of lignin. In the rice genome 33 members of this family were identified. In a recent study Park et al (2017) characterized several members of the CCR family in rice and OsCCR19 was among those. They found it is closely related to constitutive CCRs, that are highly expressed in actively lignifying tissues, including stems and roots throughout all the developmental stages (Park, Bhoo et al. 2017). The wheat ortholog was characterized by Ma and colleagues, finding that wheat varieties with higher activity levels of TaCCR1 in stem were characterized by higher levels of lignin in the stem (Ma 2007). Nonetheless, in *Arabidopsis* down-regulation of AtCCR1, involved in lignin biosynthesis during vascular development, has been observed to reduce lignin content up to 50% (Lauvergeat, Lacomme et al. 2001, Goujon, Ferret et al. 2003). AtCCR1 influences also cell proliferation and biomass accumulation, suggesting a hypothetical role of the CCR gene family in plant development (Xue, Luo et al. 2015, De Meester, de Vries et al. 2018).

The last groups of markers is located on chromosome 2H between the position 12.238.955 and 14.345.320 base pair. This group of markers is associated with the number of vascular bundles in the two trials at Zadoks stage 83-85. The first marker falls within a Cullin-associated NEDD8-dissociated protein 1 (CAND1) (position 12.232.966-12.244.042, HORVU2Hr1G005650). Homolog searches on online databases revealed the existence of an ortholog in *Arabidopsis* AtCAND1. Mutants with recessive forms of this gene showed a reduced fertility and dwarfism due to auxin insensitivity (Feng, Shen et al. 2004). Auxin positively induces its own transport through cells, and those who transport the hormone more efficiently have more chance to became a part of vascular bundle (canalization hypothesis by Sachs)(Sachs 1991). Based on this model is possible to state that reduction in auxin sensitivity should produce a sparse vascular network: Alonso-Peral and collegues in 2006 found that *hve1/*CAND1 *Arabidopsis* recessive mutants show a reduced complexity pattern in leaf venation with reduced growth (Alonso-Peral, Candela et al. 2006). AtCAND1 has been found to interact with CUL1 hindering the ubiquitin protein degradation,

essential for auxin signalin and transport (Alonso-Peral, Candela et al. 2006). Mutated alleles of *hve* altering its function and expression don't stop the formation of the primary vascular structure, but partially inhibit the formation of the secondary and tertiary veins (Alonso-Peral, Candela et al. 2006).

5. DISCUSSION AND CONCLUSION

To our knowledge, this work represents the first genetic analysis of quantitative variation for culm morphological traits in barley. Despite the well-established links between lodging resistance and culm diameter, thickness and number of vascular bundles in various cereals (Ookawa, Hobo et al. 2010, Berry 2013), no published work addressed the genetic and molecular control of these traits and their correlations with other agronomic traits in barley. To fill this gap, we applied newly developed protocols to phenotype a diverse collection of European barley cultivars in multi-environment field trials, analyzed correlations with plant height, lodging and yield-related traits, and carried out GWAS to identify marker-trait associations and candidate genes. The methods and knowledge generated in this work provide a solid foundation for further characterization of culm architecture traits in barley and other crops and their deployment in genetic improvement of lodging resistance.

The phenotyping methods we developed for the characterization of the barley sections in this project are straightforward and do not require the use of specialized equipment. In the case of plants at harvest stage (Zadoks 90), sample preparation requires no particular instruments: an electric circular saw can be used to dissect internodes without deforming the samples, producing blunt edges - a clear-cut surface is very important for the production of precise images. Attaching the samples on a dark cardboard facilitated the sorting of samples and allowed optimal contrast with the background during image analysis. High resolution images were obtained with a flat office scanner and a laptop was used for image editing and filtering. These instruments are cheap compared to modern phenotyping platforms and can produce accurate images of the samples. For plants at dough stage (Zadoks 83) sample preparation was more time demanding but allowed us to analyze and investigate also the number of vascular bundles and its correlation with other culm-related traits. Another important feature of our protocols is the use of an open-access software like ImageJ to perform image analysis. The software requires a basic understanding of Java programming language and gives the user full control over the editing process avoiding the production of artifacts that can affect results.

We compared the reliability and the precision of this methodology with culm diameter measurements taken with a caliper from the same set of specimens (paragraph 4.1): similar distributions and high correlation (Pearson correlation = 0.796) between the two datasets indicate that the image analysis-based protocol is an efficient alternative to caliper measurements of culm diameter, while also providing access to additional traits that can hardly be measured manually as the medullar cavity diameter, the perimeter of the sections and the circularity. Distribution descriptors, skewness and kurtosis, are closer to normality for the data extracted by the software. Finally, once properly set up, software-driven data extraction improves the analysis under several points of view:

1. Standardized methodology: the sample preparation protocol and the Java script used to run the data extraction can be easily shared and used; no knowledge of Java language is needed, unless some parameters in the analysis have to be changed.
2. Sensitivity of the analysis: the software can analyze large numbers of samples iteratively with the same approach increasing precision and sensitivity.
3. Shape descriptors: beside diameter, the software can extract other quantitative data such as perimeter of the sections, area and circularity, allowing comprehensive morphological evaluation of the samples. Data can be saved directly into an excel file.
4. Storage: images of the samples can be stored and will not be altered by time or accidentally damaged. These pictures can be easily shared and utilized again for further analysis.

All these considerations support the use of the image analysis-based protocol for low-cost, fast and reliable phenotyping. Furthermore, flexibility of the ImageJ software allows users with little knowledge of Java language to modify the protocol scripts, adapting it to score other traits from other plant organs such as leaves, seeds, roots, ears, etc.
More sophisticated analyses can be performed using the different segmentation plug-ins available on-line, that can identify and analyze specific traits such as leaf size or plant height directly from field pictures.

These phenotyping protocols were used to study the genetic control of culm morphology in barley. Based on the literature (Berry, Sterling et al. 2004, Berry, Sylvester-Bradley et al. 2007), we decided to focus our attention on the second basal internode of the barley main stem as a critical point for lodging resistance, reasoning that this internode may also be considered as a good proxy

for the overall structure of the main culm. Our analysis on twenty randomly selected barley varieties in ITA 2017 and UK 2017 trials (paragraph 4.2) confirmed current knowledge about barley morphology (Briggs 1978) and highlighted new important features of culm architecture that were not yet described. Accurate phenotyping of six successive internodes revealed characteristic patterns for internode length, diameter and culm wall thickness. For internode length, a linear relationship was observed between internode number and internode length: basal internodes are shorter while upper internodes are longer. The length of apical internodes is more variable than basal internodes. Thickness follows a trend that is opposite to internode length with basal internodes being thicker compared to upper internodes, i.e. internode number is negatively correlated with thickness.

Diameter instead is maximum in the central internodes (3rd and 4th) and declines in more basal and apical internodes. While showing that the barley culm does not have a straight cylindrical geometry, results support the use of the second internode as a good descriptor for other plant internodes. In both trials varieties with a wider diameter and higher thickness at the second internode, possessed on average large and thick internodes along the whole the stem, although for internode 5 and 6 this trend was not consistent. ANOVA results show that genotype and row-type factors account for a significant proportion of phenotypic variation for culm diameter with six-row varieties having a wider diameter. Thickness instead was not influenced by row-type, but it was significantly affected by genotype and internode position. Genotype effects on these two traits provide a basis for more specific investigation of the genetic control of culm features. Of note, the barley stem should not be seen as a straight pipe but instead as a “ogival-shaped” pipe, with its central part wider than the extremities. In addition, the most basal and apical internodes differ with long and thin internodes in the upper part of the culm, and short and sturdy basal internodes. Probably, this particular structure can confer more flexibility at the top of the plant and improved rigidity near the root crown, while the wider diameter of the central internodes may prevent any shear effect due to lodging agents as wind and rain. Studies of the biomechanical and biochemical features of this stem organization are needed to better understand its properties.

Second internode straw samples were collected from field trials in eight different environments (location x year combinations) and phenotypic data extracted for culm diameter and thickness. As data for plant height were also available for each plot, we were able to calculate two indexes that proved to be good descriptors of the relationship between the different traits related to lodging

resistance: stem index (ratio of the 2nd internode diameter over plant height times 100) and stiffness (ratio of 2nd internode diameter over thickness). All these data showed good normal distribution across the trials. Plant height data (and consequently stem index) were absent in the Spanish 2016 trial; 2nd internode thickness data (and consequently stiffness) were lacking for the Finnish 2016 trial. Furthermore, data from the 2016 Italian trial follow a different trend compared to other trials, likely due to the strong storm that struck the field just before the heading stage. Plant height, culm diameter and thickness generally showed larger mean values in southern locations compared to the northern ones in agreement with previous reports (Wolabu and Tadege 2016, Liu, Ji et al. 2019). This could be due to the longer vegetative phase in Italian and Spanish trials. Stem Index and stiffness are similar across all environments, showing a stable proportion of the traits under study.

Diameter on average showed high heritability values across all trials, spanning from a minimum of 53.6% in the 2017 Italian trial up to 82.4% in the 2016 UK trial. Heritability values for thickness ranged from 18.45% to 81.13% in the 2016 Italian and 2017 Spanish trials, respectively, and are generally lower than those for culm diameter. This could be due to greater effects of environmental conditions and agronomic practices on thickness compared to diameter.

AMMI analysis confirmed these findings showing a clear latitudinal trend for the diameter between the north and south of Europe. AMMI analysis for thickness appeared more complex, suggesting a less clear interaction of this trait with the environments.

Pearson correlation tests considering the culm traits under study, along with plot grain yield, lodging score and harvest index (when available), allowed us to evaluate how culm related traits interact with other important yield related features. Diameter has negative or null correlations with both harvest index and grain yield. To further investigate these correlations, we introduced stem index and stiffness, which take into account the relationships between diameter and other important architectural traits to explore how the stem structure interacts with yield related traits. Diameter has a positive correlation with plant height, but never superior to 0.6: this means that it is possible to identify genotypes combining a wider culm and reduced plant height for improved lodging resistance. Stem index takes into account this relation and has significant positive correlations with both grain yield and harvest index. Plant height largely drives these correlations, since it always has negative and significant correlation with harvest index and grain yield, but these results suggest that plants with low stature and wider diameter have improved yield. Further insight is offered by the stiffness: correlation between diameter and thickness is always

positive but never superior to 0.6, and varieties with higher diameter and low thickness were observed in the trials. The stiffness index was elaborated in order to examine how the diameter itself interacts with other traits without the effect of the thickness. Stiffness exhibited positive or null correlations with grain yield and harvest index across all trials. These data suggest that thickness, which quantify the parenchymatic tissues in the internodes, probably works as a resource-sink, diverting resources from spikes. It would be interesting to identify mutants with altered culm wall thickness in order to evaluate the effect of this trait on yield related traits.

In all trials, lodging scores have positive and significant correlations with plant height (and therefore negative correlations with stem index), in agreement with many studies from the 1960 up to now (Kuczynska and Wyka 2011, Kuczyńska, Surma et al. 2013). Diameter and thickness were thought to have positive effect on the lodging resistance, but from our data, they have positive or null correlations with the lodging score. On the other hand, stiffness has small negative but still significant correlations with the lodging scores, this could mean that thickness has no positive effect on lodging resistance whereas an increase in diameter without thickness increase could reduce lodging occurrence. These results suggest a positive effect of the diameter itself on the improvement of lodging resistance, while thickness and plant height on the other hand increase lodging occurrence. Breeding for lodging resistance may thus benefit from genes allowing specific control of diameter independent from plant height and thickness. Other studies are needed also in order to evaluate if the variation in diameter/thickness ratio is related to different cell wall composition, if the thickness could be related to sclerenchymatic tissue and more in general how reduced thickness influence the mechanical resistance of the stem.

Results for Zadoks stage 83-85 (Italian trials 2016 and 2017) are generally consistent with those for Zadoks stage 90, although with marked differences between the two trials. In 2016, when the field was struck by a storm, mean diameter and thickness of the whole population were higher at Zadoks stage 90 compared to Zadoks stage 83-85. It would be interesting to further investigate the effects of mechanical stress on culm morphology and composition. Instead in the next year, plants were not subjected to extreme weather events and mean values decreased between dough stage and harvest: this can be related to translocation of resources from the internodes up to the ear as previously reported (Scofield, Ruuska et al. 2009). Future research is needed also to better understand the mechanisms underlying the plant ability to translocate resources from the stem to the ear, toward anthesis an interesting feature to guarantee improved lodging resistance during the vegetative phase, without hindering grain filling.

The number of vascular bundles was correlated with internode diameter, as expected. Of note, in 2017, this trait was negatively and significantly correlated with lodging occurrence: investigation of the effect of the size of vascular bundles should be further evaluated in order to explore potential correlation with internode diameter, lodging resistance and yield related traits.
In this study, we used a panel of European spring varieties, mainly structured according to row-type as shown by PCA and STRUCTURE analyses. This is a well-known pattern in barley germplasm (Comadran, Kilian et al. 2012). The results from the t-tests showed a clear effect of row-type on culm diameter. For this reason, correction for population structure was incorporated in GWAS analyses.
Supporting the validity of the selected model, GWAS on plant height identified the *sdw1/denso* gene known to have an important effect on plant height control (Kuczyńska, Surma et al. 2013). GWAS for culm diameter, culm wall thickness and number of vascular bundles identified several marker-trait associations including shared associations across trials. Scanning of the underlying genomic regions based on available barley genome annotation allowed us to identify several possible candidate genes. Among them, WRKY DNA-binding protein 33 is an interesting example for culm diameter for its known interaction with the gibberellin pathway (Spielmeyer, Ellis et al. 2002, Kuczyńska, Surma et al. 2013). Further research is needed to evaluate the possible involvement of this gene in controlling transverse growth of stem internodes in barley. Other candidate genes we found are involved in cell wall composition control, especially pectin, lignin and cellulose. All these molecules are part of the cell wall matrix and have an important effect on plant development and growth (Serrano-Mislata and Sablowski 2018). These findings suggest a possible influence of the cell wall composition on the stem morphology and architecture, pointing to future areas of study for a better understanding of culm development.

In conclusion, we successfully developed and applied image-based phenotyping protocols to investigate the architecture of the barley culm and dissect the genetic basis of several traits related to its morphology in different environments and developmental stages. Results show a complex series of correlations among traits, with the internode diameter positively correlated with plant height, internode thickness and number of vascular bundles. The two indexes we adopted to describe the diameter's relation to other traits (stem Index and stiffness), underline the positive effect of increased diameter in lodging resistance while identifying the negative effect of plant height and thickness. GWAS analyses allowed the identification of genomic regions associated

with the target traits across different trials, encompassing candidate genes involved in the regulation of gibberellin and auxin hormonal pathways and in the control of the cell wall biochemical composition and organization.

Future research into the biochemical and mechanical characterization of barley internodes will provide a more comprehensive understanding of the genetic and molecular networks that shape of the stem and their interactions.

APPENDIX-

APPENDIX A – LIST OF THE BARLEY ACCESSION USED

Name	Rows	Habitus	Source
Aapo	2	Spring	ExBarDiv
Abava	2	Spring	ExBarDiv
Agneta	6	Spring	ExBarDiv
Akcent	2	Spring	ExBarDiv
Akka	2	Spring	ExBarDiv
Alexis	2	Spring	ExBarDiv
Alis	2	Spring	ExBarDiv
Alliot	2	Spring	ExBarDiv
Annabell	2	Spring	ExBarDiv
Anni	2	Spring	ExBarDiv
Ansis	2	Spring	ExBarDiv
Apex	2	Spring	ExBarDiv
Aramir	2	Spring	ExBarDiv
Armelle	2	Spring	ExBarDiv
Arra	6	Spring	ExBarDiv
Artturi	6	Spring	ExBarDiv
Arvo	2	Spring	ExBarDiv
Asplund	6	Spring	ExBarDiv
Athos	2	Spring	ExBarDiv
Atlas	2	Spring	ExBarDiv
Atribut	2	Spring	ExBarDiv
Balder J	2	Spring	ExBarDiv
Balga	2	Spring	ExBarDiv
Barabas	2	Spring	ExBarDiv
Barke	2	Spring	ExBarDiv
Baronesse	2	Spring	ExBarDiv
Beatrix	2	Spring	ExBarDiv
Berenice	2	Spring	ExBarDiv
Binder	2	Spring	ExBarDiv
Birgitta	2	Spring	ExBarDiv
Birka	2	Spring	ExBarDiv
Blenheim	2	Spring	ExBarDiv
Bonus	2	Spring	ExBarDiv
Botnia	6	Spring	ExBarDiv
Braemar	2	Spring	ExBarDiv
Brazil	2	Spring	ExBarDiv
Britta A	2	Spring	ExBarDiv
Caja	2	Spring	ExBarDiv
Calgary	2	Spring	ExBarDiv

Carlsberg II	2	Spring	ExBarDiv
Cellar	2	Spring	ExBarDiv
Ceylon	2	Spring	ExBarDiv
Chanell	2	Spring	ExBarDiv
Chariot	2	Spring	ExBarDiv
Claret	2	Spring	ExBarDiv
Class	2	Spring	ExBarDiv
Cleopatra	2	Spring	ExBarDiv
Cooper	2	Spring	ExBarDiv
Corgi	2	Spring	ExBarDiv
Corniche	2	Spring	ExBarDiv
Cristalia	2	Spring	ExBarDiv
Croydon	2	Spring	ExBarDiv
Dandy	2	Spring	ExBarDiv
Danuta	2	Spring	ExBarDiv
Deba Abed	2	Spring	ExBarDiv
Delta	2	Spring	ExBarDiv
Derkado	2	Spring	ExBarDiv
Dialog	2	Spring	ExBarDiv
Diamant	2	Spring	ExBarDiv
Digersano	2	Spring	ExBarDiv
Drost	2	Spring	ExBarDiv
Druvis	6	Spring	ExBarDiv
Edda	6	Spring	ExBarDiv
Eero	6	Spring	ExBarDiv
Egmont	2	Spring	ExBarDiv
Elantra	2	Spring	ExBarDiv
Elo	2	Spring	ExBarDiv
Emir	2	Spring	ExBarDiv
Erkki	6	Spring	ExBarDiv
Etu	6	Spring	ExBarDiv
Eunova	2	Spring	ExBarDiv
Famin	2	Spring	ExBarDiv
Favorit	2	Spring	ExBarDiv
Felicitas	2	Spring	ExBarDiv
Formula	2	Spring	ExBarDiv
Forum	2	Spring	ExBarDiv
Freja	2	Spring	ExBarDiv
Frisia	6	Spring	ExBarDiv
Galan	2	Spring	ExBarDiv
Gate	2	Spring	ExBarDiv
Gizmo	2	Spring	ExBarDiv
Golden Promise	2	Spring	ExBarDiv
Golf	2	Spring	ExBarDiv
Gorm	2	Spring	ExBarDiv

Gull	2	Spring	ExBarDiv
Hana	2	Spring	ExBarDiv
Hanka	2	Spring	ExBarDiv
Hankkija_673	6	Spring	ExBarDiv
Hanna	2	Spring	ExBarDiv
Harry	2	Spring	ExBarDiv
Helmi	2	Spring	ExBarDiv
Heris	2	Spring	ExBarDiv
Herse	6	Spring	ExBarDiv
Hydrogen	2	Spring	ExBarDiv
Ida	2	Spring	ExBarDiv
Idumeja	2	Spring	ExBarDiv
Ilga	2	Spring	ExBarDiv
Imber	2	Spring	ExBarDiv
Impala	2	Spring	ExBarDiv
Imula	2	Spring	ExBarDiv
Ingrid	2	Spring	ExBarDiv
Isaria	2	Spring	ExBarDiv
Jadar	6	Spring	ExBarDiv
Jarek	2	Spring	ExBarDiv
Jyvà	6	Spring	ExBarDiv
Karat	2	Spring	ExBarDiv
Kenia	2	Spring	ExBarDiv
Keops	2	Spring	ExBarDiv
Kilta	6	Spring	ExBarDiv
Koral	2	Spring	ExBarDiv
Kristaps	2	Spring	ExBarDiv
Krystal	2	Spring	ExBarDiv
Ladik	2	Spring	ExBarDiv
Latvijas_Vietejie	2	Spring	ExBarDiv
Leeni	2	Spring	ExBarDiv
Lenta	2	Spring	ExBarDiv
Lise	6	Spring	ExBarDiv
Lofa Abed	2	Spring	ExBarDiv
Loviisa	6	Spring	ExBarDiv
Lud	2	Spring	ExBarDiv
Lux	2	Spring	ExBarDiv
Lysimax	2	Spring	ExBarDiv
Maris Mink	2	Spring	ExBarDiv
Marthe	2	Spring	ExBarDiv
Maskin	6	Spring	ExBarDiv
Midas	2	Spring	ExBarDiv
Mona	2	Spring	ExBarDiv
Morex	6	Spring	ExBarDiv
Nathalie	2	Spring	ExBarDiv

Niina	6	Spring	ExBarDiv
Nordal	2	Spring	ExBarDiv
Odessa	2	Spring	ExBarDiv
Odin	2	Spring	ExBarDiv
Okos	2	Spring	ExBarDiv
Olli	6	Spring	ExBarDiv
Optic	2	Spring	ExBarDiv
Orza	2	Spring	ExBarDiv
Otis	2	Spring	ExBarDiv
Otra	6	Spring	ExBarDiv
Otto	2	Spring	ExBarDiv
Paavo	6	Spring	ExBarDiv
Pasadena	2	Spring	ExBarDiv
Perun	2	Spring	ExBarDiv
Pirkka	6	Spring	ExBarDiv
Pohto	6	Spring	ExBarDiv
Pokko	6	Spring	ExBarDiv
Potra	6	Spring	ExBarDiv
Priora	2	Spring	ExBarDiv
Prisma	2	Spring	ExBarDiv
Proctor	2	Spring	ExBarDiv
Prosa	2	Spring	ExBarDiv
Quartz	2	Spring	ExBarDiv
Quench	2	Spring	ExBarDiv
Rapid	2	Spring	ExBarDiv
Rika	2	Spring	ExBarDiv
Riviera	2	Spring	ExBarDiv
Rondo	6	Spring	ExBarDiv
Roxana	2	Spring	ExBarDiv
Ruja	2	Spring	ExBarDiv
Saana	2	Spring	ExBarDiv
Salka	2	Spring	ExBarDiv
Salve	2	Spring	ExBarDiv
Scandium	2	Spring	ExBarDiv
Scarlett	2	Spring	ExBarDiv
Silja	6	Spring	ExBarDiv
Simba	2	Spring	ExBarDiv
Smilla	2	Spring	ExBarDiv
Spartan	2	Spring	ExBarDiv
Static	2	Spring	ExBarDiv
Steina	2	Spring	ExBarDiv
Stella	6	Spring	ExBarDiv
Stendes	2	Spring	ExBarDiv
Suvi	6	Spring	ExBarDiv
Tammi	6	Spring	ExBarDiv

Tarm92	2	Spring	ExBarDiv
Teele	6	Spring	ExBarDiv
Teemu	6	Spring	ExBarDiv
Tellus	2	Spring	ExBarDiv
Terno	2	Spring	ExBarDiv
Thuringia	2	Spring	ExBarDiv
Tidone	2	Spring	ExBarDiv
Tocada	2	Spring	ExBarDiv
Tremois	2	Spring	ExBarDiv
Triumph	2	Spring	ExBarDiv
Tyra	2	Spring	ExBarDiv
Union	2	Spring	ExBarDiv
Ursel	2	Spring	ExBarDiv
Vada	2	Spring	ExBarDiv
Vairogs	6	Spring	ExBarDiv
Valticky	2	Spring	ExBarDiv
vankkuri	2	Spring	ExBarDiv
Varde	6	Spring	ExBarDiv
Viivi	2	Spring	ExBarDiv
Volla	2	Spring	ExBarDiv
Welam	2	Spring	ExBarDiv
Wisa	2	Spring	ExBarDiv
Zenit	2	Spring	ExBarDiv
Zephyr	2	Spring	ExBarDiv

APPENDIX B – Macro command for samples at harvest stage (Zadoks 90)

```
// OUTER // To extract data for the overall shape//

//FILTERS
run("Enhance Contrast...", "saturated=3.3");
run("Bandpass Filter...", "filter_large=40 filter_small=3 suppress=None tolerance=5 autoscale
saturate");
run("8-bit");
setAutoThreshold("Default dark");
//run("Threshold...");
setThreshold(70, 255);
setOption("BlackBackground", false);
run("Convert to Mask");
run("Remove Outliers...", "radius=5 threshold=0 which=Bright");
run("Remove Outliers...", "radius=5 threshold=0 which=Dark");
//ANALYSIS outer
makeRectangle(3480, 360, 1040, 680);
run("Analyze Particles...", "size=.03-0.5 circularity=0.60-1.00 display include summarize add");
makeRectangle(3480, 1080, 1040, 680);
run("Analyze Particles...", "size=.03-0.5 circularity=0.60-1.00 display include summarize add");
makeRectangle(3480, 1780, 1040, 680);
run("Analyze Particles...", "size=.03-0.5 circularity=0.60-1.00 display include summarize add");
makeRectangle(3480, 2520, 1040, 680);
run("Analyze Particles...", "size=.03-0.5 circularity=0.60-1.00 display include summarize add");
makeRectangle(3480, 3200, 1040, 680);
run("Analyze Particles...", "size=.03-0.5 circularity=0.60-1.00 display include summarize add");
makeRectangle(3480, 3900, 1040, 680);
run("Analyze Particles...", "size=.03-0.5 circularity=0.60-1.00 display include summarize add");
makeRectangle(3480, 4600, 1040, 680);
run("Analyze Particles...", "size=.03-0.5 circularity=0.60-1.00 display include summarize add");
makeRectangle(3480, 5300, 1040, 680);
run("Analyze Particles...", "size=.03-0.5 circularity=0.60-1.00 display include summarize add");
makeRectangle(3480, 6050, 1040, 680);
run("Analyze Particles...", "size=.03-0.5 circularity=0.60-1.00 display include summarize add");

makeRectangle(2300, 432, 1040, 680);
run("Analyze Particles...", "size=.03-0.5 circularity=0.60-1.00 display include summarize add");
makeRectangle(2300, 1080, 1040, 680);
run("Analyze Particles...", "size=.03-0.5 circularity=0.60-1.00 display include summarize add");
makeRectangle(2300, 1780, 1040, 680);
run("Analyze Particles...", "size=.03-0.5 circularity=0.60-1.00 display include summarize add");
makeRectangle(2300, 2520, 1040, 680);
run("Analyze Particles...", "size=.03-0.5 circularity=0.60-1.00 display include summarize add");
makeRectangle(2300, 3200, 1040, 680);
run("Analyze Particles...", "size=.03-0.5 circularity=0.60-1.00 display include summarize add");
makeRectangle(2300, 3900, 1040, 680);
run("Analyze Particles...", "size=.03-0.5 circularity=0.60-1.00 display include summarize add");
```

```
makeRectangle(2300, 4600, 1040, 680);
run("Analyze Particles...", "size=.03-0.5 circularity=0.60-1.00 display include summarize add");
makeRectangle(2300, 5300, 1040, 680);
run("Analyze Particles...", "size=.03-0.5 circularity=0.60-1.00 display include summarize add");
makeRectangle(2300, 6050, 1040, 680);
run("Analyze Particles...", "size=.03-0.5 circularity=0.60-1.00 display include summarize add");

makeRectangle(1150, 360, 1040, 680);
run("Analyze Particles...", "size=.03-0.5 circularity=0.60-1.00 display include summarize add");
makeRectangle(1150, 1080, 1040, 680);
run("Analyze Particles...", "size=.03-0.5 circularity=0.60-1.00 display include summarize add");
makeRectangle(1150, 1780, 1040, 680);
run("Analyze Particles...", "size=.03-0.5 circularity=0.60-1.00 display include summarize add");
makeRectangle(1150, 2520, 1040, 680);
run("Analyze Particles...", "size=.03-0.5 circularity=0.60-1.00 display include summarize add");
makeRectangle(1150, 3200, 1040, 680);
run("Analyze Particles...", "size=.03-0.5 circularity=0.60-1.00 display include summarize add");
makeRectangle(1150, 3900, 1040, 680);
run("Analyze Particles...", "size=.03-0.5 circularity=0.60-1.00 display include summarize add");
makeRectangle(1150, 4600, 1040, 680);
run("Analyze Particles...", "size=.03-0.5 circularity=0.60-1.00 display include summarize add");
makeRectangle(1150, 5300, 1040, 680);
run("Analyze Particles...", "size=.03-0.5 circularity=0.60-1.00 display include summarize add");
makeRectangle(1150, 6050, 1040, 680);
run("Analyze Particles...", "size=.03-0.5 circularity=0.60-1.00 display include summarize add");

makeRectangle(0, 360, 1040, 680);
run("Analyze Particles...", "size=.03-0.5 circularity=0.60-1.00 display include summarize add");
makeRectangle(0, 1080, 1040, 680);
run("Analyze Particles...", "size=.03-0.5 circularity=0.60-1.00 display include summarize add");
makeRectangle(0, 1780, 1040, 680);
run("Analyze Particles...", "size=.03-0.5 circularity=0.60-1.00 display include summarize add");
makeRectangle(0, 2520, 1040, 680);
run("Analyze Particles...", "size=.03-0.5 circularity=0.60-1.00 display include summarize add");
makeRectangle(0, 3200, 1040, 680);
run("Analyze Particles...", "size=.03-0.5 circularity=0.60-1.00 display include summarize add");
makeRectangle(0, 3900, 1040, 680);
run("Analyze Particles...", "size=.03-0.5 circularity=0.60-1.00 display include summarize add");
makeRectangle(0, 4600, 1040, 680);
run("Analyze Particles...", "size=.03-0.5 circularity=0.60-1.00 display include summarize add");
makeRectangle(0, 5300, 1040, 680);
run("Analyze Particles...", "size=.03-0.5 circularity=0.60-1.00 display include summarize add");
makeRectangle(0, 6050, 1040, 680);
run("Analyze Particles...", "size=.03-0.5 circularity=0.60-1.00 display include summarize add");


//  INNER  // To extract data for the medullar cavity//
```

```
//FILTERS
run("Bandpass Filter...", "filter_large=40 filter_small=3 suppress=None tolerance=5 autoscale
saturate");
run("8-bit");
setAutoThreshold("Default");
//run("Threshold...");
run("Convert to Mask");
run("Remove Outliers...", "radius=5 threshold=0 which=Bright");
run("Remove Outliers...", "radius=5 threshold=0 which=Dark");
//ANALYSIS inner
makeRectangle(3480, 360, 1040, 680);
run("Analyze Particles...", "size=0.01-0.2 circularity=0.60-1.00 display exclude summarize add");
makeRectangle(3480, 1080, 1040, 680);
run("Analyze Particles...", "size=0.01-0.2 circularity=0.60-1.00 display exclude summarize add");
makeRectangle(3480, 1780, 1040, 680);
run("Analyze Particles...", "size=0.01-0.2 circularity=0.60-1.00 display exclude summarize add");
makeRectangle(3480, 2520, 1040, 680);
run("Analyze Particles...", "size=0.01-0.2 circularity=0.60-1.00 display exclude summarize add");
makeRectangle(3480, 3200, 1040, 680);
run("Analyze Particles...", "size=0.01-0.2 circularity=0.60-1.00 display exclude summarize add");
makeRectangle(3480, 3900, 1040, 680);
run("Analyze Particles...", "size=0.01-0.2 circularity=0.60-1.00 display exclude summarize add");
makeRectangle(3480, 4600, 1040, 680);
run("Analyze Particles...", "size=0.01-0.2 circularity=0.60-1.00 display exclude summarize add");
makeRectangle(3480, 5300, 1040, 680);
run("Analyze Particles...", "size=0.01-0.2 circularity=0.60-1.00 display exclude summarize add");
makeRectangle(3480, 6050, 1040, 680);
run("Analyze Particles...", "size=0.01-0.2 circularity=0.60-1.00 display exclude summarize add");

makeRectangle(2300, 432, 1040, 680);
run("Analyze Particles...", "size=0.01-0.2 circularity=0.60-1.00 display exclude summarize add");
makeRectangle(2300, 1080, 1040, 680);
run("Analyze Particles...", "size=0.01-0.2 circularity=0.60-1.00 display exclude summarize add");
makeRectangle(2300, 1780, 1040, 680);
run("Analyze Particles...", "size=0.01-0.2 circularity=0.60-1.00 display exclude summarize add");
makeRectangle(2300, 2520, 1040, 680);
run("Analyze Particles...", "size=0.01-0.2 circularity=0.60-1.00 display exclude summarize add");
makeRectangle(2300, 3200, 1040, 680);
run("Analyze Particles...", "size=0.01-0.2 circularity=0.60-1.00 display exclude summarize add");
makeRectangle(2300, 3900, 1040, 680);
run("Analyze Particles...", "size=0.01-0.2 circularity=0.60-1.00 display exclude summarize add");
makeRectangle(2300, 4600, 1040, 680);
run("Analyze Particles...", "size=0.01-0.2 circularity=0.60-1.00 display exclude summarize add");
makeRectangle(2300, 5300, 1040, 680);
run("Analyze Particles...", "size=0.01-0.2 circularity=0.60-1.00 display exclude summarize add");
makeRectangle(2300, 6050, 1040, 680);
run("Analyze Particles...", "size=0.01-0.2 circularity=0.60-1.00 display exclude summarize add");
```

```
makeRectangle(1150, 360, 1040, 680);
run("Analyze Particles...", "size=0.01-0.2 circularity=0.60-1.00 display exclude summarize add");
makeRectangle(1150, 1080, 1040, 680);
run("Analyze Particles...", "size=0.01-0.2 circularity=0.60-1.00 display exclude summarize add");
makeRectangle(1150, 1780, 1040, 680);
run("Analyze Particles...", "size=0.01-0.2 circularity=0.60-1.00 display exclude summarize add");
makeRectangle(1150, 2520, 1040, 680);
run("Analyze Particles...", "size=0.01-0.2 circularity=0.60-1.00 display exclude summarize add");
makeRectangle(1150, 3200, 1040, 680);
run("Analyze Particles...", "size=0.01-0.2 circularity=0.60-1.00 display exclude summarize add");
makeRectangle(1150, 3900, 1040, 680);
run("Analyze Particles...", "size=0.01-0.2 circularity=0.60-1.00 display exclude summarize add");
makeRectangle(1150, 4600, 1040, 680);
run("Analyze Particles...", "size=0.01-0.2 circularity=0.60-1.00 display exclude summarize add");
makeRectangle(1150, 5300, 1040, 680);
run("Analyze Particles...", "size=0.01-0.2 circularity=0.60-1.00 display exclude summarize add");
makeRectangle(1150, 6050, 1040, 680);
run("Analyze Particles...", "size=0.01-0.2 circularity=0.60-1.00 display exclude summarize add");

makeRectangle(0, 360, 1040, 680);
run("Analyze Particles...", "size=0.01-0.2 circularity=0.60-1.00 display exclude summarize add");
makeRectangle(0, 1080, 1040, 680);
run("Analyze Particles...", "size=0.01-0.2 circularity=0.60-1.00 display exclude summarize add");
makeRectangle(0, 1780, 1040, 680);
run("Analyze Particles...", "size=0.01-0.2 circularity=0.60-1.00 display exclude summarize add");
makeRectangle(0, 2520, 1040, 680);
run("Analyze Particles...", "size=0.01-0.2 circularity=0.60-1.00 display exclude summarize add");
makeRectangle(0, 3200, 1040, 680);
run("Analyze Particles...", "size=0.01-0.2 circularity=0.60-1.00 display exclude summarize add");
makeRectangle(0, 3900, 1040, 680);
run("Analyze Particles...", "size=0.01-0.2 circularity=0.60-1.00 display exclude summarize add");
makeRectangle(0, 4600, 1040, 680);
run("Analyze Particles...", "size=0.01-0.2 circularity=0.60-1.00 display exclude summarize add");
makeRectangle(0, 5300, 1040, 680);
run("Analyze Particles...", "size=0.01-0.2 circularity=0.60-1.00 display exclude summarize add");
makeRectangle(0, 6050, 1040, 680);
run("Analyze Particles...", "size=0.01-0.2 circularity=0.60-1.00 display exclude summarize add");
```

APPENDIX C – Macro command for samples at dough stage (Zadoks 83-85)

```
   macro "Outer [s]" {
     run("Bandpass Filter...", "filter_large=40 filter_small=3 suppress=None tolerance=5 autoscale
saturate");
run("Subtract Background...", "rolling=50 light separate sliding");
run("Enhance Contrast...", "saturated=3");
run("Find Edges");
run("8-bit");
setAutoThreshold("Default dark");
//run("Threshold...");
setThreshold(71, 255);
setOption("BlackBackground", false);
run("Convert to Mask");
run("Remove Outliers...", "radius=4 threshold=0 which=Dark");
run("Fill Holes");
run("Remove Outliers...", "radius=15 threshold=0 which=Dark");
setAutoThreshold("Default");
//run("Threshold...");
setOption("BlackBackground", false);
run("Convert to Mask");
   }
  run("Set Scale...", "global");
run("Analyze Particles...", "size=12000-Infinity pixel circularity=0.60-1.00 pixel display  include
summarize add");

   macro "Inner [d]" {
      run("Bandpass Filter...", "filter_large=40 filter_small=3 suppress=None tolerance=5 autoscale
saturate");
run("Subtract Background...", "rolling=50 light separate sliding");
run("Enhance Contrast...", "saturated=3");
run("Find Edges");
run("8-bit");
setAutoThreshold("Default dark");
//run("Threshold...");
setAutoThreshold("Default");
setThreshold(0, 100);
run("Convert to Mask");
run("Remove Outliers...", "radius=2 threshold=0 which=Dark");
run("Remove Outliers...", "radius=6 threshold=0 which=Bright");
setAutoThreshold("Default");
//run("Threshold...");
setOption("BlackBackground", false);
run("Convert to Mask");
}
run("Remove Outliers...", "radius=7 threshold=0 which=Dark");
run("Set Scale...", "global");
```

```
run("Analyze Particles...", "size=12000-Infinity pixel circularity=0.60-1.00 pixel display exclude
include summarize add");
```

APPENDIX D - Graphics for the specific proportionality trend of diameter and thickness in the Italian and English trials of 2017.

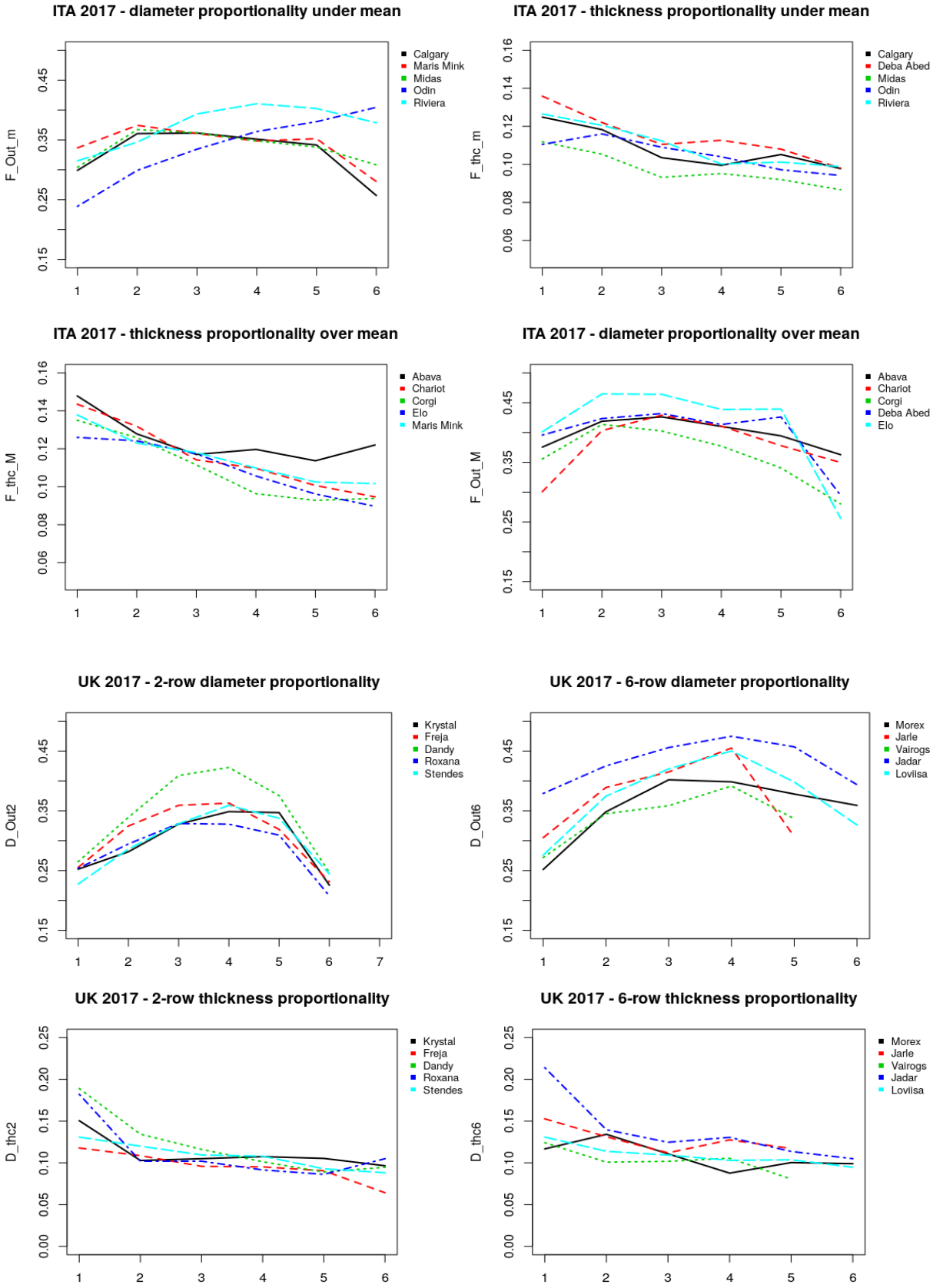

APPENDIX E - Data histogram distribution, skewness and kurtosis values

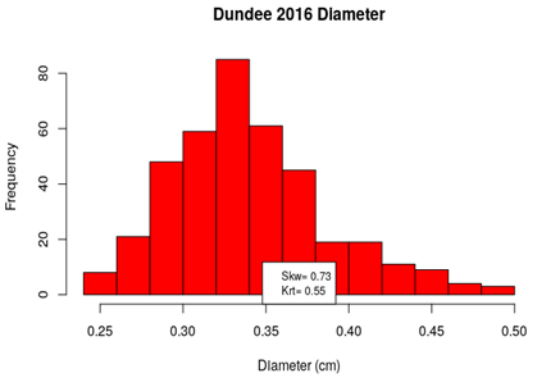

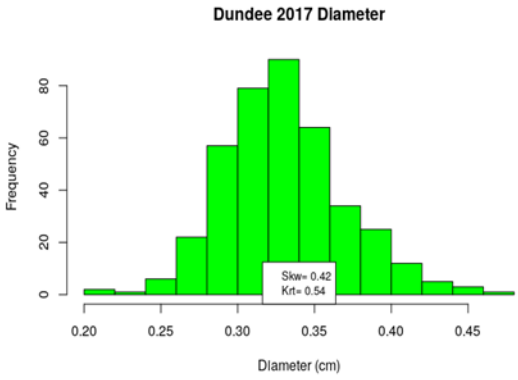

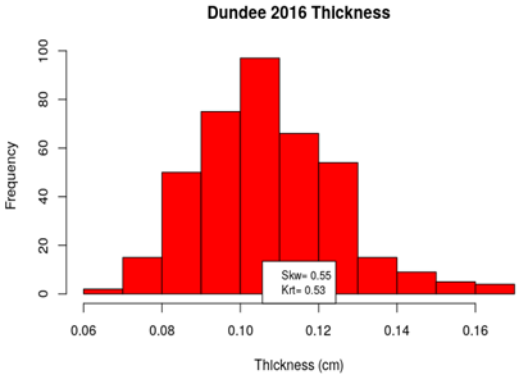

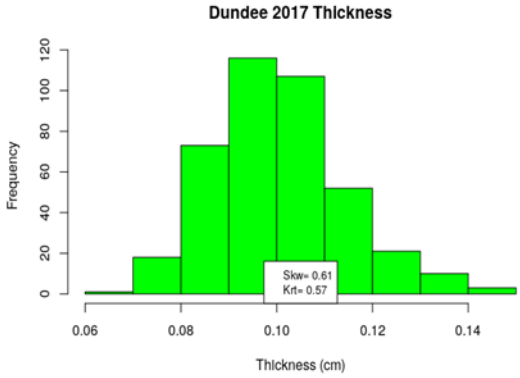

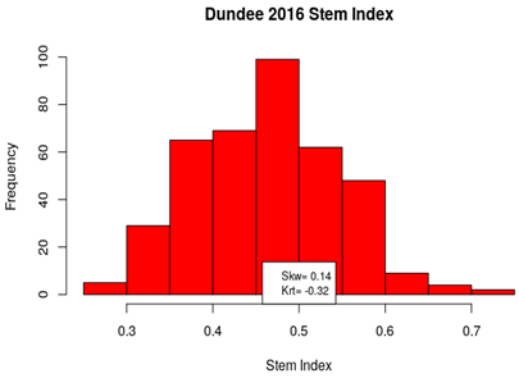

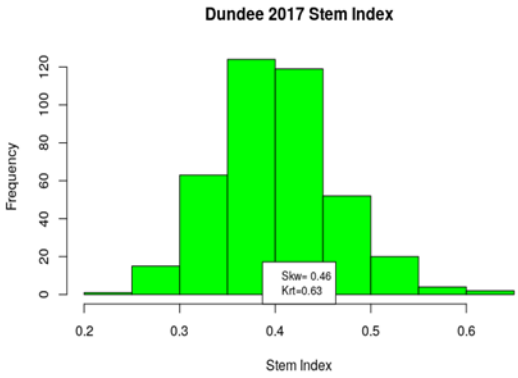

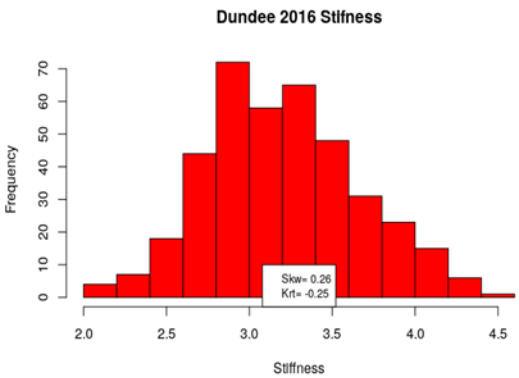

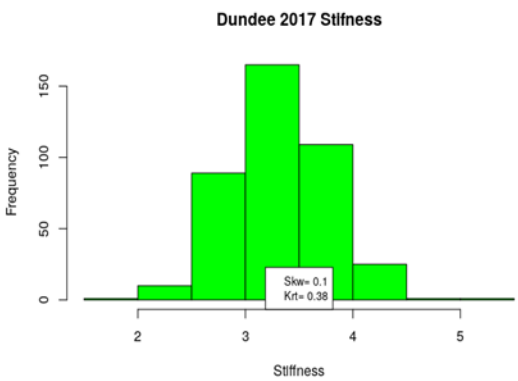

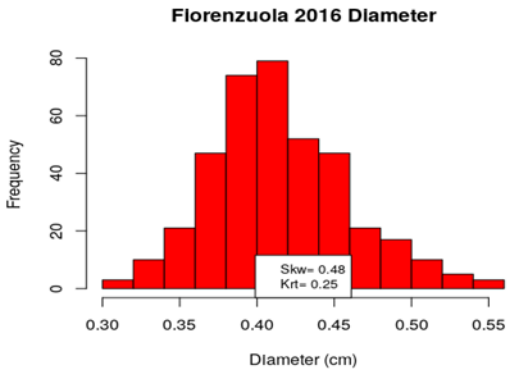
Florenzuola 2016 Diameter
Frequency
Skw= 0.48
Krt= 0.25
Diameter (cm)

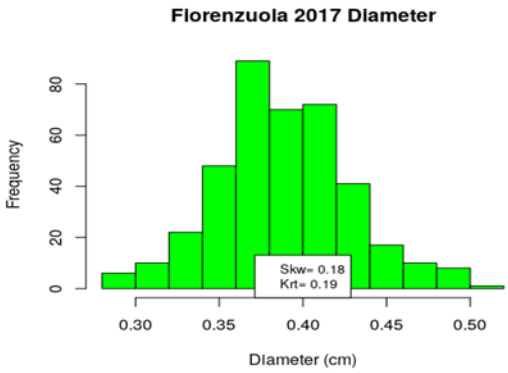
Florenzuola 2017 Diameter
Frequency
Skw= 0.18
Krt= 0.19
Diameter (cm)

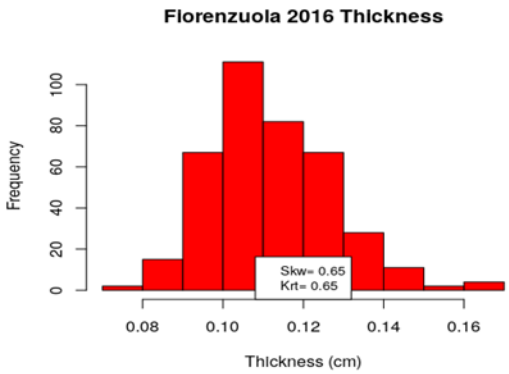
Florenzuola 2016 Thickness
Frequency
Skw= 0.65
Krt= 0.65
Thickness (cm)

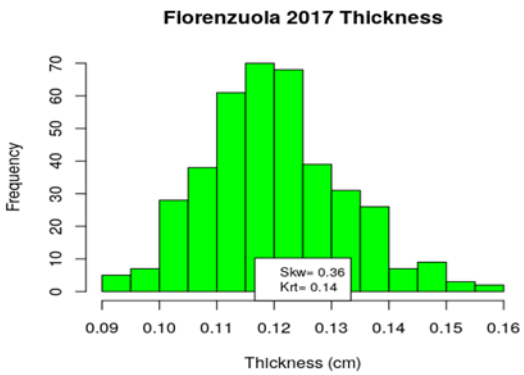
Florenzuola 2017 Thickness
Frequency
Skw= 0.36
Krt= 0.14
Thickness (cm)

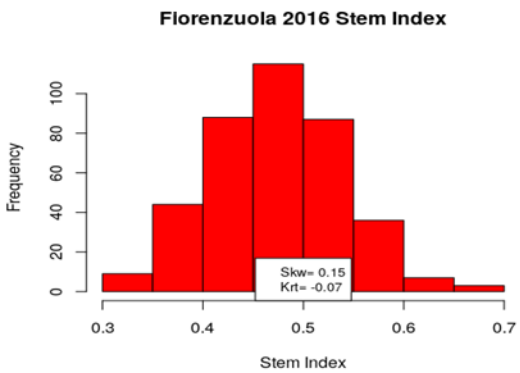
Florenzuola 2016 Stem Index
Frequency
Skw= 0.15
Krt= -0.07
Stem Index

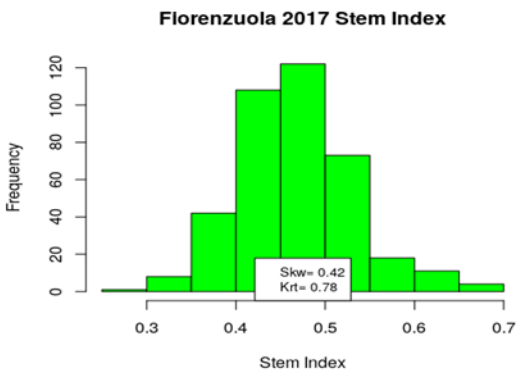
Florenzuola 2017 Stem Index
Frequency
Skw= 0.42
Krt= 0.78
Stem Index

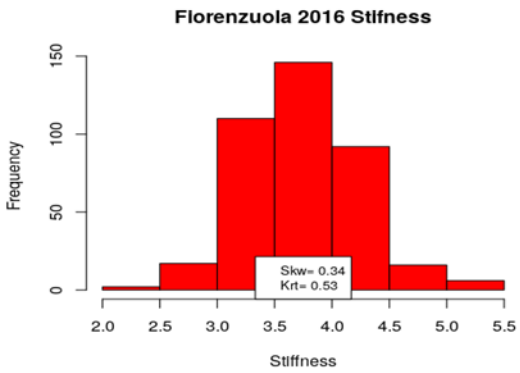
Florenzuola 2016 Stiffness
Frequency
Skw= 0.34
Krt= 0.53
Stiffness

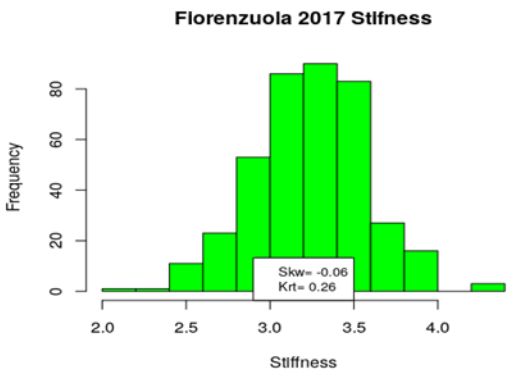
Florenzuola 2017 Stiffness
Frequency
Skw= -0.06
Krt= 0.26
Stiffness

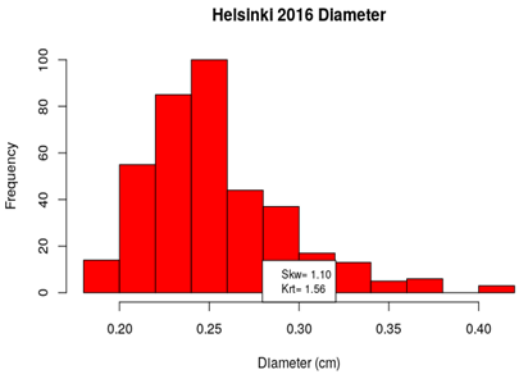
Helsinki 2016 Diameter
Frequency
Diameter (cm)
Skw= 1.10
Krt= 1.56

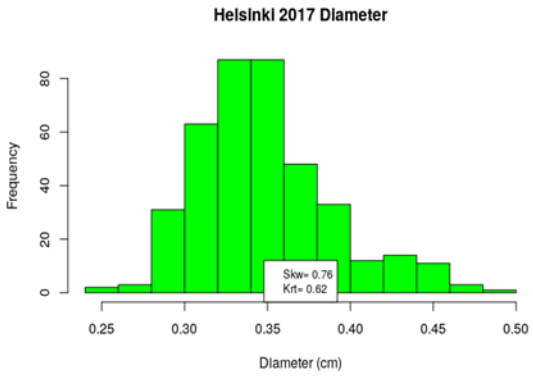
Helsinki 2017 Diameter
Frequency
Diameter (cm)
Skw= 0.76
Krt= 0.62

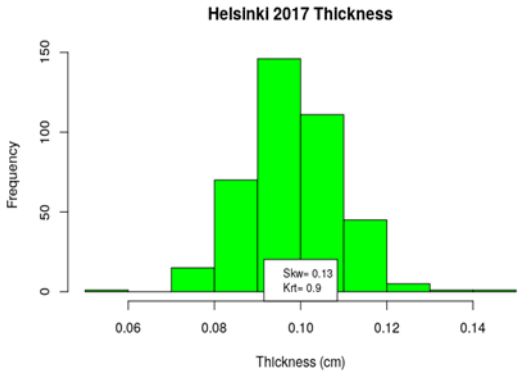
Helsinki 2017 Thickness
Frequency
Thickness (cm)
Skw= 0.13
Krt= 0.9

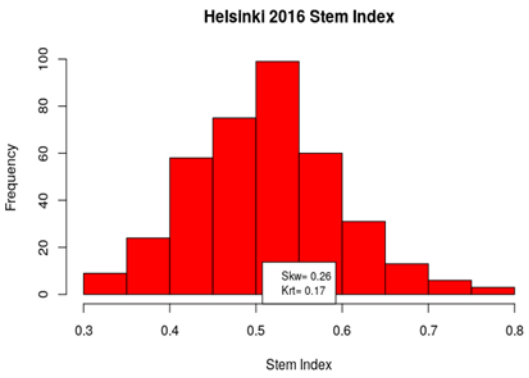
Helsinki 2016 Stem Index
Frequency
Stem Index
Skw= 0.26
Krt= 0.17

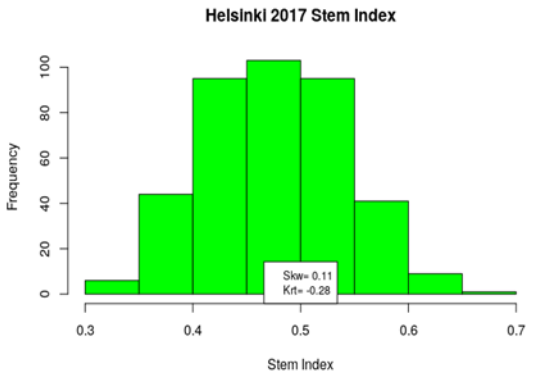
Helsinki 2017 Stem Index
Frequency
Stem Index
Skw= 0.11
Krt= -0.28

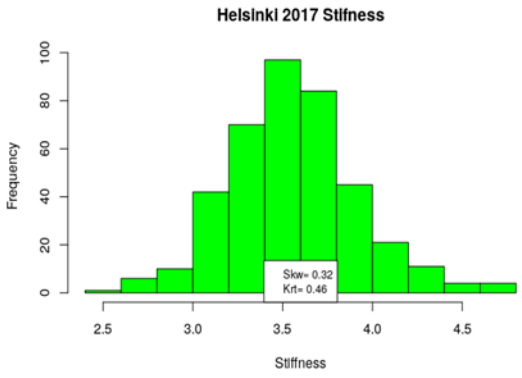
Helsinki 2017 Stiffness
Frequency
Stiffness
Skw= 0.32
Krt= 0.46

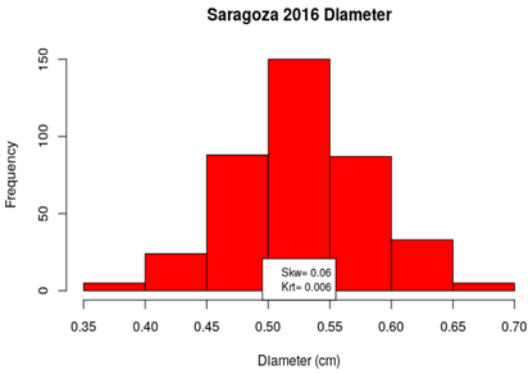
Saragoza 2016 Diameter
Frequency
Diameter (cm)
Skw= 0.06
Krt= 0.006

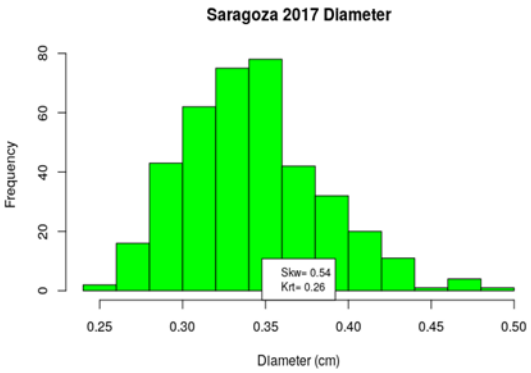
Saragoza 2017 Diameter
Frequency
Diameter (cm)
Skw= 0.54
Krt= 0.26

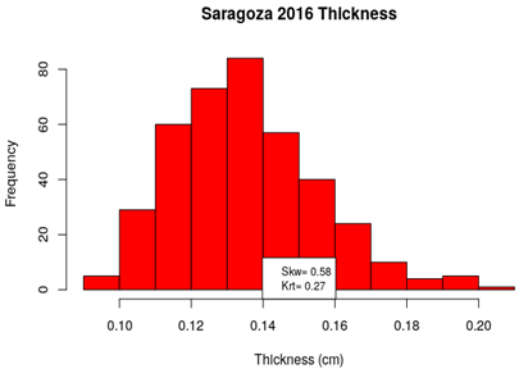
Saragoza 2016 Thickness
Frequency
Thickness (cm)
Skw= 0.58
Krt= 0.27

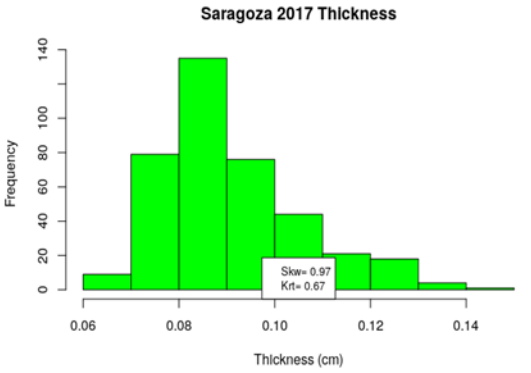
Saragoza 2017 Thickness
Frequency
Thickness (cm)
Skw= 0.97
Krt= 0.67

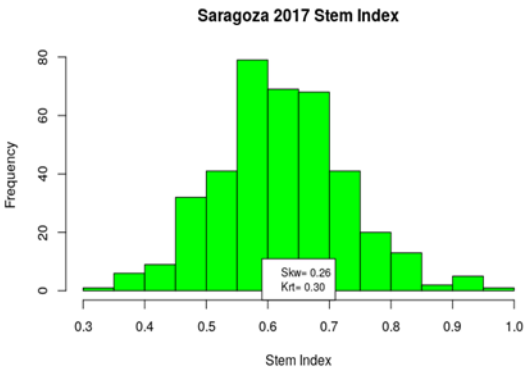
Saragoza 2017 Stem Index
Frequency
Stem Index
Skw= 0.26
Krt= 0.30

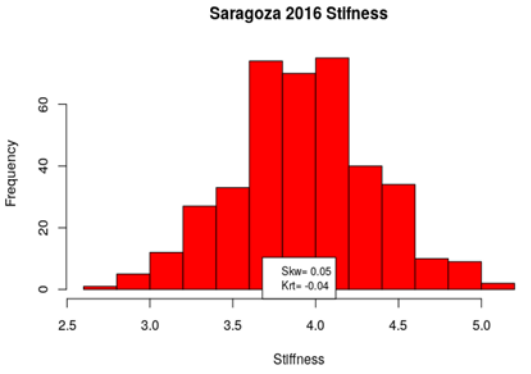
Saragoza 2016 Stiffness
Frequency
Stiffness
Skw= 0.05
Krt= -0.04

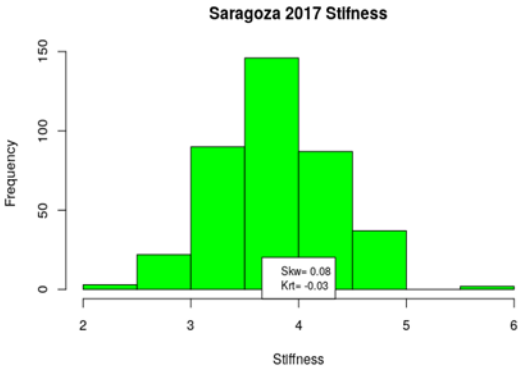
Saragoza 2017 Stiffness
Frequency
Stiffness
Skw= 0.08
Krt= -0.03

APPENDIX F – List of the ten most significant markers found with GWAS analyzing the harvest stage samples (Zadoks 90)

location	year	trait	SNP	Chromosome	Position	P.value	maf	effect
UK	2016	ph	JHI-Hv50k-2016-47922	1	528.008.766,00	4,84E-07	0,253807	4,528435
UK	2016	ph	JHI-Hv50k-2016-127497	2	722.462.781,00	1,72E-06	0,19797	3,233249
UK	2016	ph	JHI-Hv50k-2016-168035	3	183.307.804,00	3,4E-09	0,218274	4,380374
UK	2016	ph	JHI-Hv50k-2016-197260	3	592.639.168,00	3,04E-14	0,494924	-3,598494
UK	2016	ph	JHI-Hv50k-2016-205269	3	633.303.897,00	1,12E-19	0,101523	8,76089
UK	2016	ph	JHI-Hv50k-2016-325943	5	577.523.180,00	2,19E-17	0,21066	4,943762
UK	2016	ph	JHI-Hv50k-2016-384516	6	40.455.405,00	3,9E-07	0,248731	3,280706
UK	2016	ph	JHI-Hv50k-2016-434164	6	583.100.615,00	5,48E-06	0,30203	-3,464528
UK	2016	ph	JHI-Hv50k-2016-462640	7	50.290.694,00	2,6E-07	0,050761	4,716918
UK	2016	ph	JHI-Hv50k-2016-516867	7	650.218.642,00	2,16E-06	0,106599	2,968065
UK	2017	ph	12_30674	2	626.233.860,00	2,38E-12	0,147208	-5,818416
UK	2017	ph	JHI-Hv50k-2016-107364	2	650.902.508,00	4,97E-12	0,172589	5,889714
UK	2017	ph	JHI-Hv50k-2016-197260	3	592.639.168,00	4,08E-11	0,494924	-3,156936
UK	2017	ph	JHI-Hv50k-2016-205269	3	633.303.897,00	6,21E-09	0,101523	5,003685
UK	2017	ph	JHI-Hv50k-2016-258057	4	580.170.243,00	5,43E-06	0,274112	2,0853
UK	2017	ph	JHI-Hv50k-2016-271595	4	636.431.808,00	7,65E-08	0,187817	-3,409512
UK	2017	ph	SCRI_RS_196437	5	577.776.518,00	7,11E-10	0,401015	-6,120794
UK	2017	ph	JHI-Hv50k-2016-359307	5	654.512.591,00	0,000132	0,439086	4,858178
UK	2017	ph	JHI-Hv50k-2016-420333	6	550.728.798,00	1,19E-05	0,314721	-1,897092
UK	2017	ph	JHI-Hv50k-2016-478948	7	276.089.800,00	9,36E-08	0,228426	3,180538
ITA	2016	ph	JHI-Hv50k-2016-23330	1	321.609.883,00	4,39E-15	0,050761	-7,294976
ITA	2016	ph	JHI-Hv50k-2016-51959	1	539.104.723,00	1,55E-05	0,441624	-1,655402
ITA	2016	ph	JHI-Hv50k-2016-103187	2	626.236.144,00	3,66E-06	0,147208	3,421059
ITA	2016	ph	JHI-Hv50k-2016-126452	2	720.094.564,00	7,98E-08	0,370558	2,317963
ITA	2016	ph	JHI-Hv50k-2016-139740	2	751.639.819,00	5,35E-05	0,182741	-1,934059
ITA	2016	ph	JHI-Hv50k-2016-164401	3	48.638.313,00	7,48E-05	0,205584	3,377976
ITA	2016	ph	JHI-Hv50k-2016-197188	3	592.449.859,00	1,47E-05	0,454315	1,72609
ITA	2016	ph	JHI-Hv50k-2016-205000	3	632.318.274,00	1,9E-05	0,34264	1,794925
ITA	2016	ph	JHI-Hv50k-2016-277307	5	1.316.159,00	2,46E-07	0,177665	3,111987
ITA	2016	ph	JHI-Hv50k-2016-325943	5	577.523.180	0,000212	0,21066	1,427209
ITA	2016	ph	JHI-Hv50k-2016-453450	7	25.008.942,00	5,48E-05	0,205584	-3,103259
ITA	2017	ph	JHI-Hv50k-2016-16180	1	23.014.757,00	4,16E-05	0,154822	-1,609831
ITA	2017	ph	JHI-Hv50k-2016-28416	1	401.233.540,00	0,000102	0,228426	-3,517591
ITA	2017	ph	SCRI_RS_185319	2	22.770.072,00	7,86E-05	0,238579	-1,059233
ITA	2017	ph	JHI-Hv50k-2016-109823	2	672.895.449,00	4,41E-09	0,06599	-4,123477
ITA	2017	ph	JHI-Hv50k-2016-168594	3	198.163.084,00	8,56E-07	0,170051	2,628413
ITA	2017	ph	12_31220	3	627.362.478,00	8,85E-05	0,236041	1,670291
ITA	2017	ph	JHI-Hv50k-2016-210860	3	657.531.316,00	5,06E-06	0,091371	-2,65096
ITA	2017	ph	JHI-Hv50k-2016-263698	4	613.806.644,00	3,37E-05	0,13198	-1,633665
ITA	2017	ph	JHI-Hv50k-2016-325943	5	577.523.180	4,1E-07	0,21066	2,274116
ITA	2017	ph	SCRI_RS_236610	5	615.389.047,00	1,46E-05	0,225888	-2,521923
ITA	2017	ph	JHI-Hv50k-2016-384272	6	39.432.626,00	2,1E-07	0,137056	-2,816749
FIN	2016	ph	JHI-Hv50k-2016-112543	2	683.621.286,00	8,47E-05	0,091371	-1,699253
FIN	2016	ph	JHI-Hv50k-2016-168594	3	198.163.084,00	2,66E-14	0,170051	4,136276
FIN	2016	ph	JHI-Hv50k-2016-205398	3	634.190.153,00	6,65E-08	0,162437	2,624816
FIN	2016	ph	JHI-Hv50k-2016-229280	4	9.702.683,00	0,000176	0,390863	-1,147985
FIN	2016	ph	JHI-Hv50k-2016-261434	4	600.666.147,00	0,000197	0,15736	-2,367231
FIN	2016	ph	JHI-Hv50k-2016-282099	5	12.381.196,00	6,47E-09	0,086294	-3,530439

FIN	2016	ph	JHI-Hv50k-2016-345599	5	623.478.661,00	6,78E-05	0,380711	1,274182
FIN	2016	ph	JHI-Hv50k-2016-383072	6	35.446.334,00	0,000233	0,406091	-3,01053
FIN	2016	ph	JHI-Hv50k-2016-407341	6	462.119.913,00	0,000231	0,111675	2,194588
FIN	2016	ph	JHI-Hv50k-2016-415299	6	531.680.609,00	2,93E-05	0,19797	-1,434782
FIN	2017	ph	JHI-Hv50k-2016-4715	1	4.228.577,00	4,06E-05	0,167513	1,866605
FIN	2017	ph	JHI-Hv50k-2016-9983	1	9.238.603,00	0,000176	0,352792	-1,235468
FIN	2017	ph	JHI-Hv50k-2016-50842	1	536.784.046,00	0,000111	0,322335	1,350786
FIN	2017	ph	JHI-Hv50k-2016-71005	2	22.374.676,00	0,0001	0,403553	1,419487
FIN	2017	ph	JHI-Hv50k-2016-130637	2	729.223.465,00	1,64E-07	0,121827	-2,917194
FIN	2017	ph	JHI-Hv50k-2016-197260	3	592.639.168,00	4,21E-07	0,494924	-1,893357
FIN	2017	ph	JHI-Hv50k-2016-204244	3	627.766.338,00	2,39E-06	0,385787	-4,130157
FIN	2017	ph	JHI-Hv50k-2016-205154	3	633.069.492,00	1,17E-05	0,30203	1,703317
FIN	2017	ph	JHI-Hv50k-2016-231885	4	22.299.665,00	1,69E-17	0,177665	-6,061009
FIN	2017	ph	JHI-Hv50k-2016-325973	5	577.531.748,00	4,86E-07	0,347716	2,099005
SPA	2017	ph	JHI-Hv50k-2016-23330	1	321.609.883,00	8,77E-15	0,050761	-7,835694
SPA	2017	ph	JHI-Hv50k-2016-52024	1	539.382.635,00	0,000154	0,152284	-2,328797
SPA	2017	ph	JHI-Hv50k-2016-130257	2	728.298.636,00	6,36E-06	0,274112	1,718661
SPA	2017	ph	JHI-Hv50k-2016-177998	3	406.856.316,00	3,26E-06	0,456853	-5,356774
SPA	2017	ph	JHI-Hv50k-2016-197229	3	592.562.958,00	2,32E-05	0,393401	-1,361612
SPA	2017	ph	JHI-Hv50k-2016-205616	3	634.928.088,00	1,25E-08	0,177665	-3,233612
SPA	2017	ph	JHI-Hv50k-2016-206017	3	638.071.042,00	5,58E-06	0,101523	-3,455332
SPA	2017	ph	JHI-Hv50k-2016-231066	4	17.919.789,00	8,71E-07	0,192893	3,229996
SPA	2017	ph	JHI-Hv50k-2016-339272	5	609.412.755,00	9,92E-07	0,314721	-1,765601
SPA	2017	ph	JHI-Hv50k-2016-413252	6	517.888.942,00	1,9E-05	0,060914	-3,158149
UK	2016	out	JHI-Hv50k-2016-37634	1	486.872.133	2,71E-07	0,081218	-0,012689
UK	2016	out	JHI-Hv50k-2016-45614	1	522.492.014	5,11E-07	0,373096	-0,018654
UK	2016	out	JHI-Hv50k-2016-103260	2	626.588.015	6E-05	0,129442	0,010332
UK	2016	out	JHI-Hv50k-2016-159033	3	23.192.839	6,28E-05	0,088832	-0,010218
UK	2016	out	SCRI_RS_168538	3	531.627.065	1,57E-06	0,423858	0,007255
UK	2016	out	JHI-Hv50k-2016-231992	4	22.933.768	1,34E-11	0,177665	0,02218
UK	2016	out	SCRI_RS_135637	4	350.047.931	8,68E-05	0,411168	-0,005898
UK	2016	out	JHI-Hv50k-2016-309227	5	499.578.571	1,02E-06	0,464467	-0,01824
UK	2016	out	JHI-Hv50k-2016-428308	6	572.800.892	2,7E-05	0,22335	-0,008057
UK	2016	out	JHI-Hv50k-2016-478948	7	276.089.800	3,37E-07	0,228426	0,009786
UK	2017	out	JHI-Hv50k-2016-4228	1	3.879.550	3,06E-05	0,230964	-0,006369
UK	2017	out	JHI-Hv50k-2016-19334	1	67.288.382	2,85E-12	0,162437	-0,023228
UK	2017	out	JHI-Hv50k-2016-37651	1	488.799.253	1,1E-05	0,266497	-0,014005
UK	2017	out	SCRI_RS_198603	2	656.021.079	1,09E-05	0,340102	0,008413
UK	2017	out	JHI-Hv50k-2016-164745	3	64.674.446	1,37E-05	0,258883	-0,008956
UK	2017	out	JHI-Hv50k-2016-291801	5	71.634.568	3,4E-07	0,332487	-0,010188
UK	2017	out	JHI-Hv50k-2016-313788	5	535.816.147	9,82E-05	0,06599	0,01175
UK	2017	out	JHI-Hv50k-2016-418362	6	545.707.275	2,01E-06	0,172589	0,0089
UK	2017	out	JHI-Hv50k-2016-449628	7	14.569.906	0,000144	0,294416	0,005577
UK	2017	out	JHI-Hv50k-2016-498048	7	610.741.494	9,09E-06	0,451777	0,023832
ITA	2016	out	JHI-Hv50k-2016-6845	1	5.757.469	1,28E-11	0,390863	-0,024799
ITA	2016	out	JHI-Hv50k-2016-30938	1	420.360.366	8,76E-09	0,213198	0,019502
ITA	2016	out	JHI-Hv50k-2016-58973	2	834.687	3,53E-05	0,309645	0,006574
ITA	2016	out	JHI-Hv50k-2016-71066	2	22.399.825	0,000113	0,22335	0,006136
ITA	2016	out	JHI-Hv50k-2016-199959	3	606.944.760	4,21E-07	0,469543	-0,028577
ITA	2016	out	JHI-Hv50k-2016-207160	3	644.743.206	3,41E-07	0,258883	0,007355
ITA	2016	out	JHI-Hv50k-2016-309221	5	499.576.853	1,05E-06	0,423858	-0,021763
ITA	2016	out	JHI-Hv50k-2016-339891	5	610.099.259	3,25E-07	0,36802	0,016433
ITA	2016	out	SCRI_RS_222315	6	397.016.089	0,00012	0,266497	0,010201
ITA	2016	out	SCRI_RS_149650	7	538.394.571	3,91E-07	0,114213	-0,012349

ITA	2017	out	JHI-Hv50k-2016-36433	1	468.709.160	1,91E-06	0,314721	-0,01539
ITA	2017	out	JHI-Hv50k-2016-37651	1	488.799.253	1,12E-12	0,266497	-0,025986
ITA	2017	out	JHI-Hv50k-2016-77027	2	44.783.613	7,97E-07	0,147208	0,011146
ITA	2017	out	JHI-Hv50k-2016-224992	3	695.452.819	3,73E-06	0,327411	-0,014484
ITA	2017	out	JHI-Hv50k-2016-225548	3	696.305.192	4,22E-06	0,081218	0,012655
ITA	2017	out	SCRI_RS_164399	4	584.895.026	1,38E-06	0,413706	0,01478
ITA	2017	out	JHI-Hv50k-2016-282068	5	12.333.919	2,19E-07	0,164975	-0,011471
ITA	2017	out	11_10414	5	552.512.589	1,62E-06	0,329949	0,014184
ITA	2017	out	JHI-Hv50k-2016-486462	7	443.574.291	3,98E-06	0,401015	0,006743
ITA	2017	out	SCRI_RS_164623	7	640.721.112	7,89E-07	0,416244	0,006508
FIN	2016	out	JHI-Hv50k-2016-46233	1	523.388.034	2,3E-05	0,345178	0,011664
FIN	2016	out	JHI-Hv50k-2016-130413	2	728.831.999	7,99E-10	0,324873	-0,009666
FIN	2016	out	JHI-Hv50k-2016-152840	3	7.707.729	2,99E-06	0,121827	-0,00928
FIN	2016	out	SCRI_RS_205949	3	425.219.535	6,2E-09	0,172589	-0,011583
FIN	2016	out	JHI-Hv50k-2016-232164	4	23.603.729	4,58E-19	0,195431	0,026068
FIN	2016	out	JHI-Hv50k-2016-232560	4	26.357.667	1,22E-05	0,459391	0,015981
FIN	2016	out	JHI-Hv50k-2016-282260	5	12.611.988	5,98E-05	0,477157	-0,018087
FIN	2016	out	JHI-Hv50k-2016-309227	5	499.578.571	1,99E-05	0,464467	-0,014575
FIN	2016	out	JHI-Hv50k-2016-362392	5	659.533.445	6,99E-06	0,494924	-0,005418
FIN	2016	out	JHI-Hv50k-2016-444797	7	9.412.503	1,02E-05	0,13198	-0,010706
FIN	2017	out	JHI-Hv50k-2016-40173	1	507.640.878	0,000907	0,142132	0,004659
FIN	2017	out	JHI-Hv50k-2016-103130	2	626.117.006	2,75E-06	0,205584	0,008783
FIN	2017	out	JHI-Hv50k-2016-163305	3	39.377.199	0,000126	0,147208	-0,00605
FIN	2017	out	SCRI_RS_213950	3	656.385.446	9,37E-05	0,071066	-0,008823
FIN	2017	out	JHI-Hv50k-2016-231888	4	22.324.263	8,72E-19	0,162437	0,02392
FIN	2017	out	JHI-Hv50k-2016-259863	4	594.797.259	1,6E-08	0,337563	-0,014419
FIN	2017	out	JHI-Hv50k-2016-263116	4	609.239.133	5,02E-05	0,401015	-0,005006
FIN	2017	out	JHI-Hv50k-2016-301773	5	392.998.087	1,53E-09	0,314721	-0,008542
FIN	2017	out	JHI-Hv50k-2016-393040	6	163.345.036	0,000451	0,286802	-0,004175
FIN	2017	out	JHI-Hv50k-2016-515270	7	647.631.915	0,001219	0,398477	-0,00824
SPA	2016	out	JHI-Hv50k-2016-65882	2	13.109.325	6,52E-09	0,370558	-0,014089
SPA	2016	out	JHI-Hv50k-2016-163473	3	39.742.753	1,23E-07	0,284264	0,024448
SPA	2016	out	JHI-Hv50k-2016-183072	3	489.394.052	2,44E-06	0,170051	-0,01648
SPA	2016	out	JHI-Hv50k-2016-204050	3	627.062.037	5,97E-06	0,444162	0,027244
SPA	2016	out	JHI-Hv50k-2016-231905	4	22.331.283	1,1E-07	0,167513	-0,022696
SPA	2016	out	JHI-Hv50k-2016-279226	5	6.372.914	2E-05	0,243655	0,010077
SPA	2016	out	SCRI_RS_41519	5	361.700.802	0,00016	0,42132	0,006942
SPA	2016	out	JHI-Hv50k-2016-317209	5	552.550.469	0,000242	0,406091	0,008116
SPA	2016	out	JHI-Hv50k-2016-383173	6	35.936.517	0,000322	0,220812	0,009953
SPA	2016	out	JHI-Hv50k-2016-425343	6	565.056.659	0,000155	0,093909	0,017082
SPA	2017	out	JHI-Hv50k-2016-9519	1	8.915.870	0,000125	0,228426	0,006182
SPA	2017	out	JHI-Hv50k-2016-60352	2	2.848.265	6,87E-05	0,119289	-0,008641
SPA	2017	out	SCRI_RS_124301	2	728.302.402	0,000214	0,126904	-0,007809
SPA	2017	out	JHI-Hv50k-2016-203509	3	625.215.146	9,09E-05	0,461929	0,005129
SPA	2017	out	JHI-Hv50k-2016-231992	4	22.933.768	3,97E-18	0,177665	0,027531
SPA	2017	out	JHI-Hv50k-2016-236621	4	57.051.148	0,000276	0,101523	-0,008137
SPA	2017	out	JHI-Hv50k-2016-262054	4	604.399.654	0,00048	0,050761	-0,010883
SPA	2017	out	JHI-Hv50k-2016-407644	6	465.690.233	1,51E-05	0,294416	-0,00707
SPA	2017	out	JHI-Hv50k-2016-424507	6	563.148.579	0,000237	0,13198	-0,008092
SPA	2017	out	JHI-Hv50k-2016-431436	6	578.952.851	0,000121	0,060914	0,012308
UK	2016	tk	JHI-Hv50k-2016-208690	3	651.951.711	9,86E-10	0,182741	-0,00778
UK	2016	tk	JHI-Hv50k-2016-215375	3	667.841.770	6,58E-05	0,147208	0,003708
UK	2016	tk	JHI-Hv50k-2016-241134	4	287.937.638	2,47E-05	0,360406	-0,003083
UK	2016	tk	JHI-Hv50k-2016-247992	4	492.501.535	5,31E-06	0,431472	-0,007746

UK	2016	tk	SCRI_RS_231208	4	578.906.086	3,25E-05	0,279188	0,00304
UK	2016	tk	JHI-Hv50k-2016-279209	5	6.367.937	7,97E-07	0,162437	-0,004412
UK	2016	tk	JHI-Hv50k-2016-359083	5	653.924.576	1,76E-06	0,477157	0,008747
UK	2016	tk	JHI-Hv50k-2016-371529	6	7.665.476	9,61E-15	0,182741	-0,010655
UK	2016	tk	JHI-Hv50k-2016-393040	6	163.345.036	1,72E-05	0,286802	-0,002876
UK	2016	tk	JHI-Hv50k-2016-478948	7	276.089.800	1,58E-06	0,228426	0,004573
UK	2017	tk	JHI-Hv50k-2016-81421	2	76.447.452	0,000573	0,208122	0,001737
UK	2017	tk	JHI-Hv50k-2016-231962	4	22.861.735	6,92E-23	0,177665	-0,008462
UK	2017	tk	JHI-Hv50k-2016-249439	4	509.004.236	5,76E-05	0,142132	0,002639
UK	2017	tk	JHI-Hv50k-2016-256852	4	572.901.621	1,83E-05	0,472081	0,001855
UK	2017	tk	JHI-Hv50k-2016-266341	4	622.619.557	0,000214	0,060914	0,002938
UK	2017	tk	SCRI_RS_168359	5	3.438.902	5,48E-05	0,253807	0,001949
UK	2017	tk	JHI-Hv50k-2016-348277	5	630.450.966	4,17E-05	0,472081	-0,001661
UK	2017	tk	SCRI_RS_165400	5	639.992.381	5,17E-05	0,253807	0,00215
UK	2017	tk	SCRI_RS_143492	6	411.163.274	2,35E-05	0,406091	0,001549
UK	2017	tk	JHI-Hv50k-2016-459243	7	37.308.520	1,71E-05	0,050761	0,003777
ITA	2016	tk	JHI-Hv50k-2016-52533	1	541.005.990	2,6E-06	0,431472	-0,002625
ITA	2016	tk	JHI-Hv50k-2016-121503	2	710.200.434	0,000167	0,360406	0,004627
ITA	2016	tk	JHI-Hv50k-2016-209442	3	654.328.050	2,86E-06	0,243655	-0,003332
ITA	2016	tk	JHI-Hv50k-2016-267833	4	626.164.301	3,91E-07	0,06599	0,005098
ITA	2016	tk	JHI-Hv50k-2016-309125	5	498.937.052	5,72E-08	0,177665	0,004508
ITA	2016	tk	JHI-Hv50k-2016-379986	6	25.305.342	0,000116	0,06599	0,003075
ITA	2016	tk	JHI-Hv50k-2016-407801	6	467.893.908	3,16E-05	0,256345	-0,002213
ITA	2016	tk	JHI-Hv50k-2016-420432	6	551.435.769	5,86E-10	0,190355	-0,006923
ITA	2016	tk	JHI-Hv50k-2016-457880	7	32.899.627	2,35E-07	0,42132	0,010334
ITA	2016	tk	JHI-Hv50k-2016-519440	7	656.055.552	0,000115	0,413706	-0,005298
ITA	2017	tk	JHI-Hv50k-2016-41042	1	509.664.457	6,54E-11	0,182741	-0,005085
ITA	2017	tk	JHI-Hv50k-2016-81372	2	75.777.178	1,56E-06	0,228426	0,002227
ITA	2017	tk	JHI-Hv50k-2016-104859	2	639.342.580	5,43E-06	0,449239	-0,006859
ITA	2017	tk	JHI-Hv50k-2016-162781	3	36.781.480	0,000175	0,335025	0,002884
ITA	2017	tk	JHI-Hv50k-2016-215021	3	666.223.665	9,92E-06	0,167513	0,002238
ITA	2017	tk	SCRI_RS_175862	4	8.710.605	0,000214	0,373096	-0,001517
ITA	2017	tk	JHI-Hv50k-2016-263116	4	609.239.133	6,57E-05	0,401015	-0,001669
ITA	2017	tk	JHI-Hv50k-2016-274974	4	642.588.044	2,47E-05	0,106599	0,00288
ITA	2017	tk	JHI-Hv50k-2016-346776	5	626.023.597	5,08E-06	0,106599	-0,003776
ITA	2017	tk	JHI-Hv50k-2016-421275	6	553.917.550	0,001486	0,055838	-0,002407
FIN	2017	tk	12_31467	1	66.850.934	1,5E-11	0,177665	-0,003903
FIN	2017	tk	JHI-Hv50k-2016-26878	1	368.399.789	0,00021	0,053299	-0,002331
FIN	2017	tk	JHI-Hv50k-2016-53414	1	545.323.619	3,72E-06	0,192893	0,001797
FIN	2017	tk	JHI-Hv50k-2016-103558	2	630.949.219	8,13E-08	0,106599	0,003183
FIN	2017	tk	JHI-Hv50k-2016-114163	2	688.527.287	5,1E-07	0,091371	-0,002938
FIN	2017	tk	JHI-Hv50k-2016-157160	3	17.953.416	2,67E-05	0,472081	-0,001381
FIN	2017	tk	JHI-Hv50k-2016-263040	4	608.379.093	7,69E-08	0,403553	-0,001873
FIN	2017	tk	JHI-Hv50k-2016-277765	5	2.886.922	0,000122	0,086294	0,002246
FIN	2017	tk	JHI-Hv50k-2016-357799	5	651.049.650	2,86E-06	0,28934	-0,002056
FIN	2017	tk	JHI-Hv50k-2016-417281	6	542.065.422	1,21E-05	0,050761	0,002993
SPA	2016	tk	JHI-Hv50k-2016-49178	1	532.325.642	1,49E-05	0,093909	0,004458
SPA	2016	tk	JHI-Hv50k-2016-112938	2	685.275.740	0,00024	0,474619	-0,008287
SPA	2016	tk	JHI-Hv50k-2016-144956	2	760.935.052	5,52E-07	0,076142	0,00607
SPA	2016	tk	JHI-Hv50k-2016-153935	3	11.262.948	3,96E-05	0,385787	0,002731
SPA	2016	tk	JHI-Hv50k-2016-158850	3	23.094.971	0,000156	0,213198	-0,002789
SPA	2016	tk	JHI-Hv50k-2016-183831	3	495.139.792	0,000593	0,248731	-0,002483
SPA	2016	tk	JHI-Hv50k-2016-221303	3	684.258.533	0,000291	0,086294	0,003552
SPA	2016	tk	JHI-Hv50k-2016-231078	4	18.335.761	2,85E-12	0,152284	-0,008963

SPA	2016	tk	JHI-Hv50k-2016-279888	5	7.561.397	5,27E-07	0,06599	-0,007894
SPA	2016	tk	JHI-Hv50k-2016-348170	5	630.308.397	0,000148	0,474619	-0,00825
SPA	2017	tk	JHI-Hv50k-2016-164735	3	59.146.283	4,47E-05	0,126904	0,002421
SPA	2017	tk	SCRI_RS_199887	3	592.564.317	2,89E-05	0,27665	-0,003024
SPA	2017	tk	JHI-Hv50k-2016-214406	3	664.905.459	1,72E-08	0,22335	-0,003114
SPA	2017	tk	JHI-Hv50k-2016-231008	4	17.377.960	8,34E-14	0,182741	0,007098
SPA	2017	tk	JHI-Hv50k-2016-307573	5	482.424.008	6,1E-05	0,357868	-0,00176
SPA	2017	tk	JHI-Hv50k-2016-309465	5	501.183.003	6,95E-06	0,086294	0,003291
SPA	2017	tk	JHI-Hv50k-2016-384952	6	41.711.777	2,11E-05	0,258883	0,002408
SPA	2017	tk	SCRI_RS_234548	6	571.872.209	2,7E-07	0,294416	0,002347
SPA	2017	tk	JHI-Hv50k-2016-461354	7	47.480.839	0,000256	0,192893	0,002009
SPA	2017	tk	JHI-Hv50k-2016-518669	7	654.170.650	1,01E-07	0,256345	0,003033
UK	2016	si	JHI-Hv50k-2016-31326	1	424.145.541	2,44E-11	0,309645	0,029471
UK	2016	si	JHI-Hv50k-2016-130387	2	728.830.270	3,03E-06	0,238579	0,016156
UK	2016	si	JHI-Hv50k-2016-167755	3	176.202.147	6,5E-05	0,076142	0,021945
UK	2016	si	JHI-Hv50k-2016-196043	3	585.501.770	0,000117	0,083756	-0,019542
UK	2016	si	JHI-Hv50k-2016-230686	4	14.605.479	2,18E-07	0,076142	0,027435
UK	2016	si	JHI-Hv50k-2016-279847	5	7.555.392	0,00012	0,408629	-0,010976
UK	2016	si	JHI-Hv50k-2016-309465	5	501.183.003	4,72E-05	0,086294	0,018617
UK	2016	si	JHI-Hv50k-2016-370633	6	6.017.183	4,83E-05	0,441624	0,011277
UK	2016	si	JHI-Hv50k-2016-384360	6	39.513.268	0,000233	0,076142	-0,024055
UK	2016	si	JHI-Hv50k-2016-499413	7	614.823.922	1,78E-05	0,07868	-0,02193
UK	2017	si	JHI-Hv50k-2016-71249	2	22.853.879	2,88E-11	0,238579	0,015739
UK	2017	si	JHI-Hv50k-2016-130387	2	728.830.270	8,28E-06	0,238579	0,012147
UK	2017	si	JHI-Hv50k-2016-168594	3	198.163.084	1,36E-06	0,170051	-0,015174
UK	2017	si	JHI-Hv50k-2016-225850	4	370.915	7,84E-06	0,492386	0,024946
UK	2017	si	JHI-Hv50k-2016-284310	5	19.790.707	1,08E-07	0,106599	0,017566
UK	2017	si	JHI-Hv50k-2016-325943	5	577.523.180	1,66E-05	0,21066	-0,01032
UK	2017	si	JHI-Hv50k-2016-340086	5	610.334.796	5,15E-06	0,050761	-0,019191
UK	2017	si	JHI-Hv50k-2016-347472	5	629.054.092	5,91E-07	0,42132	-0,011028
UK	2017	si	JHI-Hv50k-2016-384360	6	39.513.268	4,8E-05	0,076142	-0,022055
UK	2017	si	JHI-Hv50k-2016-470580	7	87.622.649	4,12E-10	0,347716	0,01649
ITA	2016	si	JHI-Hv50k-2016-30793	1	419.585.828	5,75E-15	0,208122	-0,046444
ITA	2016	si	SCRI_RS_185319	2	22.770.072	8,41E-10	0,238579	0,01644
ITA	2016	si	JHI-Hv50k-2016-126411	2	720.092.358	7,17E-07	0,482234	0,013269
ITA	2016	si	JHI-Hv50k-2016-130413	2	728.831.999	6,49E-08	0,324873	-0,014278
ITA	2016	si	JHI-Hv50k-2016-140869	2	753.303.143	1,1E-08	0,096447	0,022687
ITA	2016	si	JHI-Hv50k-2016-197188	3	592.449.859	9,84E-08	0,454315	-0,012404
ITA	2016	si	JHI-Hv50k-2016-309221	5	499.576.853	3,58E-05	0,423858	-0,026157
ITA	2016	si	JHI-Hv50k-2016-365856	5	665.299.072	1,19E-09	0,365482	0,017179
ITA	2016	si	JHI-Hv50k-2016-449235	7	13.700.279	9,31E-06	0,403553	-0,035921
ITA	2016	si	JHI-Hv50k-2016-500129	7	617.098.010	1,71E-05	0,208122	-0,013569
ITA	2017	si	JHI-Hv50k-2016-27002	1	372.664.480	3,41E-06	0,19797	0,019969
ITA	2017	si	SCRI_RS_145336	1	448.694.456	7,5E-09	0,304569	0,017229
ITA	2017	si	JHI-Hv50k-2016-109787	2	672.596.429	1,51E-12	0,106599	-0,03197
ITA	2017	si	SCRI_RS_205658	2	742.795.239	1,44E-05	0,294416	0,01116
ITA	2017	si	JHI-Hv50k-2016-155182	3	14.177.483	4,5E-05	0,205584	-0,010935
ITA	2017	si	JHI-Hv50k-2016-206708	3	642.583.918	8,81E-07	0,238579	0,014732
ITA	2017	si	JHI-Hv50k-2016-210860	3	657.531.316	2,8E-05	0,091371	0,016085
ITA	2017	si	JHI-Hv50k-2016-225480	3	696.220.141	6,02E-06	0,208122	0,014037
ITA	2017	si	JHI-Hv50k-2016-308350	5	487.521.224	4,7E-06	0,436548	-0,02912
ITA	2017	si	JHI-Hv50k-2016-309207	5	499.573.029	1,56E-05	0,13198	-0,015652
FIN	2016	si	SCRI_RS_198643	2	23.189.369	5,67E-08	0,281726	-0,017574
FIN	2016	si	JHI-Hv50k-2016-129614	2	727.317.312	3,16E-06	0,411168	0,01557

FIN	2016	si	JHI-Hv50k-2016-130257	2	728.298.636	2,43E-06	0,274112	-0,018027
FIN	2016	si	JHI-Hv50k-2016-168470	3	196.391.413	3,11E-20	0,053299	0,086225
FIN	2016	si	JHI-Hv50k-2016-197342	3	593.275.528	2,14E-06	0,162437	0,023792
FIN	2016	si	12_11322	3	596.522.095	9,41E-06	0,411168	-0,036251
FIN	2016	si	JHI-Hv50k-2016-205269	3	633.303.897	4,43E-05	0,101523	-0,029491
FIN	2016	si	JHI-Hv50k-2016-383738	6	37.279.181	5,04E-05	0,309645	0,027339
FIN	2016	si	JHI-Hv50k-2016-421484	6	554.795.897	2,11E-05	0,428934	0,034208
FIN	2016	si	JHI-Hv50k-2016-508056	7	635.331.405	0,00028	0,454315	-0,011102
FIN	2017	si	JHI-Hv50k-2016-19345	1	67.299.632	3,7E-15	0,172589	-0,038605
FIN	2017	si	JHI-Hv50k-2016-71784	2	23.484.021	7,32E-12	0,494924	-0,018315
FIN	2017	si	JHI-Hv50k-2016-78161	2	50.936.915	0,000285	0,296954	-0,013756
FIN	2017	si	JHI-Hv50k-2016-111555	2	680.106.090	1,93E-07	0,111675	0,016928
FIN	2017	si	SCRI_RS_205658	2	742.795.239	0,000225	0,294416	0,008705
FIN	2017	si	JHI-Hv50k-2016-163268	3	39.285.297	2,79E-07	0,137056	0,017397
FIN	2017	si	JHI-Hv50k-2016-168748	3	200.572.004	1,51E-08	0,137056	-0,021332
FIN	2017	si	JHI-Hv50k-2016-204951	3	632.243.848	7,23E-09	0,406091	-0,014975
FIN	2017	si	JHI-Hv50k-2016-351467	5	640.766.892	4,26E-05	0,185279	-0,013854
FIN	2017	si	JHI-Hv50k-2016-446917	7	10.941.934	2,68E-05	0,071066	-0,017301
SPA	2017	si	JHI-Hv50k-2016-34688	1	454.174.291	2,76E-05	0,213198	-0,026449
SPA	2017	si	JHI-Hv50k-2016-130260	2	728.298.989	9,97E-10	0,274112	0,035378
SPA	2017	si	JHI-Hv50k-2016-167889	3	181.659.464	1,12E-11	0,050761	-0,071186
SPA	2017	si	JHI-Hv50k-2016-230936	4	16.668.758	1,13E-06	0,208122	0,033834
SPA	2017	si	JHI-Hv50k-2016-334221	5	596.204.796	0,000108	0,15736	-0,023115
SPA	2017	si	JHI-Hv50k-2016-389970	6	96.885.354	2,44E-07	0,494924	0,081769
SPA	2017	si	JHI-Hv50k-2016-402364	6	396.227.520	6,78E-06	0,142132	-0,029602
SPA	2017	si	11_21271	6	560.160.262	3,37E-07	0,385787	0,031725
SPA	2017	si	JHI-Hv50k-2016-501203	7	620.308.808	6,99E-06	0,06599	-0,034426
SPA	2017	si	JHI-Hv50k-2016-512270	7	641.787.418	0,000105	0,091371	0,031264
UK	2016	st	JHI-Hv50k-2016-7238	1	6.251.406	7,27E-07	0,050761	-0,181853
UK	2016	st	SCRI_RS_211923	2	4.332.694	2,62E-05	0,088832	-0,131316
UK	2016	st	JHI-Hv50k-2016-220055	3	681.465.029	2E-08	0,172589	0,14381
UK	2016	st	SCRI_RS_165273	5	586.615.927	2,5E-05	0,309645	0,149736
UK	2016	st	JHI-Hv50k-2016-351024	5	639.841.468	2,25E-06	0,233503	0,13462
UK	2016	st	SCRI_RS_194030	5	640.004.946	3,64E-07	0,213198	0,125522
UK	2016	st	JHI-Hv50k-2016-367980	6	342.696	1,19E-05	0,159898	-0,132178
UK	2016	st	JHI-Hv50k-2016-407276	6	461.870.555	5,47E-05	0,375635	-0,078763
UK	2016	st	JHI-Hv50k-2016-411510	6	503.723.396	0,001053	0,190355	-0,068158
UK	2016	st	JHI-Hv50k-2016-499145	7	614.236.763	0,000514	0,253807	0,063748
UK	2017	st	JHI-Hv50k-2016-71819	2	23.655.274	0,000514	0,124365	-0,081524
UK	2017	st	JHI-Hv50k-2016-166365	3	121.713.867	0,000359	0,063452	0,104034
UK	2017	st	JHI-Hv50k-2016-286093	5	25.827.621	0,000668	0,362944	-0,125494
UK	2017	st	JHI-Hv50k-2016-288219	5	34.675.800	0,000172	0,050761	-0,127733
UK	2017	st	JHI-Hv50k-2016-318848	5	554.922.246	0,000548	0,390863	0,057229
UK	2017	st	JHI-Hv50k-2016-376790	6	16.354.894	0,000111	0,205584	-0,096465
UK	2017	st	SCRI_RS_114741	6	148.640.702	0,00111	0,370558	-0,070769
UK	2017	st	JHI-Hv50k-2016-417942	6	545.088.823	0,000705	0,15736	0,073131
UK	2017	st	SCRI_RS_142893	7	14.439.972	1,34E-09	0,299492	0,120639
UK	2017	st	JHI-Hv50k-2016-451294	7	16.918.517	5,2E-06	0,093909	-0,129945
ITA	2016	st	JHI-Hv50k-2016-53147	1	543.804.916	6,62E-06	0,111675	-0,113423
ITA	2016	st	JHI-Hv50k-2016-111835	2	681.291.986	4,77E-06	0,111675	0,120782
ITA	2016	st	SCRI_RS_168042	3	680.221.782	6,35E-07	0,403553	-0,089758
ITA	2016	st	JHI-Hv50k-2016-321365	5	564.407.996	5,56E-09	0,050761	0,202344
ITA	2016	st	JHI-Hv50k-2016-352900	5	642.963.370	2,56E-07	0,347716	0,085839
ITA	2016	st	JHI-Hv50k-2016-379057	6	21.817.399	4,67E-07	0,329949	-0,082887

ITA	2016	st	JHI-Hv50k-2016-437996	7	2.725.936	6,28E-08	0,296954	-0,175427
ITA	2016	st	JHI-Hv50k-2016-492998	7	591.507.390	1,26E-05	0,137056	0,096048
ITA	2016	st	SCRI_RS_4556	7	593.836.026	8,96E-10	0,492386	-0,117822
ITA	2016	st	SCRI_RS_131173	7	638.446.503	2,86E-07	0,053299	0,16393
ITA	2017	st	JHI-Hv50k-2016-63218	2	8.697.665	7,2E-05	0,454315	0,181333
ITA	2017	st	JHI-Hv50k-2016-72276	2	26.014.126	3,12E-10	0,152284	0,130145
ITA	2017	st	JHI-Hv50k-2016-87627	2	122.769.327	0,000526	0,446701	0,036159
ITA	2017	st	JHI-Hv50k-2016-137072	2	744.833.374	3,41E-05	0,243655	-0,068443
ITA	2017	st	JHI-Hv50k-2016-153544	3	9.234.983	7,79E-05	0,370558	-0,090851
ITA	2017	st	JHI-Hv50k-2016-231345	4	19.488.685	1,18E-06	0,42132	-0,07518
ITA	2017	st	JHI-Hv50k-2016-278437	5	4.133.092	0,000665	0,055838	0,074457
ITA	2017	st	JHI-Hv50k-2016-322571	5	568.800.689	1,88E-05	0,22335	-0,059656
ITA	2017	st	JHI-Hv50k-2016-371886	6	7.944.777	0,000293	0,081218	0,067322
ITA	2017	st	JHI-Hv50k-2016-456765	7	31.300.831	7E-07	0,203046	0,132901
FIN	2017	st	JHI-Hv50k-2016-28073	1	394.196.032	3,93E-05	0,238579	0,086415
FIN	2017	st	JHI-Hv50k-2016-58018	1	557.776.124	5,97E-07	0,284264	-0,060372
FIN	2017	st	JHI-Hv50k-2016-120084	2	706.917.614	1,12E-07	0,091371	0,10037
FIN	2017	st	JHI-Hv50k-2016-130234	2	728.241.085	9,52E-07	0,152284	0,109608
FIN	2017	st	JHI-Hv50k-2016-148635	3	575.645	7,7E-08	0,111675	0,100984
FIN	2017	st	JHI-Hv50k-2016-225850	4	370.915	7,91E-07	0,492386	0,166417
FIN	2017	st	JHI-Hv50k-2016-258850	4	585.756.767	2,95E-05	0,408629	-0,116198
FIN	2017	st	JHI-Hv50k-2016-303229	5	418.818.037	5,07E-10	0,431472	-0,098499
FIN	2017	st	JHI-Hv50k-2016-376742	6	16.280.175	2,89E-05	0,271574	0,086265
FIN	2017	st	JHI-Hv50k-2016-417942	6	545.088.823	2,96E-06	0,15736	0,075039
SPA	2016	st	JHI-Hv50k-2016-6652	1	5.575.404	6,12E-05	0,246193	-0,086323
SPA	2016	st	JHI-Hv50k-2016-104276	2	637.284.878	0,000182	0,317259	-0,117952
SPA	2016	st	JHI-Hv50k-2016-131986	2	733.393.195	7,22E-06	0,071066	0,13049
SPA	2016	st	SCRI_RS_189757	3	24.614.927	4,46E-05	0,411168	-0,065343
SPA	2016	st	JHI-Hv50k-2016-162155	3	34.063.640	0,000397	0,385787	0,057577
SPA	2016	st	JHI-Hv50k-2016-212176	3	660.704.394	0,00022	0,13198	-0,070316
SPA	2016	st	JHI-Hv50k-2016-231078	4	18.335.761	2,83E-14	0,152284	0,292265
SPA	2016	st	JHI-Hv50k-2016-232609	4	26.681.950	1,59E-06	0,327411	0,169941
SPA	2016	st	JHI-Hv50k-2016-380301	6	26.119.865	9,17E-05	0,055838	-0,105306
SPA	2016	st	JHI-Hv50k-2016-501105	7	619.984.056	0,000442	0,225888	-0,060854
SPA	2017	st	JHI-Hv50k-2016-77818	2	49.749.337	1,27E-05	0,345178	0,091958
SPA	2017	st	JHI-Hv50k-2016-92456	2	361.283.173	0,000409	0,474619	-0,066486
SPA	2017	st	JHI-Hv50k-2016-102625	2	621.473.170	0,000141	0,324873	0,149377
SPA	2017	st	JHI-Hv50k-2016-103114	2	626.114.015	0,000861	0,147208	0,08322
SPA	2017	st	JHI-Hv50k-2016-110124	2	674.236.491	0,000747	0,322335	-0,123695
SPA	2017	st	12_10739	2	708.561.161	2,55E-05	0,071066	0,12413
SPA	2017	st	JHI-Hv50k-2016-132250	2	733.685.021	9,32E-06	0,233503	0,098619
SPA	2017	st	JHI-Hv50k-2016-211108	3	658.332.355	2,32E-12	0,152284	0,249334
SPA	2017	st	JHI-Hv50k-2016-307201	5	480.421.570	0,000306	0,06599	0,116828
SPA	2017	st	JHI-Hv50k-2016-489796	7	520.200.609	6,93E-05	0,423858	-0,082989

APPENDIX G – List of the ten most significant markers found with GWAS analyzing the dough stage samples (Zadoks 83-85)

location	year	trait	SNP	Chromosome	Position	P.value	maf	effect
ZK83	2016	out	SCRI_RS_14227	1	15.691.817	0,001714	0,213198	-0,01014
ZK83	2016	out	JHI-Hv50k-2016-46776	1	524.629.926	5,94E-07	0,203046	-0,02596
ZK83	2016	out	SCRI_RS_152485	2	686.489.408	0,000177	0,479695	0,011013
ZK83	2016	out	JHI-Hv50k-2016-132465	2	733.932.939	0,001731	0,370558	-0,01917
ZK83	2016	out	JHI-Hv50k-2016-206088	3	638.547.478	1,16E-05	0,21066	0,015982
ZK83	2016	out	JHI-Hv50k-2016-211623	3	659.544.025	0,002191	0,055838	0,019626
ZK83	2016	out	JHI-Hv50k-2016-216358	3	670.405.528	9,27E-05	0,279188	-0,01312
ZK83	2016	out	JHI-Hv50k-2016-379653	6	24.645.743	0,002313	0,106599	-0,01706
ZK83	2016	out	JHI-Hv50k-2016-382667	6	34.832.737	5,46E-08	0,393401	0,019952
ZK83	2016	out	JHI-Hv50k-2016-503319	7	624.137.785	2,42E-07	0,058376	-0,03519
ZK83	2017	out	JHI-Hv50k-2016-13583	1	16.061.886	0,000403	0,360406	-0,00711
ZK83	2017	out	JHI-Hv50k-2016-29428	1	408.789.476	0,000232	0,142132	-0,01202
ZK83	2017	out	SCRI_RS_145336	1	448.694.456	3,15E-05	0,304569	0,009425
ZK83	2017	out	JHI-Hv50k-2016-63299	2	8.945.111	1,54E-11	0,296954	-0,02974
ZK83	2017	out	JHI-Hv50k-2016-77454	2	47.176.639	2,5E-06	0,327411	0,019722
ZK83	2017	out	JHI-Hv50k-2016-142570	2	757.198.932	6,3E-05	0,142132	0,015973
ZK83	2017	out	12_30839	4	494.332.468	4,49E-05	0,167513	0,009463
ZK83	2017	out	JHI-Hv50k-2016-357952	5	651.207.847	1,91E-06	0,109137	-0,01288
ZK83	2017	out	JHI-Hv50k-2016-431826	6	579.522.437	0,000117	0,449239	0,023359
ZK83	2017	out	JHI-Hv50k-2016-515120	7	647.471.990	0,000386	0,06599	0,011232
ZK83	2016	tk	JHI-Hv50k-2016-184137	3	497.610.969	4E-05	0,401015	-0,00458
ZK83	2016	tk	JHI-Hv50k-2016-197703	3	594.959.864	3,28E-06	0,19797	-0,0036
ZK83	2016	tk	JHI-Hv50k-2016-202183	3	620.952.301	1,1E-06	0,304569	0,002847
ZK83	2016	tk	JHI-Hv50k-2016-207099	3	644.700.024	4,5E-06	0,253807	-0,00241
ZK83	2016	tk	JHI-Hv50k-2016-424200	6	562.681.018	7,02E-06	0,096447	0,003718
ZK83	2016	tk	JHI-Hv50k-2016-427749	6	571.737.763	1,89E-06	0,266497	-0,00436
ZK83	2016	tk	JHI-Hv50k-2016-458666	7	34.820.696	1,03E-05	0,172589	0,004141
ZK83	2016	tk	JHI-Hv50k-2016-505609	7	628.366.691	1,2E-05	0,200508	0,002637
ZK83	2016	tk	JHI-Hv50k-2016-509139	7	637.355.063	3,67E-09	0,279188	0,003181
ZK83	2016	tk	JHI-Hv50k-2016-512713	7	642.284.726	1,65E-05	0,352792	0,002145
ZK83	2017	tk	JHI-Hv50k-2016-7222	1	6.249.020	4,31E-06	0,106599	-0,00983
ZK83	2017	tk	JHI-Hv50k-2016-28480	1	401.746.356	2,09E-15	0,172589	-0,01885
ZK83	2017	tk	JHI-Hv50k-2016-58521	2	27.431	1,2E-05	0,147208	0,006343
ZK83	2017	tk	JHI-Hv50k-2016-113052	2	685.490.952	0,000232	0,375635	0,007995
ZK83	2017	tk	JHI-Hv50k-2016-278792	5	5.590.301	0,000281	0,319797	-0,00389
ZK83	2017	tk	JHI-Hv50k-2016-309480	5	501.227.291	0,000115	0,152284	0,005866
ZK83	2017	tk	JHI-Hv50k-2016-365364	5	664.717.590	9,16E-05	0,467005	-0,00346
ZK83	2017	tk	JHI-Hv50k-2016-407217	6	461.114.068	1,78E-05	0,451777	0,004288
ZK83	2017	tk	JHI-Hv50k-2016-433810	6	582.685.735	1,05E-05	0,340102	-0,0095
ZK83	2017	tk	JHI-Hv50k-2016-453643	7	25.438.196	1,49E-08	0,411168	0,006198
ZK83	2016	si	JHI-Hv50k-2016-10993	1	11.457.309	0,000308	0,42132	0,030815
ZK83	2016	si	JHI-Hv50k-2016-123934	2	713.895.999	0,000546	0,492386	-0,01187
ZK83	2016	si	JHI-Hv50k-2016-126153	2	719.151.649	0,00031	0,279188	0,024704
ZK83	2016	si	JHI-Hv50k-2016-205398	3	634.190.153	3,75E-08	0,162437	-0,03414
ZK83	2016	si	JHI-Hv50k-2016-206969	3	643.885.123	0,0003	0,279188	-0,01562
ZK83	2016	si	JHI-Hv50k-2016-355641	5	647.457.994	0,000444	0,408629	-0,01562
ZK83	2016	si	11_21141	5	650.559.496	3,17E-05	0,477157	-0,01865
ZK83	2016	si	JHI-Hv50k-2016-377725	6	16.900.243	0,000232	0,218274	0,016877
ZK83	2016	si	JHI-Hv50k-2016-487389	7	458.681.828	0,000316	0,091371	0,023156

ZK83	2016	si	JHI-Hv50k-2016-500794	7	618.945.999	2,35E-05	0,441624	-0,0384
ZK83	2017	si	JHI-Hv50k-2016-1422	1	1.430.891	0,000238	0,203046	-0,01174
ZK83	2017	si	JHI-Hv50k-2016-27002	1	372.664.480	1,8E-11	0,19797	0,037532
ZK83	2017	si	SCRI_RS_145336	1	448.694.456	0,000159	0,304569	0,013908
ZK83	2017	si	JHI-Hv50k-2016-71784	2	23.484.021	0,000282	0,494924	-0,01088
ZK83	2017	si	JHI-Hv50k-2016-132814	2	735.082.241	9,25E-11	0,22335	-0,02652
ZK83	2017	si	JHI-Hv50k-2016-135565	2	742.067.766	0,000993	0,388325	-0,01737
ZK83	2017	si	JHI-Hv50k-2016-161120	3	29.172.502	0,0009	0,327411	-0,0175
ZK83	2017	si	JHI-Hv50k-2016-197188	3	592.449.859	7,49E-05	0,454315	-0,01147
ZK83	2017	si	JHI-Hv50k-2016-214829	3	665.969.626	1,33E-05	0,22335	0,014701
ZK83	2017	si	JHI-Hv50k-2016-237717	4	68.270.905	2,27E-05	0,126904	0,022032
ZK83	2016	st	JHI-Hv50k-2016-107614	2	651.532.271	2,85E-06	0,383249	4,09615
ZK83	2016	st	JHI-Hv50k-2016-127604	2	722.897.646	3,7E-07	0,081218	-3,06188
ZK83	2016	st	SCRI_RS_161490	2	735.203.017	1,76E-10	0,106599	-3,41857
ZK83	2016	st	JHI-Hv50k-2016-146568	2	763.215.871	5,99E-06	0,464467	3,155805
ZK83	2016	st	JHI-Hv50k-2016-193742	3	569.482.311	7,12E-11	0,200508	3,216977
ZK83	2016	st	JHI-Hv50k-2016-197703	3	594.959.864	5,35E-07	0,19797	2,274027
ZK83	2016	st	SCRI_RS_165313	5	27.485.132	5,91E-06	0,456853	-2,35793
ZK83	2016	st	JHI-Hv50k-2016-384271	6	39.432.561	4,78E-07	0,43401	4,308586
ZK83	2016	st	JHI-Hv50k-2016-437045	7	2.083.567	4,12E-07	0,395939	-1,33118
ZK83	2016	st	JHI-Hv50k-2016-506060	7	629.241.801	1,79E-05	0,243655	-1,32294
ZK83	2017	st	JHI-Hv50k-2016-9518	1	8.915.797	0,000161	0,13198	0,098731
ZK83	2017	st	JHI-Hv50k-2016-60309	2	2.834.583	5,34E-11	0,134518	-0,20005
ZK83	2017	st	JHI-Hv50k-2016-228683	4	8.227.143	2,53E-05	0,055838	0,159313
ZK83	2017	st	JHI-Hv50k-2016-238924	4	85.354.636	8,11E-06	0,431472	0,355678
ZK83	2017	st	JHI-Hv50k-2016-249748	4	516.113.262	0,000298	0,319797	0,078625
ZK83	2017	st	JHI-Hv50k-2016-307484	5	481.616.199	0,000412	0,479695	-0,06012
ZK83	2017	st	SCRI_RS_11206	5	532.482.529	2,67E-06	0,401015	-0,10236
ZK83	2017	st	JHI-Hv50k-2016-332105	5	590.123.028	3,02E-09	0,352792	-0,32851
ZK83	2017	st	JHI-Hv50k-2016-335778	5	598.395.471	0,000164	0,098985	-0,10706
ZK83	2017	st	JHI-Hv50k-2016-348315	5	630.457.747	2,14E-05	0,116751	-0,18824
ZK83	2016	VB	JHI-Hv50k-2016-15414	1	19956443	3,35E-05	0,408629	0,674908
ZK83	2016	VB	JHI-Hv50k-2016-17894	1	35727080	8,52E-10	0,335025	2,137931
ZK83	2016	VB	JHI-Hv50k-2016-65236	2	12238955	6,56E-05	0,286802	-1,31145
ZK83	2016	VB	JHI-Hv50k-2016-65476	2	12863581	0,000164	0,154822	0,739947
ZK83	2016	VB	JHI-Hv50k-2016-188196	3	534536343	0,000117	0,177665	0,632068
ZK83	2016	VB	JHI-Hv50k-2016-225548	3	696305192	1,1E-06	0,081218	1,539399
ZK83	2016	VB	JHI-Hv50k-2016-264540	4	618295701	9,31E-06	0,492386	-0,6981
ZK83	2016	VB	JHI-Hv50k-2016-309586	5	501845352	4,84E-06	0,101523	1,287578
ZK83	2016	VB	JHI-Hv50k-2016-316219	5	547124504	5,51E-05	0,385787	-0,70276
ZK83	2016	VB	JHI-Hv50k-2016-418468	6	545760337	2,54E-06	0,213198	-0,86181
ZK83	2017	VB	JHI-Hv50k-2016-66847	2	14345320	0,000374	0,492386	-0,62198
ZK83	2017	VB	JHI-Hv50k-2016-94279	2	475599524	5,9E-06	0,467005	-0,83287
ZK83	2017	VB	JHI-Hv50k-2016-207635	3	647436977	8,09E-06	0,431472	-0,78715
ZK83	2017	VB	JHI-Hv50k-2016-255180	4	564008849	1,87E-05	0,147208	0,9352
ZK83	2017	VB	JHI-Hv50k-2016-259863	4	594797259	2,52E-05	0,337563	-1,55961
ZK83	2017	VB	JHI-Hv50k-2016-279859	5	7557066	0,000298	0,071066	1,259322
ZK83	2017	VB	JHI-Hv50k-2016-364164	5	663156749	0,000137	0,109137	1,012839
ZK83	2017	VB	JHI-Hv50k-2016-378443	6	19567779	0,000358	0,076142	1,145553
ZK83	2017	VB	JHI-Hv50k-2016-425580	6	565496900	1,83E-06	0,451777	-3,30211
ZK83	2017	VB	SCRI_RS_131173	7	638446503	2E-09	0,053299	2,617289

BIBLIOGRAPHY

Abdallah, J. M., B. Goffinet, C. Cierco-Ayrolles and M. Pérez-Enciso (2003). "Linkage disequilibrium fine mapping of quantitative trait loci: A simulation study." Genetics Selection Evolution **35**(6): 513.

Abdurakhmonov, I. Y. and A. Abdukarimov (2008). "Application of Association Mapping to Understanding the Genetic Diversity of Plant Germplasm Resources." International Journal of Plant Genomics **2008**: 574927.

Agnew, E., A. Bray, E. Floro, N. Ellis, J. Gierer, C. Lizárraga, D. O'Brien, M. Wiechert, T. C. Mockler, N. Shakoor and C. N. Topp (2017). "Whole-Plant Manual and Image-Based Phenotyping in Controlled Environments." Current Protocols in Plant Biology **2**(1): 1-21.

Alonso-Peral, M. M., H. Candela, J. C. del Pozo, A. Martínez-Laborda, M. R. Ponce and J. L. Micol (2006). "The HVE/CAND1 gene is required for the early patterning of leaf venation in Arabidopsis." Development **133**(19): 3755-3766.

Arai-Sanoh, Y., M. Ida, R. Zhao, S. Yoshinaga, T. Takai, T. Ishimaru, H. Maeda, K. Nishitani, Y. Terashima, M. Gau, N. Kato, M. Matsuoka and M. Kondo (2011). "Genotypic Variations in Non-Structural Carbohydrate and Cell-Wall Components of the Stem in Rice, Sorghum, and Sugar Vane." Bioscience, Biotechnology, and Biochemistry **75**(6): 1104-1112.

Araus, J. L., S. C. Kefauver, M. Zaman-Allah, M. S. Olsen and J. E. Cairns (2018). "Translating High-Throughput Phenotyping into Genetic Gain." Trends in Plant Science **23**(5): 451-466.

Armengaud, P., K. Zambaux, A. Hills, R. Sulpice, R. J. Pattison, M. R. Blatt and A. Amtmann (2009). "EZ-Rhizo: integrated software for the fast and accurate measurement of root system architecture." The Plant Journal **57**(5): 945-956.

Ashikari, M., H. Sakakibara, S. Lin, T. Yamamoto, T. Takashi, A. Nishimura, E. R. Angeles, Q. Qian, H. Kitano and M. Matsuoka (2005). "Cytokinin Oxidase Regulates Rice Grain Production." Science **309**(5735): 741-745.

Atkinson, J. A., M. P. Pound, M. J. Bennett and D. M. Wells (2019). "Uncovering the hidden half of plants using new advances in root phenotyping." Current Opinion in Biotechnology **55**: 1-8.

Atwell, S., Y. S. Huang, B. J. Vilhjálmsson, G. Willems, M. Horton, Y. Li, D. Meng, A. Platt, A. M. Tarone, T. T. Hu, R. Jiang, N. W. Muliyati, X. Zhang, M. A. Amer, I. Baxter, B. Brachi, J. Chory, C. Dean, M. Debieu, J. de Meaux, J. R. Ecker, N. Faure, J. M. Kniskern, J. D. G. Jones, T. Michael, A. Nemri, F. Roux, D. E. Salt, C. Tang, M. Todesco, M. B. Traw, D. Weigel, P. Marjoram, J. O. Borevitz, J. Bergelson and M. Nordborg (2010). "Genome-wide association study of 107 phenotypes in Arabidopsis thaliana inbred lines." Nature **465**: 627.

Austenfeld, M. and W. Beyschlag (2012). A Graphical User Interface for R in a Rich Client Platform for Ecological Modeling.

Aya, K., T. Hobo, K. Sato-Izawa, M. Ueguchi-Tanaka, H. Kitano and M. Matsuoka (2014). "A Novel AP2-Type Transcription Factor, SMALL ORGAN SIZE1, Controls Organ Size Downstream of an Auxin Signaling Pathway." Plant and Cell Physiology **55**(5): 897-912.

Backhaus, A., A. Kuwabara, M. Bauch, N. Monk, G. Sanguinetti and A. Fleming (2010). "leafprocessor: a new leaf phenotyping tool using contour bending energy and shape cluster analysis." New Phytologist **187**(1): 251-261.

Badr, A., K. M, R. Sch, H. E. Rabey, S. Effgen, H. H. Ibrahim, C. Pozzi, W. Rohde and F. Salamini (2000). "On the Origin and Domestication History of Barley (Hordeum vulgare)." Molecular Biology and Evolution **17**(4): 499-510.

Baik, B.-K. and S. E. Ullrich (2008). "Barley for food: Characteristics, improvement, and renewed interest." Journal of Cereal Science **48**(2): 233-242.

Baker, C. J., P. M. Berry, J. H. Spink, R. Sylvester-Bradley, J. M. Griffin, R. K. Scott and R. W. Clare (1998). "A Method for the Assessment of the Risk of Wheat Lodging." Journal of Theoretical Biology **194**(4): 587-603.

Bakshi, M. and R. Oelmüller (2014). "WRKY transcription factors: Jack of many trades in plants." Plant signaling & behavior **9**(2): e27700-e27700.

Balding, D. J. (2006). "A tutorial on statistical methods for population association studies." Nature Reviews Genetics **7**: 781.

Basu, P., A. Pal, J. P. Lynch and K. M. Brown (2007). "A Novel Image-Analysis Technique for Kinematic Study of Growth and Curvature." Plant Physiology **145**(2): 305-316.

Bates, D., M. Maechler, B. Bolker and S. Walker (2015). "Fitting Linear Mixed-Effects Models using 'lme4'." Journal of Statistic Software **67**(1): 1-48.
Bayer, M. M., P. Rapazote-Flores, M. Ganal, P. E. Hedley, M. Macaulay, J. Plieske, L. Ramsay, J. Russell, P. D. Shaw, W. Thomas and R. Waugh (2017). "Development and Evaluation of a Barley 50k iSelect SNP Array." Front Plant Sci **8**: 1792.
Bellucci, A., A. Tondelli, J. U. Fangel, A. M. Torp, X. Xu, G. T. William, A. J. Flavell, L. Cattivelli and K. R. Soren (2017). "Genome/wide association mapping in winter barley for grain yield and culm cell wall polymer content using the high-throughput CoMPP technique." PLOS ONE **12**(3): e0173313.
Bencivenga, S., A. Serrano-Mislata, M. Bush, S. Fox and R. Sablowski (2016). "Control of Oriented Tissue Growth through Repression of Organ Boundary Genes Promotes Stem Morphogenesis." Developmental Cell **39**(2): 198-208.
Bengtsson, T., I. Åhman, T. Bengtsson, O. Manninen, M. Veteläinen, L. Reitan, M. Alsheikh, B. Gertsson, S. Tuvesson, M. Jalli, A. Jahoor, J. D. Jensen, J. Orabi, G. Backes, L. Krusell, R. L. Hjortshøj, Á. Helgadóttir, M. Göransson, S. Sveinsson, O. Manninen, A. Jahoor, J. Orabi and T. P. B. Consortium (2017). "Genetic diversity, population structure and linkage disequilibrium in Nordic spring barley (Hordeum vulgare L. subsp. vulgare)." Genetic Resources and Crop Evolution **64**(8): 2021-2033.
Bergez, J. E., N. Colbach, O. Crespo, F. Garcia, M. H. Jeuffroy, E. Justes, C. Loyce, N. Munier-Jolain and W. Sadok (2010). "Designing crop management systems by simulation." European Journal of Agronomy **32**(1): 3-9.
Berry, P., M. Sterling, J. Spink, C. J. Baker, R. Sylvester-Bradley, S. Mooney, A. R. Tams and R. Ennos (2004). Understanding and Reducing Lodging in Cereals.
Berry, P. M. (2013). Lodging Resistance in Cereals. Sustainable Food Production. P. Christou, R. Savin, B. A. Costa-Pierce, I. Misztal and C. B. A. Whitelaw. New York, NY, Springer New York**:** 1096-1110.
Berry, P. M., J. M. Griffin, R. Sylvester-Bradley, R. K. Scott, J. H. Spink, C. J. Baker and R. W. Clare (2000). "Controlling plant form through husbandry to minimise lodging in wheat." Field Crops Research **67**(1): 59-81.
Berry, P. M. and J. Spink (2012). "Predicting yield losses caused by lodging in wheat." Field Crops Research **137**: 19-26.
Berry, P. M., R. Sylvester-Bradley and S. Berry (2007). "Ideotype design for lodging-resistant wheat." Euphytica **154**(1-2): 165-179.
Blattner, F. R. (2018). Taxonomy of the Genus Hordeum and Barley (Hordeum vulgare). The Barley Genome. N. Stein and G. J. Muehlbauer. Cham, Springer International Publishing**:** 11-23.
Bolger, M. E., B. Weisshaar, U. Scholz, N. Stein, B. Usadel and K. F. X. Mayer (2014). "Plant genome sequencing — applications for crop improvement." Current Opinion in Biotechnology **26**: 31-37.
Bradbury, P. J., Z. Zhang, D. E. Kroon, T. M. Casstevens, Y. Ramdoss and E. S. Buckler (2007). "TASSEL: software for association mapping of complex traits in diverse samples." Bioinformatics **23**(19): 2633-2635.
Breseghello, F. and M. E. Sorrells (2006). "Association Mapping of Kernel Size and Milling Quality in Wheat (Triticum aestivum L.) Cultivars." Genetics **172**(2): 1165-1177.
Briggs, D. E. (1978). The morphology of barley; the vegetative phase. Barley. Dordrecht, Springer Netherlands**:** 1-38.
Browning, Brian L. and Sharon R. Browning (2016). "Genotype Imputation with Millions of Reference Samples." American Journal of Human Genetics **98**(1): 116-126.
Bucklin, R. A., P. A. Fowler, V. Y. Rygalov, R. M. Wheeler, Y. Mu, I. Hublitz and E. G. Wilkerson (2004). "Greenhouse design for the mars environment: Development of a prototype, deployable dome." Acta Horticulturae **659**(November): 127-134.
Chandler, P. M. and C. A. Harding (2013). "'Overgrowth' mutants in barley and wheat: new alleles and phenotypes of the 'Green Revolution' Della gene." Journal of Experimental Botany **64**(6): 1603-1613.
Chandler, P. M., A. Marion-Poll, M. Ellis and F. Gubler (2002). "Mutants at the Slender1 Locus of Barley cv Himalaya. Molecular and Physiological Characterization." Plant Physiology **129**(1): 181-190.
Chanock, S. J., T. Manolio, M. Boehnke, E. Boerwinkle, D. J. Hunter, G. Thomas, J. N. Hirschhorn, G. Abecasis, D. Altshuler, J. E. Bailey-Wilson, L. D. Brooks, L. R. Cardon, M. Daly, P. Donnelly, J. F. Fraumeni Jr, N. B. Freimer, D. S. Gerhard, C. Gunter, A. E. Guttmacher, M. S. Guyer, E. L. Harris, J. Hoh, R. Hoover, C. A.

Kong, K. R. Merikangas, C. C. Morton, L. J. Palmer, E. G. Phimister, J. P. Rice, J. Roberts, C. Rotimi, M. A. Tucker, K. J. Vogan, S. Wacholder, E. M. Wijsman, D. M. Winn and F. S. Collins (2007). "Replicating genotype–phenotype associations." Nature **447**: 655.
Chen, H., C. Wang, Matthew P. Conomos, Adrienne M. Stilp, Z. Li, T. Sofer, Adam A. Szpiro, W. Chen, John M. Brehm, Juan C. Celedón, S. Redline, George J. Papanicolaou, Timothy A. Thornton, Cathy C. Laurie, K. Rice and X. Lin (2016). "Control for Population Structure and Relatedness for Binary Traits in Genetic Association Studies via Logistic Mixed Models." The American Journal of Human Genetics **98**(4): 653-666.
Chen, L., A. L. Phillips, A. G. Condon, M. A. J. Parry and Y.-G. Hu (2013). "GA-Responsive Dwarfing Gene Rht12 Affects the Developmental and Agronomic Traits in Common Bread Wheat." PLoS ONE **8**(4): e62285.
Chono, M., I. Honda, H. Zeniya, K. Yoneyama, D. Saisho, K. Takeda, S. Takatsuto, T. Hoshino and Y. Watanabe (2003). "A Semidwarf Phenotype of Barley uzu Results from a Nucleotide Substitution in the Gene Encoding a Putative Brassinosteroid Receptor." Plant Physiology **133**(3): 1209-1219.
Chuanren, D., W. Bochu, W. Pingqing, W. Daohong and C. Shaoxi (2004). "Relationship between the minute structure and the lodging resistance of rice stems." Colloids and Surfaces B: Biointerfaces **35**(3): 155-158.
Civáň, P. and T. A. Brown (2017). "A novel mutation conferring the nonbrittle phenotype of cultivated barley." New Phytologist **214**(1): 468-472.
Clark, R. T., A. N. Famoso, K. Zhao, J. E. Shaff, E. J. Craft, C. D. Bustamante, S. R. Mccouch, D. J. Aneshanley and L. V. Kochian (2013). "High-throughput two-dimensional root system phenotyping platform facilitates genetic analysis of root growth and development." Plant, Cell & Environment **36**(2): 454-466.
Clark, R. T., R. B. MacCurdy, J. K. Jung, J. E. Shaff, S. R. McCouch, D. J. Aneshansley and L. V. Kochian (2011). "Three-Dimensional Root Phenotyping with a Novel Imaging and Software Platform." Plant Physiology **156**(2): 455-465.
Close, T. J., P. R. Bhat, S. Lonardi, Y. Wu, N. Rostoks, L. Ramsay, A. Druka, N. Stein, J. T. Svensson, S. Wanamaker, S. Bozdag, M. L. Roose, M. J. Moscou, S. Chao, R. K. Varshney, P. Szűcs, K. Sato, P. M. Hayes, D. E. Matthews, A. Kleinhofs, G. J. Muehlbauer, J. DeYoung, D. F. Marshall, K. Madishetty, R. D. Fenton, P. Condamine, A. Graner and R. Waugh (2009). "Development and implementation of high-throughput SNP genotyping in barley." BMC Genomics **10**(1): 582.
Cobb, J. N., G. DeClerck, A. Greenberg, R. Clark and S. McCouch (2013). "Next-generation phenotyping: requirements and strategies for enhancing our understanding of genotype–phenotype relationships and its relevance to crop improvement." Theoretical and Applied Genetics **126**(4): 867-887.
Comadran, J., B. Kilian, J. Russell, L. Ramsay, N. Stein, M. Ganal, P. Shaw, M. Bayer, W. Thomas, D. Marshall, P. Hedley, A. Tondelli, N. Pecchioni, E. Francia, V. Korzun, A. Walther and R. Waugh (2012). "Natural variation in a homolog of Antirrhinum CENTRORADIALIS contributed to spring growth habit and environmental adaptation in cultivated barley." Nature Genetics **44**: 1388.
Coppens, F., N. Wuyts, D. Inzé and S. Dhondt (2017). "Unlocking the potential of plant phenotyping data through integration and data-driven approaches." Current Opinion in Systems Biology **4**: 58-63.
Darwin, C. (1859). On the origin of species by means of natural selection, or, The preservation of favoured races in the struggle for life. London, John Murray.
Darwin, C. and A. Gray (1868). The variation of animals and plants under domestication. New York Orange Judd & Co.
Dawson, I. K., J. Russell, W. Powell, B. Steffenson, W. T. B. Thomas and R. Waugh (2015). "Barley: a translational model for adaptation to climate change." New Phytologist **206**(3): 913-931.
de la Candolle, A. (1882). Origine des plantes cultivées, Paris : Librairie Germer Baillière et C.ie, 108, Boulevard Saint-Germain.
De Meester, B., L. de Vries, M. Özparpucu, N. Gierlinger, S. Corneillie, A. Pallidis, G. Goeminne, K. Morreel, M. De Bruyne, R. De Rycke, R. Vanholme and W. Boerjan (2018). "Vessel-Specific Reintroduction of CINNAMOYL-COA REDUCTASE1 (CCR1) in Dwarfed ccr1 Mutants Restores Vessel and Xylary Fiber Integrity and Increases Biomass." Plant Physiology **176**(1): 611.
Deery, D., J. Jimenez-Berni, H. Jones, X. Sirault and R. Furbank (2014). "Proximal Remote Sensing Buggies and Potential Applications for Field-Based Phenotyping." Agronomy **4**(3): 349.
Desrousseaux, D., F. Sandron, A. Siberchicot, C. Cierco-Ayrolles and B. Mangin (2017). LDcorSV: Linkage Disequilibrium Corrected by the Structure and the Relatedness.

Diaz-Garcia, L., G. Covarrubias-Pazaran, B. Schlautman, E. Grygleski and J. Zalapa (2018). "Image-based phenotyping for identification of QTL determining fruit shape and size in American cranberry (Vaccinium macrocarpon L.)." PeerJ **6**: e5461.
Doebley, J. F., B. S. Gaut and B. D. Smith (2006). "The Molecular Genetics of Crop Domestication." Cell **127**(7): 1309-1321.
Donald, C. M. (1968). "The breeding of crop ideotypes." Euphytica **17**(3): 385-403.
Dornbusch, T. and B. Andrieu (2010). "Lamina2Shape—An image processing tool for an explicit description of lamina shape tested on winter wheat (Triticum aestivum L.)." Computers and Electronics in Agriculture **70**(1): 217-224.
Druka, A., J. Franckowiak, U. Lundqvist, N. Bonar, J. Alexander, K. Houston, S. Radovic, F. Shahinnia, V. Vendramin, M. Morgante, N. Stein and R. Waugh (2011). "Genetic Dissection of Barley Morphology and Development." Plant Physiology **155**(2): 617-627.
Dumont, B., B. Basso, B. Bodson, J. P. Destain and M. F. Destain (2015). "Climatic risk assessment to improve nitrogen fertilisation recommendations: A strategic crop model-based approach." European Journal of Agronomy **65**: 10-17.
Dunn, G. J. and K. G. Briggs (1989). "Variation in culm anatomy among barley cultivars differing in lodging resistance." Canadian Journal of Botany **67**(6): 1838-1843.
Earl, D. A. and B. M. vonHoldt (2012). "STRUCTURE HARVESTER: a website and program for visualizing STRUCTURE output and implementing the Evanno method." Conservation Genetics Resources **4**(2): 359-361.
Etchells, J. P., L. Moore, W. Z. Jiang, H. Prescott, R. Capper, N. J. Saunders, A. M. Bhatt and H. G. Dickinson (2012). "A role for BELLRINGER in cell wall development is supported by loss-of-function phenotypes." BMC Plant Biology **12**(1): 212.
Falcioni, R., T. Moriwaki, D. M. de Oliveira, G. C. Andreotti, L. A. de Souza, W. D. dos Santos, C. M. Bonato and W. C. Antunes (2018). "Increased Gibberellins and Light Levels Promotes Cell Wall Thickness and Enhance Lignin Deposition in Xylem Fibers." Frontiers in Plant Science **9**(1391).
Falconer, D. S. and T. E. C. Mackay (2004). Introduction to Quantitative Genetics.
Fallah, A. (2012). "Silicon effect on lodging parameters of rice plants under hydroponic culture." International Journal of AgriScience **2**(7): 630-634.
Fan, J. B., K. L. Gunderson, M. Bibikova, J. M. Yeakley, J. Chen, E. Wickham Garcia, L. L. Lebruska, M. Laurent, R. Shen and D. Barker (2006). Illumina Universal Bead Arrays. Methods in Enzymology, Academic Press. **410:** 57-73.
Feng, S., Y. Shen, J. A. Sullivan, V. Rubio, Y. Xiong, T.-p. Sun and X. W. Deng (2004). "Arabidopsis CAND1, an Unmodified CUL1-Interacting Protein, Is Involved in Multiple Developmental Pathways Controlled by Ubiquitin/Proteasome-Mediated Protein Degradation." The Plant Cell **16**(7): 1870-1882.
Fiorani, F. and U. Schurr (2013). "Future Scenarios for Plant Phenotyping." Annual Review of Plant Biology **64**(1): 267-291.
Flint-Garcia, S. A., J. M. Thornsberry and E. S. Buckler (2003). "Structure of Linkage Disequilibrium in Plants." Annual Review of Plant Biology **54**(1): 357-374.
Forster, B. P., J. D. Franckowiak, U. Lundqvist, J. Lyon, I. Pitkethly and W. T. B. Thomas (2007). "The Barley Phytomer." Annals of Botany **100**(4): 725-733.
Foulkes, M. J., G. A. Slafer, W. J. Davies, P. M. Berry, R. Sylvester-Bradley, P. Martre, D. F. Calderini, S. Griffiths and M. P. Reynolds (2011). "Raising yield potential of wheat. III. Optimizing partitioning to grain while maintaining lodging resistance." Journal of Experimental Botany **62**(2): 469-486.
Francone, C., V. Pagani, M. Foi, G. Cappelli and R. Confalonieri (2014). "Comparison of leaf area index estimates by ceptometer and PocketLAI smart app in canopies with different structures." Field Crops Research **155**: 38-41.
Fu, X.-q., J. Feng, B. Yu, Y.-j. Gao, Y.-l. Zheng and B. Yue (2013). "Morphological, Biochemical and Genetic Analysis of a Brittle Stalk Mutant of Maize Inserted by Mutator." Journal of Integrative Agriculture **12**(1): 12-18.
Gage, J. L., N. D. Miller, E. P. Spalding, S. M. Kaeppler and N. de Leon (2017). "TIPS: a system for automated image-based phenotyping of maize tassels." Plant Methods **13**(1): 21.

Galkovskyi, T., Y. Mileyko, A. Bucksch, B. Moore, O. Symonova, C. A. Price, C. N. Topp, A. S. Iyer-Pascuzzi, P. R. Zurek, S. Fang, J. Harer, P. N. Benfey and J. S. Weitz (2012). "GiA Roots: software for the high throughput analysis of plant root system architecture." BMC Plant Biology **12**(1): 116.
Garris, A. J., T. H. Tai, J. Coburn, S. Kresovich and S. McCouch (2005). "Genetic Structure and Diversity in Oryza sativa L." Genetics **169**(3): 1631-1638.
Gauch, H. G. (1992). Statistical analysis of regional yield trials: AMMI analysis of factorial designs. Amsterdam, Elsevier Science Publishers.
Ghanem, M. E., H. Marrou and T. R. Sinclair (2015). "Physiological phenotyping of plants for crop improvement." Trends in Plant Science **20**(3): 139-144.
Gibbs, J. A., M. Pound, A. P. French, D. M. Wells, E. Murchie and T. Pridmore (2018). "Plant Phenotyping: An Active Vision Cell for Three-Dimensional Plant Shoot Reconstruction." Plant Physiology **178**(2): 524-534.
Gill, B. S., R. Appels, A.-M. Botha-Oberholster, C. R. Buell, J. L. Bennetzen, B. Chalhoub, F. Chumley, J. Dvořák, M. Iwanaga, B. Keller, W. Li, W. R. McCombie, Y. Ogihara, F. Quetier and T. Sasaki (2004). "A Workshop Report on Wheat Genome Sequencing: International Genome Research on Wheat Consortium." Genetics **168**(2): 1087-1096.
Giunta, F., R. Motzo, G. Fois and P. Bacciu (2015). "Developmental ideotype in the context of the dual-purpose use of triticale, barley and durum wheat." Annals of Applied Biology **166**(1): 118-128.
Golzarian, M. R., R. A. Frick, K. Rajendran, B. Berger, S. Roy, M. Tester and D. S. Lun (2011). "Accurate inference of shoot biomass from high-throughput images of cereal plants." Plant Methods **7**(1): 2.
González-Curbelo, M. Á., A. V. Herrera-Herrera, L. M. Ravelo-Pérez and J. Hernández-Borges (2012). "Sample-preparation methods for pesticide-residue analysis in cereals and derivatives." TrAC Trends in Analytical Chemistry **38**: 32-51.
Gooding, M. J., M. Addisu, R. K. Uppal, J. W. Snape and H. E. Jones (2012). "Effect of wheat dwarfing genes on nitrogen-use efficiency." Journal of Agricultural Science **150**(1): 3-22.
Górny, A. G. (2001). "Variation in utilization efficiency and tolerance to reduced water and nitrogen supply among wild and cultivated barleys." Euphytica **117**(1): 59-66.
Gouache, D., M. Bogard, M. Pegard, S. Thepot, C. Garcia, D. Hourcade, E. Paux, F.-X. Oury, M. Rousset, J.-C. Deswarte and X. Le Bris (2017). "Bridging the gap between ideotype and genotype: Challenges and prospects for modelling as exemplified by the case of adapting wheat (Triticum aestivum L.) phenology to climate change in France." Field Crops Research **202**: 108-121.
Goujon, T., V. Ferret, I. Mila, B. Pollet, K. Ruel, V. Burlat, J.-P. Joseleau, Y. Barrière, C. Lapierre and L. Jouanin (2003). "Down-regulation of the AtCCR1 gene in Arabidopsis thaliana: effects on phenotype, lignins and cell wall degradability." Planta **217**(2): 218-228.
Granier, C., L. Aguirrezabal, K. Chenu, S. J. Cookson, M. Dauzat, P. Hamard, J.-J. Thioux, G. Rolland, S. Bouchier-Combaud, A. Lebaudy, B. Muller, T. Simonneau and F. Tardieu (2006). "PHENOPSIS, an automated platform for reproducible phenotyping of plant responses to soil water deficit in Arabidopsis thaliana permitted the identification of an accession with low sensitivity to soil water deficit." New Phytologist **169**(3): 623-635.
Gregory, T. R., J. A. Nicol, H. Tamm, B. Kullman, K. Kullman, I. J. Leitch, B. G. Murray, D. F. Kapraun, J. Greilhuber and M. D. Bennett (2007). "Eukaryotic genome size databases." Nucleic Acids Research **35**(suppl_1): D332-D338.
Gui, M. Y., D. Wang, H. H. Xiao, M. Tu, F. L. Li, W. C. Li, S. D. Ji, T. X. Wang and J. Y. Li (2018). "Studies of the relationship between rice stem and lodging resistance. ." The Journal of Agricultural Science **156**(3): 387-395.
Gupta, P. K., S. Rustgi and P. L. Kulwal (2005). "Linkage disequilibrium and association studies in higher plants: Present status and future prospects." Plant Molecular Biology **57**(4): 461-485.
Hai, L., H. Guo, S. Xiao, G. Jiang, X. Zhang, C. Yan, Z. Xin and J. Jia (2005). "Quantitative trait loci (QTL) of stem strength and related traits in a doubled-haploid population of wheat (Triticum aestivum L.)." Euphytica **141**(1): 1-9.
Hall, H. and B. Ellis (2013). "Transcriptional programming during cell wall maturation in the expanding Arabidopsis stem." BMC Plant Biology **13**(1): 14.

Hall, H. C., J. Cheung and B. E. Ellis (2013). "Immunoprofiling reveals unique cell-specific patterns of wall epitopes in the expanding Arabidopsis stem." The Plant Journal **74**(1): 134-147.
Halperin, E. and D. A. Stephan (2009). "SNP imputation in association studies." Nature Biotechnology **27**: 349.
Han, M., K. E. Kang, Y. Kim and G.-W. Choi (2013). "High efficiency bioethanol production from barley straw using a continuous pretreatment reactor." Process Biochemistry **48**(3): 488-495.
Harlan, J. R. (1951). "Anatomy of Gene Centers." The American Naturalist **85**(821): 97-103.
Harlan, J. R. (1971). "Agricultural Origins: Centers and Noncenters." Science **174**(4008): 468-474.
Harlan, J. R. and D. Zohary (1966). "Distribution of Wild Wheats and Barley." Science **153**(3740): 1074-1080.
Hartmann, A., T. Czauderna, R. Hoffmann, N. Stein and F. Schreiber (2011). "HTPheno: An image analysis pipeline for high-throughput plant phenotyping." BMC Bioinformatics **12**(1): 148.
Hellewell, K. B., D. C. Rasmusson and M. Gallo-Meagher (2000). "Enhancing Yield of Semidwarf Barley." Crop Science **40**(2): 352-358.
Herridge, R. P., R. C. Day, S. Baldwin and R. C. Macknight (2011). "Rapid analysis of seed size in Arabidopsis for mutant and QTL discovery." Plant Methods **7**(1): 3.
Hirano, K., A. Okuno, T. Hobo, R. Ordonio, Y. Shinozaki, K. Asano, H. Kitano and M. Matsuoka (2014). "Utilization of Stiff Culm Trait of Rice smos1 Mutant for Increased Lodging Resistance." PLOS ONE **9**(7): e96009.
Hirano, K., R. L. Ordonio and M. Matsuoka (2017). "Engineering the lodging resistance mechanism of post-Green Revolution rice to meet future demands." Proceedings of the Japan Academy, Series B **93**(4): 220-233.
Hochberg, Y. and Y. Benjamini (1990). "More powerful procedures for multiple significance testing." Statistics in Medicine **9**(7): 811-818.
Houston, K., R. A. Burton, B. Sznajder, A. J. Rafalski, K. S. Dhugga, D. E. Mather, J. Taylor, B. J. Steffenson, R. Waugh and G. B. Fincher (2015). "A Genome-Wide Association Study for Culm Cellulose Content in Barley Reveals Candidate Genes Co-Expressed with Members of the CELLULOSE SYNTHASE A Gene Family." PLOS ONE **10**(7): e0130890.
Howie, B., C. Fuchsberger, M. Stephens, J. Marchini and G. R. Abecasis (2012). "Fast and accurate genotype imputation in genome-wide association studies through pre-phasing." Nature Genetics **44**: 955.
Huang, X. and B. Han (2014). "Natural Variations and Genome-Wide Association Studies in Crop Plants." Annual Review of Plant Biology **65**(1): 531-551.
Huang, X., N. Kurata, X. Wei, Z.-X. Wang, A. Wang, Q. Zhao, Y. Zhao, K. Liu, H. Lu, W. Li, Y. Guo, Y. Lu, C. Zhou, D. Fan, Q. Weng, C. Zhu, T. Huang, L. Zhang, Y. Wang, L. Feng, H. Furuumi, T. Kubo, T. Miyabayashi, X. Yuan, Q. Xu, G. Dong, Q. Zhan, C. Li, A. Fujiyama, A. Toyoda, T. Lu, Q. Feng, Q. Qian, J. Li and B. Han (2012). "A map of rice genome variation reveals the origin of cultivated rice." Nature **490**: 497.
Huang, X. Q., S. Cloutier, L. Lycar, N. Radovanovic, D. G. Humphreys, J. S. Noll, D. J. Somers and P. D. Brown (2006). "Molecular detection of QTLs for agronomic and quality traits in a doubled haploid population derived from two Canadian wheats (Triticum aestivum L.)." Theoretical and Applied Genetics **113**(4): 753-766.
Hubisz, M. J., D. Falush, M. Stephens and J. K. Pritchard (2009). "Inferring weak population structure with the assistance of sample group information." Molecular Ecology Resources **9**(5): 1322-1332.
Hufford, M. B., X. Xu, J. van Heerwaarden, T. Pyhäjärvi, J.-M. Chia, R. A. Cartwright, R. J. Elshire, J. C. Glaubitz, K. E. Guill, S. M. Kaeppler, J. Lai, P. L. Morrell, L. M. Shannon, C. Song, N. M. Springer, R. A. Swanson-Wagner, P. Tiffin, J. Wang, G. Zhang, J. Doebley, M. D. McMullen, D. Ware, E. S. Buckler, S. Yang and J. Ross-Ibarra (2012). "Comparative population genomics of maize domestication and improvement." Nature Genetics **44**: 808.
Hummer, K. E. and J. F. Hancock (2015). "Vavilovian centers of plant diversity: Implications and impacts." HortScience **50**(6): 780-783.
Ishimaru, K., E. Togawa, T. Ookawa, T. Kashiwagi, Y. Madoka and N. Hirotsu (2008). "New target for rice lodging resistance and its effect in a typhoon." Planta **227**(3): 601-609.
Islam, M. S., S. Peng, R. M. Visperas, N. Ereful, M. S. U. Bhuiya and A. W. Julfiquar (2007). "Lodging-related morphological traits of hybrid rice in a tropical irrigated ecosystem." Field Crops Research **101**(2): 240-248.

Iwata, H. and Y. Ukai (2002). "SHAPE: A Computer Program Package for Quantitative Evaluation of Biological Shapes Based on Elliptic Fourier Descriptors." Journal of Heredity **93**(5): 384-385.
Jain, M., A. Srivastava, Balwinder-Singh, R. Joon, A. McDonald, K. Royal, M. Lisaius and D. Lobell (2016). "Mapping Smallholder Wheat Yields and Sowing Dates Using Micro-Satellite Data." Remote Sensing **8**(10): 860.
Jander, G., S. R. Norris, S. D. Rounsley, D. F. Bush, I. M. Levin and R. L. Last (2002). "Arabidopsis Map-Based Cloning in the Post-Genome Era." Plant Physiology **129**(2): 440-450.
Jedel, P. E. and J. H. Helm (1991). "Lodging Effects on a Semidwarf and Two Standard Barley Cultivars." Agronomy Journal **83**: 158-161.
Jia, P. and Z. Zhao (2014). "Network-assisted analysis to prioritize GWAS results: principles, methods and perspectives." Human Genetics **133**(2): 125-138.
Jia, Q., X.-Q. Zhang, S. Westcott, S. Broughton, M. Cakir, J. Yang, R. Lance and C. Li (2011). "Expression level of a gibberellin 20-oxidase gene is associated with multiple agronomic and quality traits in barley." Theoretical and Applied Genetics **122**(8): 1451-1460.
Johnson, R. C., G. W. Nelson, J. L. Troyer, J. A. Lautenberger, B. D. Kessing, C. A. Winkler and S. J. O'Brien (2010). "Accounting for multiple comparisons in a genome-wide association study (GWAS)." BMC Genomics **11**(1): 724.
Jones, L., A. R. Ennos and S. R. Turner (2001). "Cloning and characterization of irregular xylem4 (irx4): a severely lignin-deficient mutant of Arabidopsis." The Plant Journal **26**(2): 205-216.
Jung, M., A. Ching, D. Bhattramakki, M. Dolan, S. Tingey, M. Morgante and A. Rafalski (2004). "Linkage disequilibrium and sequence diversity in a 500-kbp region around the adh1 locus in elite maize germplasm." Theoretical and Applied Genetics **109**(4): 681-689.
Kaack, K., K.-U. Schwarz and P. E. Brander (2003). "Variation in morphology, anatomy and chemistry of stems of Miscanthus genotypes differing in mechanical properties." Industrial Crops and Products **17**(2): 131-142.
Kacira, M., G. A. Giacomelli, R. L. Patterson, R. Furfaro, P. D. Sadler, G. Boscheri, C. Lobascio, M. Lamantea, R. M. Wheeler and S. Rossignoli (2012). System dynamics and performance factors of a lunar greenhouse prototype bioregenerative life support system, International Society for Horticultural Science.
Kashiwagi, T., N. Hirotsu, Y. Madoka, T. Ookawa and K. Ishimaru (2007). "Improvement of Resistance to Bending-Type Lodging in Rice." Japanese Journal of Crop Science **76**(1): 1-9.
Kashiwagi, T. and K. Ishimaru (2004). "Identification and Functional Analysis of a Locus for Improvement of Lodging Resistance in Rice." Plant Physiology **134**(2): 676-683.
Kashiwagi, T., Y. Madoka, N. Hirotsu and K. Ishimaru (2006). "Locus prl5 improves lodging resistance of rice by delaying senescence and increasing carbohydrate reaccumulation." Plant Physiology and Biochemistry **44**(2): 152-157.
Kashiwagi, T., H. Sasaki and K. Ishimaru (2005). "Factors Responsible for Decreasing Sturdiness of the Lower Part in Lodging of Rice (Oryza sativa L.)." Plant Production Science **8**(2): 166-172.
Kashiwagi, T., E. Togawa, N. Hirotsu and K. Ishimaru (2008). "Improvement of lodging resistance with QTLs for stem diameter in rice (Oryza sativa L.)." Theoretical and Applied Genetics **117**(5): 749-757.
Kawano, K., J. Yamaguchi and A. Tanaka (1966). Photosynthesis, respiration, and plant type of the tropical rice plant.
Kelbert, A. J., D. Spaner, K. G. Briggs and J. R. King (2004). "The association of culm anatomy with lodging susceptibility in modern spring wheat genotypes." Euphytica **136**(2): 211-221.
Khush, G. S. (2001). "Green revolution: the way forward." Nature Reviews Genetics **2**: 815.
Khush, G. S. (2013). "Strategies for increasing the yield potential of cereals: Case of rice as an example." Plant Breeding **132**(5): 433-436.
Kilian, B., H. Özkan, C. Pozzi and F. Salamini (2009). Domestication of the Triticeae in the Fertile Crescent. Genetics and Genomics of the Triticeae. G. J. Muehlbauer and C. Feuillet. New York, NY, Springer US**:** 81-119.
Kim, J., S. Lee, H. Ahn, D. Seo, S. Park and C. Choi (2013). "Feasibility of employing a smartphone as the payload in a photogrammetric UAV system." ISPRS Journal of Photogrammetry and Remote Sensing **79**: 1-18.

Kislev, M. E., D. Nadel and I. Carmi (1992). "Epipalaeolithic (19,000 BP) cereal and fruit diet at Ohalo II, Sea of Galilee, Israel." Review of Palaeobotany and Palynology **73**(1): 161-166.
Klinghammer, M. and R. Tenhaken (2007). "Genome-wide analysis of the UDP-glucose dehydrogenase gene family in Arabidopsis, a key enzyme for matrix polysaccharides in cell walls." Journal of Experimental Botany **58**(13): 3609-3621.
Knapp, S. J., W. W. Stroup and W. M. Ross (1985). "Exact Confidence Intervals for Heritability on a Progeny Mean Basis1." Crop Science **25**(1): 192-194.
Komatsuda, T., P. Maxim, N. Senthil and Y. Mano (2004). "High-density AFLP map of nonbrittle rachis 1 (btr1) and 2 (btr2) genes in barley (Hordeum vulgare L.)." Theoretical and Applied Genetics **109**(5): 986-995.
Komatsuda, T., M. Pourkheirandish, C. He, P. Azhaguvel, H. Kanamori, D. Perovic, N. Stein, A. Graner, T. Wicker, A. Tagiri, U. Lundqvist, T. Fujimura, M. Matsuoka, T. Matsumoto and M. Yano (2007). "Six-rowed barley originated from a mutation in a homeodomain-leucine zipper I-class homeobox gene." Proceedings of the National Academy of Sciences **104**(4): 1424-1429.
Kong, E., D. Liu, X. Guo, W. Yang, J. Sun, X. Li, K. Zhan, D. Cui, J. Lin and A. Zhang (2013). "Anatomical and chemical characteristics associated with lodging resistance in wheat." The Crop Journal **1**(1): 43-49.
Koppolu, R., N. Anwar, S. Sakuma, A. Tagiri, U. Lundqvist, M. Pourkheirandish, T. Rutten, C. Seiler, A. Himmelbach, R. Ariyadasa, H. M. Youssef, N. Stein, N. Sreenivasulu, T. Komatsuda and T. Schnurbusch (2013). "Six-rowed spike4 (Vrs4) controls spikelet determinacy and row-type in barley." Proceedings of the National Academy of Sciences **110**(32): 13198-13203.
Kuczyńska, A., M. Surma, T. Adamski, K. Mikołajczak, K. Krystkowiak and P. Ogrodowicz (2013). "Effects of the semi-dwarfing sdw1/denso gene in barley." Journal of Applied Genetics **54**(4): 381-390.
Kuczynska, A. and T. Wyka (2011). "The effect of the denso dwarfing gene on morpho-anatomical characters in barley recombinant inbred lines." Breeding Science **61**(3): 275-280.
Kumar Malav, A., Indu and K. S. Chandrawat (2016). Gene Pyramiding: An Overview.
Lander, E. S. and D. Botstein (1989). "Mapping mendelian factors underlying quantitative traits using RFLP linkage maps." Genetics **121**(1): 185-199.
Langridge, P. (2018). Economic and Academic Importance of Barley. The Barley Genome. N. Stein and G. J. Muehlbauer. Cham, Springer International Publishing**:** 1-10.
Lauvergeat, V., C. Lacomme, E. Lacombe, E. Lasserre, D. Roby and J. Grima-Pettenati (2001). "Two cinnamoyl-CoA reductase (CCR) genes from Arabidopsis thaliana are differentially expressed during development and in response to infection with pathogenic bacteria." Phytochemistry **57**(7): 1187-1195.
Le Bot, J., V. Serra, J. Fabre, X. Draye, S. Adamowicz and L. Pagès (2010). "DART: a software to analyse root system architecture and development from captured images." Plant and Soil **326**(1): 261-273.
Lee, U., S. Chang, G. A. Putra, H. Kim and D. H. Kim (2018). "An automated, high-throughput plant phenotyping system using machine learning-based plant segmentation and image analysis." PLOS ONE **13**(4): e0196615.
Lewontin, R. C. (1964). "THE INTERACTION OF SELECTION AND LINKAGE. I. GENERAL CONSIDERATIONS; HETEROTIC MODELS." Genetics **49**(1): 49-67.
Li, G., Q. M. Deng, S. C. Li, S. Q. Wang and P. Li (2009). "Correlation analysis between RVA profile characteristics and quality in rice." Chin J. Rice Sci. **23**(99-102).
Li, J., H. C. Zhang, J. L. Gong, Y. Chang, Q. G. Dai, Z. Y. Huo and H. Y. Wei (2011). "Effects of different planting methods on the culm lodging resitance of super rice." Sci Agric Sin **44**: 2234-2243.
Li, R., J. Zhang, J. Li, G. Zhou, Q. Wang, W. Bian, M. Erb and Y. Lou (2015). "Prioritizing plant defence over growth through WRKY regulation facilitates infestation by non-target herbivores." eLife **4**: e04805.
Li, X., C. Zhu, J. Wang and J. Yu (2012). Computer Simulation in Plant Breeding.
Li, Y.-M., R. L. Chaney, E. P. Brewer, J. S. Angle and J. Nelkin (2003). "Phytoextraction of Nickel and Cobalt by Hyperaccumulator Alyssum Species Grown on Nickel-Contaminated Soils." Environmental Science & Technology **37**(7): 1463-1468.
Li, Y., G. Haseneyer, C.-C. Schön, D. Ankerst, V. Korzun, P. Wilde and E. Bauer (2011). "High levels of nucleotide diversity and fast decline of linkage disequilibrium in rye (Secale cerealeL.) genes involved in frost response." BMC Plant Biology **11**(1): 6.

Liller, C. B., R. Neuhaus, M. Von Korff, M. Koornneef and W. Van Esse (2015). "Mutations in barley row type genes have pleiotropic effects on shoot branching." PLoS ONE **10**(10): 1-20.
Lippert, C., J. Listgarten, Y. Liu, C. M. Kadie, R. I. Davidson and D. Heckerman (2011). "FaST linear mixed models for genome-wide association studies." Nature Methods **8**: 833.
Listgarten, J., C. Lippert, C. M. Kadie, R. I. Davidson, E. Eskin and D. Heckerman (2012). "Improved linear mixed models for genome-wide association studies." Nature Methods **9**: 525.
Liu, L., H. Ji, J. An, K. Shi, J. Ma, B. Liu, L. Tang, W. Cao and Y. Zhu (2019). "Response of biomass accumulation in wheat to low-temperature stress at jointing and booting stages." Environmental and Experimental Botany **157**: 46-57.
Liu, X., M. Huang, B. Fan, E. S. Buckler and Z. Zhang (2016). "Iterative Usage of Fixed and Random Effect Models for Powerful and Efficient Genome-Wide Association Studies." PLOS Genetics **12**(2): e1005767.
Lobet, G. (2017). "Image Analysis in Plant Sciences: Publish Then Perish." Trends in Plant Science **22**(7): 559-566.
Lobet, G., X. Draye and C. Périlleux (2013). "An online database for plant image analysis software tools." Plant Methods **9**(1): 38.
Lobet, G., L. Pagès and X. Draye (2011). "A Novel Image-Analysis Toolbox Enabling Quantitative Analysis of Root System Architecture." Plant Physiology **157**(1): 29-39.
Lowder, L. G., D. Zhang, N. J. Baltes, J. W. Paul, X. Tang, X. Zheng, D. F. Voytas, T.-F. Hsieh, Y. Zhang and Y. Qi (2015). "A CRISPR/Cas9 Toolbox for Multiplexed Plant Genome Editing and Transcriptional Regulation." Plant Physiology **169**(2): 971-985.
Lowry, D. B., S. Hoban, J. L. Kelley, K. E. Lotterhos, L. K. Reed, M. F. Antolin and A. Storfer (2017). "Breaking RAD: an evaluation of the utility of restriction site-associated DNA sequencing for genome scans of adaptation." Molecular Ecology Resources **17**(2): 142-152.
Luo, C. M., C. T. Tian, X. J. Li and J. X. Lin (2007). "Relationship between morpho-anatomical traits together with chemical components and lodging resistance of stem in rice (*Oryza sativa L.)* " Acta Botanica Boreali-Occidentalia Sinica **27**: 2346-2353.
Ma, J. F. and N. Yamaji (2006). "Silicon uptake and accumulation in higher plants." Trends in Plant Science **11**(8): 392-397.
Ma, Q.-H. (2007). "Characterization of a cinnamoyl-CoA reductase that is associated with stem development in wheat." Journal of Experimental Botany **58**(8): 2011-2021.
Ma, Q. H., Y. Xu, Z. B. Lin and P. He (2002). "Cloning of cDNA encoding COMT from wheat which is differentially expressed in lodging-sensitive and -resistant cultivars." Journal of Experimental Botany **53**(378): 2281-2282.
Macholdt, J. and B. Honermeier (2016). "Impact of Climate Change on Cultivar Choice: Adaptation Strategies of Farmers and Advisors in German Cereal Production." Agronomy **6**(3): 40.
Mackay, T. F. C., E. A. Stone and J. F. Ayroles (2009). "The genetics of quantitative traits: challenges and prospects." Nature Reviews Genetics **10**: 565.
MacLeod, A. M. and G. H. Palmer (1966). "THE EMBRYO OF BARLEY IN RELATION TO MODIFICATION OF THE ENDOSPERM." Journal of the Institute of Brewing **72**(6): 580-589.
Mangin, B., A. Siberchicot, S. Nicolas, A. Doligez, P. This and C. Cierco-Ayrolles (2012). "Novel measures of linkage disequilibrium that correct the bias due to population structure and relatedness." Heredity (Edinb) **108**(3): 285-291.
Marchini, J. and B. Howie (2010). "Genotype imputation for genome-wide association studies." Nature Reviews Genetics **11**: 499.
Martin, J. M., T. K. Blake and E. A. Hockett (1991). "Diversity among North American Spring Barley Cultivars Based on Coefficients of Parentage." Crop Science **31**(5): 1131-1137.
Martre, P., B. Quilot-Turion, D. Luquet, M.-M. O.-S. Memmah, K. Chenu and P. Debaeke (2015). Model-assisted phenotyping and ideotype design, Elsevier**:** 349-373.
Mascher, M., H. Gundlach, A. Himmelbach, S. Beier, S. O. Twardziok, T. Wicker, V. Radchuk, C. Dockter, P. E. Hedley, J. Russell, M. Bayer, L. Ramsay, H. Liu, G. Haberer, X.-Q. Zhang, Q. Zhang, R. A. Barrero, L. Li, S. Taudien, M. Groth, M. Felder, A. Hastie, H. Šimková, H. Staňková, J. Vrána, S. Chan, M. Muñoz-Amatriaín, R. Ounit, S. Wanamaker, D. Bolser, C. Colmsee, T. Schmutzer, L. Aliyeva-Schnorr, S. Grasso, J. Tanskanen, A.

Chailyan, D. Sampath, D. Heavens, L. Clissold, S. Cao, B. Chapman, F. Dai, Y. Han, H. Li, X. Li, C. Lin, J. K. McCooke, C. Tan, P. Wang, S. Wang, S. Yin, G. Zhou, J. A. Poland, M. I. Bellgard, L. Borisjuk, A. Houben, J. Doležel, S. Ayling, S. Lonardi, P. Kersey, P. Langridge, G. J. Muehlbauer, M. D. Clark, M. Caccamo, A. H. Schulman, K. F. X. Mayer, M. Platzer, T. J. Close, U. Scholz, M. Hansson, G. Zhang, I. Braumann, M. Spannagl, C. Li, R. Waugh and N. Stein (2017). "A chromosome conformation capture ordered sequence of the barley genome." Nature **544**: 427.
Mascher, M., G. J. Muehlbauer, D. S. Rokhsar, J. Chapman, J. Schmutz, K. Barry, M. Muñoz-Amatriaín, T. J. Close, R. P. Wise, A. H. Schulman, A. Himmelbach, K. F. X. Mayer, U. Scholz, J. A. Poland, N. Stein and R. Waugh (2013). "Anchoring and ordering NGS contig assemblies by population sequencing (POPSEQ)." The Plant Journal **76**(4): 718-727.
Mascher, M., T. A. Richmond, D. J. Gerhardt, A. Himmelbach, L. Clissold, D. Sampath, S. Ayling, B. Steuernagel, M. Pfeifer, M. D'Ascenzo, E. D. Akhunov, P. E. Hedley, A. M. Gonzales, P. L. Morrell, B. Kilian, F. R. Blattner, U. Scholz, K. F. X. Mayer, A. J. Flavell, G. J. Muehlbauer, R. Waugh, J. A. Jeddeloh and N. Stein (2013). "Barley whole exome capture: a tool for genomic research in the genus Hordeum and beyond." The Plant Journal **76**(3): 494-505.
Mascher, M., V. J. Schuenemann, U. Davidovich, N. Marom, A. Himmelbach, S. Hübner, A. Korol, M. David, E. Reiter, S. Riehl, M. Schreiber, S. H. Vohr, R. E. Green, I. K. Dawson, J. Russell, B. Kilian, G. J. Muehlbauer, R. Waugh, T. Fahima, J. Krause, E. Weiss and N. Stein (2016). "Genomic analysis of 6,000-year-old cultivated grain illuminates the domestication history of barley." Nature Genetics **48**: 1089.
Masuka, B., G. N. Atlin, M. Olsen, C. Magorokosho, M. Labuschagne, J. Crossa, M. Bänziger, K. V. Pixley, B. S. Vivek, A. von Biljon, J. Macrobert, G. Alvarado, B. M. Prasanna, D. Makumbi, A. Tarekegne, B. Das, M. Zaman-Allah and J. E. Cairns (2017). "Gains in Maize Genetic Improvement in Eastern and Southern Africa: I. CIMMYT Hybrid Breeding Pipeline." Crop Science **57**: 168-179.
Mathan, J., J. Bhattacharya and A. Ranjan (2016). "Enhancing crop yield by optimizing plant developmental features." Development **143**(18): 3283-3294.
Mather, K. A., A. L. Caicedo, N. R. Polato, K. M. Olsen, S. McCouch and M. D. Purugganan (2007). "The Extent of Linkage Disequilibrium in Rice (Oryza sativa L.)." Genetics **177**(4): 2223-2232.
Mayer, K. F. X., M. Martis, P. E. Hedley, H. Šimková, H. Liu, J. A. Morris, B. Steuernagel, S. Taudien, S. Roessner, H. Gundlach, M. Kubaláková, P. Suchánková, F. Murat, M. Felder, T. Nussbaumer, A. Graner, J. Salse, T. Endo, H. Sakai, T. Tanaka, T. Itoh, K. Sato, M. Platzer, T. Matsumoto, U. Scholz, J. Doležel, R. Waugh and N. Stein (2011). "Unlocking the Barley Genome by Chromosomal and Comparative Genomics." The Plant Cell **23**(4): 1249-1263.
Mayer, K. F. X., R. Waugh, P. Langridge, T. J. Close, R. P. Wise, A. Graner, T. Matsumoto, K. Sato, A. Schulman, G. J. Muehlbauer, N. Stein, R. Ariyadasa, D. Schulte, N. Poursarebani, R. Zhou, B. Steuernagel, M. Mascher, U. Scholz, B. Shi, P. Langridge, K. Madishetty, J. T. Svensson, P. Bhat, M. Moscou, J. Resnik, T. J. Close, G. J. Muehlbauer, P. Hedley, H. Liu, J. Morris, R. Waugh, Z. Frenkel, A. Korol, H. Bergès, A. Graner, N. Stein, B. Steuernagel, U. Scholz, S. Taudien, M. Felder, M. Groth, M. Platzer, N. Stein, B. Steuernagel, U. Scholz, A. Himmelbach, S. Taudien, M. Felder, M. Platzer, S. Lonardi, D. Duma, M. Alpert, F. Cordero, M. Beccuti, G. Ciardo, Y. Ma, S. Wanamaker, T. J. Close, N. Stein, F. Cattonaro, V. Vendramin, S. Scalabrin, S. Radovic, R. Wing, D. Schulte, B. Steuernagel, M. Morgante, N. Stein, R. Waugh, T. Nussbaumer, H. Gundlach, M. Martis, R. Ariyadasa, N. Poursarebani, B. Steuernagel, U. Scholz, R. P. Wise, J. Poland, N. Stein, K. F. X. Mayer, M. Spannagl, M. Pfeifer, H. Gundlach, K. F. X. Mayer, H. Gundlach, C. Moisy, J. Tanskanen, S. Scalabrin, A. Zuccolo, V. Vendramin, M. Morgante, K. F. X. Mayer, A. Schulman, M. Pfeifer, M. Spannagl, P. Hedley, J. Morris, J. Russell, A. Druka, D. Marshall, M. Bayer, D. Swarbreck, D. Sampath, S. Ayling, M. Febrer, M. Caccamo, T. Matsumoto, T. Tanaka, K. Sato, R. P. Wise, T. J. Close, S. Wannamaker, G. J. Muehlbauer, N. Stein, K. F. X. Mayer, R. Waugh, B. Steuernagel, T. Schmutzer, M. Mascher, U. Scholz, S. Taudien, M. Platzer, K. Sato, D. Marshall, M. Bayer, R. Waugh, N. Stein, K. F. X. Mayer, R. Waugh, J. W. S. Brown, A. Schulman, P. Langridge, M. Platzer, G. B. Fincher, G. J. Muehlbauer, K. Sato, T. J. Close, R. P. Wise and N. Stein (2012). "A physical, genetic and functional sequence assembly of the barley genome." Nature **491**: 711.
Miller, N. D., N. J. Haase, J. Lee, S. M. Kaeppler, N. Leon and E. P. Spalding (2017). "A robust, high-throughput method for computing maize ear, cob, and kernel attributes automatically from images." The Plant Journal **89**(1): 169-178.

Minic, Z., E. Jamet, H. San-Clemente, S. Pelletier, J.-P. Renou, C. Rihouey, D. P. O. Okinyo, C. Proux, P. Lerouge and L. Jouanin (2009). "Transcriptomic analysis of Arabidopsis developing stems: a close-up on cell wall genes." BMC Plant Biology **9**(1): 6.
Moore, C. R., D. S. Gronwall, N. D. Miller and E. P. Spalding (2013). "Mapping Quantitative Trait Loci Affecting Arabidopsis thaliana Seed Morphology Features Extracted Computationally From Images." G3: Genes|Genomes|Genetics **3**(1): 109-118.
Morrell, P. L. and M. T. Clegg (2007). "Genetic evidence for a second domestication of barley Hordeum vulgare east of the Fertile Crescent." Proceedings of the National Academy of Sciences **104**(9): 3289-3294.
Müller, K. J., N. Romano, O. Gerstner, F. Garcia-Marotot, C. Pozzi, F. Salamini and W. Rohde (1995). "The barley Hooded mutation caused by a duplication in a homeobox gene intron." Nature **374**: 727.
Myles, S., J. Peiffer, P. J. Brown, E. S. Ersoz, Z. Zhang, D. E. Costich and E. S. Buckler (2009). "Association Mapping: Critical Considerations Shift from Genotyping to Experimental Design." The Plant Cell **21**(8): 2194-2202.
Nadolska-Orczyk, A., I. K. Rajchel, W. Orczyk and S. Gasparis (2017). "Major genes determining yield-related traits in wheat and barley." Theoretical and Applied Genetics **130**(6): 1081-1098.
Naeem, A., A. P. French, D. M. Wells and T. P. Pridmore (2011). "High-throughput feature counting and measurement of roots." Bioinformatics **27**(9): 1337-1338.
Nagel, K. A., A. Putz, F. Gilmer, K. Heinz, A. Fischbach, J. Pfeifer, M. Faget, S. Blossfeld, M. Ernst, C. Dimaki, B. Kastenholz, A.-K. Kleinert, A. Galinski, H. Scharr, F. Fiorani and U. Schurr (2012). "GROWSCREEN-Rhizo is a novel phenotyping robot enabling simultaneous measurements of root and shoot growth for plants grown in soil-filled rhizotrons." Functional Plant Biology **39**(11): 891-904.
Nair, S. K., N. Wang, Y. Turuspekov, M. Pourkheirandish, S. Sinsuwongwat, G. Chen, M. Sameri, A. Tagiri, I. Honda, Y. Watanabe, H. Kanamori, T. Wicker, N. Stein, Y. Nagamura, T. Matsumoto and T. Komatsuda (2010). "Cleistogamous flowering in barley arises from the suppression of microRNA-guided HvAP2 mRNA cleavage." Proceedings of the National Academy of Sciences **107**(1): 490-495.
Nakajima, T., M. Yoshida and K. Tomimura (2008). "Effect of lodging on the level of mycotoxins in wheat, barley, and rice infected with the Fusarium graminearum species complex." Journal of General Plant Pathology **74**(4): 289.
Nordborg, M. (2000). "Linkage disequilibrium, gene trees and selfing: an ancestral recombination graph with partial self-fertilization." Genetics **154**(2): 923-929.
Ohashi, J., S. Yamamoto, N. Tsuchiya, Y. Hatta, T. Komata, M. Matsushita and K. Tokunaga (2001). "Comparison of statistical power between 2×2 allele frequency and allele positivity tables in case-control studies of complex disease genes." Annals of Human Genetics **65**(2): 197-206.
Okuno, A., K. Hirano, K. Asano, W. Takase, R. Masuda, Y. Morinaka, M. Ueguchi-Tanaka, H. Kitano and M. Matsuoka (2014). "New Approach to Increasing Rice Lodging Resistance and Biomass Yield Through the Use of High Gibberellin Producing Varieties." PLOS ONE **9**(2): e86870.
Olsen, K. M. and J. F. Wendel (2013). "A Bountiful Harvest: Genomic Insights into Crop Domestication Phenotypes." Annual Review of Plant Biology **64**(1): 47-70.
Ookawa, T., R. Aoba, T. Yamamoto, T. Ueda, T. Takai, S. Fukuoka, T. Ando, S. Adachi, M. Matsuoka, T. Ebitani, Y. Kato, I. W. Mulsanti, M. Kishii, M. Reynolds, F. Piñera, T. Kotake, S. Kawasaki, T. Motobayashi and T. Hirasawa (2016). "Precise estimation of genomic regions controlling lodging resistance using a set of reciprocal chromosome segment substitution lines in rice." Scientific Reports **6**: 30572.
Ookawa, T., T. Hobo, M. Yano, K. Murata, T. Ando, H. Miura, K. Asano, Y. Ochiai, M. Ikeda, R. Nishitani, T. Ebitani, H. Ozaki, E. R. Angeles, T. Hirasawa and M. Matsuoka (2010). "New approach for rice improvement using a pleiotropic QTL gene for lodging resistance and yield." Nature Communications **1**: 132.
Ookawa, T. and K. Ishihara (1992). "Varietal difference of physical characteristics of the culm related to lodging resistance in paddy rice. ." Jpn. J. Crop. Sci. **61**(3): 419-425.
Ookawa, T., K. Yasuda, H. Kato, M. Sakai, M. Seto, K. Sunaga, T. Motobayashi, S. Tojo and T. Hirasawa (2010). "Biomass Production and Lodging Resistance in 'Leaf Star', a New Long-Culm Rice Forage Cultivar." Plant Production Science **13**(1): 58-66.
Pankin, A., J. Altmüller, C. Becker and M. von Korff (2018). "Targeted re-sequencing reveals the genomic signatures of multiple barley domestications." New Phytologist **218**: 1247-1259.

Pankin, A. and M. von Korff (2017). "Co-evolution of methods and thoughts in cereal domestication studies: a tale of barley (Hordeum vulgare)." Current Opinion in Plant Biology **36**: 15-21.
Park, H. L., S. H. Bhoo, M. Kwon, S.-W. Lee and M.-H. Cho (2017). "Biochemical and Expression Analyses of the Rice Cinnamoyl-CoA Reductase Gene Family." Frontiers in Plant Science **8**(2099).
Pasam, R. K., R. Sharma, M. Malosetti, F. A. van Eeuwijk, G. Haseneyer, B. Kilian and A. Graner (2012). "Genome-wide association studies for agronomical traits in a world wide spring barley collection." BMC Plant Biology **12**(1): 16.
Patterson, N., A. L. Price and D. Reich (2006). "Population Structure and Eigenanalysis." PLOS Genetics **2**(12): e190.
Pauli, D., S. C. Chapman, R. Bart, C. N. Topp, C. J. Lawrence-Dill, J. Poland and M. A. Gore (2016). "The quest for understanding phenotypic variation via integrated approaches in the field environment." Plant Physiology **172**(2): 622-634.
Pease, J. B., D. C. Haak, M. W. Hahn and L. C. Moyle (2016). "Phylogenomics Reveals Three Sources of Adaptive Variation during a Rapid Radiation." PLOS Biology **14**(2): e1002379.
Peiffer, J. A., S. A. Flint-Garcia, N. De Leon, M. D. McMullen, S. M. Kaeppler and E. S. Buckler (2013). "The Genetic Architecture of Maize Stalk Strength." PLOS ONE **8**(6): e67066.
Peng, D., X. Chen, Y. Yin, K. Lu, W. Yang, Y. Tang and Z. Wang (2014). "Lodging resistance of winter wheat (Triticum aestivum L.): Lignin accumulation and its related enzymes activities due to the application of paclobutrazol or gibberellin acid." Field Crops Research **157**: 1-7.
Peng, J., D. E. Richards, N. M. Hartley, G. P. Murphy, K. M. Devos, J. E. Flintham, J. Beales, L. J. Fish, A. J. Worland, F. Pelica, D. Sudhakar, P. Christou, J. W. Snape, M. D. Gale and N. P. Harberd (1999). "'Green revolution' genes encode mutant gibberellin response modulators." Nature **400**: 256.
Peng, S., G. S. Khush, P. Virk, Q. Tang and Y. Zou (2008). "Progress in ideotype breeding to increase rice yield potential." Field Crops Research **108**(1): 32-38.
Peng, S., R. C. Laza, R. M. Visperas, G. S. Khush, P. Virk and D. Zhu (2004). New direction for a diverse planet. Proceedings of the 4th International Crop Science Congress. 4th Int. Crop Sci. Congr, Brisbane, Australia, Published on CD.
Phyo, P., T. Wang, S. N. Kiemle, H. O'Neill, S. V. Pingali, M. Hong and D. J. Cosgrove (2017). "Gradients in Wall Mechanics and Polysaccharides along Growing Inflorescence Stems." Plant Physiology **175**(4): 1593.
Piñera-Chavez, F. J., P. M. Berry, M. J. Foulkes, M. A. Jesson and M. P. Reynolds (2016). "Avoiding lodging in irrigated spring wheat. I. Stem and root structural requirements." Field Crops Research **196**: 325-336.
Poets, A. M., Z. Fang, M. T. Clegg and P. L. Morrell (2015). "Barley landraces are characterized by geographically heterogeneous genomic origins." Genome Biology **16**(1): 173.
Poland, J. A., P. J. Brown, M. E. Sorrells and J.-L. Jannink (2012). "Development of High-Density Genetic Maps for Barley and Wheat Using a Novel Two-Enzyme Genotyping-by-Sequencing Approach." PLOS ONE **7**(2): e32253.
Pourkheirandish, M., G. Hensel, B. Kilian, N. Senthil, G. Chen, M. Sameri, P. Azhaguvel, S. Sakuma, S. Dhanagond, R. Sharma, M. Mascher, A. Himmelbach, S. Gottwald, Sudha K. Nair, A. Tagiri, F. Yukuhiro, Y. Nagamura, H. Kanamori, T. Matsumoto, G. Willcox, Christopher P. Middleton, T. Wicker, A. Walther, R. Waugh, Geoffrey B. Fincher, N. Stein, J. Kumlehn, K. Sato and T. Komatsuda (2015). "Evolution of the Grain Dispersal System in Barley." Cell **162**(3): 527-539.
Pourkheirandish, M. and T. Komatsuda (2007). "The Importance of Barley Genetics and Domestication in a Global Perspective." Annals of Botany **100**(5): 999-1008.
Price, A. L., N. J. Patterson, R. M. Plenge, M. E. Weinblatt, N. A. Shadick and D. Reich (2006). "Principal components analysis corrects for stratification in genome-wide association studies." Nature Genetics **38**: 904.
Price, C. A., O. Symonova, Y. Mileyko, T. Hilley and J. S. Weitz (2011). "Leaf Extraction and Analysis Framework Graphical User Interface: Segmenting and Analyzing the Structure of Leaf Veins and Areoles." Plant Physiology **155**(1): 236-245.
Pritchard, J. K., M. Stephens and P. Donnelly (2000). "Inference of Population Structure Using Multilocus Genotype Data." Genetics **155**(2): 945-959.

Purcell, S., B. Neale, K. Todd-Brown, L. Thomas, M. A. R. Ferreira, D. Bender, J. Maller, P. Sklar, P. I. W. de Bakker, M. J. Daly and P. C. Sham (2007). "PLINK: A Tool Set for Whole-Genome Association and Population-Based Linkage Analyses." The American Journal of Human Genetics **81**(3): 559-575.
Qian, Q., L. Guo, S. M. Smith and J. Li (2016). "Breeding high-yield superior quality hybrid super rice by rational design." National Science Review **3**(3): 283-294.
Rafalski, J. A. (2010). "Association genetics in crop improvement." Current Opinion in Plant Biology **13**(2): 174-180.
Rajkumara, S. (2008). "Lodging in cereals - a review." Agricultural Reviews **29**(1): 55-60.
Ramsay, L., J. Comadran, A. Druka, D. F. Marshall, W. T. B. Thomas, M. Macaulay, K. MacKenzie, C. Simpson, J. Fuller, N. Bonar, P. M. Hayes, U. Lundqvist, J. D. Franckowiak, T. J. Close, G. J. Muehlbauer and R. Waugh (2011). "INTERMEDIUM-C, a modifier of lateral spikelet fertility in barley, is an ortholog of the maize domestication gene TEOSINTE BRANCHED 1." Nature Genetics **43**: 169.
Rasmusson, D. C. (1991). "A plant breeder's experience with ideotype breeding." Field Crops Research **26**(2): 191-200.
Rebolledo, M. C., D. Luquet, B. Courtois, A. Henry, J.-C. Soulié, L. Rouan and M. Dingkuhn (2013). "Can early vigour occur in combination with drought tolerance and efficient water use in rice genotypes?" Functional Plant Biology **40**(6): 582-594.
Reddy, N. and Y. Yang (2005). "Structure and properties of high quality natural cellulose fibers from cornstalks." Polymer **46**(15): 5494-5500.
Reuzeau, C., V. Frankard, Y. Hatzfeld, A. Sanz, W. Van Camp, P. Lejeune, C. De Wilde, K. Lievens, J. de Wolf, E. Vranken, R. Peerbolte and W. Broekaert (2007). "Traitmill™: a functional genomics platform for the phenotypic analysis of cereals." Plant Genetic Resources **4**(1): 20-24.
Ringnér, M. (2008). "What is principal component analysis?" Nature Biotechnology **26**: 303.
Rockström, J., J. Williams, G. Daily, A. Noble, N. Matthews, L. Gordon, H. Wetterstrand, F. DeClerck, M. Shah, P. Steduto, C. de Fraiture, N. Hatibu, O. Unver, J. Bird, L. Sibanda and J. Smith (2017). "Sustainable intensification of agriculture for human prosperity and global sustainability." Ambio **46**(1): 4-17.
Rötter, R. P., F. Tao, J. G. Höhn and T. Palosuo (2015). "Use of crop simulation modelling to aid ideotype design of future cereal cultivars." Journal of Experimental Botany **66**(12): 3463-3476.
Rudall, P. J., W. Stuppy, J. Cunniff, E. A. Kellogg and B. G. Briggs (2005). "Evolution of reproductive structures in grasses (Poaceae) inferred by sister-group comparison with their putative closest living relatives, Ecdeiocoleaceae." American Journal of Botany **92**(9): 1432-1443.
Rueden, C. T., J. Schindelin, M. C. Hiner, B. E. DeZonia, A. E. Walter, E. T. Arena and K. W. Eliceiri (2017). "ImageJ2: ImageJ for the next generation of scientific image data." BMC Bioinformatics **18**(1): 529.
Sachs, T. (1991). "Cell polarity and tissue patterning in plants." Development **113**(Supplement 1): 83-93.
Sakamoto, T., K. Miura, H. Itoh, T. Tatsumi, M. Ueguchi-Tanaka, K. Ishiyama, M. Kobayashi, G. K. Agrawal, S. Takeda, K. Abe, A. Miyao, H. Hirochika, H. Kitano, M. Ashikari and M. Matsuoka (2004). "An Overview of Gibberellin Metabolism Enzyme Genes and Their Related Mutants in Rice." Plant Physiology **134**(4): 1642-1653.
Salamini, F., H. Özkan, A. Brandolini, R. Schäfer-Pregl and W. Martin (2002). "Genetics and geography of wild cereal domestication in the near east." Nature Reviews Genetics **3**: 429.
Sameri, M., S. Nakamura, S. K. Nair, K. Takeda and T. Komatsuda (2009). "A quantitative trait locus for reduced culm internode length in barley segregates as a Mendelian gene." Theoretical and Applied Genetics **118**(4): 643-652.
Sasaki, A., M. Ashikari, M. Ueguchi-Tanaka, H. Itoh, A. Nishimura, D. Swapan, K. Ishiyama, T. Saito, M. Kobayashi, G. S. Khush, H. Kitano and M. Matsuoka (2002). "A mutant gibberellin-synthesis gene in rice." Nature **416**: 701.
Sayre, K. D., S. Rajaram and R. A. Fischer (1997). "Yield Potential Progress in Short Bread Wheats in Northwest Mexico." Crop Science **37**: 36-42.
Schaefer, R. J., J.-M. Michno and C. L. Myers (2017). "Unraveling gene function in agricultural species using gene co-expression networks." Biochimica et Biophysica Acta (BBA) - Gene Regulatory Mechanisms **1860**(1): 53-63.

Scheet, P. and M. Stephens (2006). "A Fast and Flexible Statistical Model for Large-Scale Population Genotype Data: Applications to Inferring Missing Genotypes and Haplotypic Phase." The American Journal of Human Genetics **78**(4): 629-644.
Schindelin, J., I. Arganda-Carreras, E. Frise, V. Kaynig, M. Longair, T. Pietzsch, S. Preibisch, C. Rueden, S. Saalfeld, B. Schmid, J.-Y. Tinevez, D. J. White, V. Hartenstein, K. Eliceiri, P. Tomancak and A. Cardona (2012). "Fiji: an open-source platform for biological-image analysis." Nature Methods **9**: 676.
Schmid, K., B. Kilian and J. Russell (2018). Barley Domestication, Adaptation and Population Genomics. The Barley Genome. N. Stein and G. J. Muehlbauer. Cham, Springer International Publishing**:** 317-336.
Schulze, T. G. and F. J. McMahon (2002). "Genetic association mapping at the crossroads: Which test and why? Overview and practical guidelines." American Journal of Medical Genetics **114**(1): 1-11.
Scofield, G. N., S. A. Ruuska, N. Aoki, D. C. Lewis, L. M. Tabe and C. L. D. Jenkins (2009). "Starch storage in the stems of wheat plants: localization and temporal changes." Annals of botany **103**(6): 859-868.
Segura, V., B. J. Vilhjálmsson, A. Platt, A. Korte, Ü. Seren, Q. Long and M. Nordborg (2012). "An efficient multi-locus mixed-model approach for genome-wide association studies in structured populations." Nature Genetics **44**: 825.
Serrano-Mislata, A., S. Bencivenga, M. Bush, K. Schiessl, S. Boden and R. Sablowski (2017). "DELLA genes restrict inflorescence meristem function independently of plant height." Nature Plants **3**(9): 749-754.
Serrano-Mislata, A. and R. Sablowski (2018). "The pillars of land plants: new insights into stem development." Current Opinion in Plant Biology **45**: 11-17.
Shakoor, N., S. Lee and T. C. Mockler (2017). "High throughput phenotyping to accelerate crop breeding and monitoring of diseases in the field." Current Opinion in Plant Biology **38**: 184-192.
Slatkin, M. (2008). "Linkage disequilibrium — understanding the evolutionary past and mapping the medical future." Nature Reviews Genetics **9**: 477.
Small, I. (2007). "RNAi for revealing and engineering plant gene functions." Current Opinion in Biotechnology **18**(2): 148-153.
Soto-Cerda, B. J. and S. Cloutier (2012). Association Mapping in Plant Genomes. Genetic Diversity in Plants. Mahmut, IntechOpen.
Sowadan, O., D. Li, Y. Zhang, S. Zhu, X. Hu, L. B. Bhanbhro, W. M. Edzesi, X. Dang and D. Hong (2018). "Mining of favorable alleles for lodging resistance traits in rice (oryza sativa) through association mapping." Planta **248**(1): 155-169.
Spielmeyer, W., M. H. Ellis and P. M. Chandler (2002). "Semidwarf (sd-1), “green revolution” rice, contains a defective gibberellin 20-oxidase gene." Proceedings of the National Academy of Sciences of the United States of America **99**(13): 9043-9048.
Stadler, L. J. (1928). "MUTATIONS IN BARLEY INDUCED BY X-RAYS AND RADIUM." Science **68**(1756): 186-187.
Sternberg, S. (1983). "Biomedical Image Processing." Computer **16**: 22-34.
Stützel, H., N. Brüggemann and D. Inzé (2016). "The Future of Field Trials in Europe: Establishing a Network Beyond Boundaries." Trends in Plant Science **21**(2): 92-95.
Su, J., C. Hu, X. Yan, Y. Jin, Z. Chen, Q. Guan, Y. Wang, D. Zhong, C. Jansson, F. Wang, A. Schnürer and C. Sun (2015). "Expression of barley SUSIBA2 transcription factor yields high-starch low-methane rice." Nature **523**: 602.
Sun, C., S. Palmqvist, H. Olsson, M. Borén, S. Ahlandsberg and C. Jansson (2003). "A Novel WRKY Transcription Factor, SUSIBA2, Participates in Sugar Signaling in Barley by Binding to the Sugar-Responsive Elements of the iso1 Promoter." The Plant Cell **15**(9): 2076-2092.
Szareski, V. J., I. R. Carvalho, T. Corazza, S. M. Dellagostin, A. J. D. Pelegrin, M. H. Barbosa, O. Pires, D. S. Muraro, V. Q. D. Souza and T. Pedó (2018). "Oryza Wild Species : An Alternative for Rice Breeding under Abiotic Stress Conditions." 1093-1104.
Takeda, S. and M. Matsuoka (2008). "Genetic approaches to crop improvement: responding to environmental and population changes." Nature Reviews Genetics **9**: 444.
Taketa, S., S. Amano, Y. Tsujino, T. Sato, D. Saisho, K. Kakeda, M. Nomura, T. Suzuki, T. Matsumoto, K. Sato, H. Kanamori, S. Kawasaki and K. Takeda (2008). "Barley grain with adhering hulls is controlled by an ERF

family transcription factor gene regulating a lipid biosynthesis pathway." Proceedings of the National Academy of Sciences **105**(10): 4062-4067.
Tamm, Ü. (2003). The variation of agronomic characteristics of European malting barley varieties.
Tanabata, T., T. Shibaya, K. Hori, K. Ebana and M. Yano (2012). "SmartGrain: High-Throughput Phenotyping Software for Measuring Seed Shape through Image Analysis." Plant Physiology **160**(4): 1871-1880.
Tanaka, K., K. Murata, M. Yamazaki, K. Onosato, A. Miyao and H. Hirochika (2003). "Three Distinct Rice Cellulose Synthase Catalytic Subunit Genes Required for Cellulose Synthesis in the Secondary Wall." Plant Physiology **133**(1): 73-83.
Tanger, P., S. Klassen, J. P. Mojica, J. T. Lovell, B. T. Moyers, M. Baraoidan, M. E. B. Naredo, K. L. McNally, J. Poland, D. R. Bush, H. Leung, J. E. Leach and J. K. McKay (2017). "Field-based high throughput phenotyping rapidly identifies genomic regions controlling yield components in rice." Scientific Reports **7**: 42839.
Tanksley, S. D., M. W. Ganal and G. B. Martin (1995). "Chromosome landing: a paradigm for map-based gene cloning in plants with large genomes." Trends in Genetics **11**(2): 63-68.
Tanno, K.-i. and G. Willcox (2006). "How Fast Was Wild Wheat Domesticated?" Science **311**(5769): 1886-1886.
Tao, F., R. P. Rötter, T. Palosuo, C. G. H. Díaz-Ambrona, M. I. Mínguez, M. A. Semenov, K. C. Kersebaum, C. Nendel, D. Cammarano, H. Hoffmann, F. Ewert, A. Dambreville, P. Martre, L. Rodríguez, M. Ruiz-Ramos, T. Gaiser, J. G. Höhn, T. Salo, R. Ferrise, M. Bindi and A. H. Schulman (2016). "Designing future barley ideotypes using a crop model ensemble." European Journal of Agronomy **82**: 144-162.
Tardieu, F., L. Cabrera-Bosquet, T. Pridmore and M. Bennett (2017). "Plant Phenomics, From Sensors to Knowledge." Current Biology **27**(15): R770-R783.
Tavakol, E., G. Bretani and L. Rossini (2017). Natural Genetic Diversity and Crop Improvement. R. Pilu and G. Gavazzi, BENTHAM SCIENCE PUBLISHERS**:** 185-215.
Tenaillon, M. I., M. C. Sawkins, A. D. Long, R. L. Gaut, J. F. Doebley and B. S. Gaut (2001). "Patterns of DNA sequence polymorphism along chromosome 1 of maize (Zea mays ssp. mays L.)." Proceedings of the National Academy of Sciences **98**(16): 9161-9166.
Thomas, H. and C. J. Howarth (2000). "Five ways to stay green." Journal of Experimental Botany **51**(suppl_1): 329-337.
Thomas, W. T. B., W. Powell and P. Ellis (1991). "The effects of major genes on quantitatively varying characters in barley. III. The two row/six row locus (V–v)." Heredity **65**(2): 259-264.
Thorne, G. N. (1966). Physiological aspects of grain yield in cereals. London**:** 88-105.
Townsend, T. J., J. Roy, P. Wilson, G. A. Tucker and D. L. Sparkes (2017). "Food and bioenergy: Exploring ideotype traits of a dual-purpose wheat cultivar." Field Crops Research **201**: 210-221.
Tripathi, S. C., K. D. Sayre, J. N. Kaul and R. S. Narang (2003). "Growth and morphology of spring wheat (Triticum aestivum. L.) culms and their association with lodging: Effects of genotypes, N levels and ethephon." Field Crops Research **84**(3): 271-290.
Ubbens, J. R. and I. Stavness (2017). "Deep Plant Phenomics: A Deep Learning Platform for Complex Plant Phenotyping Tasks." Frontiers in Plant Science **8**(1190).
Ullrich, S. E. (2011). Significance, Adaptation, Production, and Trade of Barley. Barley. S. E. Ullrich, Blackwell Publishing
United Nations (2017). World Population Prospects: The 2017 Revision, Key Findings and Advance Tables, United Nations. **Working Paper no. ESA/P/WP.248**.
van den Oord, E. J. C. G. (2008). "Controlling false discoveries in genetic studies." American Journal of Medical Genetics Part B: Neuropsychiatric Genetics **147B**(5): 637-644.
van Leeuwen, E. M., A. Kanterakis, P. Deelen, M. V. Kattenberg, C. The Genome of the Netherlands, A. Abdellaoui, A. Hofman, A. Schönhuth, A. Kanterakis, A. Menelaou, A. J. M. de Craen, B. D. C. van Schaik, B. H. Wolffenbuttel, C. Wijmenga, C. C. Elbers, C. M. van Duijn, C. van Duijn, D. R. Cox, D. van Enckevort, D. I. Boomsma, E. M. van Leeuwen, E.-W. Lameijer, F. Hormozdiari, F. van Dijk, G. B. van Ommen, G. Willemsen, H. E. D. Suchiman, H. Mei, H. Byelas, H. Cao, I. J. Nijman, I. Pe'er, J. Bot, J. H. Veldink, J. A. Bovenberg, J. Y. Hehir-Kwa, J. F. J. Laros, J. van Setten, J. T. den Dunnen, J. J. Hottenga, J. Wang, K. Joeri der Velde, K. Ye, L. C. Francioli, L. C. Karssen, L. H. den Berg, M. Kayser, M. van Oven, M. B. Beekman, M. Stoneking, M. Dijkstra, M. Vermaat, M. Sohail, M. Plattee, M. Kattenberg, M. H. Moed, M. Li, M. A. Swertz, N. Amin, N. Li,

P. E. Slagboom, P. Deelen, P. I. W. de Bakker, P. de Knijff, P. F. Palamara, P. B. T. Neerincx, Q. Li, R. E. Handsaker, R. Chen, S. L. Pulit, S. R. Sunyaev, S. Potluri, S. J. Pitts, S. Cao, T. Marschall, V. Guryev, V. Koval, W. P. Kloosterman, Y. Li, Y. Du, P. E. Slagboom, P. I. W. de Bakker, C. Wijmenga, M. A. Swertz, D. I. Boomsma, C. M. van Duijn, L. C. Karssen and J. J. Hottenga (2015). "Population-specific genotype imputations using minimac or IMPUTE2." Nature Protocols **10**: 1285.
Vavilov, N. I. (1926). Studies on the origin of cultivated plants. Leningrad, Institut Botanique Applique´ et d'Amelioration des Plantes.
Vavilov, N. I. (1992). Origin and geography of cultivated plants. Cambridge, Cambridge University Press.
Verma, V., A. J. Worland, E. J. Savers, L. Fish, P. Caligari and J. W. Snape (2005). Identification and characterization of quantitative trait loci related to lodging resistance and associated traits in bread wheat.
Vilhjálmsson, B. J. and M. Nordborg (2012). "The nature of confounding in genome-wide association studies." Nature Reviews Genetics **14**: 1.
Virlet, N., K. Sabermanesh, P. Sadeghi-Tehran and M. J. Hawkesford (2017). "Field Scanalyzer: An automated robotic field phenotyping platform for detailed crop monitoring." Functional Plant Biology **44**(1): 143-153.
von Bothmer, R. and T. Komatsuda (2011). Barley Origin and Related Species. Barley. S. E. Ullrich, Blackwell Publishing
von Humboldt, A. and A. Bonpland (1807). Ideen zu einer Geographie der Pflanzen nebst einem Naturgemalde alde der Tropenlander. Tübingen, Paris, Bey F.G. Cotta.
Wallach, D., L. O. Mearns, A. C. Ruane, R. P. Rötter and S. Asseng (2016). "Lessons from climate modeling on the design and use of ensembles for crop modeling." Climatic Change **139**(3): 551-564.
Wang, B., S. M. Smith and J. Li (2018). "Genetic Regulation of Shoot Architecture." Annual Review of Plant Biology **69**(1): annurev-arplant-042817-040422.
Wang, J., J. Zhu, R. Huang and Y. Yang (2012). "Investigation of cell wall composition related to stem lodging resistance in wheat (Triticum aestivum L.) by FTIR spectroscopy." Plant Signaling & Behavior **7**(7): 856-863.
Wang, J., J. Zhu, Q. Lin, X. Li, N. Teng, Z. Li, B. Li, A. Zhang and J. Lin (2006). "Effects of stem structure and cell wall components on bending strength in wheat." Chinese Science Bulletin **51**(7): 815-823.
Wang, L., I. V. Uilecan, A. H. Assadi, C. A. Kozmik and E. P. Spalding (2009). "HYPOTrace: Image Analysis Software for Measuring Hypocotyl Growth and Shape Demonstrated on Arabidopsis Seedlings Undergoing Photomorphogenesis." Plant Physiology **149**(4): 1632-1637.
Wang, M., N. Jiang, T. Jia, L. Leach, J. Cockram, R. Waugh, L. Ramsay, B. Thomas and Z. Luo (2012). "Genome-wide association mapping of agronomic and morphologic traits in highly structured populations of barley cultivars." Theoretical and Applied Genetics **124**(2): 233-246.
Watanabe, T. (1997). Lodging resistance. Science of the rice plant. Volume 3: Genetics. T. Matsuo, Y. Futsuhara, F. Kikuchi and H. Yamaguchi. Tokyo, Food and Agriculture Policy Research Center**:** 567-577.
Weibel, R. O. and J. W. Pendleton (1964). "Effect of artificial lodging on winter wheat grain yield and quality." Agron. J. **56**: 487-488.
Weight, C., D. Parnham and R. Waites (2008). "TECHNICAL ADVANCE: LeafAnalyser: a computational method for rapid and large-scale analyses of leaf shape variation." The Plant Journal **53**(3): 578-586.
Weiss, E., M. E. Kislev and A. Hartmann (2006). "Autonomous Cultivation Before Domestication." Science **312**(5780): 1608-1610.
Wenfu, C., X. Zhengjin and Z. Longbu (2007). Theories and Practices of Breeding Japonica Rice for Super High Yield. **v. 40**.
Willcox, G. (1998). Archaeobotanical evidence for the beginnings of agriculture in southwest Asia. The origins of agriculture and crop domestication. Proceedings of the Harlan Symposium. , Aleppo, ICARDA.
Willcox, G., S. Fornite and L. Herveux (2008). "Early Holocene cultivation before domestication in northern Syria." Vegetation History and Archaeobotany **17**(3): 313-325.
Wolabu, T. W. and M. Tadege (2016). "Photoperiod response and floral transition in sorghum." Plant Signaling & Behavior **11**(12): e1261232.
Xu, Y., Q. Jia, G. Zhou, X. Q. Zhang, T. Angessa, S. Broughton, G. Yan, W. Zhang and C. Li (2017). "Characterization of the sdw1 semi-dwarf gene in barley." BMC Plant Biology **17**(1): 1-10.

Xue, J., D. Luo, D. Xu, M. Zeng, X. Cui, L. Li and H. Huang (2015). "CCR1, an enzyme required for lignin biosynthesis in Arabidopsis, mediates cell proliferation exit for leaf development." The Plant Journal **83**(3): 375-387.
Yan, J., T. Shah, M. L. Warburton, E. S. Buckler, M. D. McMullen and J. Crouch (2009). "Genetic Characterization and Linkage Disequilibrium Estimation of a Global Maize Collection Using SNP Markers." PLOS ONE **4**(12): e8451.
Yang, W., S. Peng, R. C. Laza, R. M. Visperas and M. L. Dionisio-Sese (2007). "Grain yield and yield attributes of new plant type and hybrid rice." Crop Science **47**(4): 1393-1400.
Yano, K., T. Ookawa, K. Aya, Y. Ochiai, T. Hirasawa, T. Ebitani, T. Takarada, M. Yano, T. Yamamoto, S. Fukuoka, J. Wu, T. Ando, Reynante L. Ordonio, K. Hirano and M. Matsuoka (2015). "Isolation of a Novel Lodging Resistance QTL Gene Involved in Strigolactone Signaling and Its Pyramiding with a QTL Gene Involved in Another Mechanism." Molecular Plant **8**(2): 303-314.
Yao, J., H. Ma, P. Zhang, L. Ren, X. Yang, G. Yao, P. Zhang and M. Zhou (2011). "Inheritance of stem strength and its correlations with culm morphological traits in wheat (Triticum aestivum L.)." Canadian Journal of Plant Science **91**(6): 1065-1070.
Yazdanbakhsh, N. and J. Fisahn (2009). "High throughput phenotyping of root growth dynamics, lateral root formation, root architecture and root hair development enabled by PlaRoM." Functional Plant Biology **36**(11): 938-946.
Yin, X., M. Kropff and P. Stam (1999). The role of ecophysiological models in QTL analysis: The example of specific leaf area in barley.
Yu, J., G. Pressoir, W. H. Briggs, I. Vroh Bi, M. Yamasaki, J. F. Doebley, M. D. McMullen, B. S. Gaut, D. M. Nielsen, J. B. Holland, S. Kresovich and E. S. Buckler (2006). "A unified mixed-model method for association mapping that accounts for multiple levels of relatedness." Nature Genetics **38**: 203.
Yuan, L. (2017). "Progress in super-hybrid rice breeding." Crop Journal **5**(2): 100-102.
Zadoks, J. C., T. T. Chang and C. F. Konzak (1974). "A decimal code for the growth stages of cereals." Weed Research **14**(6): 415-421.
Zeid, M., G. Belay, S. Mulkey, J. Poland and M. E. Sorrells (2011). "QTL mapping for yield and lodging resistance in an enhanced SSR-based map for tef." Theoretical and Applied Genetics **122**(1): 77-93.
Zhang, C.-Q., Y. Xu, Y. Lu, H.-X. Yu, M.-H. Gu and Q.-Q. Liu (2011). "The WRKY transcription factor OsWRKY78 regulates stem elongation and seed development in rice." Planta **234**(3): 541-554.
Zhang, D., G. Bai, C. Zhu, J. Yu and B. F. Carver (2010). "Genetic Diversity, Population Structure, and Linkage Disequilibrium in U.S. Elite Winter Wheat." The Plant Genome **3**(2): 117-127.
Zhang, F.-z., Z.-x. Jin, G.-h. Ma, W.-n. Shang, H.-y. Liu, M.-l. Xu and Y. Liu (2010). "Relationship Between Lodging Resistance and Chemical Contents in Culms and Sheaths of Japonica Rice During Grain Filling." Rice Science **17**(4): 311-318.
Zhang, F., Y. Wang and H.-W. Deng (2008). "Comparison of Population-Based Association Study Methods Correcting for Population Stratification." PLOS ONE **3**(10): e3392.
Zhang, W., L. Wu, X. Wu, Y. Ding, G. Li, J. Li, F. Weng, Z. Liu, S. Tang, C. Ding and S. Wang (2016). "Lodging Resistance of Japonica Rice (Oryza Sativa L.): Morphological and Anatomical Traits due to top-Dressing Nitrogen Application Rates." Rice **9**(1): 31.
Zhang, X., C. Huang, D. Wu, F. Qiao, W. Li, L. Duan, K. Wang, Y. Xiao, G. Chen, Q. Liu, L. Xiong, W. Yang and J. Yan (2017). "High-Throughput Phenotyping and QTL Mapping Reveals the Genetic Architecture of Maize Plant Growth." Plant Physiology **173**(3): 1554-1564.
Zhou, H., G. Muehlbauer and B. Steffenson (2012). "Population structure and linkage disequilibrium in elite barley breeding germplasm from the United States." Journal of Zhejiang University. Science. B **13**(6): 438-451.
Zhu, C., M. Gore, E. S. Buckler and J. Yu (2008). "Status and Prospects of Association Mapping in Plants." The Plant Genome **1**(1): 5-20.
Zhu, X.-G., S. P. Long and D. R. Ort (2010). "Improving Photosynthetic Efficiency for Greater Yield." Annual Review of Plant Biology **61**(1): 235-261.
Zohary, D., M. Hopf and E. Weiss (2012). Domestication of Plants in the Old World: The Origin and Spread of Domesticated Plants in Southwest Asia, Europe, and the Mediterranean Basin, OUP Oxford.

Zuber, U., H. Winzeler, M. M. Messmer, M. Keller, B. Keller, J. E. Schmid and P. Stamp (1999). "Morphological Traits Associated with Lodging Resistance of Spring Wheat (Triticum aestivum L.)." Journal of Agronomy and Crop Science **182**(1): 17-24.

Acknowledgements

Questo lavoro di tesi è il frutto di una collaborazione di tre anni con ricercatori e studenti che direttamente e indirettamente mi hanno aiutato nel ideazione dei protocolli, nella raccolta di dati e nella loro analisi.

Inizio ringraziando chi ricercatore non è ma è sempre stato studente: mio padre Marino Bretani per il prezioso supporto tecnico che non dovrebbe mancare in nessun gruppo di ricerca.

Ringrazio i colleghi dell'istituto del Natural Resources Institute Finland (LUKE) a Helsinki, in particolar modo il professor Alan Schulman per la disponibilità che ha sempre dimostrato nell'inviarci i campioni di cui avevamo bisogno.

Ringrazio inoltre i colleghi del Consejo Superior de investigaciones Cetìficas (CSIC) di Aula Dei a Zaragoza, professor Ernesto Igartua Arregui e dottoressa Ana Casas che hanno da subito accettato di buon grado di ricreare una macchina per il taglio delle sezioni di orzo nel loro centro di ricerca, condividendo e discutendo sempre in maniera molto costruttiva i risultati ottenuti.

Un ringraziamento obbligatorio e sentito va ai colleghi professor Robbie Waugh, dottoressa Joanne Russel, dottor Bill Thomas, dottoressa Hazel Bull e Richard Keith del James Hutton Institute (JHI) a Dundee, che hanno accettato di ospitarmi per oltre un anno, permettendomi di raccogliere e analizzare i campioni di orzo nelle loro strutture.

Non uno ma mille grazie vanno ai colleghi e amici del Consiglio per la ricerca in agricoltura e l'analisi dell'economia agraria (CREA) di Fiorenzuola d'Arda, dottor Luigi Cattivelli, dottor Alessandro Tondelli, dottoressa Raffaella Battaglia, dottor Agostino Fricano, dottor Davide Guerra, dottoressa Francesca Desiderio, dottor Gianni Tacconi, dottoressa Vania Michelotti, Fabio Reggiani e Stefano Delbono. Non ho parole per descrivere il supporto e la disponibilità di queste persone che sempre si sono spese per aiutarmi e consigliarmi in questi tre anni.

Impossibili da dimenticare sono gli studenti che in questi anni hanno accettato di farsi seguire anche da me nei loro percorsi di tirocinio e con cui ho condiviso in prima persona fallimenti e successi; ringrazio Alessandro Vajani, Nunzio Cicero, Sofia Annovazzi, Annamaria Lodigiani e Alessandro Gerli per la loro fiducia e pazienza.

Ringrazio inoltre i tutti i membri del nostro gruppo, anche se alcuni ormai già lontani, per l'aiuto e i consigli che mi hanno sempre dato senza mai tirarsi indietro, in particolar modo la dottoressa

Noemí Trabanco Martín, il dottor Avinalappa Hotti e il dottor Stefano Gattolin. Grazie anche a Emanuele Quattrini dell' Azienda Agraria Didattico-Sperimentale "F.Dotti" (Arcagna), per averci aiutato con le prove di campo e in serra.

Un grazie enorme va al dottor Salar Shaaf, una guida e un amico, per tutto ciò che mi ha insegnato, per l'amore che mi trasmesso per la statistica e per l'incrollabile esempio di dedizione al lavoro.

Infine vorrei ringraziare di cuore la professoressa Laura Rossini.
La ringrazio perché mi ha insegnato l'importanza del lavoro di gruppo, di come il successo nasca dalla cooperazione e dalla fiducia.
La ringrazio per l'impegno, la passione contagiosa e l'allegria che mette nel fare il proprio lavoro, che sempre sono stati il primo esempio per ogni membro del gruppo.
La ringrazio per avermi fatto affacciare ad un ambiente di ricerca internazionale, dove uomini e idee hanno la possibilità di muoversi, crescere e incontrarsi.
La ringrazio per avermi permesso di affiancarla nell'attività di tutoraggio e insegnamento, facendomi scoprire che spesso chi impara di più è proprio chi spiega ad altri.
Ma soprattutto ringrazio Laura perché ha creduto in me quando io non ci credevo più.

"The sun never sets for souls on the run"

Funding

This work was supported by FACCE-ERANET on Climate Smart Agriculture, project "An integrated approach to evaluate and utilize genetic diversity for breeding climate-resilient barley" (ClimBar; ID 82).